REGULATION OF GRANULOMA FORMATION IN MURINE MODELS OF TUBERCULOSIS

by

Holly Marie Scott

Bachelors of Science, Mount Union College, 1998

Submitted to the Graduate Faculty of

School of Medicine in partial fulfillment

of the requirements for the degree of

Doctor of Philosophy

University of Pittsburgh

2003

UNIVERSITY OF PITTSBURGH

SCHOOL OF MEDICINE

This dissertation was presented

by

Holly Marie Scott

It was defended on

December 8th, 2003

and approved by

Per Basse

Robert Hendricks

Paul Kinchington

Todd Reinhart

JoAnne L. Flynn
Dissertation Director

Copyright Permission was granted for the use of parts of:

1. Scott, H.M., and J.L. Flynn. 2002. Mycobacterium tuberculosis in chemokine receptor 2-deficient mice: influence of dose on disease progression. *Infection & Immunity.* 70:5946-5954.
2. Scott, H.M., J. Chan, and J.F. Flynn. 2003. Chemokines and tuberculosis. *Cytokines and Growth Factors Reviews* 14:467-477.

The letters, indicating that the publishers granted permission, are on file with Holly M. Scott.

REGULATION OF GRANULOMA FORMATION IN MURINE MODELS OF TUBERCULOSIS

Holly M. Scott, PhD

University of Pittsburgh, 2003

Abstract

Tuberculosis is a major cause of mortality worldwide. Elucidation of the host resistance against *Mycobacterium tuberculosis* infection and the pathogenesis of tuberculosis is a priority. The host response to *M. tuberculosis* in the lungs includes the formation of granulomas, focal accumulations of mononuclear cells coming together to fight infection. The signals required for the migration of cells into the lungs and those required for the formation of granulomas have not been well defined. In this thesis, we will describe the advances we have made in understanding chemokine expression and cell migration to the lungs in response to *M. tuberculosis*. We have determined that Tumor Necrosis Factor (TNF) partially controls cell migration by modulating chemokine expression by macrophages in vitro and CD11b+ cells in vivo. In addition, we have taken the subset of chemokines that are affected by TNF and addressed their functions in vivo through knockout and neutralization models. Specifically, we have used an aerosol model of tuberculosis in the mouse to address the roles of CXCL9 (MIG), CXCL10 (IP-10), chemokine receptor–5 (CCR5) and chemokine receptor–2 (CCR2). In our studies, there was no apparent, strong phenotype in mice without functional CXCL9 or CXCL10. CCR5-/- mice had altered pathology and increased inflammation in response to *M. tuberculosis* infection, but they were able to control the infection. The CCR5 -/- mice may be hyper-responsive due to higher antigen load in the lymph nodes in conjunction with increased dendritic cell migration and more primed lymphocytes. CCR2-/- mice had a clear defect in macrophage migration and a delay in T cell

migration, and the course of the disease was governed by the initial dose. Specifically, when a low dose aerosol infection route was used, CCR2-/- mice were able to control infection with the reduced number of cells migrating into the lungs; however with a higher dose, the mice succumbed to infection. Our findings are relevant to understanding the immune response and granuloma formation during aerosol *M. tuberculosis* infection, and will contribute to an appreciation of the potential effects of anti-inflammatory or anti-chemokine therapies on infections.

Acknowledgements

The work you will read about in this thesis could not have been carried out without the hard work and support of many important people. My mentor, JoAnne Flynn, has been a great scientific advisor. JoAnne has acted as a mentor with just the right balance of patience, knowledge, persistence and support. I am grateful to Amy Myers for excellent technical assistance. Amy puts in many hours to help all of us get our work done more efficiently. I thank all the members of the Flynn lab for they have become some of my best friends.

I am grateful to all of my committee members, Dr. Basse, Dr. Hendricks, Dr. Kinchington, and Dr. Reinhart. I appreciate all the time and effort they have put into my education. Their guidance has been a strong asset to this research.

I would also like to thank the Chan (Albert Einstein College of Medicine) and Nau laboratories for helpful discussions and I am extremely grateful for the Reinhart lab's technical assistance on the ISH protocol, particularly the guidance of Craig Fuller. The graduate program and the department's administrative staff are the best, trying to keep our lives less stressful. In addition, I could not imagine having a more supportive dean than Dean Stephen Phillips. Thank you!

The love and support my family and friends have shown me over the past 5 years has been tremendous. Mom and Dad always cared enough to try to understand the research and its implications. They have taught me the value of balance, education and hard work. I thank my siblings for their love. My brother's jokes always keep me smiling. I thank my sister and brother in law for bringing me 3 wonderful nieces into this world that I might get a good laugh and a reality check every once and awhile. I will be eternally grateful to my husband, David, for his love and support. David has always supported my goals and been unbelievably patient with me when I have been at my wits end. David motivates me to do my best and because of him I believe that I can balance my life (achieving while still appreciating every beautiful moment God has given us).

This work was supported by National Institutes of Health HL71241 (J.C., J.L.F), American Lung Association CI-016-N, Western Pennsylvania Lung Association Dissertation Grant (H.M.S.) and T32 Molecular Microbial Persistence and Pathogenesis AI49820 (H.M.S).

TABLE OF CONTENTS

LIST OF TABLES

LIST OF FIGURES

1.0 Introduction

Mycobacterium tuberculosis, an intracellular bacterium, is the causative agent of tuberculosis, an ancient disease that remains a major burden in some societies. Amazingly, the diagnostic methods and treatments have remained largely unchanged in the last few decades, and the current vaccine is relatively ineffective [1]. From a public health prospective, progress toward controlling tuberculosis has advanced with the implementation of directly observed treatment, short course therapy (DOTS). In addition, recent scientific advances over the last decade have raised hopes that new therapies and strategies for immunization will emerge. A wealth of knowledge has been gained towards understanding the immune response to *M. tuberculosis*. This thesis describes the advances we have made in understanding immune cell migration into the lung during *M. tuberculosis* infection in a murine model. These studies have focused on the influence of tumor necrosis factor on cell migration and chemokine expression. In addition, we addressed the roles of chemokine receptors CCR2 and CCR5 and chemokines CXCL9 and CXCL10.

1.1 Global Impact of Tuberculosis

3.8 million new cases of active tuberculosis were reported in 2001 with a corresponding global incidence rate of tuberculosis growth of 0.4%. In some countries such as Russia (6%/ year) and eastern and southern African countries (5%/ year), the incidence has been rising since 1997, but in other countries the incidence has been slowly falling [2]. The number of cases reported to the World Health Organization is only 45% of the estimated new tuberculosis cases in 2001, leaving the disease underreported and probably under diagnosed. There were 1.84 million deaths from TB in 2000, with about 12% of those deaths attributable to co-infection with HIV [3].

In the United States, there has been a decline in tuberculosis cases every year since the resurgence of tuberculosis cases in 1992. The CDC has described a plan to eliminate tuberculosis in the United States (defined as <1 case per 1,000,000) by the year 2010. In 2002, there were approximately 15,000 new cases reported to the CDC, representing a 5.7% decline from 2001. Despite the decline in the percentage of cases, the rate of tuberculosis incidence remains higher than the country's target goal in its plan towards tuberculosis elimination. On a positive note, there was also a decrease in the proportion of multidrug-resistant (MDR) tuberculosis (from 2.7 to 1.3% in 10 years) [4].

Tuberculosis is in principle, a curable and preventable disease. Its continuing global impact highlights the disparity between the developing world and the industrialized nations. In the early 20th century, industrialized nations made improvements on their populations' nutrition, sanitation, and economy, leading to declines in the incidences of many infectious diseases, but today some developing countries are still struggling in these areas. In the 1940s, treatment for tuberculosis improved with the advent of anti-mycobacterial drugs such as isoniazid, streptomycin and para-amino salicylic acid (PAS). Since that time, more anti-mycobacterial drugs have been developed including pyrazinamide, ethambutol and rifampicin, but no new specific antimycobacterial drugs have been approved over the last 40 years. The current vaccine for tuberculosis (BCG) is in use in most of the world has shown its effectiveness primarily in preventing disseminated forms of tuberculosis in young children, but has shown little protection against pulmonary tuberculosis in adults [reviewed in [1]].

With the initiation the DOTS strategy in 1995, many more countries have started to address this global health problem. Under the DOTS program, each country adopts the program's 5 Pillars: government commitment, diagnosis by smear microscopy, multi-drug

chemotherapy treatment for at least 2 months, reliable supply of anti-TB drugs, and outcome evaluation and records of every patient. The number of countries implementing DOTS has increased each year since 1995, with 7 countries newly implemented DOTS in 2001 [2], increasing the number of countries currently implementing DOTS to 155. The percentage of the world's population that is consequently covered under DOTS is 61%, and the overall treatment success rate in DOTS areas is 82%.

1.2 Potential Outcomes to infection

Transmission of *M. tuberculosis* is principally human-to-human through contaminated aerosol droplets that enter the alveolar spaces. Therefore, the most common site of infection is the lung. Although the infection is initiated in the lung, infection can spread throughout the body, including lymph nodes, central nervous system, pericardium, skin, bone, kidneys, and larynx. Exposure to *M. tuberculosis* can lead to three potential outcomes (Figure 1). In ~ 90% of exposed individuals, a strong cell mediated immune response is mounted by 4-5 weeks after exposure and results in a subclinical form of the infection, defined as latent tuberculosis. Latent tuberculosis refers to *M. tuberculosis* infection without clinical signs of disease [5]; a person can remain infected for life without developing active tuberculosis, and not be infectious. The second potential outcome is active clinical tuberculosis. About 5% of exposed persons will develop active tuberculosis within 2 years of exposure. A final possibility, although it is not clear how often this occurs, is exposure without successful infection also referred to as clearance [reviewed in [6]].

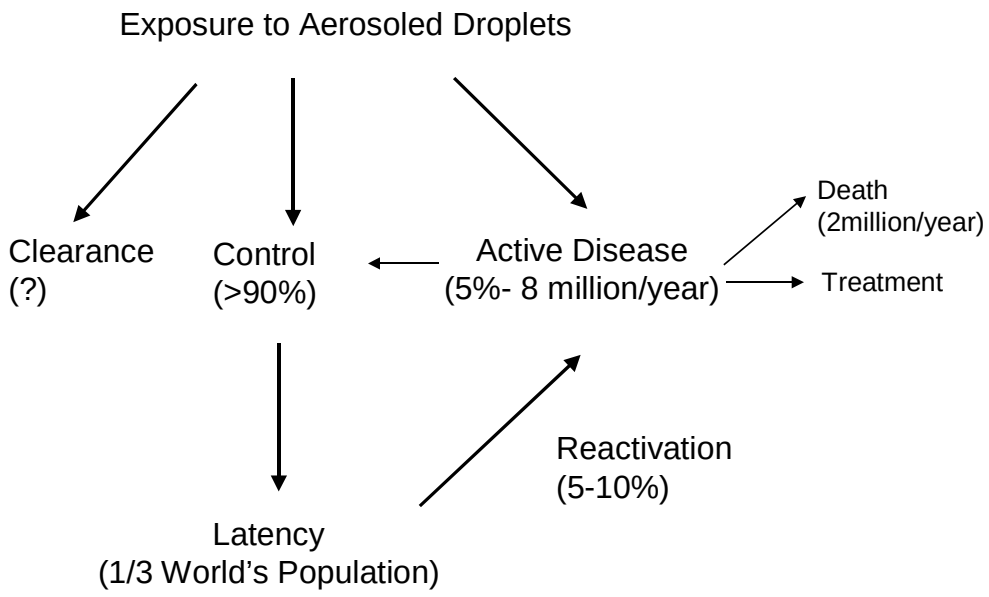

Figure 1. Potential Outcomes of exposure to the *M. tuberculosis* bacillus.

Following exposure to *M. tuberculosis* bacillus there are three potential outcomes. In some cases the bacillus may be cleared without detection by the immune system. In a majority of cases the infection is controlled through the cell mediated immune response and leads to clinical latency. About 5% of individuals exposed to *M. tuberculosis* will develop active disease in the first 1-2 years after exposure. In addition, it is possible for latent disease to become active. Reactivation of disease can result from immunosuppression.

Typical diagnosis of *M. tuberculosis* infection in the United States can be achieved through a delayed type hypersensitivity skin test to purified protein derivatives (PPD) of mycobacteria. A positive PPD test does not indicate a person has active infection, but rather that he was exposed and initiated an immune response to *M. tuberculosis*. Consequently, in the United States, a PPD positive individual without disease is often treated with isoniazid for 6 months, to reduce the risk of reactivation. In countries where BCG vaccination against tuberculosis is practiced, transmission of *M. tuberculosis* is not easy to assess, since BCG results in PPD positivity for a number of years. Persons with active tuberculosis are treated with multi-drug therapy (4 different antibiotics for 2 months and an additional 4-10 months of 2 antibiotics) to prevent drug resistant strains from emerging. Active tuberculosis can be accompanied by

night sweats and intermittent fever, weight loss and anorexia, fatigue, and coughing. Active infection is confirmed through a positive smear test, where the sputum is stained for acid-fast bacilli, and by culture of the sputum sample. Due to the presence of inflammatory lesions, granulomata, a chest radiograph can also be a diagnostic tool during or after the infection.

1.3 Influence of external factors

Many factors influence the success rate of tuberculosis control. In Russia, the increased rates of tuberculosis are related to the destruction of the health care infrastructure, the emergence of MDR strains, and the lack of monies to treat tuberculosis cases. In the United States, tuberculosis is most common among immunocompromised individuals, such as the elderly or HIV+ persons. HIV infection leads to a decline in the numbers of CD4+ lymphocytes, leaving HIV+ individuals severely immunocompromised. In the absence of CD4+ lymphocytes, *M. tuberculosis* cannot be controlled [7-10]. Immunocompromise induced by steroids, anti-inflammatory therapies, alcohol, or malnourishment causes increased risk of tuberculosis.

An estimated 10.7 million people were coinfected with *M. tuberculosis* and HIV in 1997 [reviewed in [11, 12]]. From those 10.7 million coinfected individuals, approximately 640,000 will develop tuberculosis disease. A majority of the tuberculosis/HIV coinfected patients are found in sub-Saharan Africa and southeast Asia. An estimated 60,000 reside in North America. Treating HIV in the presence of *M. tuberculosis* infection can be somewhat complicated due to significant interactions between the rifamycins and the antiretroviral protease inhibitors and non-nucleoside reverse transcriptase inhibitors. In addition HIV infection can change the progression of tuberculosis disease. Extrapulmonary tuberculosis, particularly in the lymph node is more common in HIV-positive individual than HIV-negative individuals. Although analysis of chest radiographs do not indicate any abnormalities in HIV-positive individuals with >200 CD4+

cells/μl, HIV-positive individuals with < 200 CD4+ cells/μl do having increased mediastinal adenopathy (which is also common in children with primary tuberculosis). *M.tuberculosis* infection also appears to change the progression of HIV infection because *M. tuberculosis* infection leads to induction of proinflammatory cytokines, including TNF. TNF can upregulate intracellular retroviral replication enhancing HIV infection.

2.0 Animal Models of Tuberculosis

Current animal models used to study *M. tuberculosis* include mouse, guinea pig, rabbit, and nonhuman primate models. All of these models have some features in common with human tuberculosis, including infection by depositing a few virulent bacilli directly into the lung, development of a granuloma (inflammatory lesion), and onset of a strong cell mediated immune response. However, there are differences in each animal species' ability to control infection, limit dissemination, and develop persistent infection.

The use of these animal models could not have been possible without the development of microbiology and engineering techniques to work with *M. tuberculosis*. These include growth of *M. tuberculosis* in liquid media, the improved methods for storing the bacillus and the ability to enumerate bacilli on solid media. Aerosol exposure chambers allow reproducible low dose infection via the physiologically relevant respiratory route.

2.1 Monkey

Nonhuman primates have been used as models for tuberculosis infection for years. In the 1970s these animals were used to address the efficacy of BCG vaccination, ideal route of administration, and the differences between strains of BCG [13-15]. The nonhuman primate model also served as a good model for testing new drugs as they became available, serving as a good intermediate step between testing drugs in the mouse model and in man [16]. The model was used to evaluate single and multiple drug regiments using antituberculosis drugs including isoniazid, streptomycin, p-amino-salicylic acid, cycloserine, ethambutol and others. Following these studies the use of nonhuman primates declined due to the high cost and space required for the studies. More recently, interest in using the primates has reemerged as the research has

indicated that infection of nonhuman primates leads to disease that closely resembles human disease [17]. Both primary and latent disease can be modeled in macaques, and there is an extensive array of reagents for immunologic studies in monkeys [17]. Difficulties in the use of these animals for tuberculosis research include the requirement for BSL3 primate space, out bred populations, and cost.

2.2 Rabbit

The rabbit is one of the few animal models able to form liquefied necrotic or cavitary granulomas in response to *M. tuberculosis*. Cavitation occasionally occurs in human tuberculosis and leads to the release of massive numbers of bacilli for dissemination. Interestingly, rabbits are much more susceptive to *M. bovis* than to *M. tuberculosis*. A disadvantage of rabbit models of tuberculosis is that the cost is relatively high and they require more biosafety level 3 (BSL3) space than guinea pig or mouse models. Another disadvantage is that there are limited reagents available for the immunological studies.

2.3 Guinea Pig

In contrast to mice and humans, the guinea pig is highly susceptible to *M. tuberculosis* infection and develops progressive pulmonary infection [18]. Even a single virulent tubercle bacillus can lead to progressive infection and death. In this model, there is extremely high extrapulmonary dissemination. These animals can be protected to some degree from tuberculosis with BCG vaccination, and they do develop granulomas similar to humans (except for the lack of cavitation). A drawback of this model for immunologic research is the scarcity of immunological reagents. Current efforts are being made in cloning and developing cytokine and chemokine reagents for use in this model [19-22].

2.4 Mouse

Immunological and microbiologic studies of *M. tuberculosis* have advanced most dramatically in the mouse models of tuberculosis, but as with all models, they have limitations [reviewed in [18, 23]]. The mouse models of tuberculosis are cost and space efficient. Similar to humans, the mouse is capable of generating a strong adaptive immune response to *M. tuberculosis* and can control low dose inocula. The mouse model of tuberculosis was used by Robert Koch to test his famous set of postulates on field mice inoculated with *M. tuberculosis* [24]. Over the last century, the model has evolved and played a key role in the discovery of streptomycin and other anti-mycobacterial drugs. Following drug discoveries, the mouse became a model of vaccine study with BCG immunization. Furthermore, it was the mouse model that generated data indicating a cell mediated immune response is initiated in response to *M. tuberculosis* and that control was not primarily mediated by the humoral immune response. Another advantage of the mouse model is the availability of immunological reagents. Genetic manipulation has revolutionized the use of the mouse as a model for disease. Both transgenic knockout and over-expression systems allow for in depth analyses of mechanisms by which the mouse controls *M. tuberculosis* infection. The use of monoclonal antibodies to measure cytokine production, block functioning proteins, and characterize the cell populations in response to *M. tuberculosis* infection has been instrumental in advances made in immunological research.

There are a variety of strains available for analysis of *M. tuberculosis* infection in mice. The most commonly used is the C57Bl/6 strain, which is often described as being relatively resistant to tuberculosis [mean survival time(MST)=315d] [25]. Other strains, such as the BALB/c mouse, are also considered resistant to infection administered via aerosols (MST, 245d). On the other hand, more susceptible mouse strains include the CBA, C3H, and DBA/2J strains (MST, 110d).

A clear disadvantage of the mouse model is the relatively high bacterial burden in the lungs. The bacterial burden in mice rises almost uninhibited during the first 3 weeks after infection, and the number of bacilli then reaches a plateau between 10^5 and 10^6 (Figure 2). Despite the magnitude of the bacterial burden, the mice survive for approximately a year. Immunocompromising conditions or age can spark reactivation with a rise in bacterial burden. A typical life-ending burden in the mouse is $>10^8$ CFU/lung, but can reach 10^9 CFU/lung. Our studies, some of which will be described in this thesis, indicate that the peak of the immune response in C57Bl/6 mice is actually more robust than necessary to control infection. Another disadvantage is that although mononuclear infiltrates form in the lungs of infected mice, they rarely develop necrotic or caseous granulomas, and the structure only slightly resembles that of a human pulmonary granuloma [26].

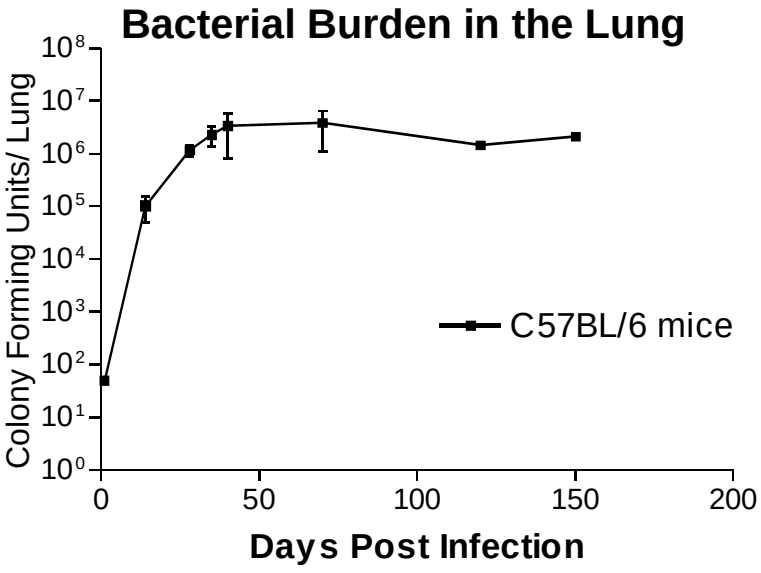

Figure 2. Bacterial burden in the lungs of wild type C57Bl/6 mice.

C57Bl/6 mice infected with 50-100 colony forming units through aerosols can control bacterial burden by approximately 4 weeks post infection. At this time point the mycobacterial burden reaches a plateau at about 10^6 colony forming units. (These data were generated in our laboratory, unpublished).

The mouse model has been modified to study latent tuberculosis. The definition of murine latency and human latency are the same, but there are differences in latency in these two species [reviewed in [27]]. Latency can be defined as a stable *M. tuberculosis* burden in the lungs without clinical signs or histological changes. In the human, the bacterial numbers are believed to be very low or almost undetectable during latency, whereas, the infection stabilizes at ~10^6 CFU/lung in the mouse. Therefore, the "latent murine model" has also been referred to as "chronic persistent tuberculosis", for there is clearly an active immune response employed to maintain control of the bacteria, resulting in a chronic infection.

Other models have been developed in mice to more closely resemble the human disease, at least in terms of bacterial numbers, such as the Cornell model [28-30]. This model relies on the use of anti-mycobacterial drugs to control the initial infection. Unfortunately, there is no standard protocol for this model. When this model was first described in the 1950s, the chemotherapy was initiated just 20 minutes post inoculum. Since that time, the dose and strain of *M. tuberculosis*, the time of initiation of chemotherapy, and the length, type, and dose of chemotherapy have varied from experiment to experiment. For immunological studies the Cornell model has proven to be inconsistent, and if chemotherapy is initiated early after infection, the antibiotics rather than the immune response is primarily responsible for controlling infection. Despite the difficulties establishing a latent tuberculosis murine model, studies of chronic persistent infection in mice have generated insights to immune responses during this stage of infection [6].

3.0 Initiation of Infection

The initiation of *M. tuberculosis* infection in mice and humans occurs through the respiratory tract. The aerosol droplets containing *M. tuberculosis* must be <5μm for the bacillus to enter the alveolar space and infect alveolar macrophages. After initial infection, dendritic cells and monocyte-derived macrophages can take up the bacillus. The *M. tuberculosis* bacillus can be taken up by the macrophage through many receptors. These include the scavenger receptor, the mannose receptor, the complement receptors 1, 3 and 4, and the most recently described CD44 receptor on macrophages [31-34]. In transgenic knockout models of these receptors, infection may use redundant methods of receptor attachment, for when one receptor is missing, another is utilized, making it difficult to confirm roles in internalization for these receptors [32, 35-37]. Phagocytic uptake via the complement receptor, CR3, can occur with both opsonized and nonopsonized bacillus [38, 39]. However, the best characterized mechanism for nonopsonized bacillus in mice and humans is the mannose receptor [32, 40]. Internalization of *M. tuberculosis* by human DCs can be mediated by DC-SIGN [41]. Although it is clear that *M. tuberculosis* has a tropism for phagocytic cells, *M. tuberculosis* also interacts with epithelial cells, possibly through its antigen 85, a fibronectin binding protein [42].

In mice whose alveolar macrophages were depleted by dichloromethylene diphosphonate liposomal treatment, there was increased survival after pulmonary challenge and 9.7 fold fewer *M. tuberculosis* in the lung and 2.7 fold less in the liver [43]. In addition, the cellular infiltrate in these mice was more diffuse and overall Th1 and Th2 cytokine production was reduced. The early replication of *M. tuberculosis* in the lung was not affected, suggesting that initial uptake of *M. tuberculosis* by alveolar macrophages was not required for establishing infection, but rather

that later in the infection the alveolar macrophages may play a role in the maintaining a pulmonary infection.

Initial uptake can lead to killing of *M. tuberculosis* through phagolysosomal fusion and acidification, but this process is dependent on the microenvironment of the macrophage. The live bacillus can inhibit phagolysosomal fusion by recruiting a host tryptophan aspartate containing coat protein (TACO), which prevents maturation of the phagosome [44]. TACO is released during normal phagosome maturation into lysosomes. With retention of TACO on the phagosome, the *M. tuberculosis* can survive and replicate. In addition to retention of TACO, the *M. tuberculosis* containing phagosome possibly accumulates Rab5 and excludes Rab7 indicating that the phagosome is arrested at the early endosomal stage [reviewed in [45]].

M. tuberculosis does not completely go under the immune radar prior to the cell mediated immune response. There is an innate immune response to the bacillus. *M. tuberculosis* and other bacteria have pathogen associated molecular patterns (PAMPs) that can be recognized by various receptors, initiating immune responses. The *M. tuberculosis* bacillus is recognized by toll-like receptors (TLRs), the mannose receptor, complement receptors, and the lipopolysaccaride (LPS) receptor. Both viable and dead *M. tuberculosis* can activate murine macrophages expressing TLR2 and TLR4 [reviewed in [46, 47]]. The LPS receptor, CD14, enhances the macrophage's ability to respond to lipoarabinomannan (LAM), a mycobacterial cell surface molecule [48]. There is evidence that mycobacterial lipoproteins, such as 19kDa protein, are recognized by TLR2. The 19kDa protein can inhibit MHC Class II expression and processing of soluble antigens through TLR-2 signaling [49-51]. In addition, the 19kDa protein can induce macrophage apoptosis through TLR2 [52]. Interaction of the bacillus with TLR2 also leads to production of IL-12, IL-8, IL-23 and TNF [47, 53-55], cytokines essential for control of

infection, while TLR4 ligation supported the production of IL-12 and CXCL10. Whether TLR2 and TLR4 are required for control of infection, or if their roles are redundant was addressed in transgenic knockout models. TLR2 and TLR4 deficient mice controlled acute infection similar to wild type mice, when a low dose aerosol route was utilized [56]. When the dose was increased 20-fold, these knockout mice both exhibit increased susceptibility to infection. In addition, during chronic infection TLR4 -/- mice succumbed to low dose aerosol infection by 5-7 months post infection exhibiting impaired macrophage recruitment and proinflammatory cytokine responses [57]. These data suggest a role for TLR4 in the adaptive immune response during chronic infection, which is somewhat surprising considering the general belief that toll-like receptors' major role is the initiation of the immune response.

Early after infection there is a neutrophilic infiltrate in the lungs, which may be important for early control of infection. When neutrophil depleted mice were infected with *M. tuberculosis*, the bacterial burden was significantly higher by one-week post infection in the liver, lung and spleen [58]. In addition the mice exhibited reduced IFNγ and NOS2 mRNA expression.

The bacillus disseminates from the lungs at least in part through lymphatic drainage to the mediastinal lymph nodes. This dissemination occurs in an aerosol infected mouse 9-11 days after infection and *M. tuberculosis* specific T lymphocytes generated in the lymph nodes 2-3 days later [59]. The dissemination of infection to the periphery organs, such as the spleen or liver occurs 11-14 days post infection and again the generation of *M. tuberculosis* specific lymphocytes follows. Dissemination appears to help initiate the cell mediated immune response in a timely manner, for when comparing C57Bl/6 mice to more susceptible C3H mice, dissemination occurred earlier in the C57Bl/6 strain [59].

4.0 Acquired Immune Response

M. tuberculosis infection is controlled primarily through the cell mediated immune (CMI) response. T cells are primed and activated within the lymphatics and the protective response is mediated within the lungs in the granuloma. This response involves many cell types including dendritic cells, macrophages, CD4+ and CD8+ T lymphocytes, and B lymphocytes [26, 60]. Although each of these cell types clearly is induced in response to infection, their functions during *M. tuberculosis* infection are still being defined. The chart below illustrates susceptibility of many transgenic knockout mice with *M. tuberculosis* infection. In addition it summarizes the cellular infiltrates found in the mice, since we have demonstrated that even resistant mice can have altered cell infiltration compared to wild type mice.

Table 1. Susceptibility chart on transgenic knockout mice infected with *M. tuberculosis.*
The table below describes the mean survival time and cellular infiltrate as described in the literature or in current studies. All infections were performed with a low dose aerosol infection, unless otherwise noted. NR = not reported, ND = not determined

Strain of Mice	Mean Survival Time (Aerosol)	Cellular Infiltrate in Lung	Reference
C57Bl/6	310 d	Organized	[23]
TNFRp55-/-	25 d	Dissorganized, neutrophilic	Section 7.0, [61]
CCR2-/-	21 d (high dose)	Dissorganized, few Mϕ, neutrophilic	[62]
CCR2-/-	>200 d (low dose)	Organized, fewer Mϕ	[63]
CCR5-/-	>200 d	Organized, more lymphocytic	Section 9.0
CXCL10-/-	>90 d	Organized	unpublished
GKO	30 d	Organized, more granulocytes	[64]
IL-10-/-	>200 d	Organized, more activated mϕ	Appendix A, [65]
IL12p40-/-	45 d	NR, Fewer lymphocytes	[66]
IL12p35-/-	ND, but >CFU than WT @ 55d	NR, Fewer lymphocytes	[67]
IL-6-/-	59 d (for i.v. infection)	ND	[68]
CD4-/-	45 d	Delayed, Some organized, smaller	[7]
β2M-/-	232 d	Organized, larger infiltrates	[69]
BKO	>200 d	Organized, smaller	[70]
NOS2-/-	>180 d, but 1 log >CFU than WT	Diffuse, more neutrophilic	[71]
CXCR3-/-	>140 d	Transiently fewer, smaller but organized	[72]
CCL2-/-	> 200 d	Organized, fewer Mϕ	[73]

4.1 Granuloma Formation

Granuloma formation is the hallmark of *M. tuberculosis* infection. Granulomas form in response to chronic local antigenic stimulation, and can be observed in other infectious diseases, including schistosomiasis, leprosy, and leishmaniasis [74-78]. Granuloma structure and composition varies depending on the organism. A tuberculous granuloma is observed concomitant with a highly activated cell mediated immune response, which generally mediates

control of mycobacterial numbers in the lungs. This is an attempt by the host to contain the infection, however the resulting pathology can cause complications for the host.

The granuloma functions to control *M. tuberculosis* infection by orchestrating communication between immune cells (Figure 3). It creates a local environment for the cells to interact leading to an effective immune response where cytokine production, macrophage activation and CD8 T cell effector functions lead to killing of *M. tuberculosis*. The granuloma also physically contains the bacilli, walling off and preventing spread of the infection. These actions lead to inhibition of growth or death of *M. tuberculosis*, in part by enhancing macrophage activation and creating an oxygen and nutrient deprived environment.

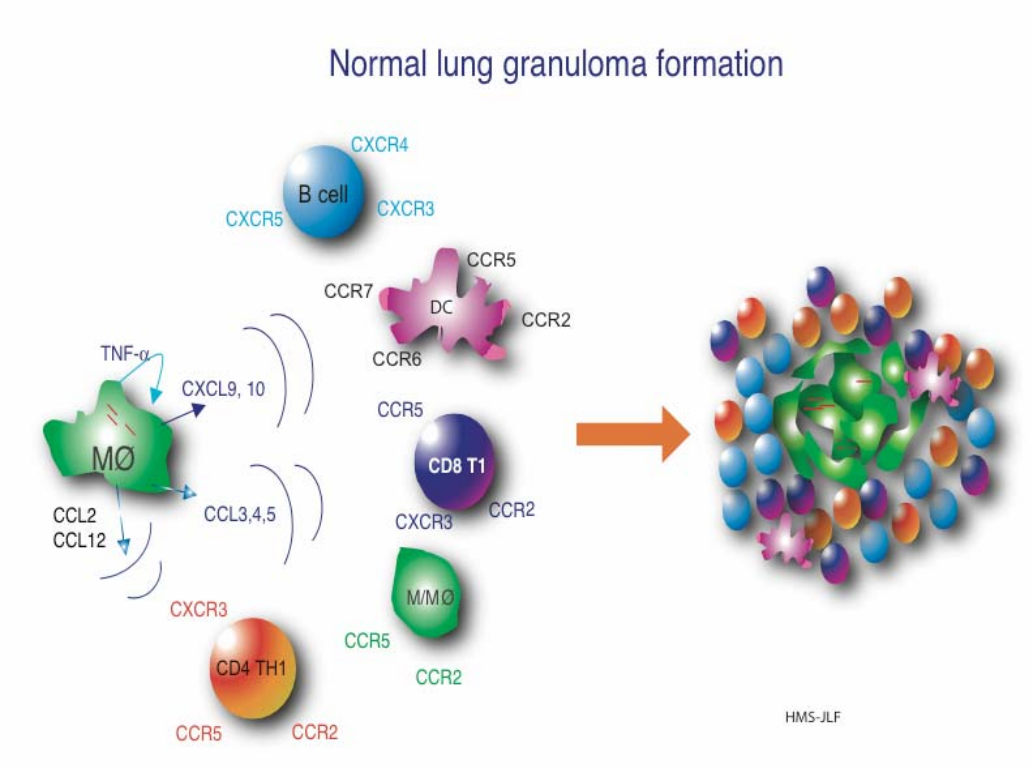

Figure 3. Granuloma formation in the lungs of *M. tuberculosis* infected mice.

This model of granuloma formation was created based on the literature and our studies. Macrophages after infection with *M. tuberculosis* produce TNF and many chemokines. These chemokines are from both the C-C and C-X-C chemokine families of inducible chemokines. The receptors for these chemokines include CCR2, CCR5, CXCR3, among others, which are present on many of the immune cells that migrated to the lungs during *M. tuberculosis* infection and ultimately play a role in the granuloma.

The granuloma is composed of many different cells, including macrophages, dendritic cells, CD4 and CD8 T lymphocytes, and B lymphocytes [26, 60]. The macrophages in human infection can differentiate into multinucleated giant cells. Occasionally, such giant cells can be observed in murine granulomas, but usually under conditions of severe inflammation. In human granulomas, the macrophages are centrally located with the lymphocytes surrounding and infiltrating the macrophage area. Some of the macrophages are infected and many have an activated appearance. Necrosis can occur in granulomas, beginning in the center of the structure, which may progress to caseous or necrosis in human tissue. The caseous material is usually solid, but if the infection is not controlled, can liquify and support extracellular replication of *M. tuberculosis*. Caseous granulomas can progress to form cavities within the lung, leading to erosion of the granuloma into a bronchus, and the subsequent release of bacteria into the airways. Solid granulomas without obvious necrosis are also observed. These granulomas may be controlling or clearing the infection, or may be simply observed prior to undergoing necrosis. Fibrosis of a granuloma seems to occur as the granuloma controls the infection and the inflammatory process is limited. In a latently infected person, one or more granulomas controlling the infection can sometimes be observed; these granulomas can also be calcified.

In murine models of tuberculosis, the granuloma is arranged differently but performs the same functions of limiting bacterial replication and spread of infection, as well as localizing the inflammatory and immune response to the site of infection within the lung. Rather than the macrophages being centrally located, they are arranged in sheets in the lungs, adjacent to loose aggregates of lymphocytes. As infection progresses, many macrophages appear foamy, an indication of activation. Lymphocytic infiltrate is observed around perivascular spaces early after aerosol infection; these cells migrate further into the lung parenchyma as the infection

progresses. The aggregates of T lymphocytes with macrophages (i.e. granuloma formation) begin to form by 2-3 weeks post infection, but are larger and more organized by 4 to 5 weeks post infection. CD4, CD8 and γδ T cells are present in these aggregates. B lymphocytes also migrate to the lung at a similar time. The aggregates of B cells form tighter clusters as the infection progresses, and can be distinguished from the T lymphocytes because the cells are more tightly packed. There is also an influx of neutrophils in the lung early after infection, which peaks ~2 to 3 weeks post-infection in mice that control infection and then decreases to very low levels. The total numbers of T and B cells stabilize by 5 to 6 weeks post infection and granulomas are well established. If bacterial numbers are not controlled by the immune response, infiltration of cells continues and the cellular aggregates increase, resulting in much of the lung filled with inflammatory cells, limiting airway space. If mice are immunocompromised (e.g. IFN-γ deficient mice) and progress to high bacterial burdens, necrosis of the granulomas is often observed, with extensive neutrophil infiltration. Necrosis in granulomas of mice is almost always associated with high *M. tuberculosis* numbers; necrosis is rarely observed in wild type mice that are controlling the infection, even in long-term infections. This may be a different situation than that of humans, where it is believed that the immune response contributes to necrosis within the granuloma.

4.2 Cellular Interactions during the protective immune response

4.21 Dendritic Cells

Dendritic cells are a key link between innate and adaptive immunity. As potent antigen presenting cells and potent responders to PAMPS, dendritic cells often influence the strength and type of adaptive immune response [79]. *M. tuberculosis* infection of bone marrow derived dendritic cells results in the upregulation of cell surface molecules, such as ICAM, B7.1, and

B7.2. In addition, infection of murine DCs leads to increased expression of inflammatory cytokines, IL-12, TNF, IL-1β, and IL-1α [80-82]. These cytokines initiate Th1 responses in T lymphocytes, stimulating the production of IFNγ and other cytokines. In addition, infected human dendritic cells produce chemokines, such as CCL3, CCL4, CXCL9 and CXCL10 [83], which appear to recruit activated NK and T lymphocytes. Beyond initiation of the immune response, the DCs may play a role in adaptive immunity, especially in chronic infections such as *M. tuberculosis*. Although murine DCs do produce reactive nitrogen intermediates (RNI) and reactive oxygen intermediates, they do not actively kill the *M. tuberculosis* bacillus (K. Bodnar and J.L.Flynn, unpublished). Rather, they produce more peroxynitrite (K. Bodnar, unpublished), a form of RNI, which is nontoxic to pathogenic mycobacterium [84]. In addition, a bacillus-containing phagosome (or vesicle) within activated DCs is structurally different than a phagosome containing *M. tuberculosis* in an activated macrophage (K. Bodnar, unpublished). Within the activated macrophage, some of the vesicles containing *M. tuberculosis* form multiple membranes around the bacillus. Studies in human DCs support the findings in the murine system [85]. The mycobacterial vacuoles of infected human DCs neither acidify nor fuse with lysosomes, explaining why the mycobacteria are not killed. In addition the lack of communication between these vacuoles and the normal host cell recycling machinery may indicate why the bacteria also do not multiply. *M. tuberculosis* survival within the dendritic cell, possibly in a non-replicating state, may be beneficial for the immune response, providing a long term source of antigen for presentation to lymphocytes. Dendritic cells have been described in the lung and within granulomas of both mice and humans [60, 86]. In the mouse model the CD11c+ dendritic cells in the lungs of infected mice appear to be of mixed phenotype, some mature, while most immature [60].

4.22 Macrophages

The role of macrophages in the CMI response is no less complicated. With many different states of macrophages (activated and unactivated), and types of macrophages (residential, alveolar and newly recruited monocytes), it can be difficult to clearly define different macrophage responses to *M. tuberculosis* infection. Macrophages, as described earlier, are a first line of defense against infection, but their role in the CMI response is a key to control of infection. Macrophages can be activated by stimulation with inflammatory cytokines, such as IFNγ, but IFNγ alone cannot stimulate a macrophage to produce RNIs and ROIs. Another signal such as TNF or LPS or another bacterial product is required. Activated macrophages are capable of bacteriocidal activity on *M. tuberculosis,* presumably within the phagolysosome, where the acidic vesicle contains hydrolases, ROI, and RNI. The importance of RNI to control of infection is a highly debated point. In the murine system, RNI appears essential for control of infection [87]. On the other hand, in the human system, a role has not clearly been defined. Immature macrophages, or newly recruited monocytes, appear to be less effective as antimicrobial forces, and may serve as a preferred host for the *M. tuberculosis* bacillus. Macrophage antimycobacterial function may also be stimulated by GM-CSF and IL12. On the other hand, IL-6 and IL-1 do not appear to have a significant affect on the mycobacterial growth. Recent evidence indicates that this may be due to a block in the IL-6 signaling via the 19Ka *M. tuberculosis* protein [49, 88].

The role of macrophages in control does not lie solely within the phagosome, but also in the context of macrophage- T cell interaction. Macrophages, like dendritic cells, also present antigen in the context of major histocompatibility class I (MHC), class II, and non classical molecules to T lymphocytes. But recent data has shown that macrophages are not as effective as

dendritic cells in priming naïve T cells to develop a Th1 phenotype. The inability of macrophages to prime Th1 cells has been attributed to the production of IL-10 by macrophages and minimal IL-12 production [80]. The presentation of antigen by macrophages in the context of MHC I may be a major factor in the ability of CD8+ lymphocytes to contribute to host defense through CTL activity.

4.23 CD4+ T lymphocytes

The continual interaction between T lymphocytes and antigen presenting cells allows for surveillance and containment of infection (Figure 4). In an oversimplified model, the macrophage produces stimulatory cytokines and presents antigen to activate the T lymphocytes, and T lymphocytes produce IFNγ and TNFα to activate the macrophages. CD4 T lymphocytes play a key role in IFNγ production and control of *M. tuberculosis*. CD4-/- mice are unable to control *M. tuberculosis* infection. Interestingly, eventually the CD8 T lymphocytes in the CD4-/- mice produce enough IFNγ to make up for the deficiency in CD4 lymphocytes, but the mice still succumb to infection [7]. Therefore, CD4 lymphocytes may perform an additional function in the CMI response that cannot be compensated for by other cells. This was also evident in chronic studies where CD4+ T lymphocytes were depleted through antibody administration. The CD4 T cell-depleted mice were unable to control infection, despite having similar levels of IFNγ compared to control mice [8].

There is increasing evidence that CD1 restricted CD4 lymphocytes may play a role in lipid antigen specific responses during infection [89]. In healthy human subjects with previous exposure to *M. tuberculosis,* CD1-restricted *M. tuberculosis* specific T cells comprise a significant portion of their circulating CD4+ blood. Interestingly, patients with active TB had

low CD1 specific proliferative responses until after two weeks of chemotherapy when their lipid specific proliferative responses increased significantly.

CD4 cells may be very important for stimulation of dendritic cells and cross priming of CD8 lymphocytes, as evidenced in many viral models. Studies addressing this hypothesis are underway. CD4 cells also can be cytolytic, acting on infected cells through the Fas – FasL interaction. Antibody blockade of CD95- CD95L interaction of CD4+ cells from healthy tuberculin skin test-positive persons with autologous monocytes decreased cytotoxicity by 25% [90]. Mice deficient in CD95 signaling were able to control acute infection similar to wild type mice, but entering the chronic stage of infection, the CD95L-/- and CD95-/- mice were gradually unable to control the bacterial burden [91].

4.24 CD8+ T lymphocytes

There is growing support for a role for CD8 lymphocytes in the CMI response to *M. tuberculosis*. MHC Class I molecule appears to be important for the control of *M. tuberculosis*, for mice deficient in beta-2-microglobulin (β2M-/-) are more susceptible to *M. tuberculosis* infection [69]. Use of this model to study CD8 T cell responses does not rule out the possibility that the increased susceptibility was due to a lack of non-classical MHC Class Ib, but the additional finding that TAP deficient mice [92], which also lack CD8+ lymphocytes, exhibited increased susceptibility to infection supports the idea that MHC Class I restricted CD8 lymphocytes are required to control infection. Vγ9/Vδ2 T cell lines generated from the peripheral blood mononuclear cells (PBMCs) of PPD+ healthy individuals can kill *M. tuberculosis* infected macrophages both by a perforin and granulysin dependent mechanisms [93]. More recently it has been shown that CD8 lymphocyte precursors can be found in the lungs and lymph nodes of *M. tuberculosis* infected mice. These precursors increase in frequency

during the first 4 weeks post aerosol infection and then their frequency wanes (V. Lazarevic, unpublished). In support of CD8 lymphocytes acting as cytotoxic cells, perforin can be detected in cells and tissues of *M. tuberculosis* infected mice [94] and T lymphocytes, isolated from infected mice and cultured short term with *M. tuberculosis* infected dendritic cells, can lyse target *M. tuberculosis* infected cells and produce IFNγ [95].

4.25 B lymphocytes

Following *M. tuberculosis* infection there is a considerable B lymphocyte infiltration in the lungs and the cells are located within the granuloma (unpublished, Flynn). Low – dose aerosol infection of B cell knockout mice (BKO) with *M. tuberculosis* led to altered dissemination and granuloma formation. The BKO mice had similar numbers of bacteria in their lungs, but the dissemination to peripheral organs was delayed and the pulmonary lesions were less severe. These differences have been linked to absence of the cells in the mice, not due to lack of antibody response [70]. During chronic infection, the absence of B lymphocytes did not appear to affect the *M. tuberculosis* infection [96] further indicating that these cells may be present as a reaction to the inflammation, but their presence is neither an advantage nor disadvantage for the host. On the other hand, when BKO mice were infected i.v. with a high dose of virulent H37Rv *M. tuberculosis*, the mice exhibited increased bacterial load in their lungs by 4-6 weeks post infection compared to wild type mice [97].

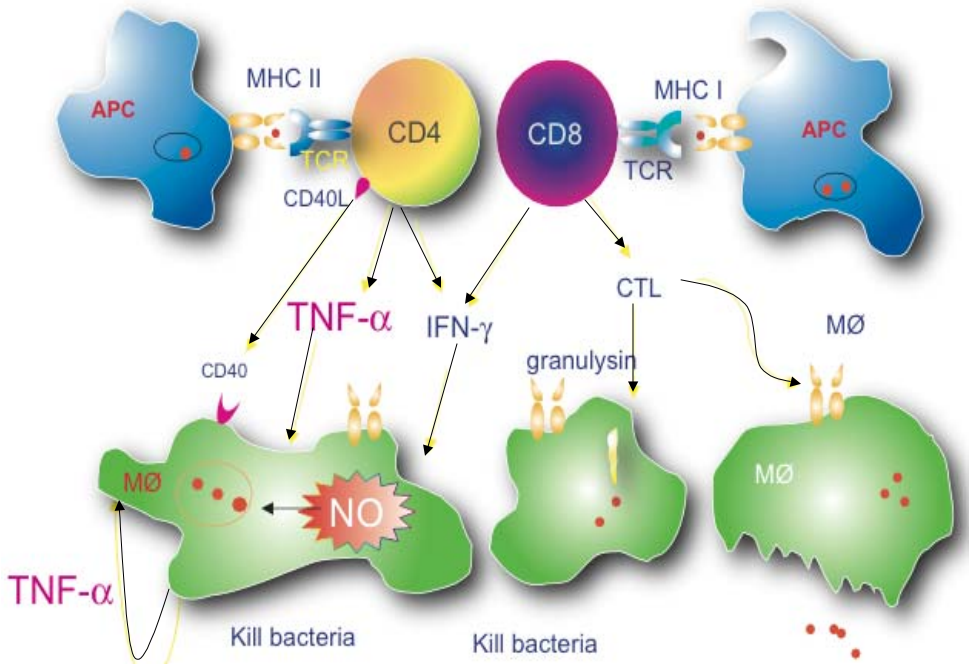

Figure 4. Cell mediated immune response to *M. tuberculosis*.

M. tuberculosis (red circles) infection of macrophages and dendritic cells (APC) leads to the presentation of antigen in the context of MHC-Class I and –Class II (MHC). Subsequently in the lymph nodes both CD4+ and CD8+ cells are primed and activated through ligation of their T cell receptors (TCR) interacting with MHC presenting *M. tuberculosis* antigens. These cells then migrate to the lungs where they are activated. They produce cytokines (IFN, TNF) and interact through macrophages (Mϕ) to initiate expression of reactive nitrogen intermediates (including NO), resulting in the killing of the bacillus. In addition CD8 lymphocytes act as cytotoxic T lymphocytes (CTL) by lysing the macrophages harboring the bacillus or by direct killing mechanisms, such as granulysin.

4.3 Cytokine mediated actions

It is evident that the communication between immune cells is not only through cell-cell interaction, but also through cytokine signaling. In this section, the roles of both pro-inflammatory and anti-inflammatory cytokines will be addressed in more detail.

It has been demonstrated both experimentally and clinically that IFNγ is an essential cytokine for the development of protective immunity against *M. tuberculosis* infection. IFNγ deficient mice (GKO) exhibit increased susceptibility to disease [**Table 1**,[64, 98]]. Infection of GKO mice led to florid bacterial growth and tissue destruction. Furthermore, patients with defective receptors for IFNγ and IL-12 are more susceptible to *M. tuberculosis* and other less

pathogenic mycobacteria [99]. GKO mice do generate antigen-specific T lymphocytes, but lack the ability to induce NOS2 in macrophages [100]. The cellular infiltrate in the lungs following aerogenic infection consisted of >50% granulocytes with many neutrophils and even eosinophils [100].

IL-12 is a key cytokine involved in differentiation of T cell responses and initiation of Th1 cytokine responses. The IL-12p70 molecule is a heterodimer, consisting of a p40 and p35 subunit acting through the IL-12R. IL-12 can also form a homodimer of p40 subunits that appears to act as an antagonist to IL-12p70. More recently the p40 subunit was found to have some IL-12 like activities. When IL-12p40-/- mice and IL-12p35-/- mice were infected with *M. tuberculosis*, p40-/- mice were more susceptible to disease than p35-/- mice (which were still more susceptible to disease than control, wild type mice) [**Table 1**,[67]]. The p35-/- mice were able to generate antigen specific responses. This finding indicates that the p40 subunit, which is also a subunit for IL-23, has functions that are independent of p35.

Another targeted cytokine deletion that leads to profound susceptibility in mice when infected with *M. tuberculosis* is disruption of the TNF gene or its p55 subunit receptor [101-103]. When infected via aerosol or intravenous routes, TNF deficient mice succumb to infection with a mean survival time of approximately 28 days. TNF deficient mice lack granuloma structure and have a large influx of neutrophils as the bacterial burdens increase. These mice are unable to activate macrophages and the production of NOS2 is reduced. Clearly, TNF's effects on tissue can be both beneficial and detrimental, and TNF's involvement in the host response is on many levels. The roles of TNF on the host response are described in more detail in chapter 1.

Recently, therapies have been developed that inhibit TNF signaling, in an effort to reduce inflammation during such chronic diseases as rheumatoid arthritis or Crohn's disease. Both a

humanized anti-TNF neutralizing antibody (Infliximab) and an antibody – TNF receptor fusion protein (Etanercept) have been implemented for this purpose. Unfortunately, use of these drugs increased the risk of reactivation of tuberculosis in latently infected (PPD+) individuals [104]. The incidence of tuberculosis was higher in patients prescribed Infliximab than Etanercept [105]. The stronger correlation between Infliximab and tuberculosis may be due the use of this treatment in Europe (where a higher percentage of the population has latent tuberculosis), or it may be a reflection of the different binding capability of the drugs. Infliximab strongly binds monomeric, trimeric and transmembrane forms of TNF, whereas Etanercept binds strongly to trimeric forms and weakly to monomeric and transmembrane forms of TNF. There is also evidence that Infliximab treatment induces drug-mediated apoptosis and monocytopenia.

The patient population receiving Infliximab treatment not only had a higher incidence of tuberculosis then the general population, but they also had a higher incidence of extrapulmonary and disseminated disease. Studies in our murine model of tuberculosis have recapitulated these findings [106]. Although the mechanisms underlying the TNF dependent control of acute and latent tuberculosis has not been clearly elucidated, TNF appears to modulate cell migration in the lungs. A major focus of this thesis is the role of TNF in chemokine expression and granuloma formation (described in Section 7.0 Chapter 1 TNF-alpha influences chemokine expression of macrophages in vitro and CD11b+ cells in vivo during *M. tuberculosis* infection, affecting cell migration and granuloma formation).

In addition to inflammatory cytokine production as a result of *M. tuberculosis* infection, expression of anti-inflammatory cytokines such as IL-10 or TGF-β increases in some infected populations of humans and mice. Expression of IL-10 can be detrimental depending on when it is expressed and how much is expressed. In the case of IL-10 transgenic mice, overexpression of

IL-10 can induce reactivation in chronically infected mice and can lead to increased susceptibility to acute infection with BCG [107, 108]. IL-10 -/- mice were reported to have increased resistance to mycobacterial infection with *M. avium* and BCG [109, 110]. However, in the case of *M. tuberculosis* infection, published results indicate that either there are no differences in control of bacterial growth or the differences are seen early after infection and over time the IL-10-/- mice have similar disease progression [Table 1,[65, 109]]. The interactive role of IL-10 and TNF in granuloma formation will be discussed in further detail in the appendix of this thesis (see Appendix A.0 IL-10 expression during aerosol *M. tuberculosis* infection is a result of increased bacterial burden and does not lead to immunosuppression).

4.4 Cytokines and cells involved in granuloma formation

Genetically engineered knockout mice have provided clues to the roles of immune cells in granuloma formation. CD4 T cell-deficient mice, which are susceptible to *M. tuberculosis* infection, experience a delay in the formation of the granulomas compared to wild type mice [7], and both disorganized and organized granulomas can be found in their lungs. Mice deficient in CD8 T cells also form granulomas in the lungs, but do not control infection as well as wild type mice [69, 111]. Interestingly, data generated using γδ T cell deficient (δ-/-) mice suggest that these T cells may play a role in granuloma formation [112]. The δ-/- mice had larger, more diffuse granulomas in the lungs following low dose aerosol infection, compared to wild type mice, but with high dose aerosol infection the δ-/- mice had a largely neutrophilic infiltrate. Severe combined immunodeficient (SCID) mice when infected with an avirulent *M. bovis* vaccine strain, BCG, do form epithelioid macrophage aggregates in the liver and spleen, but less so in the lung [113]. B-cell deficient mice have smaller, more diffuse granulomas than wild-type mice following aerosol infection, but successfully control infection in the lung [70, 96].

However, in the absence of B cells, the pathology of the lungs is altered significantly, and may point to a role for these cells in granuloma formation or maintenance, as discussed above. Interestingly, spread of the infection from the lungs to the spleen is reduced in B cell-deficient mice [70]. IFN-γ has been mentioned as being important in granuloma formation, however immune cells migrate to the lungs and aggregate to form granulomas in IFN-γ-/- mice following *M. tuberculosis* infection [64, 98]. Due to the lack of IFN-γ and subsequent poor macrophage activation, these granulomas do not function to control the infection, and quickly become necrotic. In murine models of infection where TNF is absent granuloma formation is substantially impaired, pointing to an important role for this cytokine in the signals that direct granuloma formation [101, 103]. This will be addressed to a greater extent later in the thesis.

5.0 Chemokines

Cellular trafficking and recirculation is a multi-step process including rolling, adhesion, and migration across endothelium into tissues [reviewed in [114]]. Once inside tissues, the cells continue to migrate through more locally directed mechanisms. These processes are directed by adhesin molecules, both integrins and selectins, and chemokines and chemokine receptors. Chemokines are small 8-10 kDa chemotactic cytokines, which bind to pertussis toxin-sensitive G-protein coupled receptors, inducing actin dependent processes such as membrane ruffling, pseudopod formation and assembly of adhesion complexes. Chemokines are a diverse class of molecules acting both as constitutive signals functioning to form secondary lymphoid tissues, and as inducible signals in response to physiological stress, such as inflammatory stimuli including infection.

The pattern of chemokine receptor expression dictates, to some extent, the localization of cells participating in the immune system. Many immune cells switch from constitutively expressed receptors to inflammatory receptors as a consequence of cell activation and polarization. For example, immature dendritic cells residing within tissues express CCR5 and CCR1[115]. Upon uptake of antigen and maturation, dendritic cells downregulate CCR5 and CCR1, and upregulate CXCR4 and CCR7, causing migration of these antigen presenting cells to the lymphoid tissues, such as lymph nodes, where they can encounter and prime naive T cells. The chemokines that bind to CXCR4 and CCR7, CXCL12 (SDF-1α/β), CCL19 (MIP3β) and CCL21 (SLC), are expressed primarily in lymphoid tissues [reviewed in [115]]. Naïve T lymphocytes express a different repertoire of receptors (CXCR4, CCR7) than activated T lymphocytes (CCR1, CCR2, CCR5 and CXCR3); the chemokine receptor profile influences where the cells reside or migrate within lymphoid or non-lymphoid tissue. Activated T cells will

generally migrate to sites of inflammation or infection rather than back into the lymphoid tissue. Memory cells also have different chemokine receptors, which likely play a role in where various subsets of memory cells reside following resolution of infection [116, 117].

Characterization of chemokine expression has been performed by conventional techniques such as RNA expression analysis to assess gene expression and ELISA to detect protein. Due to high homology between chemokines in many species, it has been difficult to develop useful monoclonal antibodies for studies, particularly in the murine model. Polyclonal antibodies exist, but very few monoclonal antibodies are available for flow cytometric analysis in murine models, limiting the studies that can be performed in situ or ex vivo. There is a larger collection of monoclonal antibodies available for human or nonhuman primate studies. Cell migration assays using transwell inserts or Bowden chambers have also allowed basic migration properties to be evaluated, but these systems are simplistic compared to the multi-factorial processes occurring in vivo, and cell lines, rather than primary cells from different tissues, are usually used for these studies.

The number of chemokines identified has been expanding at a rapid rate in the past few years. There appears to be redundancy in the expression of both chemokines and their receptors, since most receptors bind multiple chemokines, and specific chemokines can bind to more than one receptor. Often, more than one ligand for a chemokine receptor can be expressed at the site of infection, suggesting that both chemokines have a function, or that signals such as infection or inflammation induce a number of different chemokines. A particular chemokine receptor can be found on many different types of cells. For example, T lymphocytes, monocytes, macrophages, basophils and immature dendritic cells express CCR2 [118]. In addition, expression of inducible chemokines from a number of different cell types can be observed. Monocytes, endothelial cells,

epithelial cells, fibroblasts and keratinocytes can produce CXCL10, an IFN-γ-inducible chemokine [119]. The various signals for induction of chemokine production by different types of cells are still being determined. The true extent of redundancy in vivo, and the possible reasons for such apparent duplication of function, remains to be determined; it may simply be that our current understanding of the roles or induction of expression of each chemokine in a complex and interactive system is incomplete. However, results from CXCL9-/- mice, in which an IFN-γ inducible chemokine that recruits activated T cells via CXCR3 was not present, indicated that the absence of this chemokine had no discernible effect on control of a number of different bacterial and viral pathogens, despite the requirement for IFN-γ in control of these pathogens [120]. One can speculate that CXCR3 is not important for directing activated T cells to the site of infection, that another CXCR3 ligand [such as CXCL10 (IP-10)] is also expressed at the site of infection (which is often the case), or that other chemokine receptors can also direct activated T cells equally well to infected tissues. Surprising results from this same study were that CXCL9 was important for antibody responses to *Francisella tularensis*, and that activated B cells expressed CXCR3 [120]. Genetically engineered mouse models are likely to enlighten us about the roles these chemokines and receptors can play in induction of immune responses and control of infection.

The expression of chemokines is highly regulated. Studies are underway addressing signals required for post-transcriptional processing and secretion of the small molecular weight proteins. Several genes encoding chemokines are controlled by NF-κB, NF-IL6, activator protein 1 (AP-1) and Sp1 [reviewed in [121]]. Hydrogen peroxide (H_2O_2) not only gives rise to NF-kB signaling pathways, it also appears to production of mRNA encoding MIP1a and IL-8 in human cell lines [122]. In addition studies in the murine macrophage cell line B10R indicate

that H_2O_2 increases expression of CCL3, CCL4, CXCL2 and CCL2 [123]. H_2O_2 dependent induction of chemokines is dependent on both ERK and cAMP-dependent pathways. H_2O_2 dependent upregulation of CCL3, CCL4 and CXCL2 is at the level of gene transcription activation, but the expression of CCL2 is increased through both gene transcription activation and mRNA stabilization, indicating that there is differential post-transcriptional regulation of chemokines expression. Another type of post-transcriptional regulation that has been uncovered is regulation of the secretion of the chemokines. CCL5 secretion from memory T cells appears to be dependent on TCR stimulation [124]. These CD8+ memory T cells carry high levels of CCL5 mRNA but do not contain or secrete the protein unless the cells undergo TCR engagement.

5.1 Chemokines and *M. tuberculosis*

There have been a variety of studies aimed at characterizing expression of chemokines in response to *M. tuberculosis* in vitro and in vivo, in human and murine systems. However, synthesizing an understanding of cell infiltration and granuloma formation using results from these descriptive studies has proved difficult. This is in part due to lack of appropriate reagents for study, but also to the complexity of the system for migration of cells into tissues in response to infection. In addition chemokines also play roles in other activities of cells, such as induction of apoptosis or proliferation [reviewed in [114]]. Table 2 lists the major chemokines that will be discussed in this thesis (Table 2).

Table 2. Chemokine Nomenclature.

Systematic Name	Mouse Ligand	Receptor
CCL2	JE, MCP-1	CCR2
CCL3	MIP-1α	CCR1, CCR5
CCL4	MIP-1β	CCR5
CCL5	RANTES	CCR1, CCR3, CCR5
CCL7	MCP 3 (Human), MARC	CCR1, CCR2, CCR3
CCL8	MCP-2	CCR3
CCL11	Eotaxin	CCR3
CCL12	MCP-5	CCR2
CXCL1	GRO-α	CXCR2
CXCL2	MIP-2	CXCR2, CXCL1
CXCL8	IL-8	CXCR1, CXCR2
CXCL9	MIG	CXCR3
CXCL10	CRG-2, IP-10	CXCR3
CXCL11	I-TAC	CXCR3

5.2 Induction of chemokine expression by *M. tuberculosis*

M. tuberculosis is a strong inducer of chemokine expression. Studies to date have primarily focused on the pattern of expression of inducible chemokines following *M. tuberculosis* infection of macrophages in vitro. *M. tuberculosis* induces a rapid expression of many chemokines in murine macrophages, detectable as early as 2 hours post infection. In vitro, expression usually peaks 12 to 30 hours post-infection [125]. Human macrophages produced

chemokines CCL2, CCL3, CCL4, and CCL5 in response to virulent strains of *M. tuberculosis* [126, 127]. Responses were attenuated with infection using an avirulent strain of *M. tuberculosis* (H37Ra) for CCL3, but not CCL4 or CCL5 [127], indicating that the PAMPs or antigens that stimulate the production of these chemokines may be different. Lymph node tissue and CD14+ blood monocytes isolated from tuberculosis patients expressed more CCL2 than those from control subjects [128]. In addition human alveolar macrophages produced significantly more CCL3, CCL2 and CCL5 than blood monocytes upon infection with *M. tuberculosis* [126]**.** These results suggest that the chemokines interacting with CCR1, CCR2, and CCR5 might play a role in the trafficking of cells bearing these receptors to the site of infection. However, direct evidence for such a role for all these chemokines in tuberculosis remains elusive.

Expression of CCL2, CCL3, CCL7, CCL12, CXCL2, and CXCL10 in response to *M. tuberculosis* infection of mice has been reported [62, 63, 125]. CCL4, CCL5, and CXCL9 are also expressed by murine macrophages following infection with virulent Erdman strain of *M. tuberculosis* (see Section 7.0). These results support that *M. tuberculosis* is a strong inducer of chemokines. The cell wall components of mycobacteria may be crucial to this induction, as it was reported that infection of murine macrophages with delipidated *M. tuberculosis* strain Erdman significantly reduced production of CCL3 [129]. In addition, different strains of *M. tuberculosis* can induce different levels of chemokines in the tissues of infected mice[125], although in this study, the control of infection was similar for the strains tested.

Macrophages are not the only cells in the lungs responding to *M. tuberculosis* by producing chemokines. Expression of CXCL8 and CCL2 mRNA, but not CCL3, CCL4, or CCL5 was detected in human alveolar epithelial cell line A549 in response to virulent strains of *M. tuberculosis* [128]. *M. avium* and heat-killed *M. tuberculosis* could not elicit the same

responses in these cells. Murine pleural mesothelial cells stimulated with BCG and rIFNγ induced CCL4 and CCL2 expression in a dose dependent manner [130]. This production could be inhibited by IL-4. Granulocytes from the blood of patients with active tuberculosis produced CXCL8 and CXCL1 in response to LAM from *M. tuberculosis*. Human bronchial epithelial cells produce the CXCR3 ligands (CXCL9, 10 and 11) [131] and this expression is upregulated by IFN-γ. CXCL10 was expressed at higher levels in the bronchial epithelium of tuberculosis patients, compared to control subjects [132]. These studies imply that cells other than macrophages or monocytes participate in recruiting cells by producing chemokines in response to mycobacteria.

The expression of chemokines in vivo has been characterized to a limited degree. Studies performed using bronchoalveolar lavage (BAL) fluid indicate that there are elevated levels of CCL2, CCL5, CCL7, CCL12, CXCL8 and CXCL10 in tuberculosis patients compared to uninfected controls [126, 133, 134]. Increased expression of CCL5 correlated with higher numbers of cells in BAL fluid [134]. Although the production of many chemokines has not been examined, CCL11 (Eotaxin) [133] and CCL3 [126] were not detected in human BAL fluid.

With the emergence of HIV/*M. tuberculosis* co-infection, a number of studies have addressed the ability of *M. tuberculosis* to enhance HIV infection. PBMC from HIV+ patients with tuberculosis produced more HIV than those from patients without tuberculosis, even with similar numbers of CD4+ lymphocytes [135]. The increase of CCR5 and CXCR4 (HIV co-receptors) expression on monocytes in response to *M. tuberculosis* was hypothesized to result in increased productivity of HIV infection. Stimulation of whole blood with *M. tuberculosis* LAM upregulated expression of CCR5 and CXCR4 [136]. In addition, HIV infection reduced

production of CCL3 and CCL5 from PBMC [135], freeing up more receptors for HIV to bind and possibly interfering with recruitment of cells to fight infection.

5.3 Difficulties in studying chemokines and infectious disease

The *M. tuberculosis* infection studies performed on genetically engineered mice suggest that redundancy in the chemokine system may be real. In CCR2-/- mice the number of macrophages migrating to the lung after 3 weeks of infection increased significantly compared to two weeks post-infection. At the 3 week time point, a number of chemokines are expressed in response to both higher *M. tuberculosis* burden and expression of inflammatory cytokines. At this time, other chemokines signaling through CCR1 or CCR5 (or other receptors) may stimulate the migration of monocytes to the lungs. In the absence of CCR2 or CCR5, many immune cells still migrate to the lungs and form granulomas [62, 63], and data not shown). These results may indicate that these receptors are not essential for migration of cells to the lungs or within the lungs (e.g., for granuloma formation), or that other signals and interactions with adhesins may be more important. The breadth of the chemokine response induced following *M. tuberculosis* makes it difficult to pinpoint which subset is important at which time during infection.

Many cytokines and infectious disease products regulate chemokines. There is evidence that IFN-γ, TNF and *M. tuberculosis* itself induces expression of chemokines in vitro and in vivo. In models of infection when bacterial burdens are different (such as when comparing immunodeficient mice with wild type mice), drawing conclusions about chemokine expression can be very difficult. Higher expression of chemokines could be due to increased numbers of *M. tuberculosis* bacilli, instead of resulting from a specific immunodeficiency (for example, in a cytokine knockout mouse). Alternatively, higher chemokine levels could alter the anti-mycobacterial response, resulting in higher bacterial burdens.

Interpreting differential chemokine expression in *M. tuberculosis* infection, particularly in vivo, is challenging. Because chemokines act in a gradient, higher chemokine expression does not necessarily mean that more cells will migrate in response to that signal. Too much chemokine can saturate a receptor and desensitize the cell to the migration signal. Specifically with studies on chemokines in *M. tuberculosis* infection, the expression of chemokines is likely very different within the granuloma compared to the whole lung, if chemokines participate in the formation and maintenance of the granuloma. Indeed, in our studies designed to procure pure granulomatous tissues for the analysis of host gene expression using an approach that incorporates laser capture microdissection and real-time PCR technology, results showed that the relative levels of expression of certain immunologic genes (including chemokines and chemokine receptor genes) determined using microdissected tissue-derived RNA may differ significantly from that obtained when total lung RNA was used for analysis [137]. These data suggest the conventional use of whole infected lungs to study granuloma-specific gene expression can yield data that may not genuinely reflect intra-lesional events. In addition, BAL fluid as a source of cells or chemokines is unlikely to reflect the site of infection within the lungs. Therefore, such studies need to be interpreted cautiously.

6.0 Statement of the problem

The goal of this study was to address the hypothesis that TNF influences chemokine expression in the lung during tuberculosis, thereby playing a major role in orchestrating granuloma formation. The signals required for the complex process of granuloma formation in response to *M. tuberculosis* infection are not well understood, although this structure is important in containing the infection in the tissues. Although tumor necrosis factor–alpha (TNF) is required for control of *M. tuberculosis*, the mechanisms underlying its requirement have not been well defined. In models of chronic or latent tuberculosis, TNF was required for maintenance of macrophage activation, granuloma formation and ultimately, control of disease. One mechanism of TNF control could be its regulation of chemokine expression. Chemokines, or chemotactic cytokines, are compelling candidates for influencing cell migration and granuloma formation in tuberculosis. As part of our work on TNF and granuloma formation, we characterized chemokine expression in the lungs following *M. tuberculosis* infection and evaluated the immune response and granuloma formation in the absence of select groups of chemokines or chemokine receptors.

7.0 Chapter 1 TNF-alpha influences chemokine expression of macrophages in vitro and CD11b+ cells in vivo during *M. tuberculosis* infection, affecting cell migration and granuloma formation

This chapter has been submitted to Journal of Immunology. The chapter in this form is more inclusive that the submitted paper and includes additional data that was not shown in the submitted paper.

7.1 Introduction

Tuberculosis in immunocompromised hosts elucidated the protective immune responses to *M. tuberculosis*. In recent years, the use of anti-inflammatory drugs targeting tumor necrosis factor alpha (TNF), such as Infliximab (Remicade) and Enbrel (Etanercept), for treatment of chronic inflammatory diseases, has highlighted the importance of TNF in controlling *M. tuberculosis*, since there is an increased risk of reactivation tuberculosis in patients treated with these drugs [104, 105].

TNF has many potential effects within the lungs of an infected individual. In vitro, TNF has been reported to affect apoptosis of infected macrophages [138, 139], secondary signaling to macrophages for nitric oxide production [reviewed in [140]], and regulate activity of other inflammatory cytokines (such as IL-12) [141]. In vivo, pathology, control of bacterial numbers, and chemokine expression (in the liver) have been shown to be affected by TNF [142]. The role of TNF within the lungs in chemokine expression following *M. tuberculosis* infection has not been explored.

Antibody mediated neutralization of TNF in chronically infected mice led to severe pathology with the loss of granuloma structure [106]. Bacterial loads in the TNF-neutralized, chronically infected mice increased initially, but stabilized at a level below that generally considered fatal in C57BL/6 mice. Nonetheless, TNF-neutralized mice succumbed quickly. Granuloma structural deficiencies and uncontrolled infection in mice lacking TNF have been reported by our group and others, in both acute and chronic infection [101, 103, 106, 142],

however the mechanisms by which TNF controls granuloma development and maintenance have yet to be elucidated. Studies in the liver of *M. smegmatis and M. tuberculosis* intravenously infected mice showed that gene expression of a subset of chemokines was reduced in TNF deficient mice [143], but these studies do not reveal the localized chemokine expression patterns in the lungs- the primary site of *M. tuberculosis* infection and control.

We hypothesized that TNF influences macrophage chemokine expression and these localized differences in expression lead to changes in granuloma formation. Our results described here demonstrate for the first time that TNF affects chemokine gene and protein expression by *M. tuberculosis*-infected macrophages, both in vivo and in vitro. We also demonstrate that during the early phases of acute infection TNF deficient mice have similar numbers and types of immune cells migrating to the lungs, indicating that the lack of granuloma formation is a result of a migration defect within the lung tissue, rather than a defect in the migration of cells to the lungs. These data support that TNF affects the expression of many chemokines at the level of macrophage gene expression, suggesting that differences in localized chemokine gradients may result in disorganized cellular infiltrate within the lungs.

7.2 Materials and Methods

Animals. C57BL/6 female mice (Charles River, Rockland, Mass.) and TNFRp55-/- (breeding pairs from Dr. Tak Mak, [144] 8-14 weeks old were used in all experiments. TNFRp55-/- mice were bred in an SPF facility at the University of Pittsburgh and transferred to the Biosafety Level 3 animal facility at 7-8 weeks of age. All infected mice were maintained in the BSL3 animal laboratories and routinely monitored for murine pathogens by means of serological and histological examinations. The University Institutional Animal Care and Use Committee approved all animal protocols employed in this study.

Chemicals, antibodies and reagents. All chemicals were purchased from Sigma Chemical Co. (St. Louis, MO.) unless otherwise noted. Middlebrook 7H9 liquid medium and 7H10 agar were obtained from Difco Laboratories (Detroit, MI). Antibodies used in flow cytometric analyses were obtained from Pharmingen (San Diego, CA). The cell lines, MP6XT-22 (anti-TNF) and was obtained from DNAX and used to generate ascites (Harlan Bioproducts, Indianapolis,IN). Antibodies were purified endotoxin free from ascites fluid as previously described [106] and mice were treated with antibody intravenously every three days (0.5mg/dose) starting 4 months post infection. Control mice received normal rat IgG (Jackson Immunoresearch Laboratories Inc.,West Grove, PA) with the same dosing regiment.

Mycobacteria and infection of mice. To prepare bacterial stock, *M. tuberculosis* strain Erdman (Trudeau Institute, Saranac Lake, N.Y.) was used to infect mice, and then bacteria were harvested from their lungs, expanded in 7H9 liquid medium and stored in aliquots at -80◦C. Mice were infected via the aerosol route using a nose-only exposure unit (InTox Products, Albuquerque, N.M.), and exposed to *M. tuberculosis* (1×10^7 CFU/ml in the nebulizer chamber) for 20 minutes, followed by 5 minutes of air. This resulted in reproducible delivery of 50-100 viable CFU of *M. tuberculosis* as described previously [94], which was confirmed by CFU determination on the lungs of 2-3 mice 1 day post-infection. In acute experiments where a higher inoculum was used, the concentration of *M. tuberculosis* in the nebulizer was increased, and day 1 CFU were determined in the lungs. The tissue bacillary load was quantified by plating serial dilutions of the lung, liver, and spleen homogenates onto 7H10 agar as described previously [30].

Bone marrow derived macrophages. Macrophages were derived from C57Bl/6 bone marrow based on adherence. The mice were euthanized and bone marrow was flushed out of the femur

and tibia bones with DMEM as previously described [82]. The bone marrow suspension was washed twice with 2% FBS in PBS and the cells were counted. $2x10^6$ cells were plated on non-tissue culture treated petri dishes (Labtek) in 25 ml macrophage media (25% L cell supernatant, 20% FBS, 1% L-glutamine, 1% sodium pyruvate, and 1% nonessential amino acids). After 4 days in culture the cells were fed with 10 ml fresh macrophage media. On day 6 macrophages were infected with *M. tuberculosis* (MOI of 4). Four hours post infection the supernatant was removed, cells were washed and fresh media was added.

Flow cytometric analysis of lung cells. To determine cellular infiltrate in the lung, at 10-day intervals lungs were removed for flow cytometric analysis. Lungs were subjected to a short period (20 minutes) of digestion with 1 mg/ml collagenase A and 25 Units/ml DNAse (both from Boehringer Mannheim, Mannheim, Germany) at 37°C. The suspension was pushed through a cell strainer as previously described [63]. Red blood cells were lysed with red blood cell lysis buffer (NH_4Cl/Tris Solution) and the single cell suspension was counted. The samples were stained with 0.2 μg anti-CD4, anti-CD8, anti-CD69, or 0.15 μg anti-Gr1 and 0.2 μg anti-CD11b in FACS buffer (0.1% NaAzide, 0.1% BSA, 20% mouse serum). Following washes, the cells were fixed in 4% PFA for 1 hour and collected on a FACS Caliber (Beckon Dickinson). Analysis was performed on Cell Quest software (BD-Pharmingen, San Diego, CA).

Histopathology. Tissue samples for histological studies were fixed in 10% normal buffered formalin followed by paraffin embedment. For histopathological studies 5- to 6- μm sections were stained with Harris' hematoxylin and eosin.

Ex vivo CD11b+ isolation. To isolate CD11b+ cells from the lungs of C57Bl/6 mice, a Magnetic Cell Sorting (MACS) column isolation protocol (Miltenyi Biotech, Auburn, CA) was followed. The lungs were removed, rinsed in T cell media and pushed through a 70μm cell

strainer (Fisher, Pittsburgh, PA) using the end of a 5 ml syringe. Following red blood cell lysis and washing, the cells were labeled with CD11b Microbeads in MACs buffer (2mM EDTA and 0.5% SDS in PBS) for 15 minutes at 8°C. The cells were washed with MACS buffer and then resuspended in 0.5ml of buffer. The cells were poured over a 40μm cell strainer and then applied to a prewashed MS+ column. After initial flow through, the column was washed 3 times with 0.5ml buffer. The column was then removed from the magnet and the CD11b+ cells were eluted from the column with 1 ml of buffer. The cells were spun down and resuspended in 1ml of TRIZOL and the RNA was isolated.

RNA Isolation. RNA was isolated from the lung or cells using the TRIZOL isolation protocol with slight modifications. The lung was homogenized in 3ml (cells were lysed in 1ml TRIZOL/ $2x10^6$ cells) of TRIZOL reagent and then two chloroform extractions were performed. Following an isopropanol precipitation, the RNA was washed with 70% ethanol and treated with RNase Inhibitor (Applied Biosystems, Foster City, CA) for 45 minutes. Following complete resuspension of the RNA at 65° C for 15 minutes the RNA was cleaned and DNase digested using the Qiagen RNA isolation kit, as directed by the manufacturer (Qiagen Inc., Valencia, CA).

RNA expression of chemokines in lung granulomas isolated by Laser Capture Microdissection

Histologically distinct cell populations were procured for subsequent gene expression analysis in a precise and reliable manner using the Laser Capture Microdissection (LCM) [145]. Lung tissue for LCM was fixed in 10% normal buffered-formalin for 8 hours at room temperature, transferred to 70% ethanol overnight at 4ºC and paraffin-embedded the next day. Tissue sections (8 μm) were de-paraffinized, rehydrated, stained and dehydrated by serially immersion in xylene, 100% ethanol, 95% ethanol, 70% ethanol, Mayer's hematoxylin (Sigma, St. Louis, MO), eosin

(Sigma, St. Louis, MO), 70% ethanol, 95% ethanol, 100% ethanol, xylene and then placed in a vacuum oven with dessicant for 15 minutes. Using the Pix-Cell II (Arcturus, Mountain View, CA), cells from microscopically visualized granulomas were transferred onto a thermoplastic cap via laser beam (30 μm beam at 40mW power). Four to six tissue sections were used for LCM per animal to yield approximately one to two caps full of tissue. RNA extraction was performed using Proteinase K and Trizol (Invitrogen, Carlsbad, CA) by methods previously described [137]. The RNA pellet was further purified with a RNAse free DNAse kit (Qiagen, Valencia, CA) using the manufacturer's instructions. RNA samples were stored at -80ºC until cDNA synthesis.

Real time RT-PCR. The RNA was reverse transcribed using Superscript II enzyme, as directed by the manufacturer (Invitrogen, Carlsbad, CA). For Real time RT-PCR we used the comparative Ct method [146]. HPRT served as the endogenous control, and uninfected lung or macrophages as the calibrator. Each primer and probe set was tested for efficiency (results efficient >97% for all primer/probe sets). All samples were run in triplicate and with "no reverse transcriptase" controls on an ABI Prism Sequence Detector 7700. Relative gene expression was calculated as 2 ^-ΔΔCt, where ΔCt = Ct (gene of interest)- Ct (endogenous control) and the ΔΔCt= ΔCt (sample) - ΔCt (calibrator). Results are expressed as relative gene expression to uninfected samples. The primer and probe concentrations were used as suggested by Applied Biosystems (Foster City, CA) with the final concentration of each primer at 400nM and probe at 250nM. The primers (Gibco BRL, Grand Island, NY) and probes (Applied Biosystems) used in this assay were designed using Applied Biosystems Primer Express Software and the sequences are in Table 3.

Table 3. Primers and Probes used in the Taqman Real time RT-PCR assay.

Primers are probes were designed using the Primer Express Software. Sequences used for primer and probe synthesis are found in the table.

Gene	Forward Primer (5' to 3')	Reverse Primer (5' to 3')	Taqman Probe (5' 6-FAM, 3' TAMRA labeled)
CXCL9	TGG AGC AGT GTG GAG TTC GA	TCG GCT GGT GCT GAT GC	CCC TAG TGA TAA GGA ATG CAC GAT GCT CC
CXCL10	AGA GCA GCA CTT GGG TTC	ACG GCA GCA CTT GGG TTC	CGG AAG CCT CCC CAT CAG CAC C
CXCL11	GGG CGC TGT CTT TGC ATC	AAG CTT TCT CGA TCT CTG CCA T	CCC CGG GAT GAA AGC CGT CAA
CCL2	CTT CCT CCA CCA CCA TGC A	CCA GCC GGC AAC TGT GA	CCC TGT CAT GCT TCT GGG CCT GC
CCL3	ACC AAG TCT TCT CAG CGC CAT	TTC CGG CTG TAG GAG AAG CA	TGG AGC TGA CAC CCC GAC TGC C
CCL4	CCC GAG CAA CAC CAT GAA G	AGA AGG CAG CCA CGA GCA	TCT GCG TGT CTG CCC TCT CTC TCC TC
CCL5	CTG CAG CCG CCC TCT G	GAC TGC AAG ATT GGA GCA CTT G	CTC CCT GCT CGT TTG CCT ACC TCT CC
CCL12	GGA GGA TCA CAA GCA GCC AGT	TCA GCA CAG ATC TCC TTA TCC AGT AT	TCC CCG GGA AGC TGT GAT CTT CAG
HPRT	TTA CCT CAC TGC TTT CCG GAG	AAA AGC GGT CTG AGG AGG AAG	TAG CAC CTC CTC CGC C
TNF	TGA TCC GAG ACG TGG AA	ACC GCC TGG AGT TCT GGA A	TGG CAG AAG AGG CAC TCC CCC AA

Protein Determination.

Immunoassay. The quantity of CXCL9 and CXCL10 in the macrophage culture supernatants was determined with the Quantikine mouse CXCL9 and CXCL10 immunoassays (R&D Systems, Minneapolis, MN). These kits were used exactly as suggested by the manufacturer. The readout was performed using the *Emax* precision microplate reader (Molecular Devices, Sunnydale, CA).

SearchLight Proteome Arrays. To determine the protein concentration of TNF, IL-10, CCL2, CCL3, CCL5, CCL12, CXCL2, a multiplex sample testing service was utilized. Supernatants from uninfected and infected macrophages were filter sterilized and sent to Pierce Biotechnology (Boston, MA) for quantitative measurement using multiplexed sandwich ELISAs.

In situ hybridization.

Cloning. The pGEM-T Easy Vector System (Promega, Madison, WI) was used to clone CCL5, CXCL9, and CXCL10 PCR products. Primers were designed to amplify CCL5, CXCL9 and

CXCL10 with restriction enzyme sites specific for the pGEM-T vector cloning sites. These primers were used to amplify murine cDNA using the Applied Biosystems Thermocycler. Following amplification, the product was purified using QIAquick Nucleotide Removal Kit (Qiagen, Valencia, CA). The ends were digested and the product was ligated to prepared pGEM-T vectors. Competent *E. coli* (JM109) was transformed with the ligation reactions, using the suggested protocol (Promega). Transformed bacteria were selected based on resistance to ampicillin and interruption of the LacZ promoter, and the selected colonies were grown up in LB+AMP liquid media. The plasmid DNA was purified from this culture by the Qiagen Midiprep protocol (Qiagen). Following verification of the insert, the plasmids were linearized and used to generate probes.

Probe generation. Labeled RNA probes were synthesized by in vitro transcription of DNA cloned downstream of T7 or SP6 RNA polymerase in the pGEM-T vector using ^{35}S-UTP as substrate. The MAXIscript In vitro Transcription Kit (Ambion, Austin, TX) was used for this protocol, with slight modification. In short, linearized plasmid was incubated with the reaction mix (buffer, dATP, dCTP, dGTP ^{35}S-UTP)+ either T7 or SP6 polymerase. The reaction was incubated at 37°C for 3 h, 1µl DNase was added for an additional 20 minutes at 37°C. Following a 5 minute incubation at 65°C, the probes were brought up to 50µl and purified using the 'mini Quick Spin RNA Column' as directed by the manufacturer (Roche, Indianapolis, IN). Probes were stored at -80°C.

Tissue and slide preparation. Lungs were fixed in 4% paraformaldehyde at 40°C for 5 hours, washed in two overnight incubations of PBS followed by treatment in a sucrose gradient and then snap frozen and stored at -80°C. 14µm cryosections were cut and the slides were post fixed in 4% paraformaldehyde for 20 minutes, dehydrated in an ethanol gradient (70% EtOH 20

minutes, 80% EtOH 5 minutes, then 95% EtOH 5 minutes). After air drying the slides, antigen retrieval was performed in 0.01M sodium citrate with warming in the microwave. After the slides were cooled, the tissues were acetylated twice in 0.25% acetic anhydride- 0.1M Triethanolamine solution. Following treatment in another EtOH dehydration gradient, the slides were air dried and ready for hybridization.

Hybridization and washes. Tissue was hybridized to the ^{35}S-labelled probes as previously described [147]. In short, $5x10^4$ cpm/μl sense or anti sense probe was hybridized to the tissue under siliconized coverslips ($5x10^4$ cpm/μl sense or anti sense probe in 1x hybridization buffer containing 10% dextran sulfate formamide, 0.6M NaCl, yeast tRNA [100μg/ml], and 0.4M DTT) overnight at 50°C. Coverslips were removed and slides were washed in a series of SSC buffers: 5XSSC+0.1mM DDT 42°C for 30 minutes; 2XSSC/50% formamide+0.1mM DTT 60°C for 20 minutes; ribowash solution (0.1M Tris, 0.05M EDTA, 0.4M NaCl) 37°C for 10 minutes; ribowash solution at 37°C for 10 minutes; ribowash solution+ 6.25U of an RNAse A+T1 mix 37°C for 30 minutes; ribowash solution 37°C for 10 minutes; 2xSSC 37°C for 10 minutes; 0.2XSSC 37°C for 10 minutes. Slides were then dehydrated in 0.3M ammonium acetate+ EtOH gradient. After the slides were completely dried, they were dipped in prewarmed radiography emulsion (Kodak) and dried. Slides were wrapped in a dark box for one week. Development was in D19 developer followed by fixation in Rapid Fix. Slides were counterstained in hematoxylin.

Statistical Analysis. 3-4 mice per group per time point were used for all studies. Statistical analysis was performed on the data utilizing Prism Software for an unpaired t-test. For bacterial numbers and cell numbers, log transformation was performed prior to statistical analysis to normalize the data. P values <0.05 were considered significant.

7.3 Results

Susceptibility to tuberculosis without TNF

It is well established that mice deficient in TNF have increased susceptibility to *M. tuberculosis* infection [reviewed in [6]]. Following acute low dose aerosol infection, TNFRp55-/- mice and TNF- neutralized mice (MP6-XT22 treated) had significantly higher bacterial burdens than control mice by 18-21 days post infection (Figure 5A and data not shown). The mice succumbed by 28 days post infection.

Following TNF neutralization of chronically infected mice, the bacterial burden increased by 8 days post antibody treatment (Figure 5B), but was not significantly different until 18 days post antibody treatment. We previously reported that the mean survival time for chronically infected TNF-neutralized mice was 44 days, when infection was initiated by intravenous infection with moderate doses of *M. tuberculosis* [106]. However, using low dose inoculum delivered via aerosol to set up the chronic infection, neutralization of TNF resulted in faster progression of disease with a mean survival time of 22 days after initiation of antibody treatment (Figure 5C). In the following experiments, we analyzed the effects of TNF deficiency in acute and chronic models of infection, using aerosol delivery for all studies.

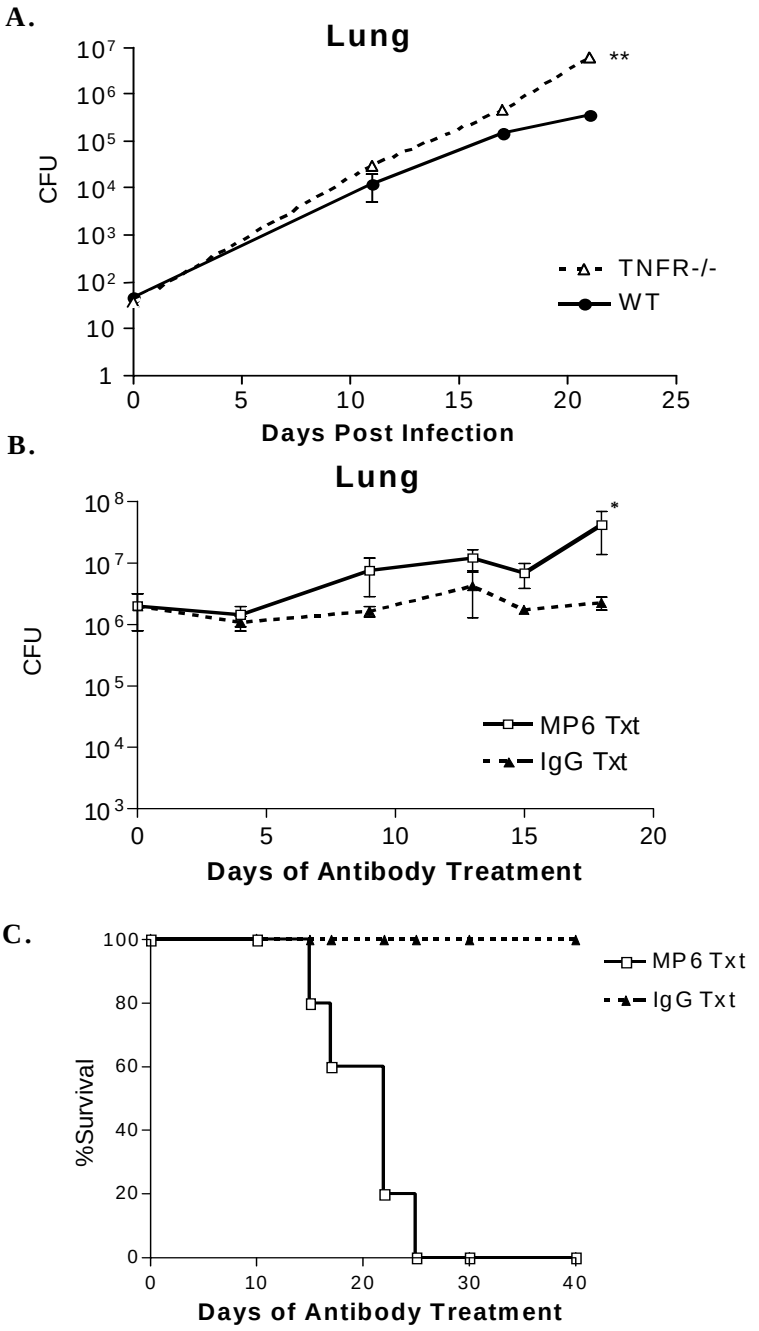

Figure 5. Deficiencies in TNF signaling led to rapid disease progression.

A. Serial dilutions of lung homogenates were plated throughout infection to determine the colony forming units. Colony forming units of TNFRp55-/- mice (open triangles) were significantly higher than wild type mice (closed circles) by day 21 post aerosol infection (**p=0.021). B. MP6-XT22 treatment of C57BL/6 wild type mice 4 months post infection led to an increase in bacterial numbers in the lungs (* p=0.04). MP6XT-22 treated mice: open squares, IgG treated mice: closed triangles. C. MP6XT-22 treatment led to rapid reactivation of disease and mice began to succumb to infection only 15 days after anti-TNF Ab treatment. The mean survival time for MP6XT-22 treated mice (when treatment began 4 months post aerosol infection) was 22 days. Each time point represents the mean of 4 mice. The graphs shown are representative of data from 1 of 4 independent experiments.

Cell infiltration during acute infection

During acute mycobacterial infections TNF deficient mice do not form proper granulomas [101-103]. The cell populations migrating into the lungs were assessed by flow cytometry. No defects in appearance of T lymphocytes and macrophages in the lungs early after infection were observed in TNF deficient mice compared to controls (Figure 7). By 21 days post infection, when bacterial burdens were already significantly higher in TNFRp55-/- mice, the number of CD8+ T lymphocytes was reduced and the number of neutrophils was significantly higher. The increased neutrophilic infiltrate was likely a result of the increased mycobacterial burden in these mice.

Histological analysis of the lung infiltrate indicated that although the cells were migrating into the lungs, they were not forming an organized granuloma structure, as previously reported [[101, 103], and Figure 6]. These data indicate that TNF is not required for migration of cells into the lung following infection, but rather may influence migration within the lung.

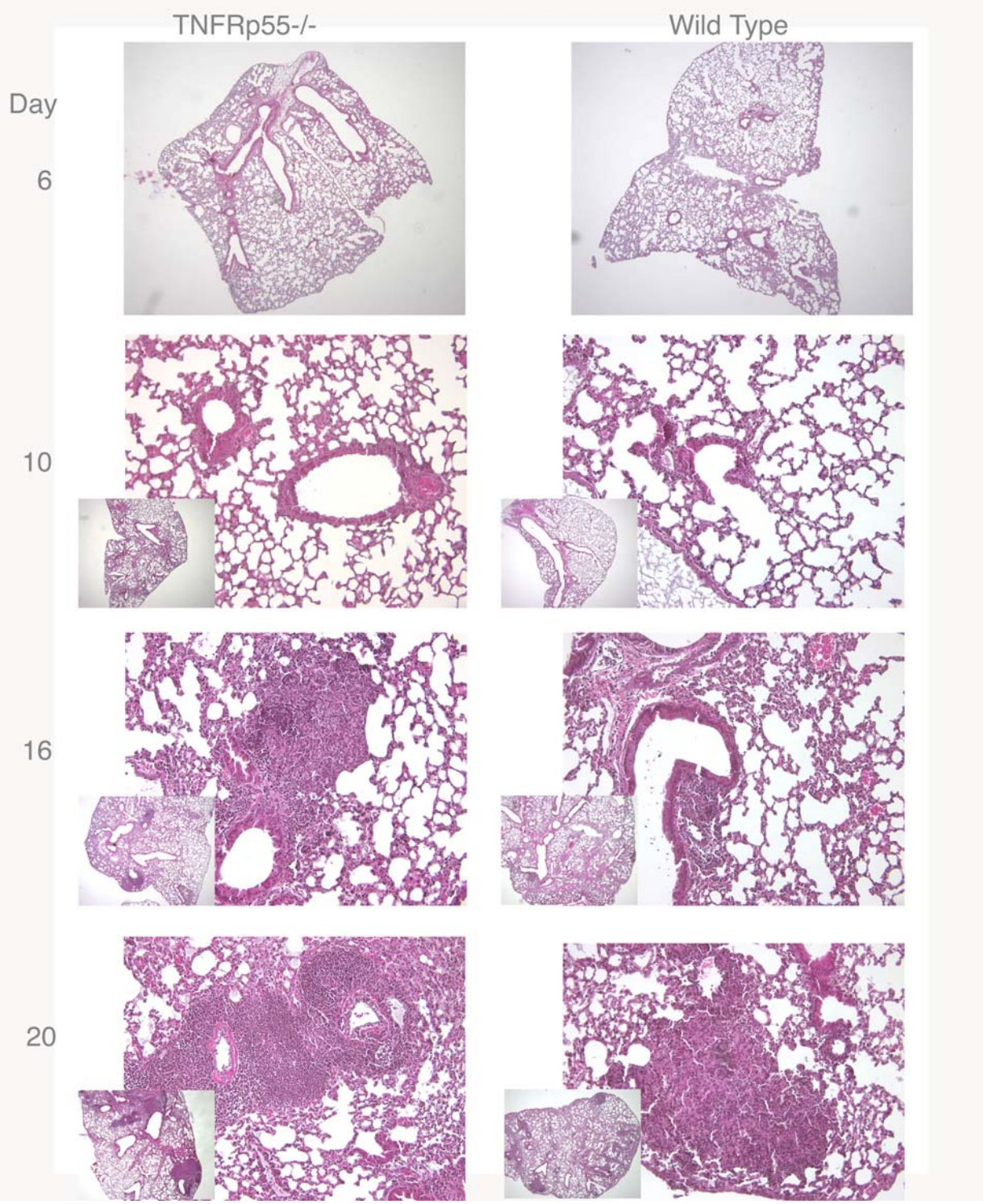

Figure 6. Lung pathology in *M. tuberculosis* infected TNFRp55-/- mice and wild type mice.

Following low dose aerosol infection, mice were sacrificed at indicated time points and a lobe of their lung was fixed in 10% formalin and then embedded, sectioned and H & E stained. TNFRp55-/- mice do have cellular migration into the lungs, but the cellular infiltrates are not organized and have higher granulocyte numbers by 20 days post infection.

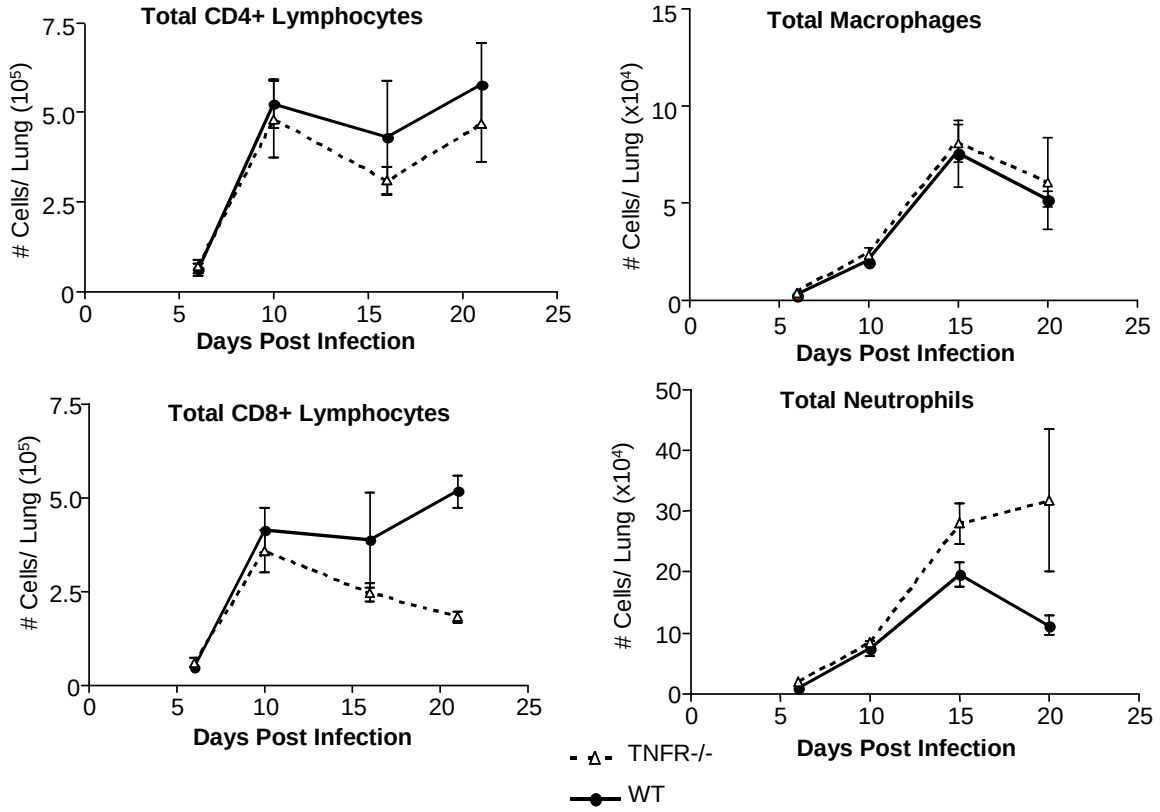

Figure 7. Immune cells migrate into the lungs in TNFRp55-/- mice.

Flow cytometric analysis of the lung was used to quantify the numbers of CD4+ and CD8+ lymphocytes, macrophages (CD11b+ Gr1-) and neutrophils (CD11b+ Gr1+) present in the lungs post aerosol infection. There were similar numbers of CD4+ lymphocytes and CD8+ lymphocytes in the lungs up to 16 days post infection. At 21 days post infection the number of CD8+ lymphocytes decreased. The number of macrophages migrating into the lungs of the TNFRp55-/- mice was similar to WT mice throughout the length of the experiment. The number of neutrophils increased in the TNFRp55-/- mice when bacterial burdens increased. Each time point represents 3-4 mice. These graphs are representative of 3 independent experiments.

Cell populations in the lung following anti-TNF treatment in chronically infected mice

The cell populations in the lungs of anti-TNF Ab treated and IgG control mice were not significantly different until the bacterial burdens significantly increased in the anti-TNF Ab-treated mice (Figure 8). There was variability among the mice during the chronic stage of infection (see error bars for day 0 time points, Figure 8), and mice in the TNF-neutralized group

succumbed to reactivation over the course of 10 days, beginning at day 12. Histological changes in the granuloma structure were observed as early as 9 days post anti-TNF Ab treatment (representative sections at 12 days shown in Figure 9). By 18 days of antibody treatment all surviving anti-TNF treated mice had diffuse cellular infiltrates in their lungs accompanied by edema within alveolar spaces.

These data indicate that TNF plays either a direct or indirect role in controlling migration of immune cells within the lungs and maintaining granuloma structure. A possible mechanism for control of migration of cells is through effects on chemokine expression.

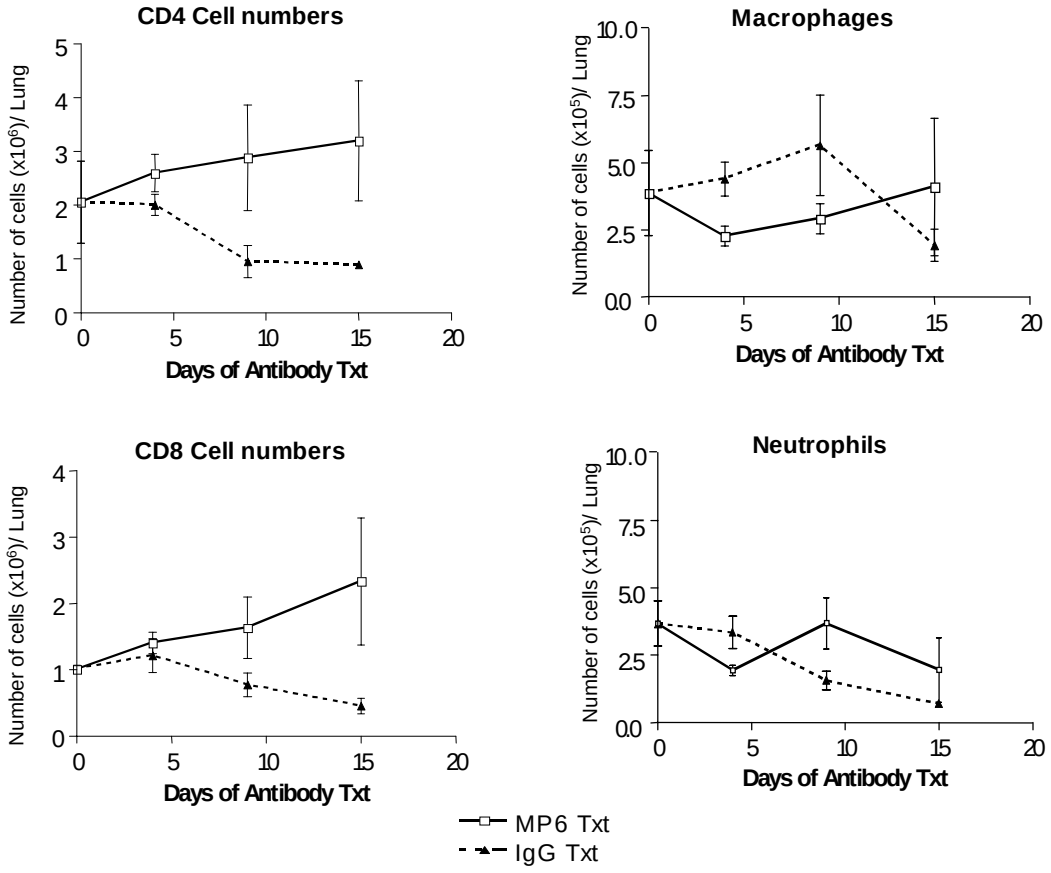

Figure 8. As bacterial burdens increased in MP6XT-22 treated mice, the numbers of cells migrating into the lung increased significantly.

MP6XT22 treatment began 4 months post aerosol infection. Following the initiation of MP6XT22 treatment, flow cytometric analysis of cellular infiltrate to the lungs revealed that as disease progressed the numbers of CD4+ and

CD8+ lymphocytes and macrophages increased, but the numbers of these cells in the IgG treated mice were stable. The number of neutrophils in the lungs of MP6 and IgG treated mice did not significantly change after antibody treatment began. Each time point represents 4 mice/group. This experiment was repeated twice with similar results.

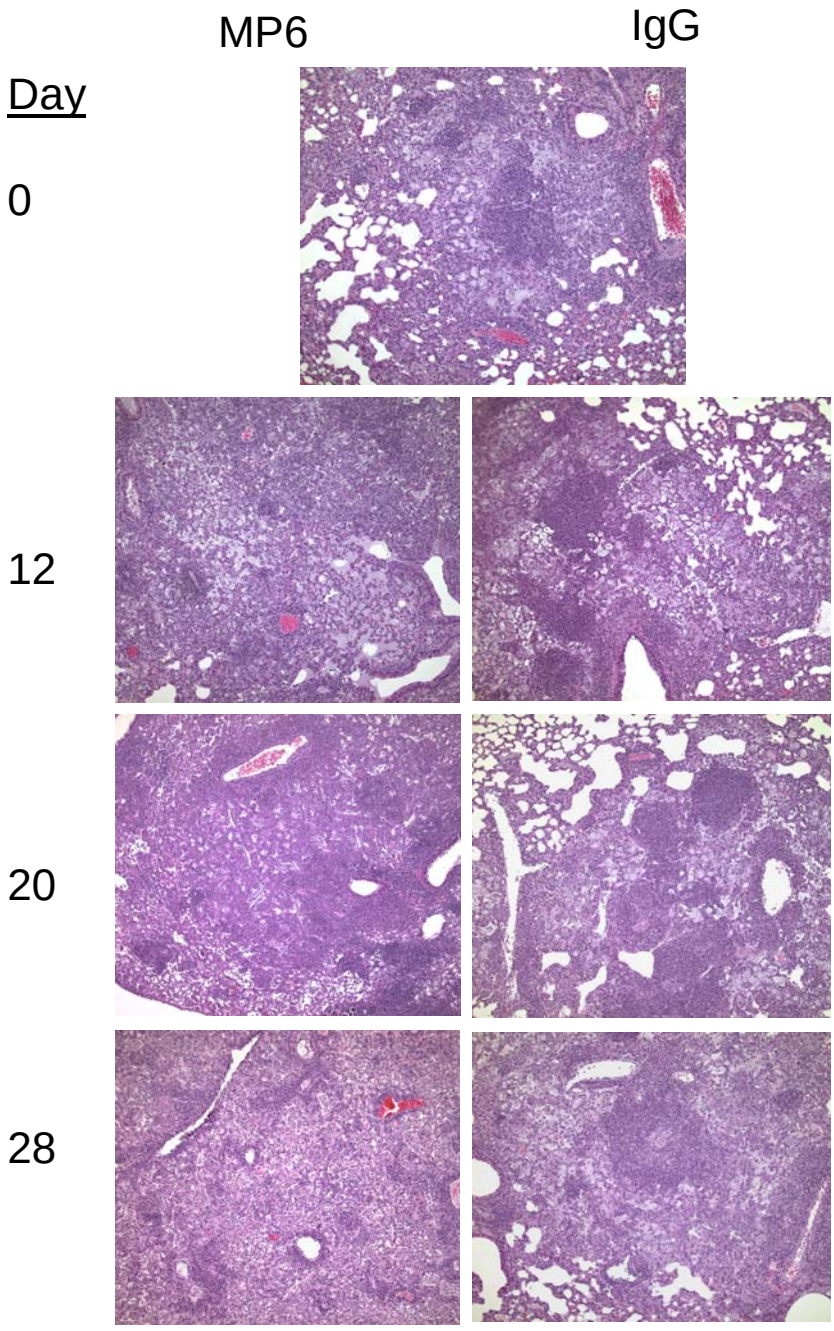

Figure 9. Neutralization of TNF in chronically infected mice leads to severe lung pathology.

MP6XT-22 treatment of mice led to disorganized cellular infiltration and fluid in the alveolar spaces of the lungs by 12 days post antibody treatment (middle panel). IgG treated mice (right panel) at day 12 post antibody treatment still exhibited organized granuloma formation, with clusters of lymphocytes and macrophages. (100x magnification). Sections shown here are representative of 4 mice/ group. This experiment was repeated with similar results 4 times.

TNF affects chemokine expression in M. tuberculosis infected macrophages

Effects of TNF on *M. tuberculosis*-induced chemokine expression by macrophages were first examined in vitro. Bone marrow derived macrophages were infected with *M. tuberculosis*. Following infection the macrophage expression of many inducible C-C and C-X-C chemokines increased relative to uninfected macrophages, and mRNA levels peaked between 4 and 12 hours post-infection depending on the gene (Figure 10). Expression of CXCL10, CCL12, CCL2 and CCL4 peaked at 4 hours, whereas expression of CXCL9, CXCL11, CCL3, and CCL5 did not peak until 12 hours post infection. Although expression decreased rapidly after 12 hours of infection, the levels remained elevated compared to uninfected macrophages.

These data were generated using a real time RT-PCR assay, which evaluates expression on a population basis relative to the chosen calibrator (in this study, uninfected macrophages). The value, ΔCt, or the change in cycle threshold between the endogenous control (HPRT) and the gene of interest (a chemokine), allows examination of constitutive expression of chemokines. Constitutive expression in macrophages (highest to lowest) was:

CCL4>CCL12>TNF>CXCL10>CCL2>CCL5>CCL3>CXCL9>CXCL11

Following *M. tuberculosis* infection of the macrophages, the relative RNA induction (normalized to the HPRT gene and relative to uninfected macrophages) of CCL5 and CXCL9 was highest in the panel of chemokines examined, followed by induction of CXCL10 and CCL3. Relative expression of CCL4 (Figure 10) and CCL12 was very low compared to other chemokines. Interestingly, these two chemokines also had the highest constitutive expression. In most cases after the reduction in expression after 12 hours, the expression of chemokines remained stable between 24 and 48 hours post infection; by 72 hours the macrophages began to die in culture.

In the first set of experiments anti-TNF Ab was added to the cell culture at the time of infection. As early as 4 hours post infection, TNF expression was induced (Figure 10). Anti-TNF Ab treatment at the time of infection reduced expression of many chemokines (Figure 10), indicating that optimal expression of these chemokines was dependent on TNF. Expression of some chemokines, such as CCL5, was sustained at a higher level as infection progressed in vitro, and in the presence of anti-TNF Ab the expression of CCL5 was reduced 30-70%. CCL2 expression was reduced by TNF neutralization only at the 4 hr time point (Figure 10). TNF neutralization modestly reduced CCL3 expression early in infection, but high levels of CCL3 mRNA were sustained in the anti-TNF Ab treated, but not control macrophage cultures (Figure 10). CCL12 also had reduced expression in TNF-neutralized cultures early after infection, but then was upregulated in the presence of anti-TNF Ab by 24 hours post infection and back down by 48 hours (Figure 10).

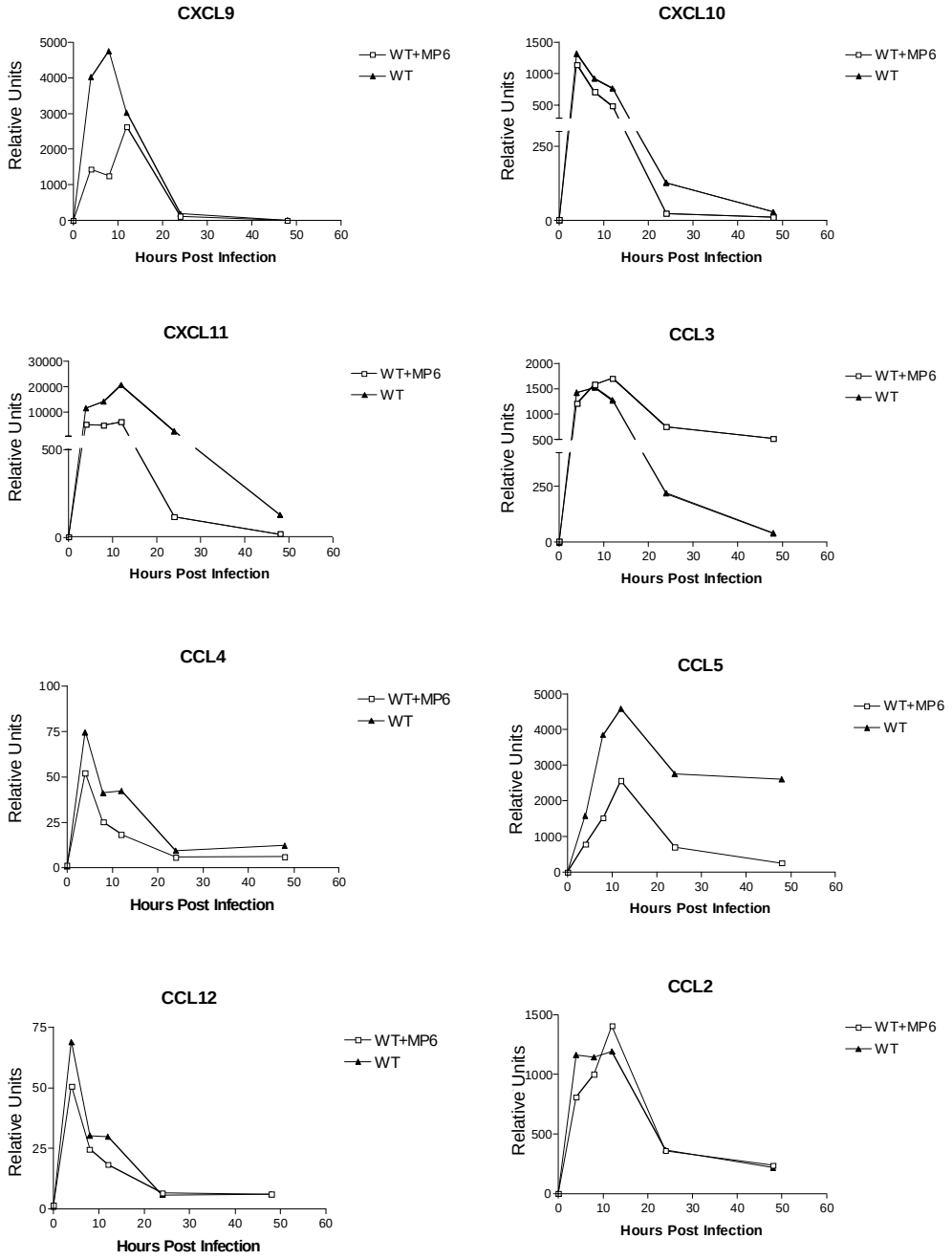

Figure 10. Macrophage expression of chemokines is partially dependent on TNF.

Real time RT-PCR was performed on RNA isolated from macrophages infected with *M. tuberculosis* at 0, 4, 8, 12, 24, and 48 hours post infection, with or without addition of anti-TNF Ab. Expression of CXCR3 ligands CXCL9 and CXCL10, CCR5 ligands CCL3, CCL4 and CCL5, and CCR2 ligands CCL2 and CCL12 were determined. Expression levels reported are relative to uninfected macrophages. This experiment was performed twice with similar results.

In a separate set of experiments, macrophages were infected with *M. tuberculosis*, and anti-TNF Ab was added 4 hours after infection (when unincorporated bacteria were removed

from the culture); expression of chemokines was examined 24 and 48 h after infection. The mRNA levels of CCL5, CXCL10, and CXCL11 were still significantly reduced at 24 and 48 hours post-infection (60%, 58%, and 84%, respectively, Figure 12). The expression of CCL12 was significantly increased (Figure 12). Treatment of infected macrophages with isotype control antibody did not alter the chemokine expression (Figure 11). Chemokines were still induced upon infection in anti-TNF Ab treated cultures, indicating that TNF was only partially responsible for controlling the expression of these chemokines. Addition of recombinant TNF to the infected macrophage cultures did not lead to additional chemokine expression (Figure 11), suggesting that the TNF induced by *M. tuberculosis* infection was sufficient to affect expression of the chemokine genes. These data indicated that TNF induced expression of CCL5, CXCL9, CXCL10 and CXCL11, but downregulated expression of CCL12.

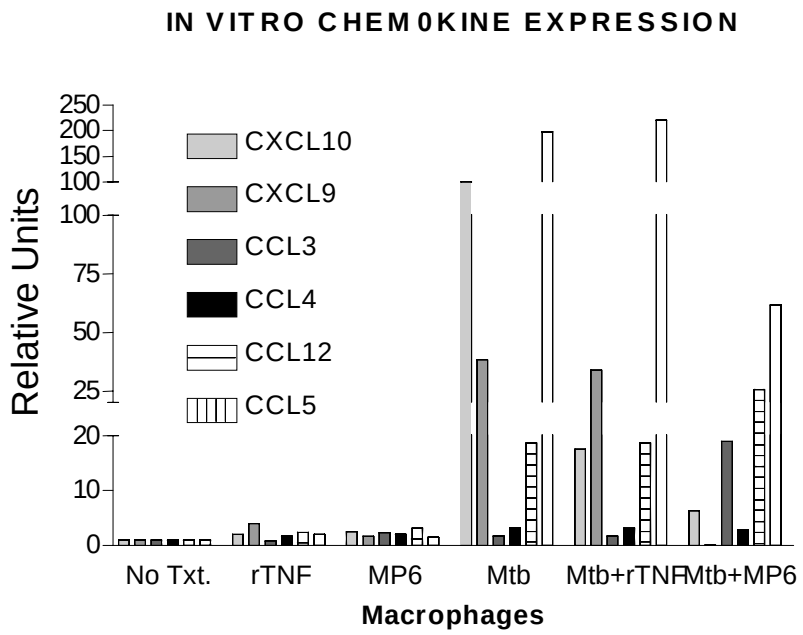

Figure 11. Control macrophage experiment.

Treating uninfected bone marrow derived macrophages with anti-TNF Ab or murine rTNF, did not significantly change expression of chemokine mRNAs. Addition of murine rTNF to infected macrophages did not increase expression of chemokine mRNAs to levels above those of untreated infected macrophages.

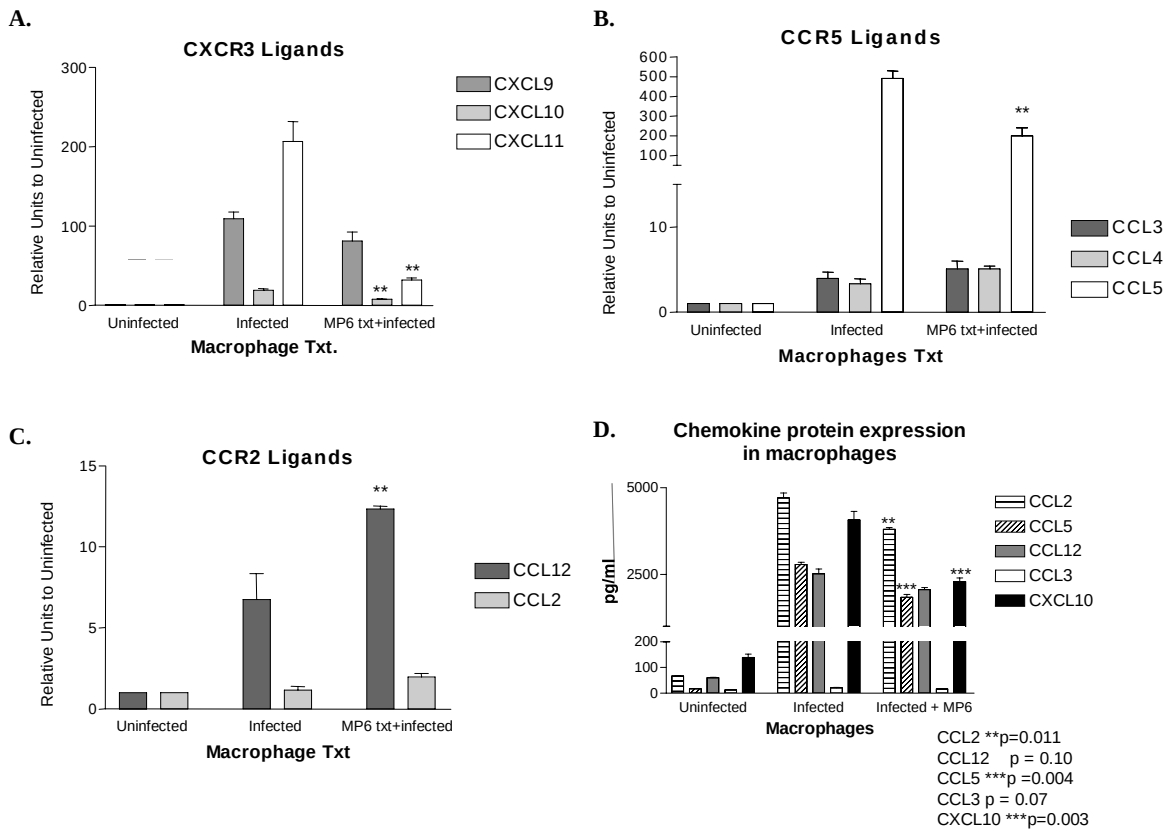

Figure 12. Macrophage expression of chemokines is partially dependent on TNF.
Real time rt PCR was performed on RNA isolated from macrophages infected with M. tuberculosis for 24 hours. A. Expression of CXCR3 ligands, CXCL10 and CXCL11, was significantly reduced by anti- TNF treatment of macrophages. B. Expression of CCR2 ligand, CCL2 was unaffected by anti-TNF treatment, but CCL12 expression increased. C. Expression of CCR5 ligand, CCL5 was also significantly reduced following anti-TNF treatment. D. Proteins were isolated from the supernatants of macrophages infected for 48 hours to look at protein expression following anti-TNF treatment of macrophages. Consistent with RNA results, CCL5 and CXCL10 expression was significantly reduced. Contrary to RNA results, expression of CCL2 was significantly reduced and expression of CCL12 was unaffected. (Protein expression of CXCL11 was not addressed.)

Chemokine protein production in M. tuberculosis infected macrophages.

There are little data regarding post-transcriptional regulation of chemokine expression [148, 149]. To confirm the gene expression results, we used two different immunoassays to quantify protein production. Supernatants were collected from uninfected and infected macrophages at time 0, 4h, 8h, 12h, 24h and 48 hours post infection (from the cultures used to make RNA in Figure 10). The supernatants were used in the immunoassay for CXCL9 and

CXCL10 in our laboratory, and used for multiplex sample testing to quantify CCL2, CCL3, CCL5, CCL12, CXCL8 and TNF.

Uninfected macrophages do make small quantities of chemokines in cell culture. Constitutive protein expression from highest to lowest was:

CCL2>CCL12>CCL3>CXCL10>CXCL8>CCL5>TNF>CXCL9.

Many of the chemokines examined had reduced levels of protein present in the supernatant in the presence of anti-TNF Ab. The protein levels, especially in the wild type mice, either increased throughout the time course (e.g., CCL5) or increased during the first 12 hours of infection and then stabilized (Figure 13). Expression of CXCL9 was reduced 30-70% in the presence of anti-TNF Ab compared to control macrophages, depending on the time point. Expression of CXCL10 was reduced 20-30%, CCL5 was reduced 50-90%, CCL3 was reduced 10-90%, and CXCL8 was reduced 25%-70% (data not shown). Expression of CCL2 and CCL12 (data not shown) followed a similar pattern where in the presence of anti-TNF Ab, expression was reduced initially, then increased, but by 48 hours post infection there was clearly a reduction in the amount of protein present.

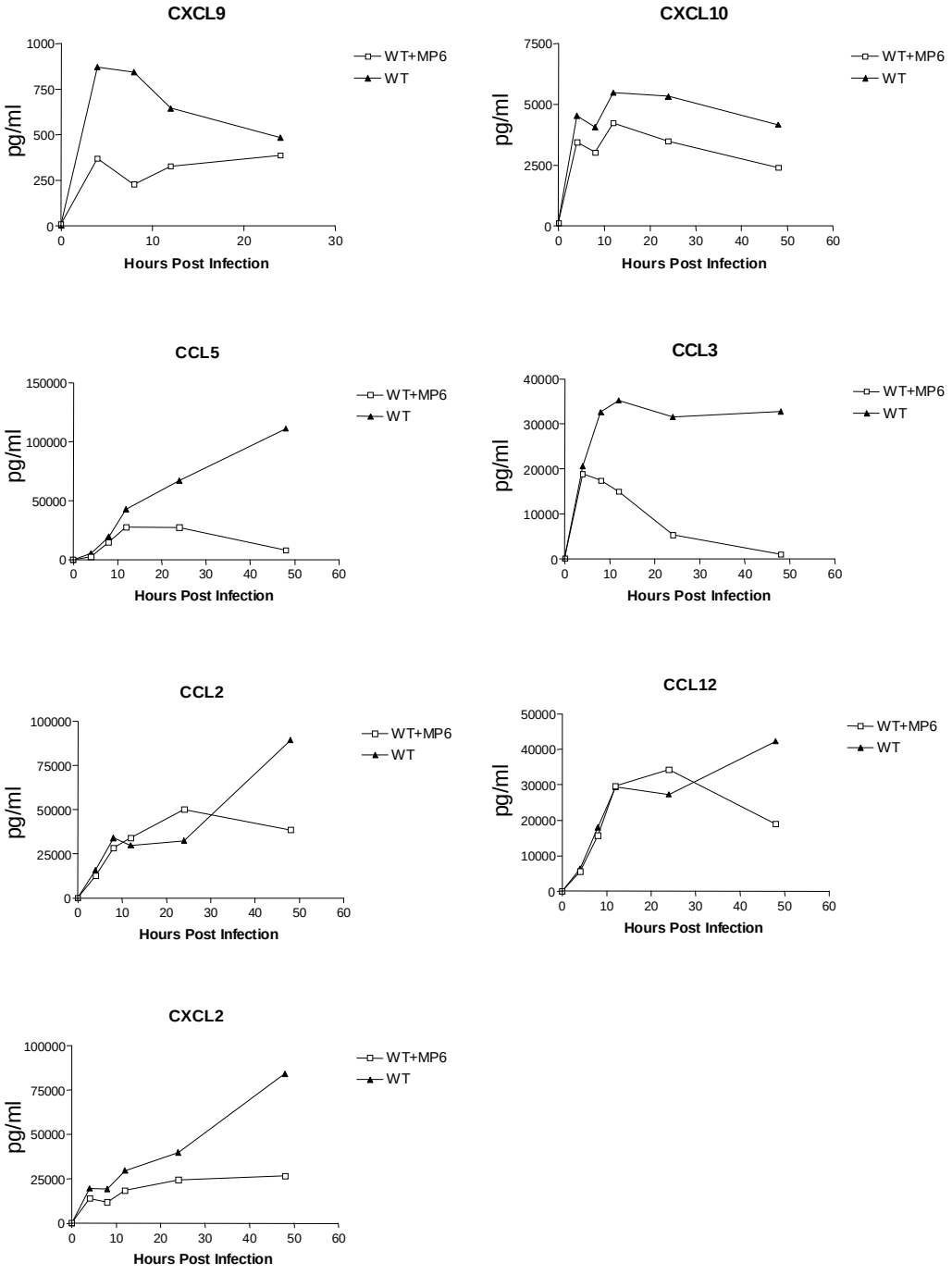

Figure 13. Chemokine protein expression in *M. tuberculosis* infected macrophages was affected by anti-TNF Ab treatment.

Supernatants from macrophages cultures infected for 0, 4, 8, 12, 24 and 48 hours were collected to quantitate protein expression following anti-TNF Ab treatment (or no treatment) of macrophages. Supernatants are from the cultures used for RNA preparations in **Figure 10**. ELISAs were performed for CXCL9 and CXCL10, while protein concentrations for the other chemokines and TNF were determined by multiplex protein array. This experiment was performed twice with similar results.

Protein analysis of supernatants from cultures where anti-TNF Ab was added at 4 hours post infection confirmed the macrophage mRNA data in that CCL2, CCL5, CCL12, CXCL9, and CXCL10 were induced by *M. tuberculosis* infection, and that CXCL9, CXCL10 and CCL5 were downregulated in the presence of anti-TNF Ab (Figure 12). On the other hand, although there was no difference in the expression of CCL2 mRNA in anti-TNF-treated macrophages, there was a significant reduction in the amount of the protein ($p=0.011$).

Chemokine expression in the whole lung of M. tuberculosis infected mice.

Based on the results from the macrophages and the findings in the spleen and liver of infected mice from a published study [150], we addressed the expression of chemokines in the whole infected lung by both RNase protection assay and real time RT-PCR. We expected to observe differences similar to our findings in the in vitro macrophage experiments, but following low dose aerosol infection, the induction of chemokines over uninfected lung was not detectable until 10-12 day post infection.

In anti-TNF Ab-treated mice, lower expression of a number of chemokines in the lungs was observed at the early times post infection using RNase protection assay and real time RT-PCR, especially at day 9 post infection, but these differences, although consistent, were not significant (Figure 14). By 15 days post infection the TNFRp55-/- or MP6-treated mice had significantly higher expression (compared to their controls) of CCL3, CCL4, CCL5, CXCL9 and CXCL10, but significantly less CCL12.

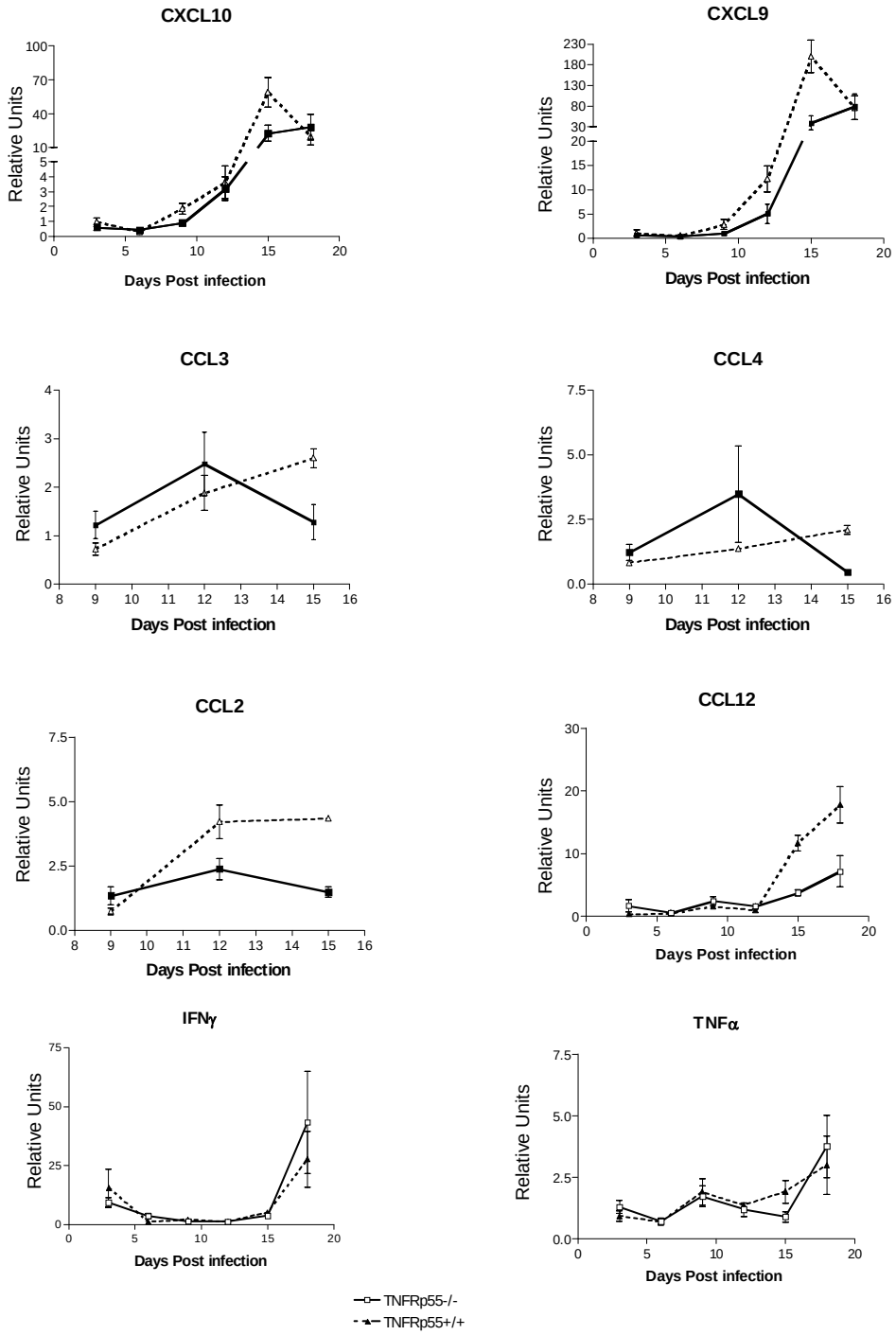

Figure 14. Chemokine RNA expression in the whole lung of TNFRp55-/- mice and wild type mice after *M. tuberculosis* infection.

Real time rtPCR was used to examine mRNA expression of chemokines in the whole lungs of mice after aerosol M. tuberculosis infection. Relative units represents a measure of the RNA relative to the endogenous control, HPRT, and the calibrated sample of uninfected lung. Expression above uninfected, or constitutive levels would be >1. Levels are not detected >1 until 9 or 10 days post infection.

We have observed repeatedly that increases in chemokine expression in the lungs correlate with increases in bacterial burden; since TNF-deficient mice have higher bacterial burdens than control mice by 10-12 days post-infection, differences in chemokine expression at these later time points were more likely due to bacterial numbers than to direct effects of TNF on gene expression. Therefore, focusing on early time points before bacterial burdens are different was essential in deciphering differences in chemokine expression due the absence of TNF independently of the effects of increased bacterial numbers. Most likely, chemokine induction was not detectable early after infection because the aerosol infection model used delivers 50-100 CFU, and only a small percentage of macrophages are infected. There is very little time between the detectable induction of expression in the whole lung and increasing bacterial growth in the TNF-deficient mice, complicating analysis of the role of TNF in control of chemokine expression.

In the chronic model of tuberculosis, TNF neutralization also resulted in increased bacterial burden in the mice relatively early after antibody treatment (within 12 days). When focusing on chemokine expression at early time points post-antibody treatment, using real time RT- PCR and RNase protection assay, there were no significant differences in the chemokine levels between anti-TNF Ab-treated and control mice; as before, chemokine expression increased in parallel with bacterial burden (Figure 15). It is important to note that granuloma disorganization was observed in the lungs of TNF-neutralized mice prior to bacterial numbers increasing, indicating that early time points were important for differentiating the effects of TNF from the effects of increased bacterial burden. In addition the increasing bacterial burden in the TNF deficient mice may result in higher numbers of cells migrating to the lungs in response to the inflammatory stimulus, complicating the analysis. (We attempted to control for bacterial

growth during chronic infection in mice by treating mice with pyrazinamide in conjunction with the anti-TNF or IgG treatment- these data represented in APPENDIX B).

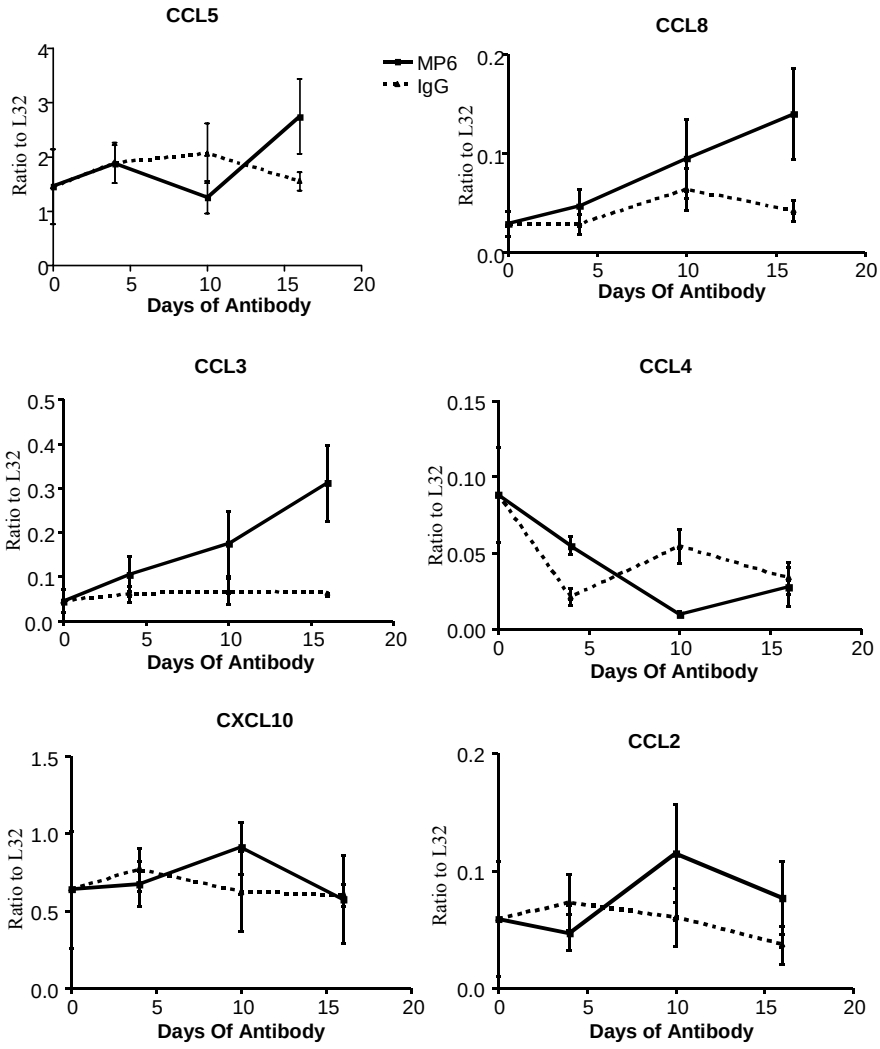

Figure 15. Chemokine expression in the lungs of chronically infected mice.

RNase protection assay was performed on pulmonary RNA isolated from whole lung. Expression is relative to the housekeeping gene L32. Mice were either treated with anti-TNF Ab (MP6- solid lines) or IgG (perforated lines).

Relative Chemokine Expression of Lung Granuloma by Laser Capture Microdissection.

The local nature of the immune response to *M. tuberculosis*, as characterized by a granuloma, suggests that gene expression measured in whole lung tissue might not accurately reflect the relevant gene expression within the granuloma [137]. For this reason, chemokine expression was measured from RNA obtained specifically from granulomatous tissue procured by LCM. Lung sections from early time points after MP6 or IgG treatment were chosen to assess the effects of TNF neutralization during a time where bacterial numbers remained similar in both groups. Relative expression of CXCL9, CXCL10 and CCL5 was measured by real-time RT-PCR at 0, 4 and 6 days post antibody treatment (Table 4). No significant differences in CXCL9, CXCL10 or CCL5 expression were detected between MP6 treated and control groups of mice. The variability within the groups was very high, indicating that the disease state or bacterial replication at the level of the granuloma varied widely within an individual mouse and between mice in chronic infection.

Table 4. Gene Expression by Laser Capture Microscopy (LCM) in granulomas isolated through Laser Capture Microscopy.

Granulomas were procured from fixed, embedded tissue and RNA was isolated to examine RNA expression of CXCL9, CXCL10 and CCL5 through real time RT-PCR. The values in the table represent relative units of expression. Each sample's analysis included comparing the expression of the chemokine to the expression of the endogenous control (HPRT) and comparing the expression relative to the calibrator (in this case uninfected lung). Tissue sections from 4 mice per time point were used to prepare RNA.

	Day 0	Day 4		Day 6	
		IgG	MP6	IgG	MP6
CXCL9	498.8 ± 276.8	333.7 ± 71.9	287.4 ± 122.1	249.4 ± 119.2	258.0 ± 300.9
CXCL10	85.6 ± 46.0	52.7 ± 32.2	41.3 ± 28.0	36.0 ± 22.5	49.3 ± 44.2
CCL5	5.0 ± 5.6	5.1 ± 2.8	2.9 ± 1.6	4.3 ±1.4	3.9 ± 1.5

Ex vivo macrophage isolation

Macrophages are a major reservoir for *M. tuberculosis*, and play a key role in orchestrating granuloma formation. Due to the low level of macrophage infection early after aerosol infection, gene expression of infected macrophages may have been diluted in the whole lung gene expression analysis. A more sensitive technique for assessing the effect of TNF on macrophage chemokine expression in vivo was needed. We enriched for macrophages by isolating CD11b+ cells from the lungs of acutely infected TNFRp55-/- and WT mice at various time points after low dose (50-100 CFU) aerosol infection. RNA was isolated from the CD11b+ population and real time RT-PCR was performed. At day 10 post infection, the CD11b+ population of cells was 50% F4/80+ and 46% Gr1+ following MACs column isolation, indicating that this technique purified both macrophages and neutrophils from the lungs (Table 5). Using this method, induction of chemokines in CD11b+ cells was still difficult to detect prior to 9 days post infection; at this time point there was reduced relative expression of chemokines in the TNF deficient mice compared to wild type, but the expression was very low (Figure 16). Just three days later (day 12) chemokine expression rose dramatically and the TNF deficient mice had higher expression of CCL5 and CCL12 chemokines (Figure 16).

Table 5. MACs column isolation of CD11b+ cells.

Flow cytometric analysis results from the MACs column isolation. These data represent the results of one sample from 3 pooled mice.

	CD3+	B220+	F4/80+	Gr1+
- selection	48%	34%	3%	15%
+ selection	1%	3%	50%	46%

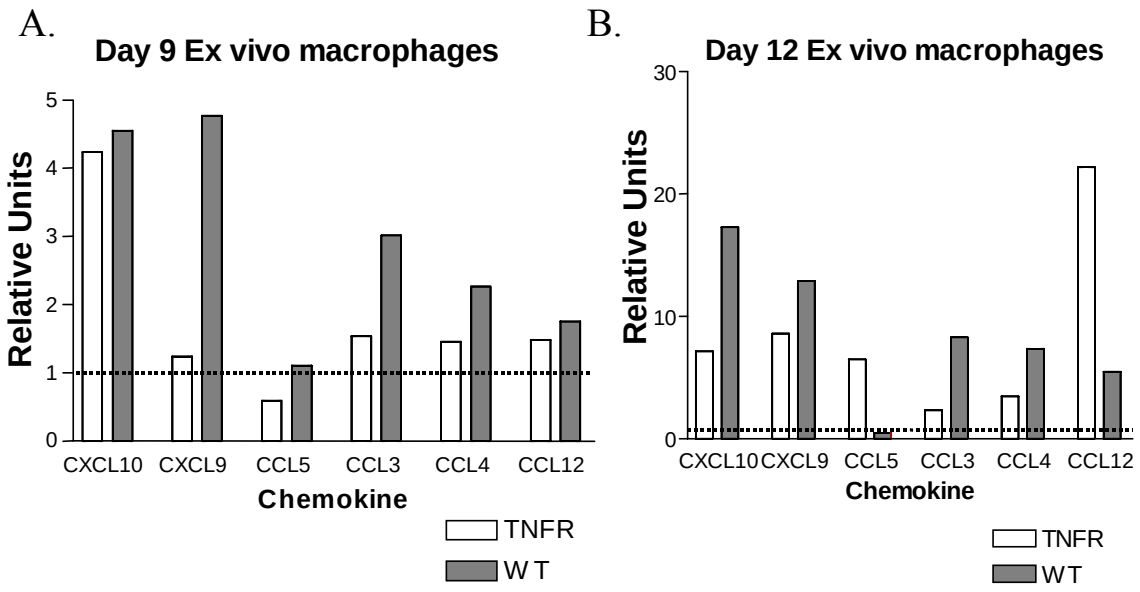

Figure 16. Chemokine expression in CD11b+ cells isolated from low dose infection of TNFR and WT mice.

A. At Day 9 chemokine expression was reduced in TNFR-/- mice in many of the chemokines tested. B. At day 12 expression of the chemokines was more highly induced. Each bar represents the combined sample of 3 mice. This experiment was repeated 3 times with similar results.

When we increased our aerosol dose 20-fold to increase the number of macrophages initially infected in the lungs, we detected induction of chemokines in the macrophage population as early as 4 days post infection. There were differences between TNFRp55-/- and wild type mice in the expression of CXCL9, CXCL10, CCL3, CCL4, CCL5 and CCL12 (Figure 17). By 7 days post infection the bacterial burdens in the TNFRp55-/- mice were significantly higher at this dose (Figure 17). There were still reduced levels of expression of CXCL9, CXCL10 and CCL4, and but now increased expression of CCL5 and CCL12 in TNFRp55-/- mice compared to wild type mice (Figure 17). By day 10 the expression was 10-fold higher than at day 7, and the differences between the mouse strains were no longer observed (Figure 17).

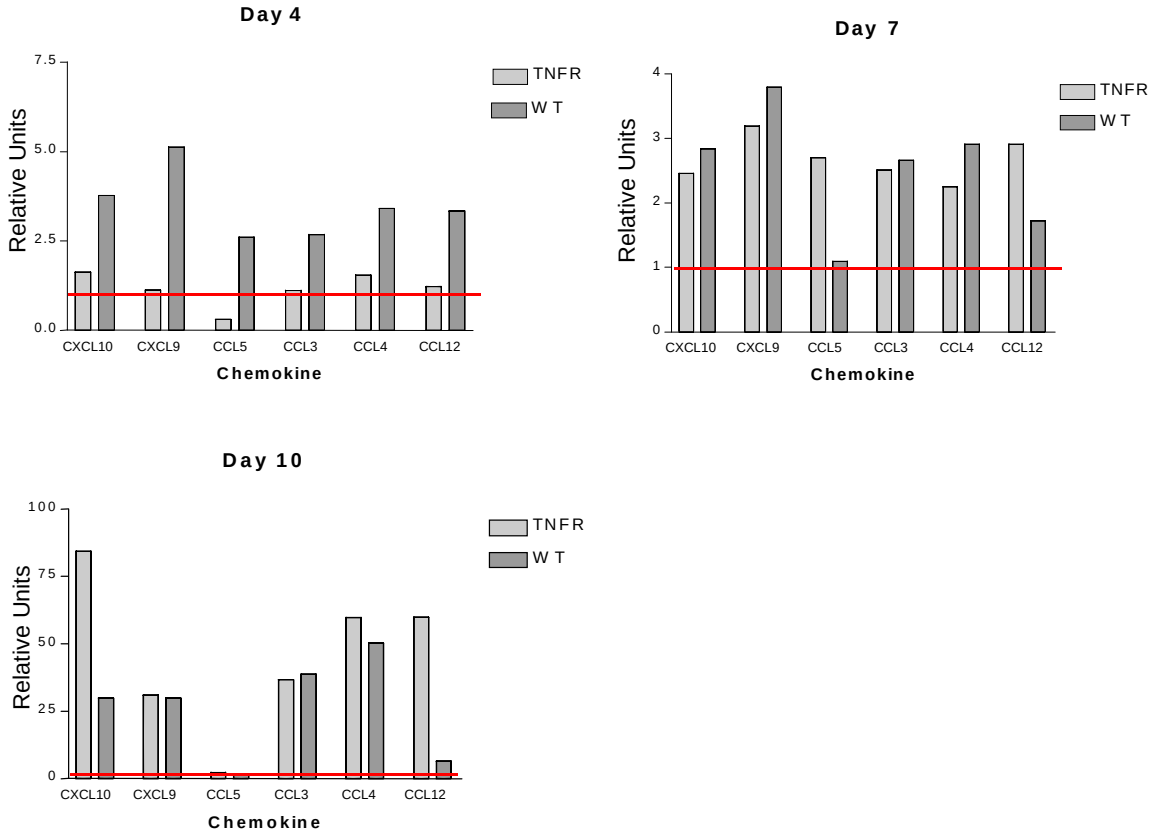

Figure 17. RNA expression of CCR5 ligands and CXCR3 ligands is transiently reduced in CD11b+ cells of TNFRp55-/- mice infected with a high dose of *M. tuberculosis*.

Ex vivo isolation of CD11b+ cells was performed on the lungs of TNFRp55-/- mice and wild type mice following high dose (300 CFU) aerosol *M. tuberculosis* infection. Real time RT-PCR performed on the RNA from those cells revealed that chemokine expression was transiently reduced in the lungs of the TNFRp55-/- mice compared to wild type mice. By day 7 post infection when bacterial burdens were higher in TNFRp55-/- mice reduced levels of expression were still observed. CD11b+ cells from 4-5 mice per time point were pooled to prepare RNA. Relative Units is used to represent the induction of chemokine expression compared to uninfected CD11b+ cells isolated from the lung (represented by line).

To follow the effect of TNF neutralization at the level of macrophages in vivo in the chronic model of tuberculosis, CD11b+ cells were isolated ex vivo from the lungs of *M. tuberculosis* chronically infected mice (treated with IgG or anti-TNF Ab) and real time RT-PCR was performed on isolated RNA. The expression of CCL3, CCL4, CCL5, CXCL9, and CXCL10 were transiently reduced in CD11b+ cells isolated from chronically infected MP6 treated mice (Figure 18). The expression of these genes increased as bacterial burdens increased and by 12

days post infection, when the bacterial burdens in MP6 treated mice were substantially higher than in IgG-treated mice, chemokine mRNA levels were higher than in control mice.

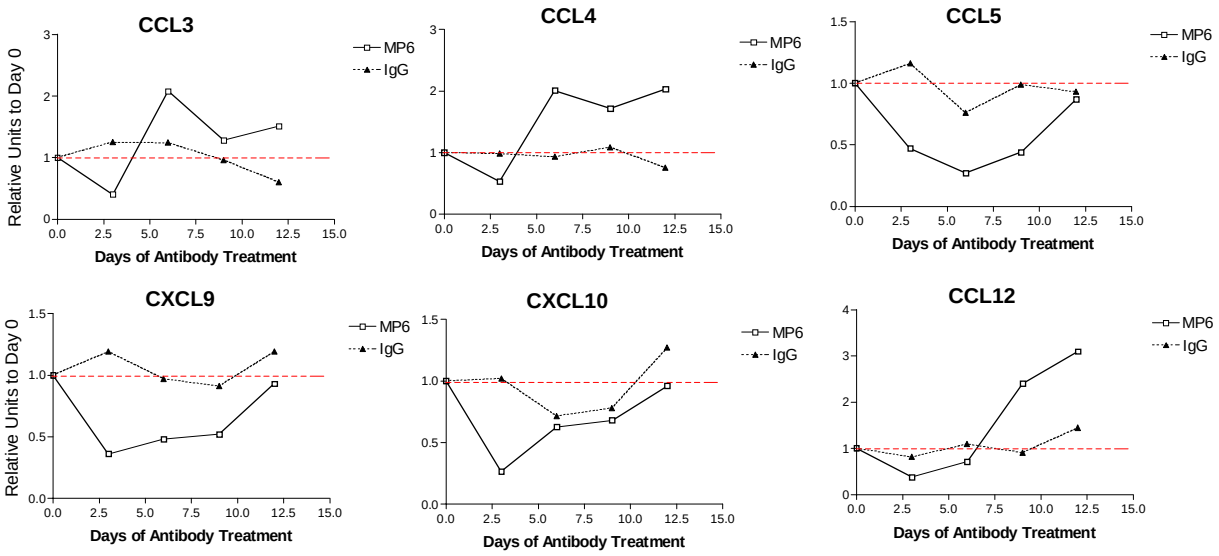

Figure 18. In chronically infected, MP6XT22 treated mice, chemokine RNA expression was transiently reduced in CD11b+ cells isolated ex vivo from the lungs.

MP6XT22 treatment of chronically infected mice led to transient reductions in the levels of many chemokines compared to IgG treatment. Relative Units in panel B are relative to day 0 of antibody treatment (represented as dashed line). CD11b+ cells from 4-5 mice per time point were pooled to prepare RNA. This experiment was repeated and similar results were obtained.

In situ hybridization

To obtain additional information on effects of TNF on the localized chemokine expression in the lungs early in infection, in situ hybridization (ISH) was performed to visualize expression of CXCL9 and CXCL10 mRNAs.

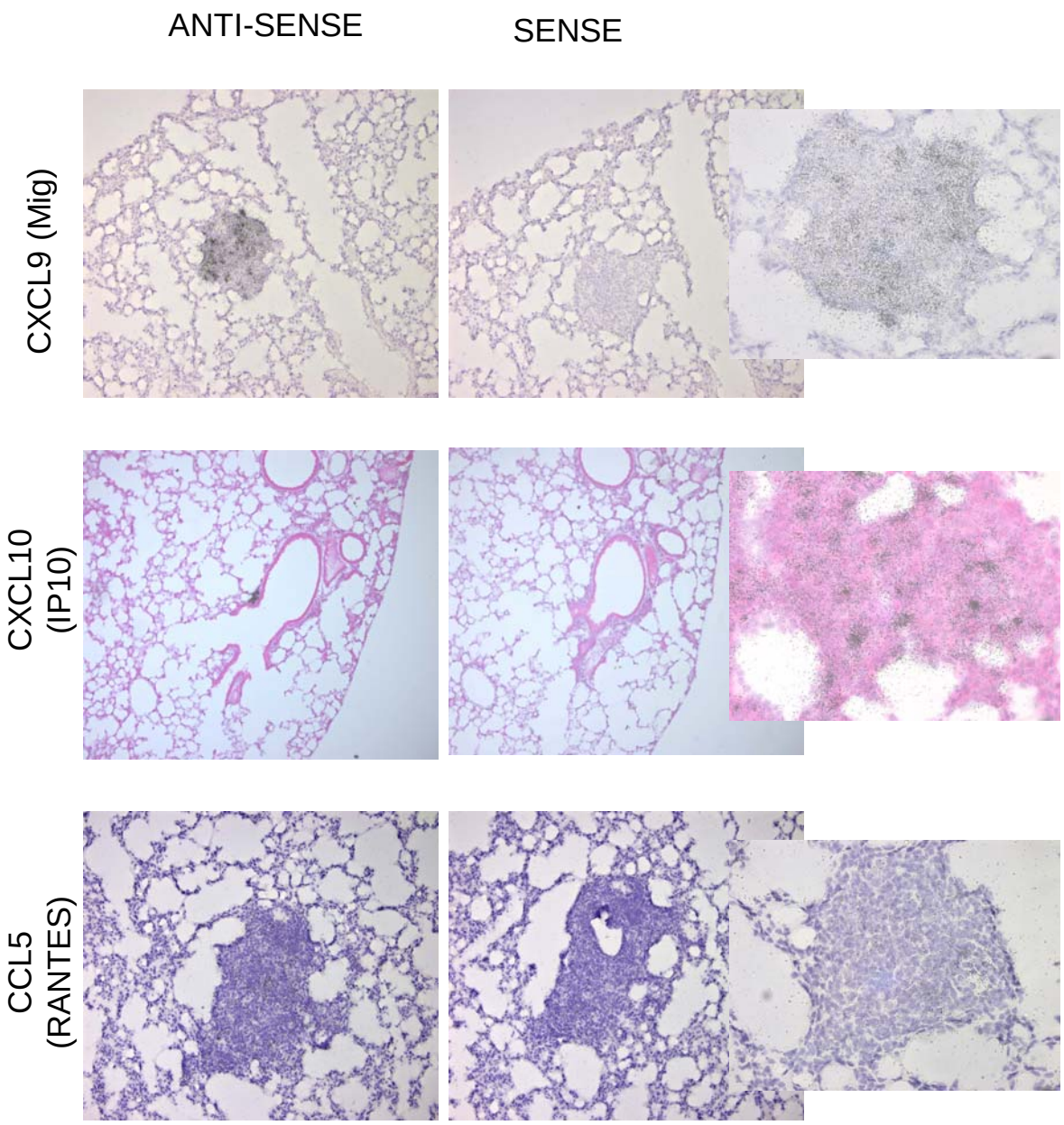

Figure 19. Sense and anti-sense in situ hybridizations to detect CXCL9, CXCL10 and CCL5 in lung tissue infected with *M. tuberculosis*.

In situ hybridization was performed using ^{35}S-labelled sense and anti-sense riboprobes. Exposures were for 7 days in all cases. The images on the left and in the middle were photographed at 20X. The images on the right were photographed at 60x.

An algorithm was designed to accurately assess two aspects of this study. First the number and size of the cellular infiltrates was studied. Second, the location and quantity of gene

expression with respect to pathology within the lung was evaluated (Table 6). Single cells or non-clustered cells (<20 cells together) that expressed the gene of interest were classified as Category 1. Infiltrating clusters of cells were classified as Category 2 or Category 3, on the basis of histology and regardless of gene expression. Category 2 infiltrates were clusters or infiltrates of 20-100 cells, whereas Category 3 infiltrates were defined as clusters of >100 cells. After classifying the infiltrates, the ISH signal for a gene was analyzed in each infiltrate. If no signal was detected, the infiltrate was designated -. If <50% of the cells within a cellular aggregation were positive for expression, the infiltrate was designated +, but if >50% of the cells within a cellular cluster were signaling for expression, the infiltrate was considered ++. Therefore each category 2 or 3 infiltrate could be either -, +, or ++.

Table 6. Algorithm used for ISH analysis.

Twenty 20X fields were counted for all analyses. All cellular infiltrates were counted and classified into a category based on their size. In addition, all signals for CXCL9 and CXCL10 were also counted and classified based on the cellular infiltrate expressing them.

Category	ISH signal	Description
1	-	Individual cells or a group of <20 cells negative for gene expression (normal tissue)
1	+	Individual cells or a group of <20 cells positive for gene expression
2	-	Clusters of 20-100 cells, negative for gene expression
2	+	Clusters of 20-100 cells, <50% of cells positive for gene expression
2	++	Clusters of 20-100 cells, >50% of cells positive for gene expression
3	-	Clusters of >100 cells, negative for gene expression
3	+	Clusters of >100 cells, <50% of cells positive for gene expression
3	++	Clusters of >100 cells, >50% of cells positive for gene expression

The number of category 1 areas expressing CXCL9 or CXCL10 was counted in twenty 20X fields. Category 1 (normal tissue) expression of CXCL10 was detected as early as 3 days post infection, and the expression increased gradually as infection progressed. By 12 days post infection the number of category 1 areas expressing CXCL10 (in the 20 fields counted) increased to an average of 8 ($\pm$2) in the IgG treated mice and 4 ($\pm$1) in the anti-TNF Ab treated mice (per 20 fields). Expression of CXCL9 was not detected until day 6 but at this time point it was not

detected in all mice. By 12 days post infection the number of category 1 areas counted was 4(±1) in the IgG treated mice and 1(±0.75) in the anti-TNF Ab treated mice in the 20 fields counted.

The overall number of category 2 and 3 infiltrates was not different between MP6 treated and control mice (Figure 20) up to 12 days post infection. This was not surprising since at these early time points the overall number of cells migrating into the lungs was not significantly affected by anti-TNF Ab treatment (Figure 7), and this is prior to true granuloma formation.

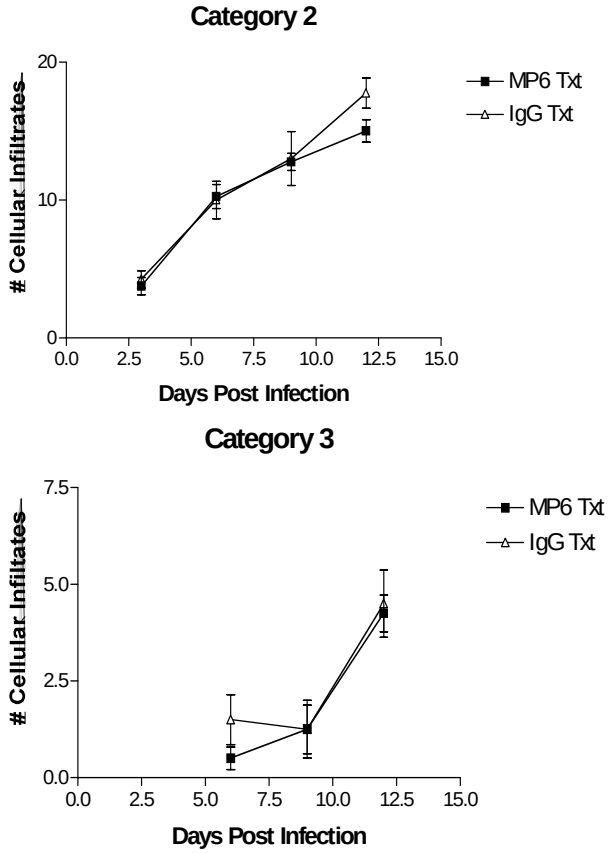

Figure 20. The number of cellular infiltrates, whether classified as category 2 or 3, was not different between anti-TNF Ab treated and IgG treated mice.

The number of CXCL9 Category 3++ clusters was significantly lower in the anti-TNF Ab treated mice by 12 days post infection, but there were no differences in the number of CXCL9 Category 2+/++ clusters (Figure 21). CXCL10 gene expression followed a different pattern:

there were significantly fewer CXCL10 Category 2+ clusters in MP6-treated mice, but no differences in the number of CXCL10 Category 3+/++ clusters (Figure 21). These data confirm that TNF neutralization affects the expression of a subset of chemokines in the lung, and that effects on timing of chemokine expression may be important in granuloma formation.

Expression of CCL5 was addressed in the tissue of MP6 and IgG treated through in situ hybridization, but the analysis was more complicated than analysis of CXCL9 and CXCL10. Due to higher background expression of CCL5 it was near impossible to apply the algorithm to CCL5 expression. There was specific expression within the inflammatory cellular infiltrates, but there is also evidence of many endothelial and epithelial cells expressing the CCL5 mRNAs.

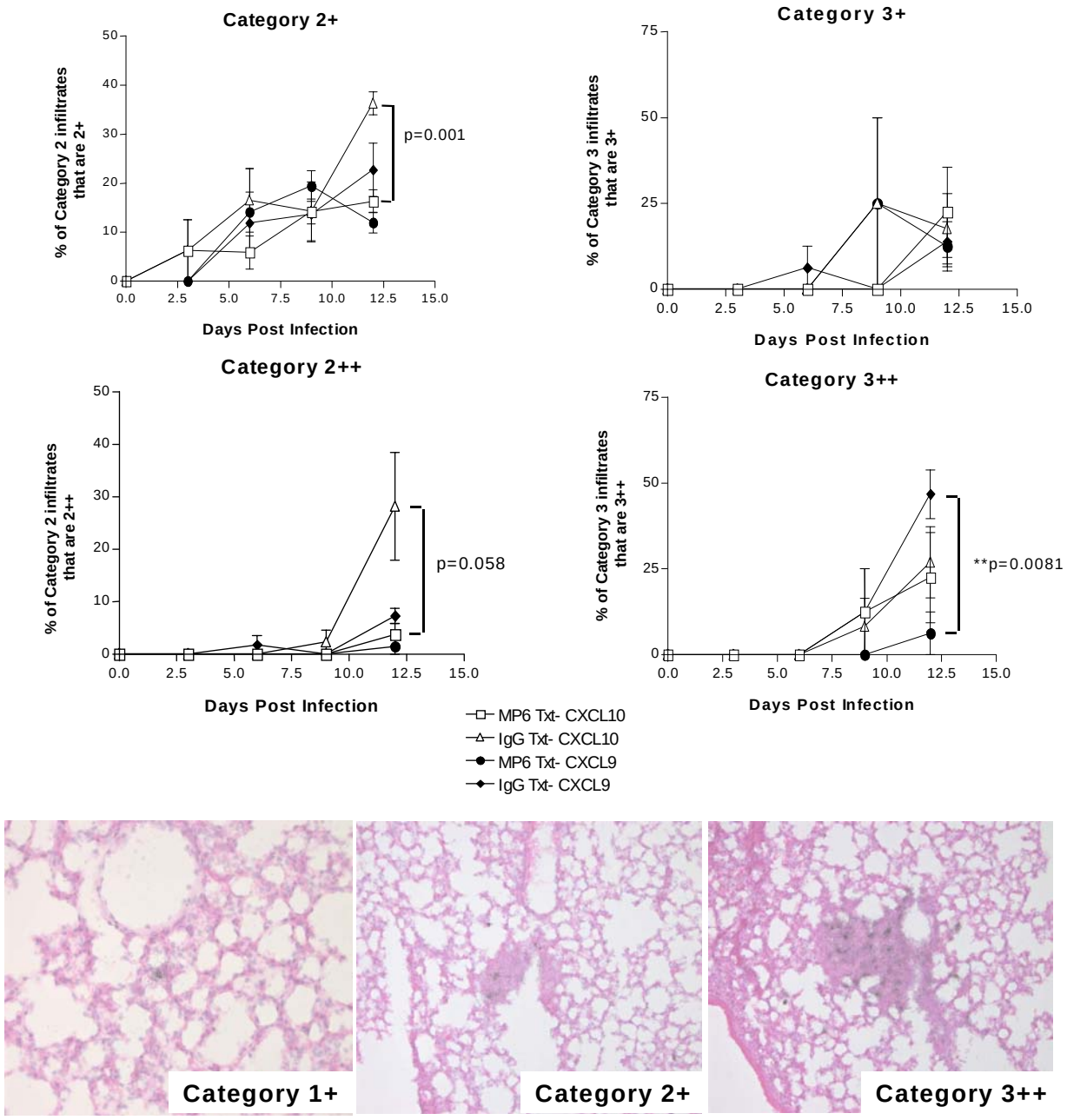

Figure 21. Expression of CXCL9 and CXCL10 are reduced in MP6XT-22 treated mice during acute aerosol

In situ hybridizations were performed on fixed frozen sections of lung tissue. Expression of CXCL10 was reduced in infiltrates of intermediate size (Category 2) in MP6XT-22 treated mice. Expression of CXCL9 was reduced in larger category 3, infiltrates in the MP6XT-22 treated mice compared to the wild type mice. Each panel represents an example of the categorization used in the algorithm, where category 1 + cells were either single positive cells or a cluster of less than <20 cells that were positive. Category 2 infiltrates were clusters of cells with 20-100 cells contained within the cluster. If <50% of the cells were positive in the cluster than the infiltrate was classified as 2+, If > 50% of the cells in the infiltrate were positive the infiltrates was classified as 2++. Category 3 infiltrates were classified as clusters of >100 cells. Again, percent % cells was used to classify the infiltrates as -, +, or ++. 20, 20X fields were counted for the analysis.

7.4 Discussion

TNF is required for granuloma formation and the absence of TNF affects the expression of many inducible chemokines in the acute and chronic models of tuberculosis. In the absence of TNF, the cell-mediated immune response fails to control infection and the bacterial burden increases. Interestingly, in the chronic model of infection, the mice succumb to infection before the bacterial burdens rise to moribund levels, indicating that lung pathology is presumably leading to a decrease in lung function and death [106]. Deciphering the difference between the influences of TNF and bacterial burden on chemokine expression, in a model where TNF affects bacterial burden, was technically challenging. Focusing attention at early time points in the experimental models allowed us to diminish the impact of higher bacterial burdens in TNF deficient mice. In addition, we focused on macrophage chemokine expression since this cell is a major *M. tuberculosis* reservoir and is responsive to TNF. This enabled detection of the effects of anti-TNF Ab on chemokine expression prior to changes in pathology, granuloma formation, and increased bacterial burden. Following increased bacterial burdens, the chemokine gradients were even more dramatically altered. The initial changes in chemokine expression may lead to a cascade of inappropriate cellular communication, impaired cell migration within the lung, and loss of cell mediated immune response.

Control of cell migration is a complex process involving not only chemokines and receptors, but also adhesion molecules. The complexity of this process has been illustrated in this study. We also examined expression of adhesion molecules, using gene expression filter arrays (GEArray Q Series SuperArray Bioscience Corporation), but no striking differences were observed after anti-TNF Ab treatment (APPENDIX C). Clearly changes in pathology are compounded by the other roles that TNF plays in control of *M. tuberculosis* infection and the effects on chemokine expression are probably not solely responsible for the severe pathology

observed in TNF-deficient mice. Studies on low dose aerosol *M. tuberculosis* infection in CCR2 and CCR5 chemokine receptor transgenic knockout mice [[63] and Section 9.3 Results.], and in vivo models of CXCL9 and CXCL10 neutralization [[72] and Section 8.3 Results.] have revealed some differences in cell migration. But even in these models, the pathology does not mirror the destructive pathology observed in the absence of TNF, where signaling by some of the same chemokines that were affected by TNF neutralization is diminished. CCR2-/- mice have fewer macrophages throughout infection, but have sufficient numbers to control low dose infection, although the mice are quite susceptible to high dose infection [62, 63], see Section 10.0. CCR5-/- mice had a greater lymphocytic infiltrate in their lungs, but controlled infection (See Section 9.0). CXCL10-/- and mice treated with both anti-CXCL9 and anti-CXCL10 antibodies controlled infection with no apparent lymphocyte migration deficiencies (See Section 8.0) to the lung but a slight delay in lymphocyte migration to the lymph nodes.

A recently published study provided data that anti-CXCL9 Ab treatment in *M. tuberculosis* infected mice did not affect control of infection, but the mice had smaller, although still organized, granulomas [72]. These authors suggested that CXCL9 was produced by neutrophils and played a key role in granuloma formation. However, the differences we observed in pathology and granuloma formation in TNF-deficient mice was not reflected in the anti-CXCL9 Ab treated mice. Therefore, TNF-mediated control of CXCL9 expression may be only one factor in the influence this cytokine has on granuloma formation.

Our studies on whole lung chemokine RNA expression consistently revealed differences in gene expression at early time points post infection and after antibody treatment when comparing control and TNF deficient mice. Although these differences were consistent (in 3 experiments), they were not significant. The laser capture microscopy technique was employed

to examine more localized gene expression patterns in granulomas. To isolate enough RNA from fixed, embedded tissue to perform real time RT PCR on the LCM samples, multiple granulomas had to be isolated from each mouse. Although the granulomas isolated were from the same lobe of the lung, there was still high variability among mice and probably between granulomas, since granuloma size and the number of bacteria in each granuloma can be variable. Although the LCM data revealed that the chemokine expression was higher within the granuloma compared to the whole lung, the pattern of expression was similar to whole lung chemokine expression.

We next focused our in vivo studies on the CD11b+ population of cells, enriching for macrophages. The technique used removed epithelial cells and lymphocytes from the lung homogenates, but the neutrophils (which are CD11b+) were not removed. We have focused on the macrophages, since direct effects of TNF on chemokine production by this population was observed in vitro. However, TNF may also affect chemokine production by neutrophils. The number of neutrophils at early time points post infection and after antibody treatment in chronically infected mice was similar to the number of macrophages present in the lungs [[63], Figure 7 and 7]. There were 3-5x10^4 macrophages and 3-5x10^4 neutrophils 6 days post infection and 4x10^5 of each cell type at 4 days after initiation of antibody treatment in the chronic model.

Recently, there has been published evidence of TNF affecting chemokine levels in the liver during intravenous *M. smegmatis* and *M. tuberculosis* infection [142, 143]. Our study has gone beyond these by focusing on the localized chemokine expression in the lungs following aerosol infection, and by addressing chemokines that have not previously been studied. We also carefully controlled for the confounding effects of bacterial numbers on chemokine expression by studying very early time points in the infection or neutralization. We demonstrated that the

chemokine deficiency in the absence of TNF was at the macrophage level, using in vivo and in vitro studies. The macrophage likely plays a key role in granuloma formation as an initial site of infection, a reservoir for *M. tuberculosis,* and a potent producer of both TNF and chemokines.

The chemokines affected by TNF are known to influence the migration of cell types found within the lung during *M. tuberculosis* infection. CCL5, produced in the lung and by macrophages at high levels, induces migration of T lymphocytes, monocytes, and immature dendritic cells through CCR1 and CCR5. Disruption in the CCL5 gradient, seen in TNF deficient mice, likely affects the migration of these cells within the lung. T lymphocyte migration in the lungs could also be affected by the reduction in CXCL9, CXCL10, CCL3 and CCL4. Monocyte and macrophage migration may be affected by similar chemokines including CCL3 and CCL4 through CCR5, and CCL2 and CCL12 through CCR2. The increased expression of these chemokines following increased bacterial load also likely leads to increased cell migration to the lungs. Therefore, we propose that the initial reduction in chemokines in the absence of TNF leads to localized changes in the gradients, decreased cell responsiveness and disorganized cellular infiltrate. As a result the cells do not interact with each other in a coordinated manner, thus reducing the cell mediated response [106]. The reduced cell mediated response leads to increased bacterial burden, increased chemokine expression and an increase in cells migrating into the lungs, including neutrophils.

Table 7. Summary of the effects of anti-TNF Ab on the expression chemokines in *M. tuberculosis* infected macrophages.

A down arrow (↓) indicates that expression was reduced in the presence of anti-TNF Ab (when added at the time of infection). The symbol (←→) indicates that there was no difference in the expression of this gene. ND= not determined. *When anti-TNF Ab was administered 4 hours after infection, expression of CCL12 increased.

CHEMOKINE	RNA	PROTEIN
CXCL9 (CXCR3 ligand)	↓	↓
CXCL10 (CXCR3 ligand)	↓	↓
CXCL11 (CXCR3 ligand)	↓	ND
CCL3 (CCR5 ligand)	↑	↓
CCL4 (CCR5 ligand)	←→	ND
CCL5 (CCR5 ligand)	↓	↓
CCL2 (CCR2 ligand)	←→	↓
CCL12* (CCR2 ligand)	↓	↓↑

The chemokine expression studies performed in vitro advance our understanding of the role of TNF in chemokine expression and in post-transcriptional regulation of chemokines. The RNA analysis serves as a snapshot of the RNA at that moment in the cell, whereas collecting supernatant from cell culture was a representation of the accumulated proteins in the media. Gene expression of most chemokines tested diminished by 48 hours post infection (except CCL5); this may indicate that there was a negative feedback loop for gene expression. CCL3 expression was interesting because although mRNA expression peaked at a similar point in the anti-TNF Ab treated and control macrophages, the mRNA levels remained higher in the TNF-neutralized cultures. However, the protein level peaked at a lower point, and was reduced in the

TNF-neutralized cultures. The anti-TNF Ab treated macrophages may continue to express the gene in these cultures because the protein has not accumulated to a level to turn down transcription. In addition the expression of CCL2 was only reduced very early after infection in the presence of anti-TNF Ab, but the protein expression was reduced as late as 48 hours post infection. This suggests that CCL2 and CCL3 post-transcriptional regulation may be affected by TNF.

The in situ hybridization analysis of CXCL9 and CXCL10 expression highlighted the extensive variability between different stages of cellular infiltrates, granuloma formation, and their chemokine expression. First, analyzing the number and size of the infiltrates confirmed that at early time points, the cellular infiltration in the lungs was not different in the anti-TNF Ab treated mice compared to control mice. As infection progressed, the control mice developed organized granulomas, while the TNF-deficient mice did not. Early patterns of chemokine expression presumably affect this organization of the cellular infiltrate. The size of the collection of cellular infiltrate in the lungs can reasonably be attributed to the time of formation: as the infiltrate grows and collects more cells, the granuloma forms. Expression of CXCL10 in smaller (early) infiltrates (Category 2) was affected by TNF, but CXCL9 expression was only influenced by TNF in larger infiltrates (Category 3). This may suggest a differential timing of chemokine expression in granuloma formation, or that expression of these chemokines is sensitive to different levels of TNF. Alternatively, in the larger infiltrates, there are more cellular interactions, and possibly more cytokines to signal CXCL10 expression, overcoming a deficiency in TNF. Comparing this to our findings in the macrophages, it was similarly observed that CXCL9 was more dramatically affected by the anti-TNF Ab treatment than was CXCL10. The kinetics of chemokine expression is clearly complex in the lungs, and the dynamics of

granuloma formation may depend on TNF signaling expression of different chemokines at specific times.

In summary, this in depth study of localized chemokine expression patterns during acute and chronic *M. tuberculosis* infection presents evidence for TNF playing a direct role in chemokine expression and granuloma formation. We demonstrated that macrophages in vitro and CD11b+ cells in vivo, are partially dependent on TNF for expression of many inducible chemokines following *M. tuberculosis* infection. Our findings are relevant to understanding the immune response and granuloma formation during aerosol *M. tuberculosis* infection, and will contribute to an appreciation of the potential effects of anti-inflammatory or anti-chemokine therapies on infections.

8.0 Chapter 2 CXCL9 and CXCL10 are not required for granuloma formation and control of *M. tuberculosis* infection

8.1 Introduction

A Th1 cell mediated immune response is required for control of *M. tuberculosis*. Th1 associated responses include both CD4 and CD8 lymphocytes and expression of inflammatory cytokines such as IL-12, TNF, IFNγ, and IL-1. The migration of T lymphocytes to the lungs during *M. tuberculosis* infection begins about one week post infection and as bacterial burdens increase, the numbers of T lymphocytes migrating to the lungs also increases in a similar pattern. The signals required for T lymphocyte migration to the lungs have been studied to a limited degree. Presumably the cells migrate through a cascade of events including rolling, adherence, transmigration and response to chemotactic gradients.

It has been reported that CXCR3, a chemokine receptor, is expressed on Th1 lymphocytes, circulating CD4 and CD8 lymphocytes, NK cells, plasmacytoid and myeloid dendritic cells and leukemic B cells. This receptor is more promiscuous than initially thought, but the highest expression appears to be on Th1 lymphocytes. The ligands for CXCR3 in the mouse include CXCL9 (Mig), CXCL10 (IP10), CXCL11 (ITAC) and CCL21 (SLC) [151]. The CXCR3 ligands were originally described as IFNγ-inducible proteins, but other signals, such as LPS or high antigenic stimulation, have also been shown to induce expression of these chemokines [119]. We observed induced expression of CXC chemokines, CXCL9, CXCL10, CXCL11, in bone marrow derived macrophages following *M. tuberculosis* infection (Figure 10 and 10). The expression of CXCL9 and CXCL10 increased in the lungs following aerosol *M. tuberculosis* infection. Until recently it was believed that CXCR3 was the only receptor for CXCL10, but there is new evidence of a receptor for CXCL10 on epithelial cells and possibly endothelial cells which may induce antiangiogenic properties [152]. The expression level of

CXCL10 appears to correlate with T lymphocyte infiltration during Th1 inflammatory responses, such as multiple sclerosis [153] and inflammatory bowel disease (unpublished, Grimm, MC, St George Clinical School, University of New South Wales).

Although CXCL9, 10 and 11 share a common receptor, there is some evidence that their functions may not be redundant [151]. Transgenic knockout models and neutralizing antibody for CXCL9 and CXCL10 have been utilized to study lymphocyte migration and effector function in various infectious disease models. Studies in a murine viral hepatitis model show that anti-CXCL10 treatment led to increased mortality and delayed viral clearance during the chronic stage of infection [154]. On the other hand, treatment with anti-CXCL9 antibody did not lead to a change in the course of disease. These data indicate that in vivo the biological function of CXCL9 and CXCL10 may be different. Treating *Toxoplasma gondii* infected mice with anti-CXCL10 antibody increased susceptibility [155] with a greater than 1000 fold increase in parasite burden. In addition CXCL10-/- mice infected with mouse hepatitis virus were unable to control viral replication in the brain. These mice exhibited decreased antigen specific lymphocyte migration to the brain and decreased IFNγ responses compared to wild type littermates [154]. However, no significant differences were found in mortality in CXCL9-/- mice infected with *Listeria monocytogenes, Salmonella typhimurium, Francisella tularensis, M. avium, T. gondii*, vaccinia virus, ectromelia virus, Herpes Simplex Virus type 1, *Histoplasma capsulatum, or Cryptococcus neoformans* [120]. The CXCL9-/- mice infected with *F. tularensis* did have lower antibody responses than control mice, suggesting that CXCL9 may play a role in the T lymphocyte/APC/B lymphocyte interaction [120].

The available data support that the primary role of CXCR3 and its ligands is in recruitment of effector T lymphocytes, especially Th1 subsets during inflammatory responses.

Given that *M. tuberculosis* induces a Th1 response and requires T lymphocytes to migrate to the lungs during infection, we hypothesized that CXCL9 and/or CXCL10 may be necessary for migration of these cells to the lungs during infection. To test this hypothesis, we used both a knockout model and an antibody neutralization model of infection. CXCL10-/- mice and their CXCL10+/+ littermates, and wild type mice treated with anti-CXCL10 and anti-CXCL9 along with control wild type mice were infected with *M. tuberculosis* via aerosol. Our results indicated that with or without bioactive CXCL9 and CXCL10, mice controlled *M. tuberculosis* infection, formed granulomas and mounted a Th1 response in the lungs.

8.2 Materials and Methods.

Mice.

B6/129 CXCL10-/- mice, their wild type littermates, 129 CXCL10-/- mice and their wild type littermates were provided by Andrew Luster (Harvard University School of Medicine). Following quarantine these mice were transferred to the BSL3 facility. Mice were 5-7 months old when infected. C57BL/6 female mice (Charles River, Rockland, MA) (8-14 weeks old) were used in chemokine neutralization experiments. All infected mice were maintained in the BSL3 animal laboratories and routinely monitored for murine pathogens. The University Institutional Animal Care and Use Committee approved all animal protocols employed in this study.

Antibodies and chemicals.

Anti-CXCL10 and anti-CXCL9 were provided by Andrew Luster (Harvard University School of Medicine). These antibodies were administered at 100μg/ i.p. every other day. Control mice received a non-specific rat IgG (Jackson ImmunoLabs). All chemicals were purchased from Sigma Chemical Co. (St. Louis, MO.) unless otherwise noted. Middlebrook 7H9 liquid medium and 7H10 agar were obtained from Difco Laboratories (Detroit, MI). Antibodies used in flow

cytometry were obtained from Pharmingen (San Diego, CA).

Bacteria and infections.

To prepare bacterial stock, *M. tuberculosis* strain Erdman (Trudeau Institute, Saranac Lake, N.Y.) was used to infect mice, and then bacteria were harvested from their lungs, expanded in 7H9 liquid medium and stored in aliquots at -80°C. Mice were infected via the aerosol route using a nose-only exposure unit (InTox Products, Albuquerque, N.M.), and exposed to *M. tuberculosis* (1×10^7 CFU/ml in the nebulizer chamber) for 20 minutes, followed by 5 minutes of air. This resulted in reproducible delivery of 50-100 viable CFU of *M. tuberculosis*, which was confirmed by CFU determination on the lungs of 2-3 infected mice 1 day post-infection. The tissue bacillary load was quantified by plating serial dilutions of the lung homogenates in 0.05% PBS/Tween 80 onto 7H10 agar. Total colony forming units were calculated.

Culture and infection of DCs.

Dendritic cells are derived from the C57Bl/6 mice bone marrow. The bone marrow was obtained as previously described [82]. After the cells were washed and counted, the cells were resuspended in two non-tissue culture treated deep dish petri dishes in 20 ml DC media/ plate (10% FBS, 1% sodium pyruvate, 1% L-glutamate) overnight. The following day, the nonadherent and semi-adherent cells were removed from the plates, spun down and cultured at $1x10^6$ cells/ ml in DC media with 20ng/ml of GM-CSF and 20ng/ml of IL-4 (PeproTech Inc., Rocky Hill, NJ) in p75 filter flasks. On day 3 of culture the cells were fed with and additional 5ml DC media and 100ng of GM-CSF and IL-4. Dendritic cells were infected with *M. tuberculosis* on day 6 of culture (MOI 4) in the presence of GM-CSF. *M. tuberculosis* culture from day 5 or 6 was centrifuged at 4000 RPM for 10 minutes and then resuspended in DC media. The *M. tuberculosis* suspension was then sonicated twice in a closed cup-horn sonicator at a

power of 5 for 10 seconds each time. Following sonication the bacillus was added to the DC culture at a multiplicity of infection of 4. Cells were infected for 14-20 hours. Extracellular bacteria were separated from the cells by low speed centrifugation. Infected and uninfected DCs were used for stimulation assays.

FACS analyses of Cell Surface Markers.

To determine cellular infiltrate in the lung, at 10-day intervals lungs were removed for flow cytometric analysis. Lungs were subjected to a short period (20 min.) of digestion with 1mg/ml collagenase A and 25 Units/ml DNAse (Boehringer Mannheim, Mannheim, Germany) at 37°C. The suspension was then pushed through a cell strainer as previously described [63]. Red blood cells were lysed with lysis buffer (0.14M NH_4Cl/ 0.017Mtris pH= 7.65) and the single cell suspension was counted. The samples were stained with 0.2 μg anti-CD4 (clone H129.19), anti-CD8 (clone 53-6.7), and anti-CD69 (clone H1.2F3) in FACS buffer (0.1% NaAzide, 0.1% BSA, 20% mouse serum). Following washes, the cells were fixed in 4% PFA for 1 hour and collected on a FACSCaliber (Beckon Dickinson). Cells were gated on the lymphocyte population by size and granularity. Analysis was performed on Cell Quest software (BD-Pharmingen, San Diego, CA).

Intracellular Cytokine Staining.

Single cell suspensions of the lung were prepared as described above. The lung cells were then cultured at $0.5x10^6$ cells/ml in the presence of 2μM monensin and with or without anti-CD3 (0.1μg/ml) and anti-CD28 (1μg/ml) for 4 hours (37°C and 5%CO) in 24 well plates. Following stimulation, the cells were collected, spun down and stained for T lymphocyte surface markers as described above, following fixation with 100μl 4% PFA, the cells were transferred to a 96 well plate, washed 2 times with permeablization buffer (FACS buffer + 0.1% saponin), stained with

anti-IFNγ (2μl neat) for 20 minutes at 4°C, and then washed 2 times with permeablization buffer and once with FACs buffer. The cells were then resuspended in 4% PFA and collected on the FACS Caliber (Beckon Dickinson).

T cell proliferation Assay.

DCs uninfected and infected at a MOI of 4 for 18 hours were plated in triplicate in a 96-well U-bottom plate (Corning Incorporated, Corning, NY) at different concentrations of DC: T cell ratios (1:25, 1:50 and 1:100) in T cell media (DMEM containing 10% certified FBS, 10mM sodium pyruvate, 2mM L-glutamine, 25mM HEPES (Gibco, Gaithersburg, MD) and 50μM 2-ME. As a source of T lymphocytes, splenocytes were obtained from CXCL10-/- and WT mice by crushing the spleens in cell strainers. Red blood cells were lysed as described above and macrophages were depleted by adherence on plastic petri dishes for 2 hours at 37°C/5% CO_2. Cells suspensions were added at $2x10^5$cells/ well (in a final volume of 100μl) and cultured in media alone (negative control), 5μg/ml ConA (a positive control), uninfected, or infected DCs for 3 days. Cells were pulsed for the final 18 hours of culture with 1μCi/well [^{3}H] thymidine (Amersham Life Sciences, Inc., Arlington Heights, IL) and the incorporation of radioactivity was measured by counting cell lysates on filters in a scintillation counter. The simulation index was determined by (CPM T Cells+infected DCs)/(CPM Tcells+uninfected DCs).

Culture of lung cells.

Lung cells from CXCL10-/- and WT mice infected for 4 weeks were obtained as described above and plated in 96-well U-bottom plates in T cell media supplemented with 30μg/ml gentamicin (Gibco, Gaithersburg, MD), 15-20 U/ml rIL-2 (Boehringer Mannheim, Indianapolis, IN), and 1mM aminoguanidine at $2x10^5$ cells/well. MHC Class II DCs were infected for 20 hours as described above and were added to the cell cultures at $6x10^3$ cells/well. After 2-3 days

of culture 100µl of media were removed from each well and replaced with fresh media containing IL-2. Cells were cultured for an additional 3-4 days prior to the CTL assay.

Cytotoxicity Assay.

Lymphocytes harvested from 5-7 day stimulation cultures were tested in a 4-h ^{51}Cr release assay. Bone marrow derived macrophages were prepared (as described in Section 7.2 Materials and Methods) and used as targets (uninfected or infected at MOI 3). $2x10^6$ macrophages were labeled with 100ul $Na^{51}CrO4$ (Amersham) in Teflon jars (Savillex, Minnetonka, MN) for 1 hour at 37°C. Macrophages were washed 3 times and then added to 96-well U-bottom plates at $4x10^3$ cells/ well. Cultured T cells were added at various effector: target ratios (1:12, 1:25, 1:50) in a total volume of 100µl in T cell media. After 4 hours, 85µl of supernatant was removed from each well and 100ml of undiluted vesphene was mixed with the supernatant. This mixture was counted in a gamma counter. Spontaneous release was determined by culturing target cells in medium along and total release was calculated by lysing target labeled macrophages with 0.1% Triton-X. Percent specific lysis was calculated using the formula: 100x[(experimental CPM-spontaneous CPM)/ (total CPM-spontaneous CPM)].

Statistics.

Statistical analysis was performed comparing CXCL10-/- vs. wild type littermates and comparing anti-CXCL10/anti-CXCL9 to their controls. Student t-test was preformed using GraphPad Prism3 software for the analyses.

8.3 Results.

In the absence of CXCL10 and CXCL9, mice control M. tuberculosis infection.

CXCL10 deficient mice (CXCL10-/-), wild type littermates, C57Bl/6 mice treated with anti-CXCL10 and anti-CXCL9 antibodies, and C57Bl/6 control mice were aerosol infected with

approximately 100 colony forming units of Erdman *M. tuberculosis*. One group of CXCL10-/- mice was from a pure 129 background, while the second group was B6/129 mixed background. These mice were matched with their wild type littermates. In all experiments performed, the data between these two groups were very similar. Data from the B6/129 mixed litters will be presented here. CXCL10-/- mice controlled *M. tuberculosis* infection as well as their wild type littermates (Figure 22). As seen in wild type C57Bl/6 mice, the bacterial burdens increased rapidly after infection, and by 3-4 weeks post infection the number of bacteria in the lungs reached a plateau. The anti-CXCL10/anti-CXCL9 treated mice also controlled infection as well as their controls (Figure 22). No mice succumbed to infection during the course of the experiment. Therefore CXCL10 and CXCL9 may not be necessary for control of mycobacterial growth.

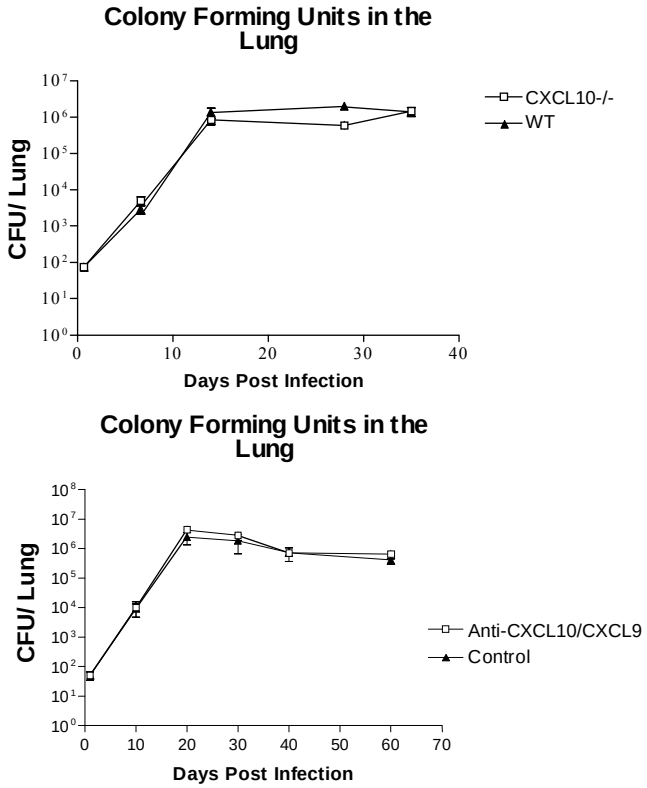

Figure 22. Mice control *M. tuberculosis* infection in the absence of functional CXCL9 and CXCL10.

CXCL10-/- mice and anti-CXCL9/anti-CXCL10 treated mice control aerosol *M. tuberculosis* infection. Total colony forming units in the lung were calculated from plating serial dilutions of lung homogenates. Each point represents 4 mice and the error bar is the standard error of the group. There were no significant differences found between experimental and control groups at any time.

Migration of lymphocytes to the lungs is unaffected after M. tuberculosis infection of mice lacking functional CXCL10 or CXCL9.

Due to evidence that the receptor for CXCL9 and CXCL10, CXCR3, is expressed on Th1 lymphocytes and a large lymphocytic infiltrate occurs in the lungs during *M. tuberculosis* infection, we examined the numbers of lymphocytes migrating to the lungs by flow cytometric analysis. Upon infection the numbers and percentages of lymphocytes migrating to the lungs of CXCL10-/- mice and anti-CXCL10 /anti-CXCL9 treated mice were similar to the experimental

control mice (Figure 23, data not shown). Despite this, two weeks after infection, the percentage of lymphocytes expressing early activation marker, CD69, was lower in CXCL10-/- mice compared to controls (Figure 24). Unfortunately, the activation of the immune response in the experiment with anti-CXCL9/anti-CXCL10 treated mice and control mice may have started slower, since at two weeks post infection, the early activation marker, CD69 was not yet observed on lymphocytes. This may have been due to a lower than expected inoculum. By three weeks post infection the numbers of CD69+ lymphocytes was similar in all groups of mice (Figure 24).

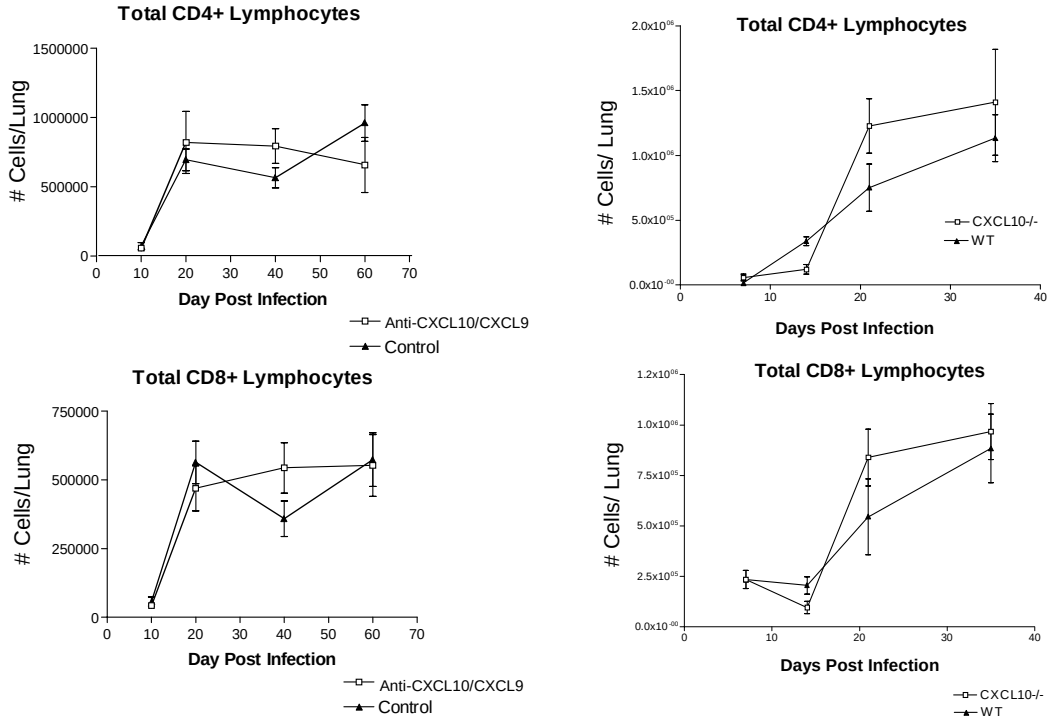

Figure 23. T lymphocytes migrate to the lungs of CXCL10-/- and anti-CXCL9/anti-CXCL10 treated mice.

Flow cytometric analysis was performed to determine the number of lymphocytes within the lungs following *M. tuberculosis* infection in CXCL10-/- and anti-CXCL9/anti-CXCL10 treated mice. CD4+ and CD8+ lymphocytes migrate to the lungs in similar numbers in the experimental and control groups. Each point represents 3-4 mice. The error bars represent standard error.

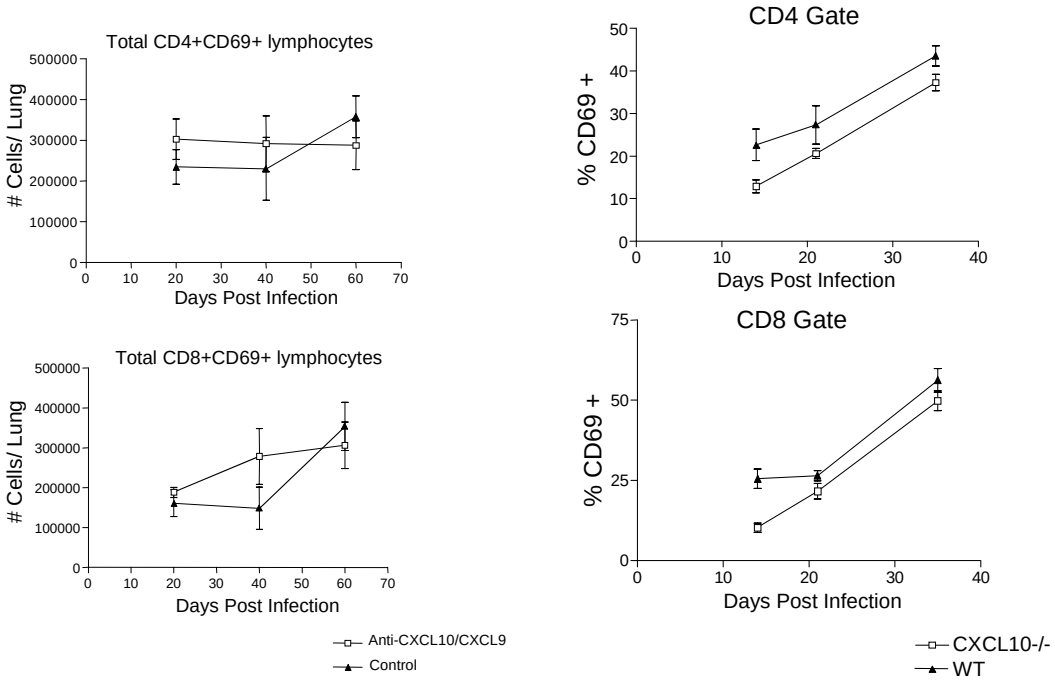

Figure 24. T lymphocytes in the lung are activated in CXCL10-/- and anti-CXCL9/anti-CXCL10 treated mice.

The number and percentage of CD69+ cells in the CXCL10-/- and anti-CXCL9/anti-CXCL10-/- is similar to control mice by 3 weeks post infection. In the CXCL10-/- mice the percentage of CD69+ lymphocytes is lower at 2 weeks post infection, but the reduction is transient. Each point represents 3-4 mice. The error bar represents the standard error.

Cell migration to the lymph nodes.

The lymph nodes serve as a priming and activation site for antigen specific lymphocytes. Naïve cells migrate to the lymph nodes, where they are primed and expanded to generate effector lymphocytes. In the anti-CXCL9 and anti-CXCL10 treated mice, we examined the numbers of cells and the number of activated cells in the lymph nodes after infection. There was either a delay in migration, activation or expansion of CD4 and CD8 lymphocytes in the antibody treated mice. Clearly the number of lymphocytes and the number of activated lymphocytes present in the lung draining lymph nodes was lower in the antibody treated mice early after infection

(Figure 25). By two months post infection, the numbers of cells in the antibody treated mice was higher than in controls, but the number of activated lymphocytes was similar.

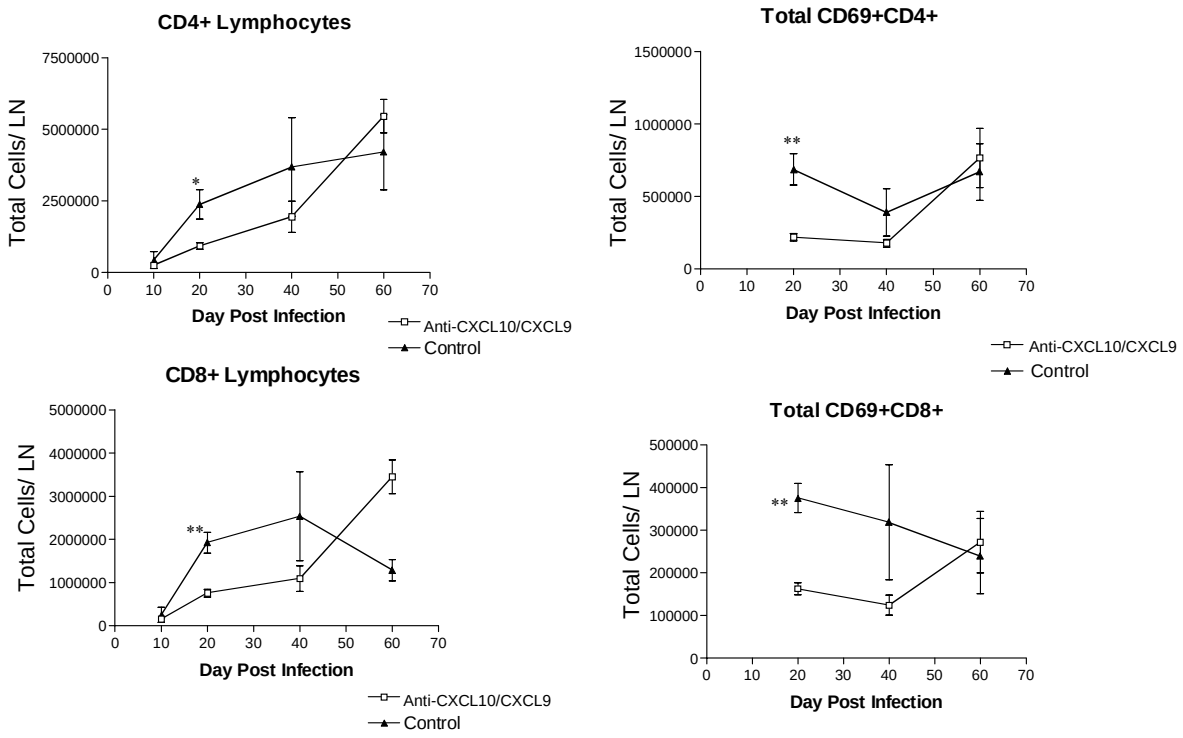

Figure 25. Cell migration to the lymph nodes was delayed in anti-CXCL9/anti-CXCL10 treated mice.

Flow cytometric analysis was performed to determine the number of lymphocytes and activated lymphocytes present in the lung draining lymph nodes of anti-CXCL9/anti-CXCL10 treated and control mice. Each point represents 3-4 mice. The error bar represents the standard error. * $p<0.05$, ** $p<0.005$

IFNγ production in the absence of functional CXCL9 and CXCL10.

IFNγ production is essential for control of *M. tuberculosis* infection [64, 98]. There is increasing evidence that the signaling of chemokines not only leads to migration of cells, but can also lead to activation. Intracellular cytokine staining was performed to determine whether the lymphocytes in the lungs were activated and capable of producing IFNγ. By three weeks post infection (the earliest we examined IFNγ production in this experiment), the lymphocytes from CXCL10-/- and anti-CXCL9/anti-CXCL10 mice produced levels of IFNγ similar to that

produced by wild type and control mice (Figure 26). There were slightly higher levels of IFNγ present in the wild type or control mice, but the differences were not significant. ELIspot analysis performed on the anti-CXCL9/anti-CXCL10 mice confirmed that there were similar amounts of IFNγ being produced in the experimental and control groups (data not shown).

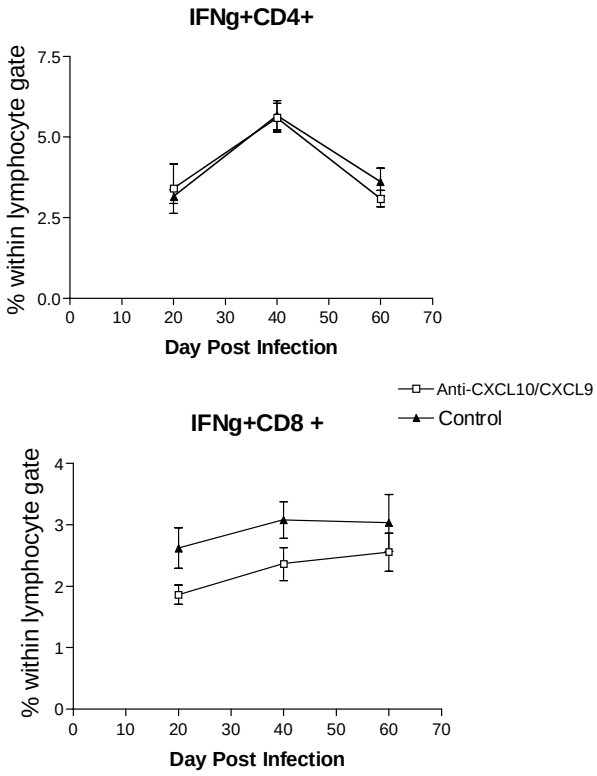

Figure 26. IFNγ production in the absence of functional CXCL9 and CXCL10.

Intracellular cytokine staining was performed on lymphocytes following a short ex vivo stimulation with anti-CD3 and anti-CD28. Each point represents 3-4 mice. The error bars represent standard error.

Lymphocytes from CXCL10-/- mice can serve as cytotoxic lymphocytes and proliferate.

To determine whether lymphocytes in the lungs were responsive to *M. tuberculosis*, we tested the cells for cytotoxicity and ability to proliferate. Following expansion of CD8 lymphocytes, a cytotoxic T cell lysis assay was performed. The lymphocytes from the lungs of CXCL10-/- or wild type mice were equally capable of lysing infected macrophage targets with

very little nonspecific lysis of uninfected macrophages. In addition the lymphocytes when stimulated with infected DCs at various ratios, proliferated in the presence of antigen. This proliferation increased as the ratio of DC: T cells decreased and the probability of interaction with antigen presenting cells increased. (Figure 27)

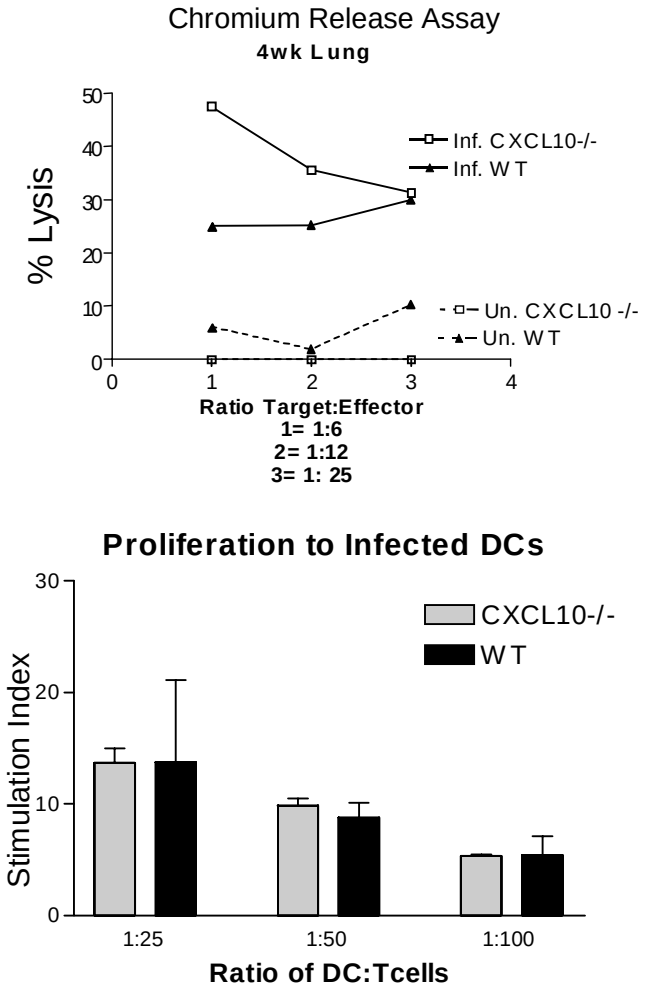

Figure 27. Cytotoxic activity and proliferative ability of T lymphocytes from CXCL10-/- mice.

A. A Cytotoxic Lysis Assay (CTL) was performed on lymphocytes isolated from the lungs at 4 weeks post infection. Targets were either infected or uninfected macrophages. The graph represents the % specific lysis for each of these targets. B. At 4 weeks post infection the ability of the lymphocytes to proliferate in response to antigen was tested in a [^{3}H] thymidine incorporation assay. The error bar represents 4 mice at each ratio of lymphocyte to antigen presenting cell.

8.4 Discussion

The signaling behind migration of cells to the lung and the formation of the granuloma appears to be a very intricate, complicated system. There has been evidence for the role of CXCL9 and CXCL10 in migration of T lymphocytes both in vitro and in vivo. The evidence for their roles in migration of cells to the lungs during an inflammatory response has been less defined, although in *T. gondii* infection there is evidence that CXCL10 is required for the recruitment of CXCR3+ cells to the lung. Our data indicates that CXCL9 and CXCL10 are not necessary for migration of effector lymphocytes to the lung and for control of *M. tuberculosis* infection. The CXCL10-/- mice showed no signs of exacerbated disease. In addition the CXCL10-/- lymphocytes migrated to the lung and were activated. The T lymphocytes produced IFNγ, proliferated and had cytolytic potential. Even when both CXCL9 and CXCL10 were neutralized with antibodies, the mice had a similar pattern of disease as control mice. The experiment utilizing the monoclonal antibody administration also addressed the migration of lymphocytes to the lymph nodes, and although there appeared to be early differences in the numbers of lymphocytes present in the lung draining lymph nodes, the mice controlled infection.

Early migration of T lymphocytes into the lung draining lymph node was affected by neutralization of CXCL9 and CXCL10, but enough T lymphocytes were primed and activated in the lymph node to travel to the lung and control infection in this model. The ability of mice to overcome deficiencies in chemokines and chemokine receptors is not a novel phenomenon. In CCR2-/- mice, the immune response was more robust than necessary to control infection (see Section 10.4 Discussion). In this case there were no differences in the numbers of cells in the lungs, even though there are fewer cells in the lymph nodes. This raises a number of questions. Where are the cells coming from in the anti-CXCL9/anti-CXCL10 treated mice? In wild type

mice, are the excess cells in the lymph nodes migrating to an organ other than the lung? Or is there more cell death in the wild type lymph nodes or lungs?

We did not test the effectiveness of the administration of the antibodies. This regimen was effective in the *T. gondii* model, where the mice were susceptible to infection following infection with a lymphocytic migration deficiency [155]. Whether redundancy exists in vivo truly is a difficult question to ask. Another CXCR3 ligand does exist, CXCL11 (I-TAC); although there was induction of this chemokine following in vitro infection of macrophages, we have been unable to find reagents to address its function in vivo.

Interestingly the experiments that drove us to study CXCR3 ligands were rooted in the regulation of chemokine expression by TNF. In the absence of TNF, there is a down regulation in the expression of CXCL10 and CXCL9 as described in Chapter 1 (Section 7.0). Although CXCL9 and CXCL10 are not the only chemokines affected by the loss of TNF, the loss of CXCL9 and CXCL10 did not recapitulate the pathology seen in the absence of TNF.

The role of CXCL10 in the immune response to *T. gondii* may be very different than the role of this chemokine in *M. tuberculosis* response for many reasons. Although both infections are controlled through a strong cell-mediated immune response, control of *T. gondii* also was very dependent on the innate immune response. Infection with *T. gondii* led to very early (day 3) detectible induction of CXCL10 in the spleen and liver by RNase protection assay, whereas during *M. tuberculosis* infection in mice, induction of CXCL10 was not detected in the lungs until at least day 9 post infection. In addition, the peak of CXCL10 expression during *T. gondii* infection was as early as day 7, on the other hand during *M. tuberculosis* infection of mice the expression of CXCL10 reached a plateau between 3-4 weeks. This implies that CXCL10 is necessary during acute infection of *T. gondii*- even at a time point where CXCL10 was difficult

to detect in *M. tuberculosis* infection. Another possible explanation for the differences observed is that *M. tuberculosis* itself can induce expression of other chemokines, which can signal lymphocyte migration. This induction could occur through the presence of PAMPs signaling through toll-like receptors or other pattern recognition molecules. The induction of these chemokines may override the necessity for IFNγ dependent induction of chemokines such as CXCL10, as in *T. gondii* infection. Another difference could purely be due to basic differences in the model. Replication of the *M. tuberculosis* bacillus is slower than replication of *T. gondii*, therefore initially the antigenic load is not as high and the immune response may have more time to develop after *M. tuberculosis* infection.

A recent study demonstrated that CXCR3-/- mice infected with *M. tuberculosis* exhibited delayed granuloma formation [72]. Surprisingly, the lymphocyte migration was not affected in these mice, but anti-CXCL9 Ab treated and PMN depleted mice had similar pathology. In short, they describe PMNs as a major producer of CXCL9 and important for early granuloma formation. Despite the differences in pathology, these mice (CXCR3-/-, anti-CXCL9 Ab treated and PMN depleted mice) are all capable of developing pulmonary granulomas and there were no differences observed in the survival or mycobacterial burden. On one hand, this study attempts to argue that early granuloma formation is not necessary for control of infection. Although there were fewer granulomas and the size of the granulomas was smaller, the granulomas that form in PMN- depleted or CXCR3-/- mice are organized. We can argue that within these granulomas the cell mediated immune response is effective in controlling the low dose aerosol infection.

9.0 Chapter 3 Enhanced dendritic cell migration and T cell priming in lymph nodes result in increased pulmonary lymphocytic infiltration in chemokine receptor 5 (CCR5)-deficient mice following *Mycobacterium tuberculosis* infection.

This chapter has been submitted to Journal of Immunology. The chapter in this form is more inclusive that the submitted paper and includes additional data that was not shown in the submitted paper.

9.1 Introduction

In this study, we addressed the role of CCR5 in murine *M. tuberculosis* infection. *M. tuberculosis* infection causes an increase in the expression of β- chemokines, CCL3, CCL4 and CCL5 and their receptors, including CCR5, in the lungs. CCR5 is a co-receptor for HIV [156], and as a result, interest has emerged in the role of CCR5 in infectious diseases and as a target for HIV therapy. CCR5 is expressed on granulocytes, macrophages, immature DCs, CD8+ lymphocytes and at a high level on T helper 1 lymphocytes [157, 158]. Studies in infectious disease models illustrate the variety of functions of CCR5 in the immune response. In CCR5-/- mice infected with *Leishmania donovani*, the boundaries of the granulomas were difficult to demarcate, yet the mice had fewer parasites than wild type mice [159]. On the other hand, CCR5-/- mice were more susceptible to influenza A virus, *Cryptococcus neoformans, Listeria monocytogenes,* and *Toxoplasma gondii* [160-163]. CCR5 was associated with elimination of extracellular polysaccharide during *C. neoformans* infection [160], induction of IL-12 during *T. gondii* infection [161], and trafficking of cells to sites of infection [162, 163]. An understanding the use of CCR5 by the immune system will benefit the development of anti-microbial drugs and vaccines.

The data presented here support a role for CCR5 in dendritic cell migration. In this study we demonstrate that CCR5 transgenic knockout mice were capable of recruiting immune cells to the lung to form granulomas. CCR5-/- mice controlled *M. tuberculosis* growth in the lungs, spleen and liver, but had higher bacterial loads in the lung-draining lymph nodes. Substantially

higher numbers of T lymphocytes were found in the lungs of CCR5-/- mice, compared to controls. Our data are consistent with the hypotheses that higher bacterial loads in the lymph nodes are due to more dendritic cells carrying *M. tuberculosis* from the lungs to the lymph nodes or that there is retention of dendritic cells in the lymph nodes presenting antigen, resulting in more priming of lymphocytes in the lymph nodes. These primed/ activated lymphocytes then migrate to the site of infection (the lungs). These results suggest that CCR5 may be important for the migration to and retention of dendritic cells in lymph nodes during infection.

9.2 Materials and Methods.

Mice.

C57BL/6 female mice (Charles River, Rockland, MA) and CCR5-/- (Cmkbr5) male and female mice (8-14 weeks old) were used in all experiments. CCR5-/- mice (Jackson Laboratory, Bar Harbor, ME) were bred at the University of Pittsburgh in specific pathogen-free facilities. All infected mice were maintained in the BSL3 animal laboratories and routinely monitored for murine pathogens. The University Institutional Animal Care and Use Committee approved all animal protocols employed in this study.

Chemical and reagents. All chemicals were purchased from Sigma Chemical Co. (St. Louis, MO.) unless otherwise noted. Middlebrook 7H9 liquid medium and 7H10 agar were obtained from Difco Laboratories (Detroit, MI). Antibodies used in flow cytometry were obtained from Pharmingen (San Diego, CA).

Mycobacteria and infection of mice.

To prepare bacterial stock, *M. tuberculosis* strain Erdman (Trudeau Institute, Saranac Lake, N.Y.) was used to infect mice, and then bacteria were harvested from their lungs, expanded in 7H9 liquid medium and stored in aliquots at -80°C. Mice were infected via the aerosol route

using a nose-only exposure unit (InTox Products, Albuquerque, N.M.), and exposed to *M. tuberculosis* (1 x 10^7 CFU/ml in the nebulizer chamber) for 20 minutes, followed by 5 minutes of air. This resulted in reproducible delivery of 50-100 viable CFU of *M. tuberculosis*, which was confirmed by CFU determination on the lungs of 2-3 infected mice 1 day post-infection. Mice were infected i.v. via tail vein with $1x10^4$ CFU in 100 μl PBS/0.05% Tween 80. The tissue bacillary load was quantified by plating serial dilutions of the lung homogenates in 0.05% PBS/Tween 80 onto 7H10 agar. Total colony forming units were calculated.

Bone marrow derived macrophages.

Macrophages were derived from the C57BL/6 mice bone marrow based on adherence. The mice were euthanized and bone marrow was flushed out of the femur and tibia bones with DMEM as previously described [82]. The bone marrow suspension was washed twice with 2% FBS in PBS and the cells were counted. $2x10^6$ cells were plated on non-tissue culture treated petri dishes (Labtek) in 25ml macrophage media (25% L cell supernatant, 20% FBS, 1% L-glutamine, 1% sodium pyruvate, and 1% nonessential amino acids). After 4 days in culture the cells were fed with 10 ml fresh macrophage media. On Day 6 macrophages were infected with *M. tuberculosis* (MOI 4). Four hours post infection the supernatant was removed, cells were washed and fresh media added.

DC preparation.

Dendritic cells are derived from the C57Bl/6 mice bone marrow. The bone marrow was obtained as described as above. After the cells were washed and counted, the cells were resuspended in two non-tissue culture treated deep dish petri dishes in 20 ml DC media/ plate (10% FBS, 1% Sodium pyruvate, 1% L-glutamate) overnight. The following day, the nonadherent and semi-adherent cells were removed from the plates, spun down and cultured at $1x10^6$ cells/ ml in DC

media with 20ng/ml of GM-CSF and 20ng/ml of IL-4 (PeproTech Inc., Rocky Hill, NJ) in p75 filter flasks. On day 3 of culture the cells were fed with and additional 5ml DC media and 100ng of GM-CSF and IL-4. Dendritic cells were infected with *M. tuberculosis* on day 6 of culture (MOI 4) as previously described [82].

Flow cytometric analysis of lung cells.

To determine cellular infiltrate in the lung, at 10-day intervals lungs were removed for flow cytometric analysis. Lungs were subjected to a short period (25 min.) of digestion with 1mg/ml collagenase A and 25 Units/ml DNAse (Boehringer Mannheim, Mannheim, Germany) at 37°C. The suspension was then pushed through a cell strainer as previously described [164]. Red blood cells were lysed with lysis buffer (0.144M NH_4Cl/ 0.017Mtris pH= 7.65) and the single cell suspension was counted. The samples were stained with 0.2 μg anti-CD4, anti-CD8, and anti-CD69, or 0.15 μg anti-Gr1 and 0.2 μg anti-CD11b in FACS buffer (0.1% NaAzide, 0.1% BSA, 20% mouse serum). Following washes, the cells were fixed in 4% PFA for 1 hour and collected on a FACSCaliber (Beckon Dickinson). Analysis was performed on Cell Quest software (BD-Pharmingen, San Diego, CA).

Intracellular Cytokine Staining.

Single cell suspensions of the lung were prepared as described above. The lung cells were then cultured at $0.5x10^6$ cells/ml in the presence of 2μM monensin and with or without anti-CD3 (0.1μg/ml) and anti-CD28 (1μg/ml) for 4 hours (37°C and 5%CO) in 24 well plates. Following stimulation, the cells were collected, spun down as stained for T lymphocyte surface markers as described above, following fixation with 100μl 4% PFA, the cells were transferred to a 96 well plate, washed 2 times with permeablization buffer (FACS buffer + 0.1% saponin) stained with anti-IFNγ (2μl neat) for 20 minutes at 4°C, and then washed 2 times with permeablization buffer

and once with FACs buffer. The cells were then resuspended in 4% PFA and collected on the FACS Caliber (Beckon Dickinson).

Histopathology.

Tissue samples for histological studies were fixed in 10% normal buffered formalin followed by paraffin embedment. For histopathological studies 5- to 6- μm sections were stained with Harris' hematoxylin and eosin.

Immunohistochemistry.

5- to 6- μm sections of formalin fixed paraffin embedded lung were stained for CCL5, using anti-CCL5 (RANTES) antibody (Santa Cruz Biotechnology, Santa Cruz, CA). Immunohistochemistry was performed as recommended by manufacturer the goat ABC Staining System (Vector Laborabories, Inc., Burlingame, CA). The slides were deparaffinized and hydrated using a xylene, EtOH, water gradient. Antigen unmasking was performed with citrate buffer by microwaving the slides for 5 minutes x2. Following a wash in PBS and blocking with 2% donkey serum, the slides were stained with anti-CCL5 or goat anti-mouse IgG (at 1:50 in 2% donkey serum) overnight at 4°C. The slides were washed, and the secondary donkey anti-goat IgG- biotin (1:200) applied for 30 minutes at room temperature. Following additional washes the sections were incubated with AB enzyme reagent for 30 minutes. Following additional washes the sections were developed in peroxidase substrate (AEC substrate with 20ml N,N dimethlyformamide in 0.02M Na Acetate Buffer + 200ul H_2O_2) for 4 minutes. The sections were then washed with deionized H_2O and counterstained by dipping aqueous hemotoxylin. After rinsing the sections they were brightened in PBS and air dried. Crystal mount was applied overnight and then the sections were coverslipped.

Apoptosis Staining.

TUNEL staining was performed on formalin fixed paraffin embedded lung sections. The procedure was followed exactly as described by the ApopTag Manual using the ApopTag Peroxidase In Situ Apoptosis Detection Kit (Intergen Co, New York).

Apoptosis staining on lung cells was also performed using Annexin V and 7-Amino-actinomycin D (7-AAD) in conjuction with surface staining for lymphocytic markers. In short, after surface staining as described above, $1x10^6$ cells were washed in 100µl binding buffer (BD-Pharmingen, San Diego, CA) resuspended in 50µl of binding buffer and stained with Annexin V and 7-AAD (3µl each neat) for 15 minutes at room temperature. The cells were then washed with binding buffer and fixed in a 1:2 solution of 4%PFA:binding buffer. Cells were collected on the FACS Caliber within 1 hour of staining.

RNase Protection Assay (RPA).

A multiprobe RNase protection assay system (Pharmingen, San Diego, Ca) was used to determine the levels of mRNA for genes of interest at 10 day intervals post-aerosol infection in murine lung or infected macrophages in vitro. At the time of harvest, the lungs were snap frozen in liquid nitrogen and stored at -80°C. Total RNA was extracted using Trizol reagent (Life Technology, Grand Island, N. Y.) followed by treatment with RNase free-DNase (Roche, Indianapolis, IN) and RNase Inhibitor (Roche). Macrophage RNA was obtained from bone marrow derived macrophages by treating ~4 x 10^6 adherent cells with 1ml Trizol reagent. The RNA was subjected to RPA according to Pharmingen's protocol. In short, mRNA from macrophages or the lungs was hybridized overnight to [^{32}P]-UTP-labeled probes. The protected

[^{32}P]-UTP-labeled RNA probes were resolved on a 6% polyacrylamide gel and analyzed by autoradiography. Cytokine analysis was performed using a custom-made template set specific for NOS2, IL-4, IL-12p40, TNF, IL-1β, IL-1α, and IFN-γ. Chemokine analysis was performed using mCK5 multiprobe template set (Pharmingen). The expression of specific genes was quantified on a densitometer (ImageQuant Software, Molecular Dynamics, Sunnyvale, CA), relative to the abundance of housekeeping gene, L32. We also performed phosphorimaging quantification on some samples but found results identical to densitometry; therefore, only densitometry quantifications are shown.

Real time RT-PCR.

RNA was isolated from the lung using the TRIZOL isolation protocol with slight modifications. The lung was homogenized in 3ml of TRIZOL reagent and then two chloroform extractions were performed. Following an isopropanol precipitation, the RNA was washed with 70% ethanol and treated with RNase Inhibitor (Applied Biosystems, Foster City, CA) for 45 minutes. Following treatment at 65° C for 15 minutes the RNA was cleaned and DNase digested using the Qiagen RNA isolation kit, as directed by the manufacturer (Qiagen Inc., Valencia, CA). The RNA was reverse transcribed using Superscript II enzyme, as directed by the manufacturer (Invitrogen, Carlsbad, CA). For Real time RT-PCR we used the relative gene expression method [165]. HPRT served as the endogenous control, and uninfected lung or macrophages as the calibrator. Each primer and probe set was tested for efficiency (results efficient >97% for all primer/probe sets). All samples were run in triplicate and with "no reverse transcriptase" controls on an ABI Prism Sequence Detector 7700. Relative gene expression was calculated as 2 ^-ΔΔCt, where ΔCt = Ct (gene of interest)- Ct (endogenous control) and the ΔΔCt= ΔCt (sample) - ΔCt (calibrator). Results are expressed as relative gene expression to uninfected samples. The primer

and probe concentrations were used as suggested by Applied Biosystems with the final concentration of each primer at 400nM and probe at 250nM.

ELIspot analysis for IFNγ.

The ELIspot plates (96-well filtration plates Millipore MultiScreen MAIPS4510, Millipore Co., Bedford, MA) were pretreated with 95% EtOH and then washed three times with sterile PBS. The rat anti-IFNγ capture antibody (clone R4-6A2 BD Pharmingen, San Diego, CA) was added to the wells overnight at a concentration of 10μg/ml. The capture antibody was washed off (all washes PBS/0.1%Tween 20) and the plate blocked with T cell media containing 20% FBS for 2 hours. Single cell suspensions were prepared from the lung by pushing the lung sections through a cell strainer (Fisher, Pittsburgh, PA) using the plunger of a 5ml syringe. The cells were treated with red blood cell lysis buffer, washed twice in 2% fetal bovine serum in PBS and counted. 150,000 cells per well were incubated for 40-48 hours in the presence of 20U/ml IL-2 and either with media alone, uninfected bone marrow derived dendritic cells, *M. tuberculosis* infected dendritic cells (MOI = 3-4), or 10μg/ml Con A. Following the incubation at 37°C in 5% CO_2, the cells were washed off, the biotinylated anti-IFN-γ detection antibody (clone XMG1.2 BD Pharmingen) added for 2 hours at 37°C at 5μg/ml, followed by more washes and the addition of streptavidin – peroxidase for 1 hour at room temperature in a humidified chamber (Vectastain ABC Kit, Vector Laboratories, Burlingame, CA). After additional washing the plate was developed using the AEC substrate kit as directed by the manufacturer. ELIspot plates were read on the Immunospot™ CTL plate reader (Cellular Technology LTD, Cleveland, OH)

Statistical Analysis.

3-4 mice per group per time point were used for all studies. Statistical analysis was performed on the data utilizing GraphPad Prism Software for an unpaired t-test. For bacterial numbers and cell numbers, log transformation was performed prior to statistical analysis to normalize the data.

9.3 Results.

Expression of CCR5 and its ligands following M. tuberculosis aerosol infection.

CCR5 and its ligands are associated with the migration of Th1 cells and macrophages, two cell types important in a protective immune response to *M. tuberculosis*. Infection of bone marrow derived macrophages with *M. tuberculosis* induced CCL3, CCL4 and CCL5 expression (Figure 28A). Next we examined in vivo expression of these chemokines as well as CCR5 following *M. tuberculosis* infection. RNA from the lungs of C57BL/6 mice infected with *M. tuberculosis* via aerosol was isolated and real-time RT-PCR was performed on the RNA (Figure 28B). The expression of all known CCR5 ligands increased within the first two weeks of infection. CCL4 had the lowest relative expression of the CCR5 ligands. The expression of CCL5, when compared with other CC- chemokines was very high. Through immunohistochemical staining for CCL5 on granulomatous lung sections, we observed CCL5 protein expressed locally in both macrophage and lymphocytic areas of the granuloma (Figure 28C). CCR5 mRNA levels also increased in the mice following infection (data not shown). Whether this is an upregulation of CCR5 or merely a reflection of cells expressing CCR5 migrating into the lungs cannot be determined by this assay, and an appropriate anti-CCR5 antibody for use in flow cytometry is not available.

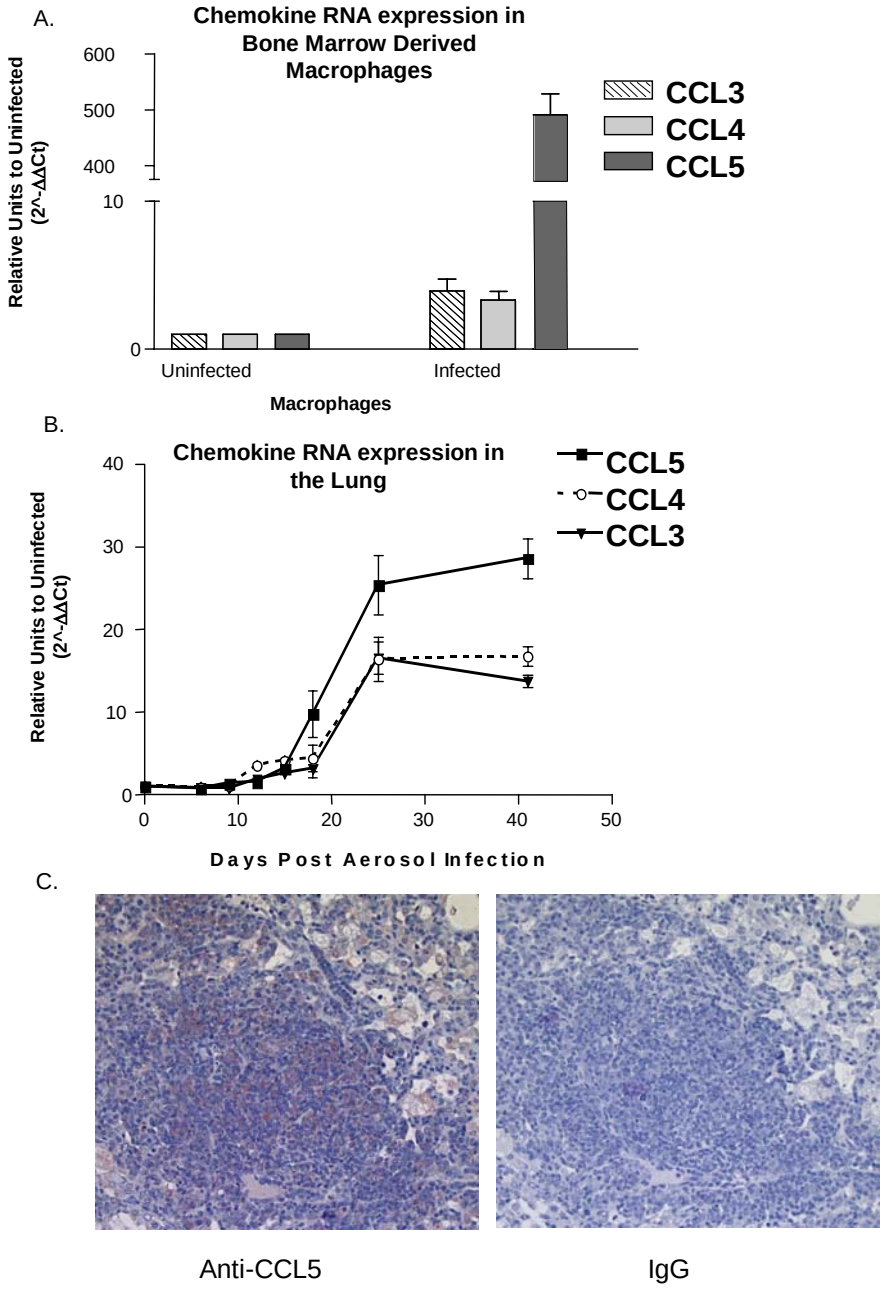

Figure 28. Expression of CCR5 ligands increased in *M. tuberculosis*-infected bone marrow derived macrophages and in the lungs of aerosol *M. tuberculosis*-infected mice.

A. Bone marrow derived macrophages were infected with Erdman strain of *M. tuberculosis* (MOI 4). RNA was isolated 24 hours post infection and real time RT-PCR was performed using HPRT as an endogenous control and uninfected macrophages as a calibrator. B. Expression of all CCR5 ligand RNAs increased in the lungs of C57Bl/6 mice during the first 4 weeks post aerosol infection. C. Protein expression of CCL5 can be localized to the granuloma during infection (100x). Immunohistochemistry was performed on lung tissue sections from C57BL/6 mice; expression of CCL5 was detected as early as 7 days post-infection. Shown are lung sections from 60 days post-infection.

M. tuberculosis infection in CCR5-/- mice.

To determine whether CCR5 plays a role in control of *M. tuberculosis* infection, C57Bl/6 and CCR5-/- mice were infected via the aerosol route with ~50 colony forming units (CFU). The survival of CCR5-/- mice was unaffected by *M. tuberculosis* infection. The mice survived >180 days, at which point experiments were terminated. There was no difference in bacterial loads, as determined by CFU, in the lungs (Figure 29A), liver or spleen (Figure 29D and E). Intravenous infection of CCR5-/- mice with $2x10^5$ CFU delivered via the tail vein, showed similar results (Figure 29B). In contrast, by 8 weeks post-aerosol infection, there were significantly higher bacterial loads in the lymph nodes of CCR5-/- mice (Figure 29C).

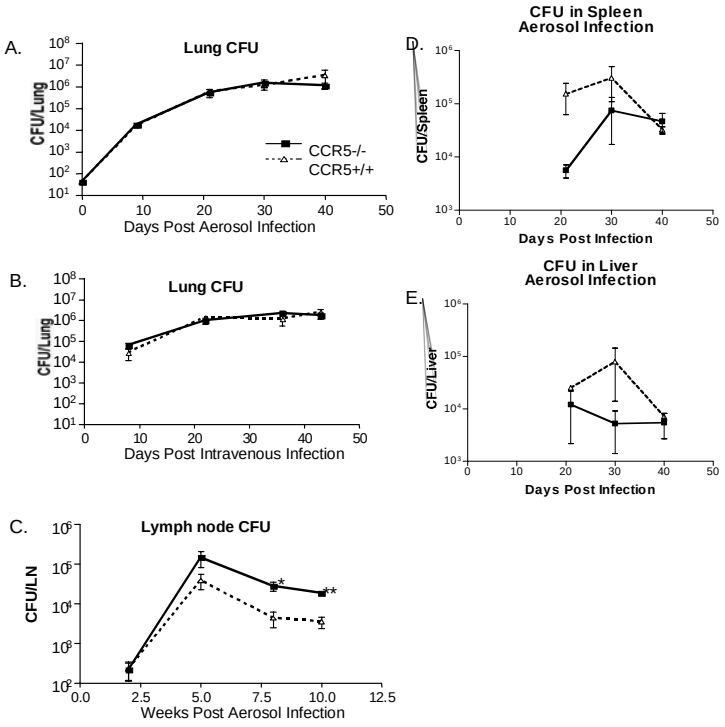

Figure 29. CCR5-/- mice control aerosol and intravenous *M. tuberculosis* infection.

A. Aerosol infection of C57Bl/6 and CCR5-/- mice led to increasing bacillary loads during the first 4 weeks post infection and then the number of colony forming units levels off as infection is controlled. Each point represents 4 mice and similar results were obtained in 3 independent experiments. B. Intravenous infection showed a similar pattern of *M. tuberculosis* growth in the lungs of the C57Bl/6 and CCR5-/- mice. C. The colony forming units in the lymph nodes of CCR5-/- mice was significantly higher by 7.5 weeks post infection (at week 5 p=0.01, week 8 p=0.03, and at week 10 p=0.008). Each point represents 3-4 mice. Similar results were obtained in 2 independent experiments.

Cell migration to the lungs and granuloma formation during M. tuberculosis infection in CCR5-/- mice.

Since CCR5 plays a role in migration of T cells and macrophages, we examined the cellular infiltrate in the lungs following infection. At predetermined time points, the lungs were removed, the total number of cells was calculated, and flow cytometric analysis was performed to determine cell populations. The single cell suspension was stained for T cell markers (CD4, CD8 and activation marker CD69) and macrophage and neutrophil differentiating markers (CD11b and Gr1). During initial infection the number of cells in the lungs was not significantly different between CCR5-/- mice and wild type mice. However, by 6 weeks post infection the numbers of CD4 and CD8 lymphocytes were significantly higher in CCR5-/- mice (Figure 30A and B). The number of macrophages and neutrophils increased in the CCR5-/- mice and the differences were significant at later time points (Figure 30C and D). The increased lymphocytic infiltrate in CCR5-/- mice was still evident at 6 months post infection (Table 8). The colony forming units in the lungs were not statistically different at this or any time point between CCR5-/- and wild type mice (Table 8).

Table 8. Cell migration in chronic infection in CCR5-/- and wild type mice (6 months post-infection).

The increased cellular infiltrate observed in CCR5-/- mice by 2 months post infection was also evident during the chronic stages of infection. CFU remained similar between the two groups of mice. (* p =0.047). For CD8 T cells, p = 0.072.

Cells ($x10^5$)	Macrophages	Neutrophils	CD4+ Cells*	CD8+ Cells	CFU (log)
CCR5-/-	1.12±0.04	1.28±1.44	**7.37±1.59**	7.97±3.25	6.39±0.25
CCR5+/+	0.88±0.02	0.49±0.08	**4.62±0.68**	4.26±0.68	6.13±0.01

The engagement of CCR5, especially by CCL5, plays a role in T lymphocyte activation in some infection diseases [166]. Therefore the expression of early activation marker, CD69, on the lymphocytes in the lungs was examined. There was no difference in the expression of the early

activation marker on CD4+ lymphocytes until 6 weeks post infection, when the CD4+ lymphocyte numbers were significantly higher in the CCR5-/- mice, $1.2x10^6 \pm 0.08x10^6$ v. $0.57x10^6 \pm 0.05x10^6$, but the percentage of CD69+ lymphocytes was continuously similar. On the other hand there was a significantly greater percentage of CD8+ lymphocytes expressing CD69 present in the lungs of the CCR5-/- mice compared to WT mice (58±2.8% vs. 41±0.5%, p=0.004).

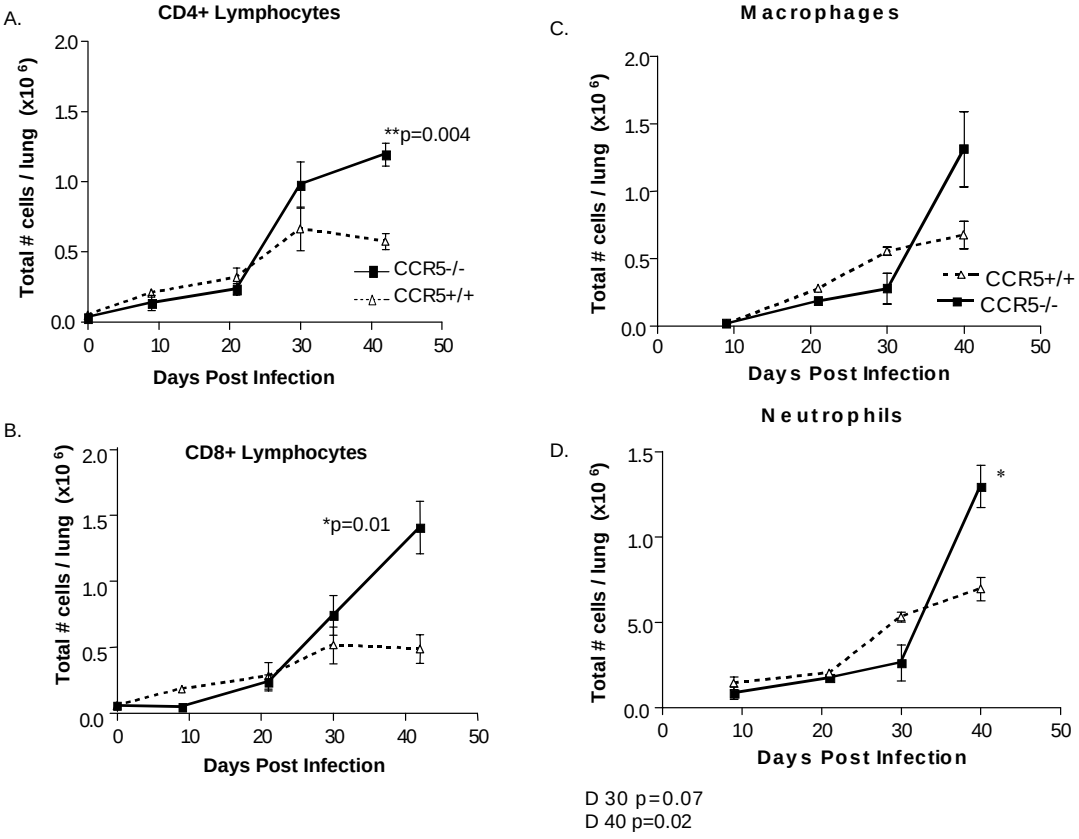

Figure 30. Infection of CCR5-/- mice led to greater numbers of lymphocytes in the lungs compared to wild type mice.

Flow cytometric analysis was performed on single cell suspensions from the lungs. The total number of CD4+ (A) and CD8 (B) lymphocytes increased to a significantly higher number in the CCR5-/- mice compared to wild type mice (**p=0.004, *p=0.01). Each point represents 3-4 mice. Similar results were obtained in three independent experiments and with intravenous infection.

Histology.

Histological analysis of the lung revealed that organized granulomas did form in CCR5-/- mice. These granulomas were similar to wild type mice granulomas at early time points. By 5 weeks post infection, the increased lymphocytic infiltrate in the lungs of CCR5-/- mice compared to lungs of wild type mice demonstrated by flow cytometry was evident in the histologic sections (Figure 31). The increased lymphocytic infiltrate is even more evident at 10 weeks post infection (Figure 31).

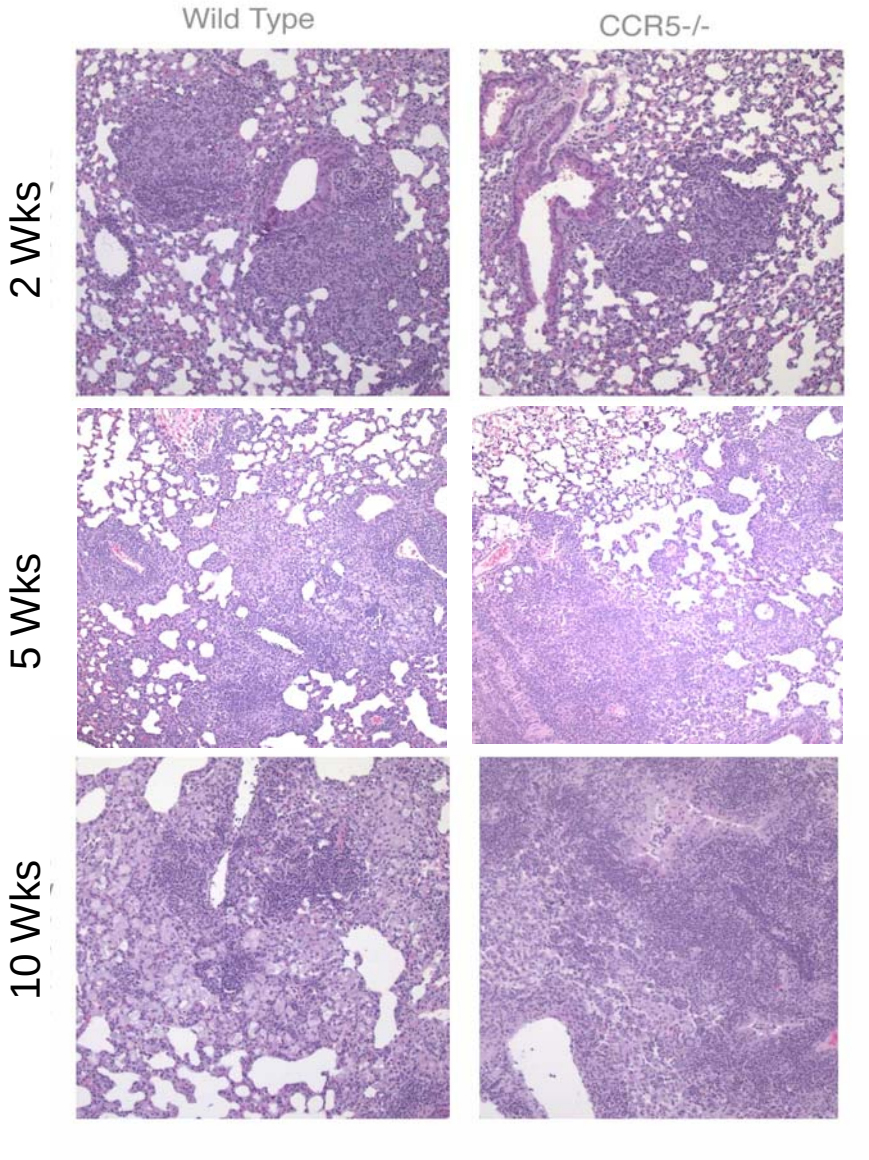

Figure 31. CCR5-/- mice formed granulomas with greater lymphocytic infiltrate.

Sections of the lung were stained with hemotoxylin and eosin (100x). Early after infection (2 weeks post infection), CCR5-/- mice and C57Bl/6 mice had similar cellular infiltrate in the lungs, but by 5 weeks post infection the greater lymphocytic infiltrate in the lung was apparent in the CCR5-/- tissue sections and granulomas.

Chemokine expression in CCR5-/- mice.

The results above indicated that CCR5-/- mice had no deficiency in cell migration to the lung, but rather have more cells migrating to the lung in response to infection. To address

potential compensatory mechanisms that could account for increased cell migration in the absence of CCR5, we looked for increased expression of CCR5 ligands and their alternative receptors, CCR1 and CCR3. Real time RT-PCR was used to determine whether there was increased expression of CCL3, CCL4, or CCL5 in the lungs of CCR5-/- mice (Figure 33). There was significantly greater CCL3 expression in CCR5-/- mice by day 41 post aerosol infection ($p=0.03$); although there was a trend toward greater expression of other inflammatory chemokines, such as CXCL10 and CCL2, these differences were not significant. Through RNase protection assays on lung RNA, no differences in the expression of CCR1 and no expression of CCR3 was detected in the CCR5-/- or C57Bl/6 mice (Figure 32).

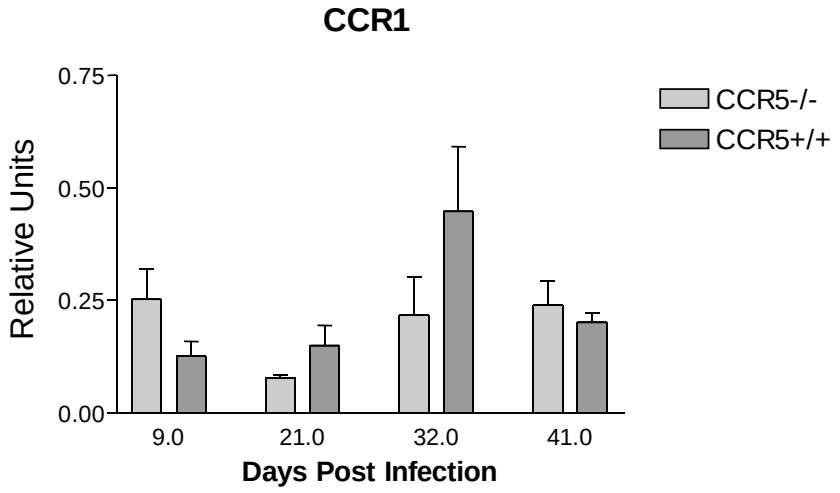

Figure 32. CCR1 mRNA expression in the lungs of *M. tuberculosis* infected, wild type and CCR5-/- mice.
RNase protection assay was used to determine the expression of CCR1 in the lungs of aerosol infected mice. Expression is measured relative to L32. There were no significant differences in the level of expression.

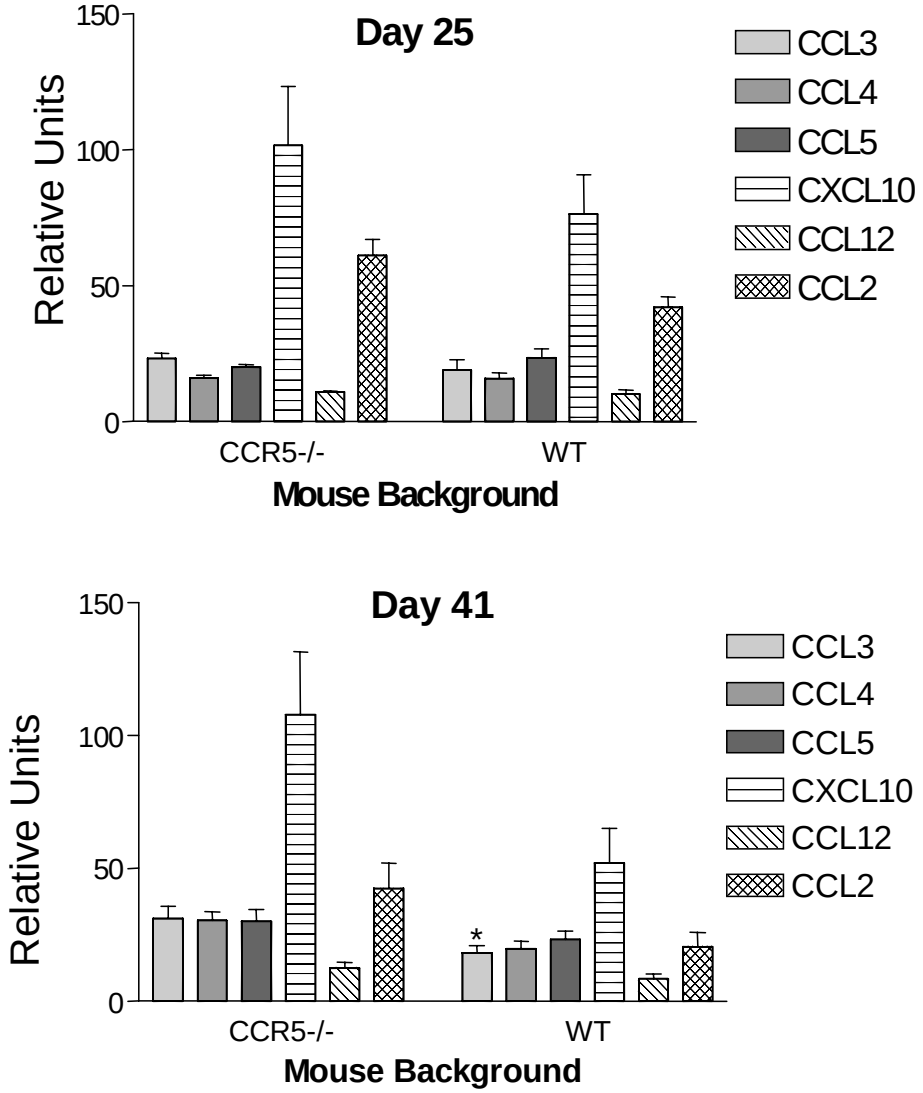

Figure 33. CCR5-/- mice had altered chemokine expression late in infection.

Real time rt PCR was performed on RNA isolated from the lungs of CCR5-/- and wild type mice. The relative units represented here are relative to uninfected wild type lung expression of these genes. There was a trend toward greater expression of chemokines in the CCR5-/- mice but only the difference in expression of CCL3 was significantly different. This could be a reason for increased cellular infiltrate to the lungs, but it could also be a result of a greater number of cells in the lungs.

Cytokine expression.

Control of *M. tuberculosis* infection depends on the activation of macrophages by IFNγ and TNF, leading to the induction of inducible nitric oxide synthase (NOS2) and production of reactive nitrogen intermediates, such as nitric oxide. To determine whether these components of the immune response were affected by CCR5 deficiency, RNase protection assay was performed on total lung RNA (Figure 34A). Early after infection the expression of TNF, IFNγ and NOS2 was similar in CCR5-/- and wild type mice, but by day 36 the CCR5-/- mice had higher expression of many inflammatory cytokines. There were significant differences in expression of NOS2 and TNF at day 36, but variability at day 45 resulted in differences that did not reach statistical significance. Relative units in the RNase protection assay is standardized to L32, a housekeeping gene, therefore the expression is relative on a per cell basis. Even though there were not significant differences per cell at later time points, since there were significantly more lymphocytes in the CCR5-/- mice, there was clearly higher expression of lymphocytic genes, such as IFNγ and TNF overall. The IFNγ gene expression differences were verified by intracellular cytokine staining (Figure 34B), and through these studies it is evident that the increased expression of IFNγ was due to an increase in the percentage of CD8+IFNγ+ lymphocytes in the lungs of CCR5-/- mice.

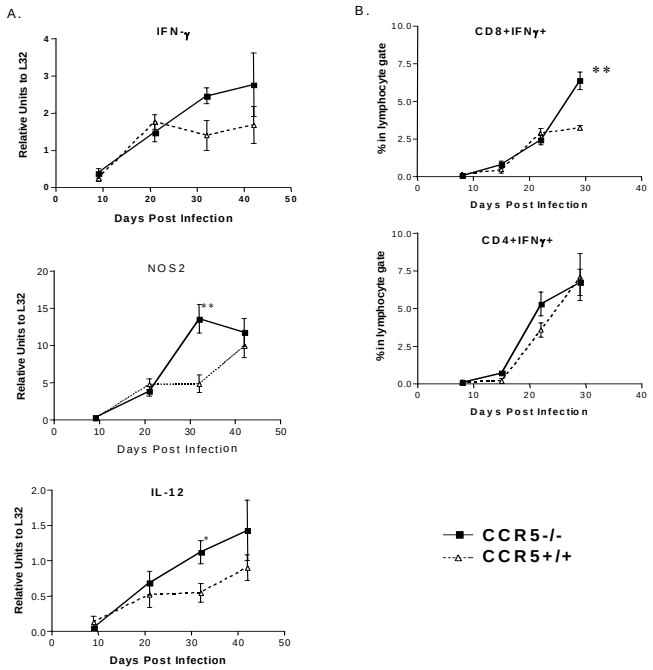

Figure 34. T helper 1 inflammatory cytokines increased to significantly higher levels in CCR5-/- mice compared to C57Bl/6 mice.

A. RNase protection assay was performed on whole lung RNA from CCR5-/- and wild type mice at predetermined time points. Expression of IFNγ, NOS2 and IL-12 is shown relative to L32 housekeeping gene. Each point represents 3-4 mice. Similar results were obtained in 2 independent experiments. *$p \leq 0.05$. B. Intracellular cytokine staining for IFNγ using anti-CD3/anti-CD28 as non-specific stimulus revealed that a similar percentage of CD4+IFNγ + cells were present in the lungs, while there were a greater percentage of CD8+IFNγ + cells in the CCR5-/- mice, compared to wild type mice. **$p<0.01$

Immune regulation in CCR5-/- mice.

There were a number of possible explanations for the higher numbers of lymphocytes in the lungs of CCR5-/- mice in response to *M. tuberculosis* infection. We hypothesized that there was less apoptosis in the CCR5-/- mice, therefore the cells were accumulating in the lungs instead of undergoing normal turnover. Using both TUNEL staining for apoptotic bodies and flow cytometric analysis for 7-AAD and Annexin V, there was no difference in the percentage of apoptotic cells between the CCR5-/- mice and wild type mice (data not shown), but due to the

increase in lymphocytes present in the lungs, there were actually significantly more apoptotic lymphocytes in the CCR5-/- mice (Figure 35).

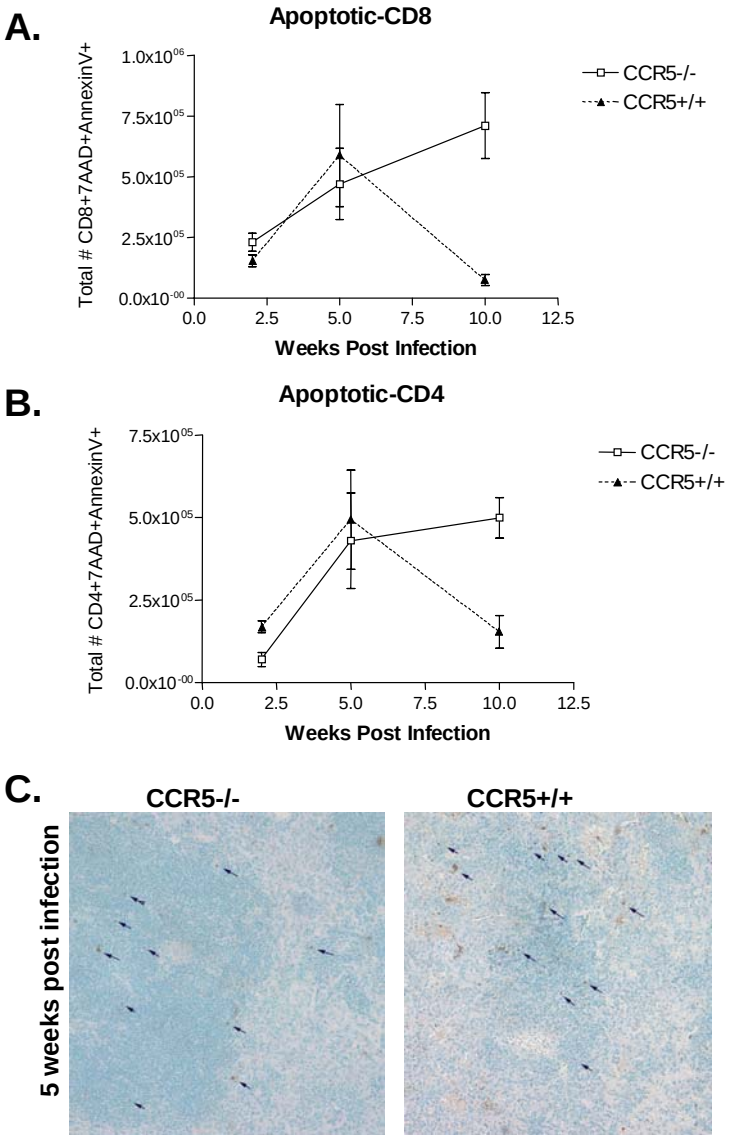

Figure 35. CCR5-/- mice did not have a decrease in apoptosis.

A. and B. Through FACS, the number of apoptotic lymphocytes was actually higher in the CCR5-/- mice. Therefore, the increase in cellular infiltrate in the CCR5-/- mice was not due to lack of apoptosis. C. Through TUNEL staining of sections of lung, it was evident that the CCR5-/- mice have similar levels of apoptotic cells present.

We also hypothesized that CCR5 was required to recruit regulatory T lymphocytes to the lungs during *M. tuberculosis* infection in mice, and that this absence could interfere with normal immune regulation in the lungs. Using CD4+ CD25+CD45RB^{lo} as markers for a regulatory T

cell population [167], flow cytometric analysis of lung cells demonstrated that significantly greater numbers of these cells infiltrated the CCR5-/- mice by 6 weeks post infection, indicating that CCR5 was not required for their recruitment to the lung (Figure 36).

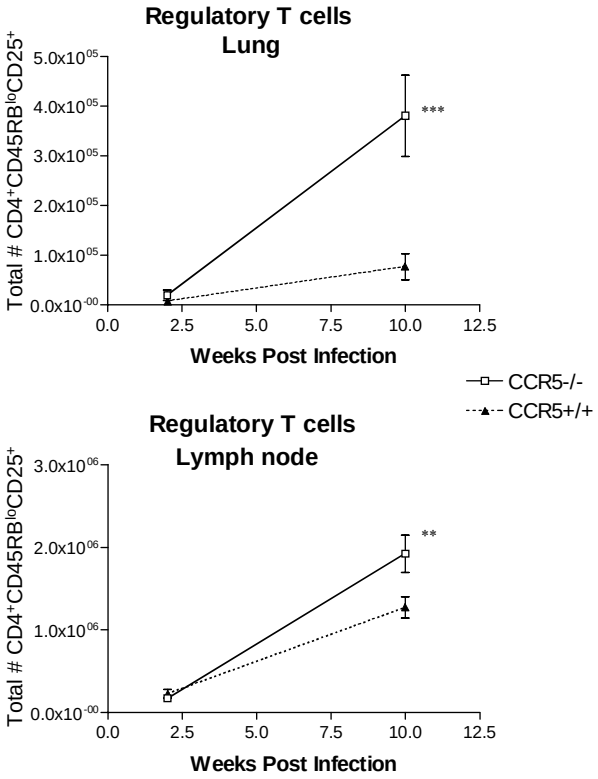

Figure 36. CCR5-/- mice do not have fewer CD4+CD45RB^{lo}CD25+ cells than wild type mice, but rather have significantly more cells of this phenotype.

This analysis was done using flow cytometric analysis on single cell suspensions from the lungs and lymph nodes of aerosol *M. tuberculosis* infected mice. Each time point represents 4 mice. ***p<0.005 **p<0.001.

Priming in the lymph nodes.

The lung-draining lymph nodes of CCR5-/- mice contained more *M. tuberculosis* bacilli than C57Bl/6 mice (Figure 29C). We hypothesized that this was due to greater numbers of dendritic cells migrating from the lungs to the lymph nodes carrying *M. tuberculosis.* As a result more T lymphocytes were being primed in the lymph node and then migrating to the lungs. To

explore this hypothesis, flow cytometric analysis was performed on the mediastinal lymph nodes of CCR5-/- mice following *M. tuberculosis* infection.

The overall total cell numbers of the lymph nodes of CCR5-/- and C57Bl/6 mice were similar, but at 5 weeks post infection there were statistically significant differences in the number of dendritic cells (defined as CD11c+CD11b$^{hi\ (or\ lo)}$ B7.2+ cells) in the CCR5-/- mice (Figure 37A). ELIspot analysis confirmed that significantly more lymphocytes from lymph nodes of CCR5-/- mice were primed to produce IFNγ when stimulated by either ConA or *M. tuberculosis*-infected dendritic cells (Figure 37B).

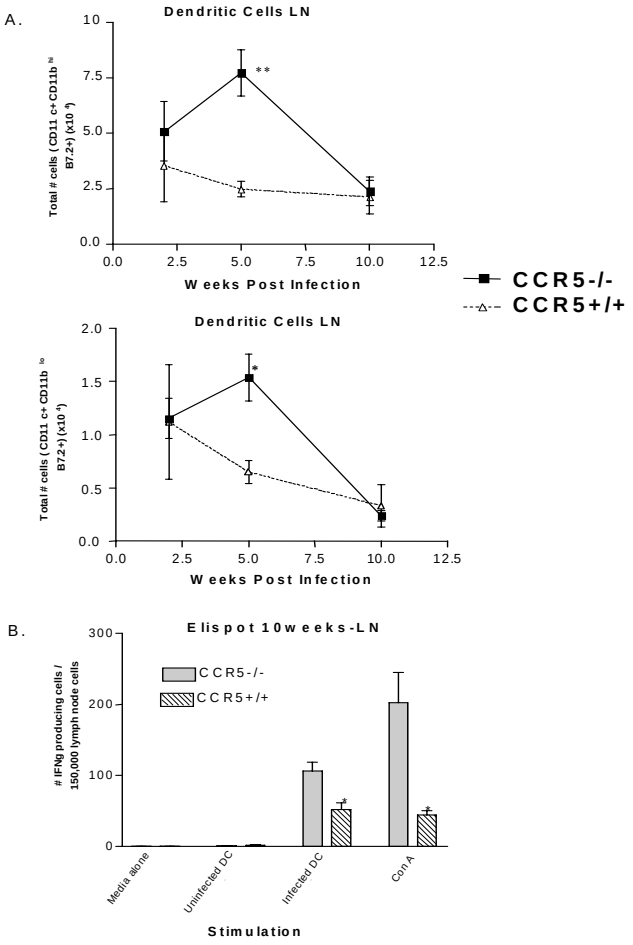

Figure 37. CCR5-/- mice had more dendritic cells and more primed lymphocytes within the lung draining lymph nodes.

The number of DCs was determined by flow cytometric analysis. A. There were significantly more CD11c+CD11b$^{hi\ (or\ lo)}$ B7.2+ cells in the lymph nodes of CCR5-/- mice at 5 weeks post infection (CD11b^{hi} **p=0.003, CD11b^{lo} *p=0.01). B. ELIspot analysis for IFNγ was performed on single cells suspensions from the lymph nodes. By 10 weeks post infection, the number of IFNγ producing cells in the lymph nodes was significantly greater when the cells were simulated with *M. tuberculosis* infected DCs (*p=0.013) or ConA (*p=0.011). Each bar represents 4 mice.

Intravenous infection.

In CCR2-/- mice, the requirement for CCR2 in control of *M. tuberculosis* infection was dose dependent. These mice were unable to control *M. tuberculosis* when it is administered at a standard dose of 2.5x10^5 CFU delivered intravenously, but could control lower dose aerosol or

i.v. infection [63]. We investigated whether the ability of CCR5-/- mice to control infection was route or dose dependent. CCR5-/- mice infected i.v. (2×10^5 CFU/mouse) controlled *M. tuberculosis* growth and the cell migration pattern were similar to that of CCR5-/- mice infected via the aerosol route (data not shown). The CCR5-/- mice again had strikingly high cell infiltration to their lungs, but with no apparent long-term detrimental effects of this increased infiltration.

9.4 Discussion.

CCR5 is expressed on many immune cells that are present in the lung following *M. tuberculosis* aerosol infection in mice, and the ligands for this receptor are induced in the lung by this infection. Whether the CCR5 is required for the migration of these cells to the lungs and subsequent control of infection was unknown. The results of this study provide evidence that CCR5 is not required for migration of immune cells to the lungs during *M. tuberculosis* infection, but may influence the retention of DCs in the lungs and migration to the lymph nodes. CCR5-/- mice had more bacilli in the lung-draining lymph nodes, as well as more dendritic cells. This coincided with enhanced priming of *M. tuberculosis*-specific T cells in the lymph nodes. Such increased priming likely accounts for the substantially increased numbers of T lymphocytes migrating to the lungs of CCR5-/- mice following *M. tuberculosis* infection.

Although CCR5 is known to be present on many immune cells, CCR5 function may be compensated for by other chemokine receptors and chemokines expressed in the lungs during infection. Although CCL4 and CCL5 can also signal through CCR1, the immune cells express many other chemokine receptors that may be responsible for the migration of these cells to the lung. These include CXCR3, CCR2, CCR1 and CXCR2. There is no reported increase in susceptibility to tuberculosis in humans carrying a deletion in the CCR5 gene (CCR5delta32).

The finding that CCR5-/- mice had more inflammation in their lungs was intriguing and unexpected. Recent data in other systems support an immunoregulatory role for CCR5. CCR5-/- mice had enhanced delayed-type hypersensitivity and humoral responses to T cell- dependent antigenic challenge [162]. When infected with influenza A virus, CCR5-/- mice had a hyperinflammatory response resulting in increased pulmonary inflammation and a decrease in survival [163]. In a murine model of colitis utilizing dextran sodium sulfate, CCR5 deficient mice had increased infiltration of CD4+ and NK1.1+ lymphocytes, along with a decrease in Th1 and an increase in Th2 cytokine expression [168].

We explored several possibilities for the increased numbers of lymphocytes in the lungs of the *M. tuberculosis*-infected CCR5-/- mice. There was increased expression of other chemokines (such as MIP1α) in the lungs of the CCR5-/- mice compared to wild type. Such increased expression/circulation of chemokines signaling through receptors other than CCR5 in the lungs could have resulted in the influx of immune cells. However, the increased expression may also have been a reaction to the numbers of cells in the lungs.

An alternative hypothesis was that there was less turnover of cells in the lungs of CCR5-/- mice. Recent studies have suggested that CCR5 signaling induces apoptosis in some situations. The HIV protein, Env, can activate CCR5 to induce the Fas and caspase-8 pathway resulting in CD4+ cell death [169]. However, in our studies there were equal or greater numbers of apoptotic cells in the CCR5-/- mice detected by two different methods, discounting this hypothesis in our system.

We also assessed whether CCR5 was important for migration of regulatory T lymphocytes to the lungs and the down regulation of Th1 responses, which could account for the observed increased inflammation in the absence of CCR5. Using the best markers known for

regulatory T cells [167] there were actually significantly more cells of this phenotype in the lungs of CCR5-/- mice. Therefore, CCR5 does not appear to be playing a role in regulatory T cell migration, but rather the increased migration may be a response to the increased inflammation, or simply related to the overall increase in cell numbers in the lungs of these mice.

A final hypothesis was that CCR5 is required for normal dendritic cell migration. We observed greater bacterial numbers in the mediastinal lymph nodes of CCR5-/- mice. Dendritic cells infected in the lungs are likely migrating and carrying *M. tuberculosis* bacilli to the lymph nodes. Previous studies demonstrated that infection of dendritic cells with *M. tuberculosis* matures the cells [26, 82, 170, 171], and mature dendritic cells migrate to the lymph nodes [172-174] where they prime naive T cells. At 5 weeks post infection there were more dendritic cells in the lymph nodes of CCR5-/- mice. The increased antigen dose (i.e. bacterial numbers) in conjunction with increased numbers of dendritic cells within the lymph nodes likely leads to enhanced priming of lymphocytes, as seen in the ELIspot assays. More primed T lymphocytes then are available to migrate to the site of infection in the lungs, resulting in the higher T lymphocyte numbers observed in the CCR5-/- mice.

Upon maturation, dendritic cells are believed to down regulate expression of CCR5 and CCR6 while they upregulate other receptors such as CXCR4 and CCR7, targeting these cells to the lymph nodes [reviewed in [175]]. We observed increased numbers of dendritic cells in the lymph nodes following infection in CCR5-/- mice, suggesting that during *M. tuberculosis* infection the expression of β-chemokines such as CCL3, CCL4 and CCL5 may normally retain CCR5+ dendritic cells in the lungs or recruit the dendritic cells out of the lymph nodes to the lungs. The absence of CCR5 apparently results in either increased migration from the lungs to the lymph nodes, or retention of dendritic cells in the lymph nodes.

This study further supports our previous finding that although there may not be striking differences in bacterial loads in the lungs of some transgenic mouse models, these models are very useful for studying the immune response [63, 176]. Addressing the function of molecules in the immune response requires careful experimental design and execution, and interpretation of experimental results. Roles may exist for molecules in the immune response even if the mouse is controlling infection at the level of bacterial burden. The immune response in the C57BL/6 mice, although not sufficient to eliminate bacterial numbers in the lungs, does control the infection. In this study, as well as other models (IL-10-/-, for example, H.M.S., J. Chan, and J.L.F, unpublished data), enhancing the Type 1 T cell response or the ability of T lymphocytes to enter the lungs over the wild type level, does not have an obvious beneficial effect on control of the infection. These data indicate that there are additional factors that must be induced or enhanced for increasing the ability of the host to eliminate *M. tuberculosis* infection.

In summary, our study supports a role for CCR5 in controlling dendritic cell migration to the lymph nodes, possibly by maintaining these cells in infected lungs. Thus, the absence of CCR5 resulted in increased numbers of both dendritic cells and *M. tuberculosis* bacilli in lymph nodes; we assume that the bacteria were carried from the lungs in dendritic cells. The result of the increased numbers of dendritic cells and antigens was enhanced T lymphocyte priming, leading to increased inflammation in the lungs.

10.0 Chapter 4 *Mycobacterium tuberculosis* in chemokine receptor 2 (CCR2) deficient mice: the influence of dose on disease progression.

This chapter has been modified from the published paper Scott, et. al. [63]. Copyright permission is on file.

10.1 Introduction

As described in the introduction to the thesis, the hallmark of *Mycobacterium tuberculosis* infection is granuloma formation. Following infection of alveolar and resident macrophages or dendritic cells in the lungs, monocytes and mycobacteria-specific lymphocytes migrate from the blood to the lungs and form granulomas. Within the localized environment of the granuloma, the immune cells control the bacterial replication and limit the spread of infection within the lung and to other organs. In *M. tuberculosis*-infected hosts, $CD4^+$ and $CD8^+$ T lymphocytes produce IFN-γ and TNF, cytokines which aid in control of infection and macrophage activation [64, 98, 103, 177]. Activated macrophages also produce TNF and reactive oxygen and nitrogen intermediates, which have anti-mycobacterial properties [177, 178]. Identifying factors involved in migration of cells to the lungs and granuloma formation is a key to understanding the immune response to *M. tuberculosis*.

There have been studies on the contribution of various chemokines to granuloma formation. Using "bead" instillation (PPD or schistosomal egg antigen beads) or injection of schistosomal eggs to induce granulomas in lungs of mice, roles for CCR1 and CCR2, as well as CCL5 and CCL2 in granuloma formation were demonstrated [179-182]. CCR2 is present on monocytes, macrophages and dendritic cells, as well as activated T cells. This chemokine receptor is a logical candidate for monocyte/macrophage recruitment to the lungs because macrophages and monocytes are chemotactic towards CCR2 ligands, macrophage chemotactic protein CCL2, CCL7 (MCP-3) and CCL12 (MCP-5). Studies in CCR2-/- mice have indicated that this receptor plays a major role in mediating monocyte/macrophage recruitment in response

to intracellular pathogens such as *Listeria monocytogenes* or *Cryptococcus neoformans* and to nonspecific inflammatory stimuli, such as thioglycollate or mycobacterial antigens [183-185], although resident macrophages were unaffected by the absence of CCR2 [185].

In this study we addressed the requirement for CCR2 in various infection models of *M. tuberculosis*, including aerosol infection and both high and low dose i.v. infection. Previously we, with co-workers, reported that CCR2-/- mice were highly susceptible to i.v. *M. tuberculosis* infection with significantly higher bacterial loads by 14 days post infection, severe pathology, and increased mortality [135]. These mice demonstrated macrophage and dendritic cell migration deficiencies and delays in IFN-γ and inducible nitric oxide synthase (NOS2) expression [135]. To determine whether the migration defects were evident following aerosol or i.v. infections with low doses of *M. tuberculosis,* we infected CCR2-/- mice and compared the development of the immune response to CCR2+/+ mice. Our results confirm that CCR2 plays a major role in migration of monocytes to the lung during *M. tuberculosis* infection. It also appears to affect early migration of T cells to the lung, which could result in the observed transient delay in IFN-γ and NOS2 expression. Surprisingly, the deficiencies in cell migration and cytokine expression did not noticeably affect the ability of CCR2-/- mice to control low dose *M. tuberculosis* infection. Finally, these data demonstrate that when studying infectious disease in knockout models, clear phenotypes may not be evident when solely evaluating bacterial numbers and survival. Functional assays may be necessary to reveal roles for components of the multifactorial immune system.

10.2 Methods and Materials

Mice.

C57BL/6 female mice (Charles River, Rockland, Mass.) and CCR2-/- [184] (8-14 weeks old) were used in all experiments. CCR2 +/- or -/- mice (heterozygous breeding pair provided by Dr. I. Charo, University of California, San Francisco) were bred and genotyped by PCR on tail DNA and maintained under specific pathogen-free conditions at the University of Pittsburgh Biotechnology Center. Only CCR2-/- mice were used. Mice were transferred to the Biomedical Science Tower Biosafety Level 3 animal facility at 7-8 weeks of age. All infected mice were maintained in the BSL3 animal laboratories and routinely monitored for murine pathogens by means of serological and histological examinations. The University Institutional Animal Care and Use Committee approved all animal protocols employed in this study.

Chemical and reagents.

All chemicals were purchased from Sigma Chemical Co. (St. Louis, MO.) unless otherwise noted. Middlebrook 7H9 liquid medium and 7H10 agar were obtained from Difco Laboratories (Detroit, MI). Antibodies used in flow cytometric analyses were obtained from Pharmingen (San Diego, CA). Pyrazinamide was purchased from Acros.

Mycobacteria and infection of mice.

To prepare bacterial stock, *M. tuberculosis* strain Erdman (Trudeau Institute, Saranac Lake, N.Y.) or H37Rv (Dr. John Belisle, Colorado State University, Fort Collins, Colorado) was used to infect mice, and then bacteria were harvested from their lungs, expanded in 7H9 liquid medium and stored in aliquots at -80°C. Mice were infected via the aerosol route using a nose-only exposure unit, as described in [94], which was confirmed by CFU determination on the lungs of 2-3 infected mice 1 day post-infection. High dose aerosol infection using $2x10^8$ or

$1x10^8$ CFU in the nebulizer resulted in delivery of 1500 or 4000 viable CFU, respectively, of H37Rv M. tuberculosis in two different experiments, and was confirmed by day 1 CFU in the lungs. Mice were infected i.v. via tail vein with either $1x10^4$ (low dose) or $2x10^5$ (high dose) CFU in 100 μl PBS/0.05% Tween 80. The tissue bacillary load was quantified by plating serial dilutions of the lung, liver, and spleen homogenates onto 7H10 agar as described previously [64].

Bone marrow derived macrophages.

Macrophages were derived from C57Bl/6 bone marrow based on adherence. The mice were euthanized and their bone marrow was flushed out of the femur and tibia bones with DMEM as previously described [82]. The bone marrow suspension was then washed twice with 2% FBS in PBS and the cells were counted. $2x10^6$ cells were plated on non-tissue culture treated petri dishes (Labtek) in 25ml macrophage media (25% L cell supernatant, 20% FBS, 1% L-glutamine, 1% sodium pyruvate, and 1% nonessential amino acids). After 4 days in culture the cells were fed with 10 ml fresh macrophage media. On Day 6 macrophages were infected with *M. tuberculosis* at an MOI of 4. Four hours post infection the supernatant was removed, cells were washed and fresh media was added.

Flow cytometric analysis of lung cells.

To determine cellular infiltrate in the lung, at 10-day intervals lungs were removed for flow cytometric analysis. Lungs were subjected to a short period (25 min.) of digestion with 1mg/ml collagenase A and 25 Units/ml DNAse (both from Boehringer Mannheim, Mannheim, Germany) at 37°C. The suspension was then pushed through a cell strainer as previously described [164]. Red blood cells were lysed with red blood cell lysis buffer (NH_4Cl/Tris Solution) and the single cell suspension was counted. The samples were stained with 0.2 μg anti-CD4, anti-CD8, anti-CD69, or 0.15 μg anti-Gr1 and 0.2 μg anti-CD11b in FACS buffer (0.1% NaAzide, 0.1% BSA,

20% mouse serum). Following washes, the cells were fixed in 4% PFA for 1 hour and collected on a FACSCaliber (Beckon Dickinson). Analysis was performed on Cell Quest software (BD-Pharmingen, San Diego, CA).

Histopathology.

Tissue samples for histological studies were fixed in 10% normal buffered formalin followed by paraffin embedment. For histopathological studies 5- to 6- μm sections were stained with Harris' hematoxylin and eosin.

RNase Protection Assay (RPA).

A multiprobe RNase protection assay system (Pharmingen, San Diego, CA) was used to determine the levels of mRNA for genes of interest at 10-day intervals post-aerosol infection in murine lung or infected macrophages *in vitro*. At the time of harvest, the lungs were snap frozen in liquid nitrogen and stored at -80°C. Total RNA was extracted using Trizol reagent (Life Technology, Grand Island, N. Y.) followed by treatment with RNase free-DNase (Roche, Indianapolis, IN) and RNase Inhibitor (Roche). Macrophage RNA was obtained from bone marrow derived macrophages by treating ~4 x 10^6 adherent cells with 1ml Trizol reagent. The RNA was subjected to RPA according to Pharmingen's protocol. In short, mRNA from macrophages or the lungs was hybridized overnight to [^{32}P]-UTP-labeled probes. The protected [^{32}P]-UTP-labeled RNA probes were resolved on a 6% polyacrylamide gel and analyzed by autoradiography. Cytokine analysis was performed using a custom-made template set specific for NOS2, IL-4, IL-12p40, TNF, IL-1β, IL-1α, and IFN-γ. Chemokine analysis was performed using either a custom-template set specific for CCL2, CCL7, CCL12, CCR2, CCL19 (MIP-3β) and CXCL10 (Pharmingen, provided by Joel Ernst, UCSF) or mCK5 multiprobe template set (Pharmingen). The expression of specific genes was quantified on a densitometer (ImageQuant

Software, Molecular Dynamics, Sunnyvale, CA), relative to the abundance of housekeeping gene, L32. We also performed phosphorimaging quantification on some samples but found results identical to densitometry; therefore, only densitometry quantifications are shown.

Statistical Analysis.

3-4 mice per group per time point were used for all studies. Statistical analysis was performed on the data utilizing Prism Software for an unpaired t-test. For bacterial numbers and cell numbers, log transformation was performed prior to statistical analysis.

10.3 Results

Expression of CCR2 ligands, CCL2, CCL7 and CCL12, increases following infection.

To determine whether expression of CCR2 ligands was enhanced following *M. tuberculosis* infection, RNase protection assays were performed on infected bone marrow derived macrophages and the lungs of infected C57Bl/6 mice. The expression of three major CCR2 ligands and CCR2 increased upon in vitro infection of macrophages (Figure 38A). There was also enhanced expression of genes for CCL3, CCL4 (MIP-1β), CCL5, CXCL2, and CXCL10 in macrophages (data not shown). In the lungs, expression of the macrophage chemotactic proteins (CCL2, 7, 12) increased following aerosol *M. tuberculosis* infection (Figure 38B). The pattern of expression was similar to that of a number of other chemokines following infection in the lung, including CCL3, CCL4, CCL5, and CXCL10 (as described in previous chapters).

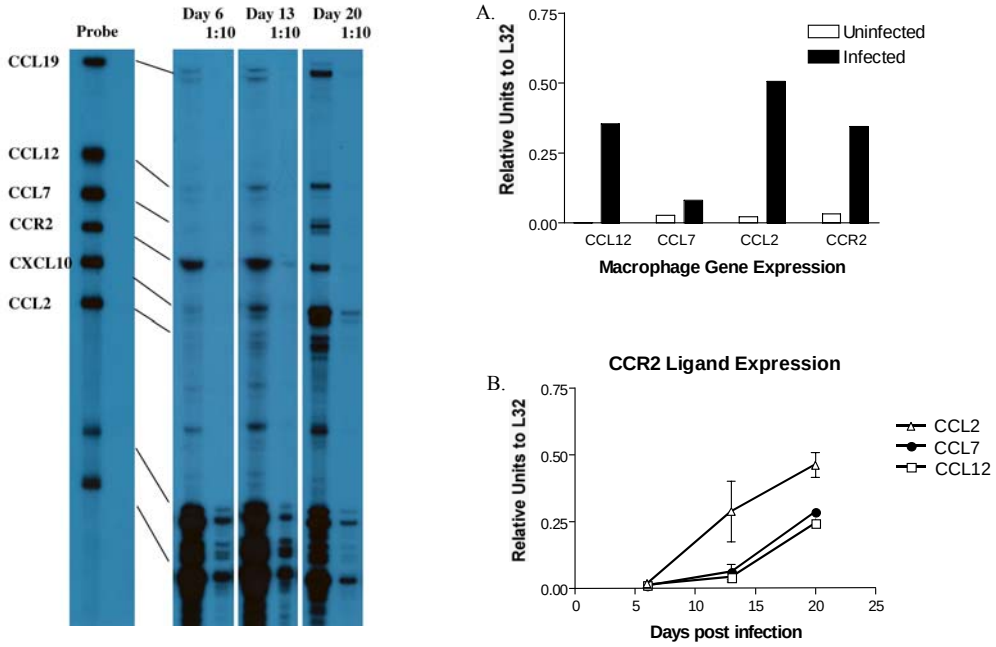

Figure 38. Expression of CCR2 ligands, CCL2, CCL7 and CCL12 increases following *M. tuberculosis* infection.

RNase protection assay on mRNA isolated from bone marrow derived macrophages (A) or C57Bl/6 mice (B) reveals enhanced expression of CCL2, CCL7 and CCL12 following *M. tuberculosis* infection. Representative samples from the lung RNase protection assay are shown (C).

CCR2-/- mice control low dose infection with M. tuberculosis.

Mice were infected via the aerosol route (~50 CFU) with *M. tuberculosis*, and sacrificed to determine bacillary burdens in the lung, liver and spleen at various time points post-infection (Figure 39A). The bacterial numbers in the lungs of CCR2-/- and wild type mice were not significantly different at any time post infection. There was no significant difference in bacterial dissemination to the spleen or liver between the mouse strains, although the initial growth of *M. tuberculosis* in the spleens of CCR2-/- was impaired compared to wild type mice (p=0.0019). However, at late time points (70 days) there were ~10-fold more CFU in the CCR2-/- spleens compared to wild type. No differences in the bacterial growth in the liver were observed (data

not shown). No CCR2-/- mice succumbed to the aerosol infection during the course of the experiment; mice were maintained up to 5 months. At 5 months post infection the CCR2-/- mice had similar bacterial loads in the lungs (data not shown). The low dose aerosol infections were performed using *M. tuberculosis* strains H37Rv (twice) and Erdman (twice) with similar results.

These results were in sharp contrast to the published results on CCR2-/- mice infected i.v. with 4-10 $x10^5$ CFU [135], where a majority of mice did not survive beyond 23 days. We repeated these studies with our standard i.v. dose of 2 x 10^5 CFU using strain H37Rv. This dose does not cause mortality in C57BL/6 mice in our hands. As reported previously [62], the CCR2-/- mice infected with a relatively high dose of *M. tuberculosis* had 5-fold higher bacterial numbers than wild type mice by 10 days post-infection, and 100-fold more CFU by 20 days post-infection (Figure 39B). The CCR2-/- mice infected with 2 x 10^5 CFU i.v. did not survive past 23 days post-infection.

The decreased susceptibility of CCR2-/- mice to the aerosol infection could have been due to either the route used to infect the mice, or the substantially lower dose that is delivered to the lungs by aerosol (compared to i.v.) infection. To distinguish between these possibilities, we infected CCR2-/- mice with a lower dose i.v., using 1 x 10^4 CFU H37Rv. This delivers <100 CFU to the lungs [7, 186] which is similar to the dose delivered directly to the lung by our aerosol infection. CCR2-/- and wild type mice infected i.v. with the lower dose were equally capable of controlling the infection, similar to aerosol-infected mice (Figure 39C). When a high dose of *M. tuberculosis* strain H37Rv was administered via aerosol (4000 CFU or 1500 CFU), the CCR2-/- mice had significantly higher bacterial loads in their lungs than wild type mice by 3 weeks post infection (data not shown), yet both strains of mice succumbed by 4 weeks post-infection to these high doses of *M. tuberculosis*. Thus, the susceptibility of CCR2-/- mice is

dependent on dose, rather than route of infection.

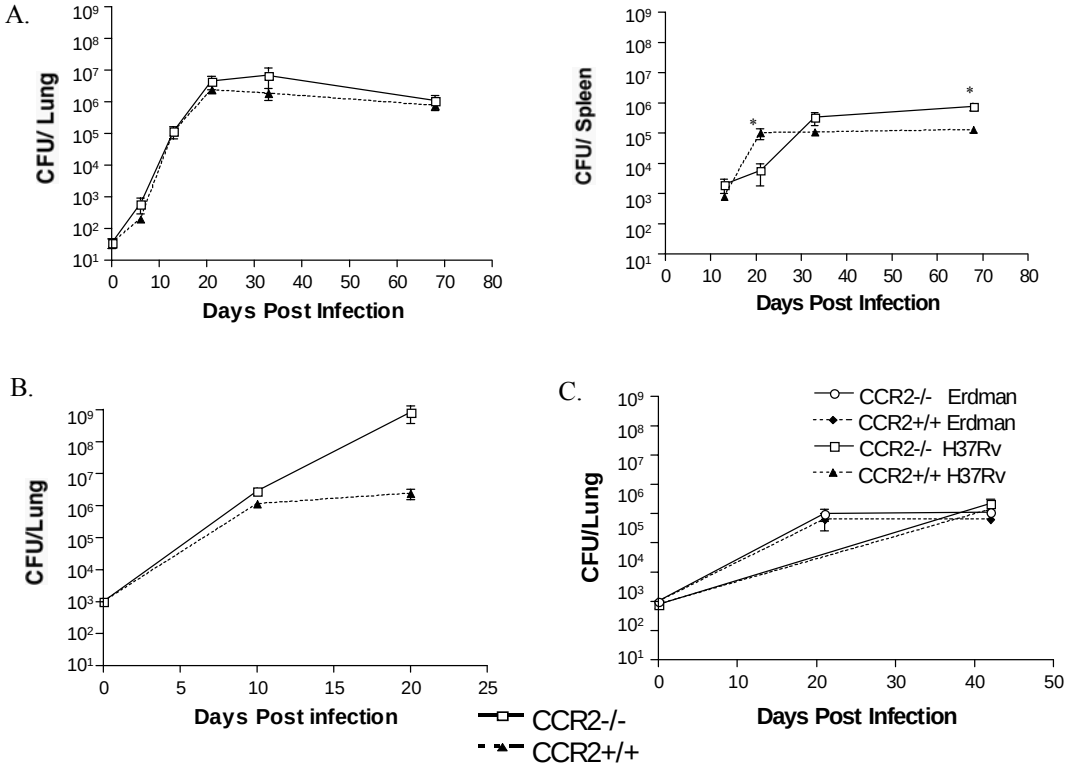

Figure 39. CCR2 deficient mice control low dose infection with *M. tuberculosis*.

CCR2-/- mice and wild type C57BL/6 mice were infected via aerosol route with ~50 CFU *M. tuberculosis* H37Rv (circles) (A), intravenously with 2x 10^5 CFU *M. tuberculosis* H37Rv (B), intravenously with 1x10^4 CFU *M. tuberculosis* Erdman (triangles) or H37Rv (C). CCR2-/- mice (open symbols) controlled growth of *M. tuberculosis* similar to wild type (closed symbols) mice in the two lower dose models (A, C), but had much higher bacterial numbers in the higher dose model (B). For (A) both lung and spleen CFU are shown; for (B, C) lung CFU only are shown. Each time point represents 3-4 mice and the bars represent standard error. The aerosol route experiment was performed twice with H37Rv and twice with Erdman strain with similar results. The i.v. route experiments were performed twice.

Monocyte/macrophage migration deficiencies were observed even in low dose infection.

Murine macrophages express CCR2 and show chemotactic ability to CCR2 ligands, CCL2, CCL7, and CCL12. Monocyte/macrophage migration deficiencies have been observed in inflammatory models in CCR2-/- mice [135, 182-185, 187-189]. Since the CCR2-/- mice were capable of controlling low dose *M. tuberculosis* infection, we examined whether the lungs of the

CCR2-/- mice were also deficient in macrophages following low dose *M. tuberculosis* infection. Antibody staining followed by flow cytometric analysis was performed on single cell lung homogenates. A substantial macrophage deficiency was observed in the CCR2-/- mice infected with a low dose of *M. tuberculosis*. There was a 10-fold increase in macrophages by 32 days post infection, but the number of macrophages in the CCR2-/- mice remained much lower than in wild type mice (Figure 40A), even up to 5 months post-infection (data not shown). In the low dose i.v. model of *M. tuberculosis* infection ($1x10^4$ CFU), the CCR2-/- also exhibited at least 2-fold fewer macrophages in the lungs (Table 9).

These data and those previously reported [135] demonstrate that CCR2 plays an essential role in macrophage migration to the lung during *M. tuberculosis* infection, regardless of dose, route or strain of *M. tuberculosis* used for infection. In high dose i.v. and aerosol infection models, the numbers of neutrophils increased to greater than 50% of the total lung homogenate [190]. An increase in neutrophils was evident in low dose models of infection in CCR2-/- mice, but by 4 weeks post infection the percentage of neutrophils was greatly reduced (Figure 40B and Table 9).

Table 9. Numbers of immune cells within the lungs 3 weeks post infection.

Numbers of macrophages, neutrophils, CD4+ lymphocytes and CD8+ lymphocytes are represented from low dose aerosol infection, low dose i.v. infection and high dose i.v. infection. Each value represents the mean of 3-4 mice and the standard error of the mean is in parentheses. *$p \leq 0.05$, **$p \leq 0.005$, and ***$p \leq 0.001$ Numbers of immune cells within the lungs 3 weeks post infection. Numbers of macrophages, neutrophils, CD4+ lymphocytes and CD8+ lymphocytes are represented from low dose aerosol infection, low dose i.v. infection and high dose i.v. infection. Each value represents the mean of 3-4 mice and the standard error of the mean is in parentheses. *$p \leq 0.05$, **$p \leq 0.005$, and ***$p \leq 0.001$

Cellular Infiltrate ($x10^5$)(3wks)	WT (aerosol)	CCR2-/- (aerosol)	WT (low dose iv)	CCR2-/- (low dose iv)	WT (high dose iv)	CCR2-/- (high dose i.v.)
Macrophages	0.81 (±0.06)	0.28 (±0.06)	0.64 (±0.10)	0.36 (±0.05)	5.06 (±0.50)	0.7 (±0.16)
Neutrophils	1.57 (±0.24)	2.35 (±0.29)	0.65 (±0.29)	1.70 (±0.45)	2.16 (±0.26)	24.54 (±7.15)
CD4 T cells	6.01 (±0.88)	3.72 (±0.62)	5.04 (±1.11)	3.58 (±0.66)	30.42 (±5.31)	16.81 (±0.53)
CD8 T cells	3.84 (±0.46)	4.28 (±0.28)	3.25 (±0.64)	2.50 (±0.36)	16.46 (±3.21)	8.7 (±0.53)

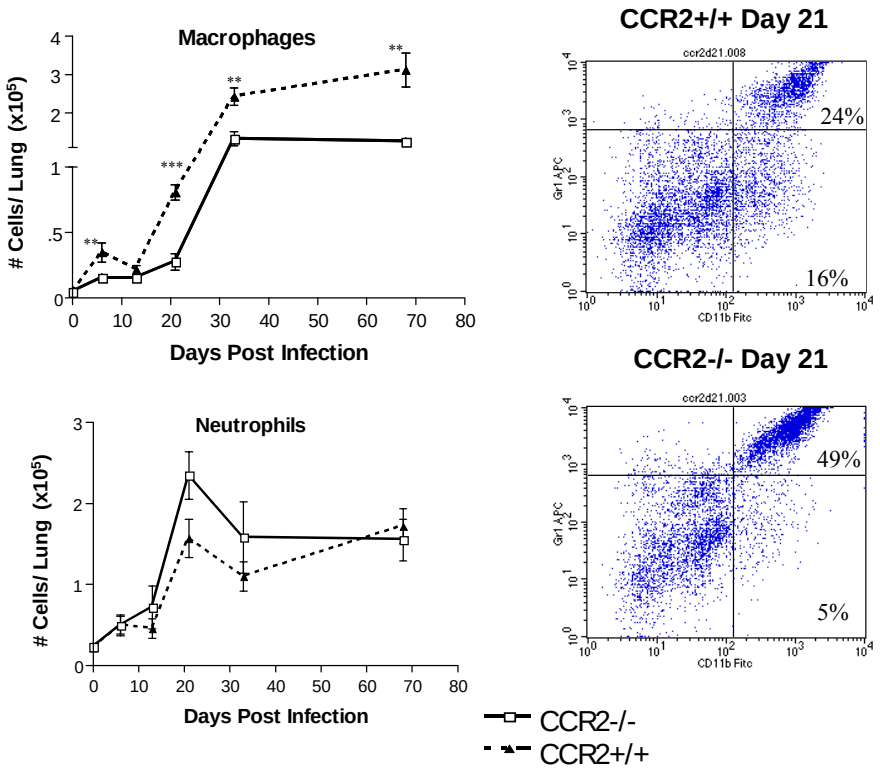

Figure 40. Macrophages are present in fewer numbers throughout *M. tuberculosis* infection in the CCR2 deficient mice.

Migration of macrophages (A) and neutrophils (B) to the lung following aerosol infection (50 CFU) with *M. tuberculosis* H37Rv in CCR2-/- mice (open squares) and CCR2+/+ mice (closed triangles). Flow cytometric analysis was performed on single cell suspensions of the lung. Within the macrophage/granulocyte gate (determined by SSC v FSC), macrophages were defined as CD11b+Gr1- and neutrophils were CD11b+ Gr1+. Each data point represents 3 to 4 mice and the bars represent standard error. *p≤0.05, **p≤0.005, and ***p≤0.001. This experiment was repeated twice with similar results.

Lymphocyte migration to the lung following aerosol infection is affected.

Because CD4+ and CD8+ lymphocytes play important roles in *M. tuberculosis* infection [reviewed in [23]] and can express CCR2, the migration of these cells to the lung following *M. tuberculosis* infection was evaluated by flow cytometry. The percentage of CD4+ T cells was significantly less in the CCR2 deficient mice compared to wild type mice up to 50 days post-infection (Figure 41A). There was a more modest delay in CD8+ lymphocyte migration to the

lung, but this delay was overcome by 4 weeks post infection (Figure 41B). We assessed activation status of the lung T cells by staining for the early activation marker, CD69. There was no difference in CD69 expression on CD4+ T cells at any time point between wild type and CCR2-/- mice. However, at 13 days post infection there was a significantly higher percentage of CD8+ lymphocytes expressing CD69 in wild type mice (p=0.004); at other time points the expression of CD69 was not significantly different between CCR2-/- and CCR2+/+ mice (data not shown).

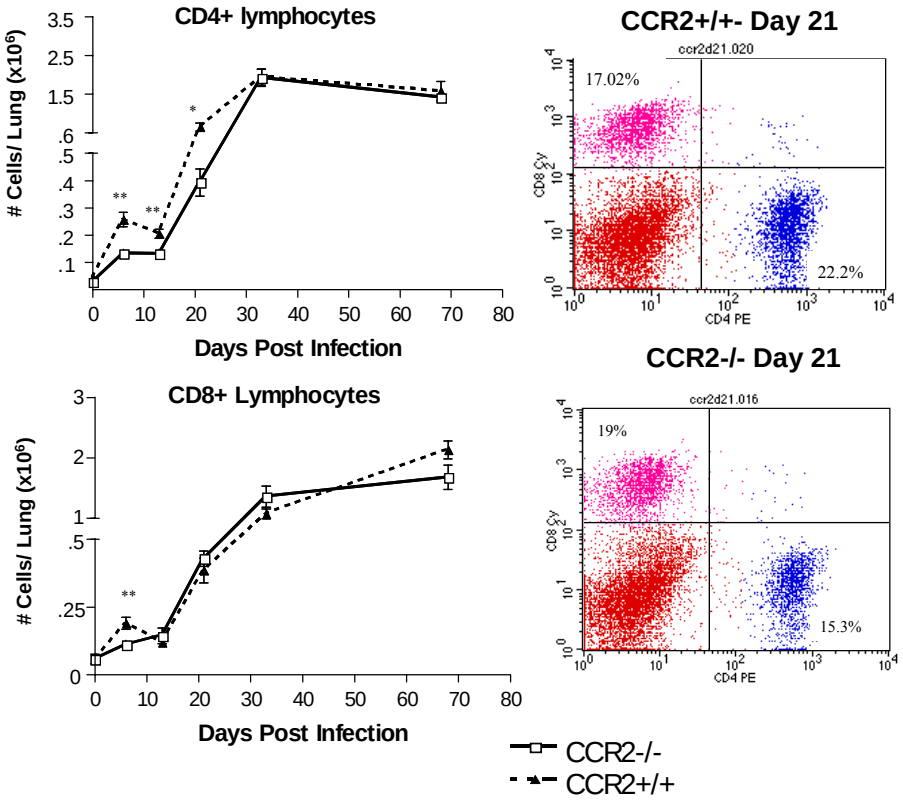

Figure 41. Migration of T lymphocytes to the lung is delayed following low dose aerosol *M. tuberculosis* infection.

Flow cytometric analysis using anti-CD4 (A) and anti-CD8 (B) antibodies was performed on single cells suspensions of the lung at various time points post infection. Points represent the percent antibody positive within the lymphocyte gate (determined by SSC v. FSC parameters). Each data point represents three to four CCR2-/- mice (open squares) or CCR2+/+ mice (closed triangles), and the bars represent standard error. *$p \leq 0.05$, **$p \leq 0.005$. This experiment was repeated twice with similar results.

Histological analysis of CCR2 deficient mice.

Granuloma formation parallels development of cell mediated immunity in murine models of tuberculosis. This occurs in the *M. tuberculosis*-infected lung 3-4 weeks post-infection. The granuloma consists primarily of clusters of macrophages, including epithelioid macrophages, and lymphocytes. In human tuberculous granulomas, typically the lymphocytes surround the macrophages, which may fuse to form multinucleated giant cells. Following aerosol infection, the CCR2-/- mice did form granulomas in the lungs, but the formation was delayed and the reduction in macrophages could clearly be observed in the overall granuloma structure and pathology of the lungs (Figure 42). By 13 days post infection, perivascular and peribronchial lymphocytic infiltrate was evident in wild type mice but to a lesser extent in CCR2 deficient mice. This correlates with the delay in lymphocytic and macrophage infiltration evident in the flow cytometric analysis of the lung (Figure 40 and Figure 41). By 21 days post infection the perivascular and peribronchial infiltrate was more noticeable in the CCR2 deficient mice, but in the wild type mice the lymphocytes were infiltrating deeper into the parenchymal space. By 33 days post-infection granulomas were evident in both groups of mice, but were more organized in wild type mice with tighter lymphocytic clusters. By day 48 the granulomas were organized in the CCR2 deficient mice, but as a result of fewer macrophages in the lungs, the granulomas consisted of lymphocytic cuffs surrounding epithelioid macrophages, rather than the lymphocytic aggregates within sheets of epithelioid macrophages as previously described in wild type mice [26]. Thus, granuloma formation in the lungs was delayed and ultimately the granulomas appeared to contain fewer macrophages in CCR2-/- mice compared to wild type mice.

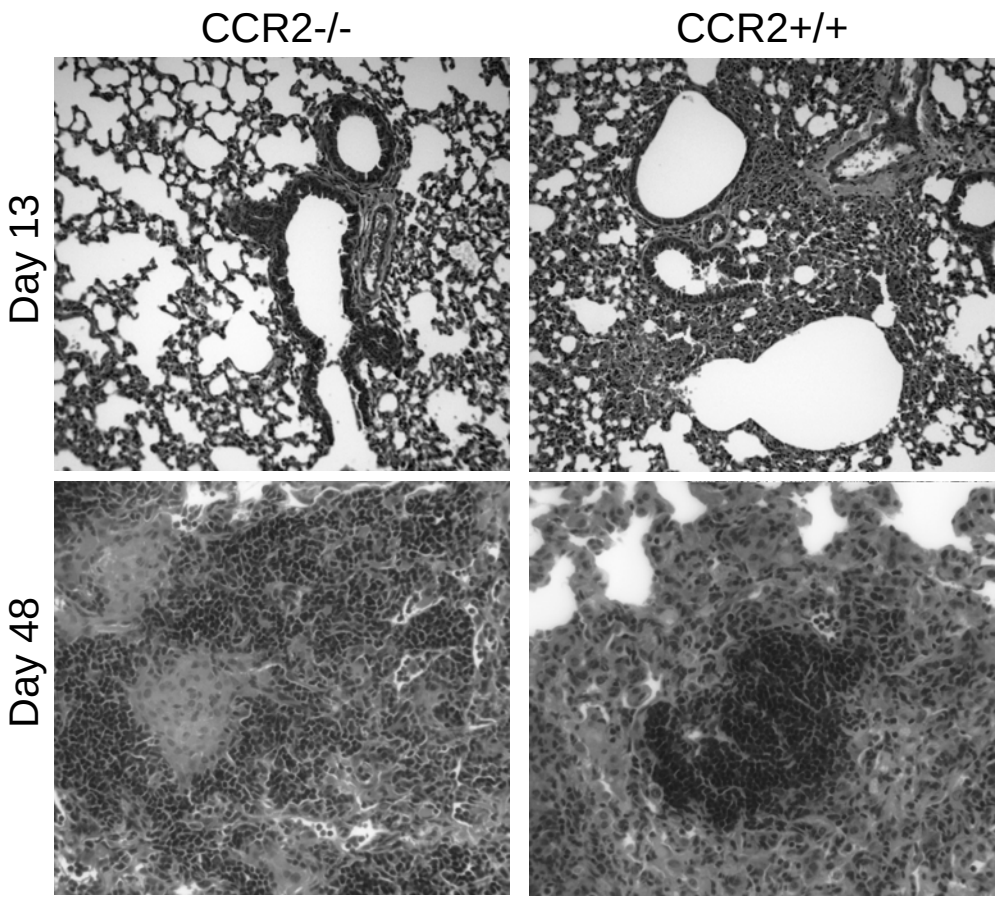

Figure 42. Granulomas form in the lungs with delayed kinetics in CCR2 deficient mice.

Hematoxylin and Eosin staining was performed on 5-6μm formalin-fixed lung tissue sections at each time point, post infection. Panels from day 13, 21, and 33 are 40X while panels from day 48 are 100x magnification. Infiltration is delayed in CCR2-/- mice, but granulomas do form, although they are histologically different from those found in CCR2+/+ mice.

IFN-γ and NOS2 production is delayed in CCR2 deficient mice.

Mice deficient in CCR2 have transient delays in IFN-γ production [159, 188, 191]. Since IFN–γ is required for control of *M. tuberculosis* [64, 98, 192] and the CCR2-/- mice control infection in the low dose models, we examined whether the defect in IFN-γ production reported in the high-dose infected mice [62] was evident in the aerosol model. Using RNase protection assays on whole lung RNA preparations, there was a substantial delay in the IFN-γ gene expression (Figure 43). Concomitant with the delay in IFN-γ there was a delay in mRNA levels

of the gene for inducible nitric oxide synthase (NOS2). RNA from the lungs of uninfected mice was also used in RNase protection assays; the genes of interest were below the level of detection with this RNA (data not shown). The delayed NOS2 gene expression was confirmed at the protein level by immunostaining of lung tissue from the mice at each time point post-infection (data not shown). Expression of a number of other cytokines was addressed through RNase Protection Assay, and no significant difference in the mRNA expression of IL-12, TNF, or IL-1 in CCR2-/- compared to wild type mice was observed (data not shown).

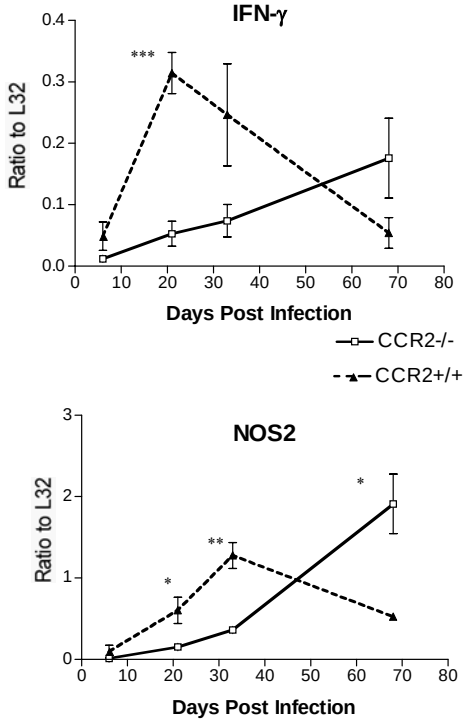

Figure 43. Expression of IFN-γ and inducible nitric oxide synthase (NOS2) is delayed in the lungs of CCR2-/- mice infected with a low dose of *M. tuberculosis* H37Rv via aerosols.

RNase Protection Assays were performed on whole lung RNA preparations, as described. Each data point represents three to four CCR2-/- mice (open squares) or CCR2+/+ mice (closed triangles), and the bars represent standard error. *$p \leq 0.05$, **$p \leq 0.005$, and ***$p \leq 0.001$. This experiment was repeated once with similar results.

Memory response

To determine whether CCR2 was required in the secondary immune or memory response to *M. tuberculosis*, we infected wild type and CCR2-/- mice via aerosol (~50 CFU/mouse) and 4 months later, treated the mice with isoniazid and pyrazinamide for 8 weeks, reducing bacillary loads below detection. After allowing the mice to "rest" for 8 weeks, the mice were challenged via the aerosol route with ~50 CFU *M. tuberculosis*. No CFU were detectable in the mice prior to challenge. Following challenge, the bacterial loads were determined and cell migration was addressed by flow cytometric analysis. The macrophage defect in CCR2-/- mice was evident throughout the 6 weeks of observation, but again there was no sign of increased susceptibility (Table 10). There was no difference in T cell migration to the lungs observed in these mice.

Table 10. Cell migration to the lung following challenge of memory mice with aerosol *M. tuberculosis*.

C57Bl/6 mice and CCR2-/- mice were infected with *M. tuberculosis* H37Rv (50 CFU) via aerosol route. Four months post infection the mice were drug-treated for 2 months. The mice were then challenged with aerosol *M. tuberculosis* H37Rv (50 CFU) and flow cytometric analysis was performed at the times indicated in the table. * p= 0.02 and ***p=0.001.

Days post Rechallenge	% CD4+T cells (+/- SEM) CCR2-/-	% CD4+T cells (+/- SEM) CCR2+/+	% CD8+T cells (+/- SEM) CCR2-/-	% CD8+T cells (+/- SEM) CCR2+/+	% Macrophages (+/- SEM) CCR2-/-	%Macrophages (+/-SEM) CCR2+/+	CFU/Lung $x10^5$ (+/-SEM) CCR2-/-	CFU/Lung $x10^5$ (+/-SEM) CCR2+/+
18	20.2 (2.6)	27.6 (7.5)	18.4 (2.4)	16.0 (2.5)	ND	ND	3.1 (0.25)	5.0 (0.4)
28	21.9 (1.5)	22.5 (1.3)	21.1 (0.9)	17.3 (1.2)	**11.2 (0.8)**	**18.3 (1.14)**	5.8 (1.56)	5.2 (1.66)
49	16.4 (1.7)	19.0 (1.4)	18.4 (1.1)	16.5 (0.9)	**8.2 (1.98)**	**16.5 (1.62)**	6.4 (1.27)	6.8 (1.94)

10.4 Discussion

CCR2-/- mice are clearly deficient in monocyte/macrophage migration to an inflammatory site [62, 184, 185, 187-189, 191, 193]. Here we confirmed the previous findings of impaired migration of cells to the lungs of CCR2-/- mice following *M. tuberculosis* infection. However, in contrast to CCR2-/- mice infected with a relatively high dose of *M. tuberculosis*, CCR2-/- mice infected with a low dose of *M. tuberculosis* controlled the infection, despite a substantially

reduced macrophage population in the lungs. Thus, in a low dose infection, a delayed or deficient immune response does not necessarily lead to higher bacterial numbers in the lungs.

The absence of CCR2 resulted in prolonged macrophage deficiency in the lungs in the low dose model of infection. There was 2-5 fold fewer macrophages in the CCR2-/- lungs compared to wild type lungs. There was also a less pronounced but definite defect in macrophage migration to the lungs following challenge of previously infected and drug-treated (i.e. immune) mice. However, the level of macrophages was apparently sufficient to control the primary or secondary infection, suggesting that the macrophage response in wild type mice to *M. tuberculosis* is more robust than necessary to control a low dose infection. However, even a very robust response is insufficient to clear the infection in mice.

T cell migration, particularly CD4 T cells, was also deficient in CCR2-/- mice during the early stages of the infection. This may be a direct effect of the absence of CCR2, since this receptor is found on activated T cells and may be important in T cell trafficking to the lungs from the bloodstream. However, the delay in T cell migration could also be an indirect effect of CCR2 deficiency. Macrophages produce additional chemokines that signal T cell migration, and the reduction in macrophages in the lungs may result in altered chemokine levels contributing to reduced T cell migration. Alternatively, priming of T cells by dendritic cells in the lymph nodes could also be affected by the absence of CCR2, and this would result in a delay in T cell responses in the lungs. The T cell migration delay was not observed in the memory response to challenge in the lungs, suggesting that chemokine responses for memory cells may differ from those required for a primary response, or that priming of T cell response by dendritic cells may be the cause of the delay in the primary response.

A significant delay in IFN-γ gene expression was also observed in the lungs. This may be due to the delayed T cell migration to the lungs, or to reduced stimulation of the T cells that are present in the lungs because of macrophage deficiencies. Regardless of the mechanism responsible, the finding that a substantial delay in IFN-γ production does not necessarily lead to increased bacterial numbers is surprising. IFN-γ is an essential cytokine for control of *M. tuberculosis* infection, regardless of dose or route of challenge [64, 98]. Nonetheless, it appears that IFN-γ levels substantially reduced from wild type levels are sufficient to control low dose infection, at least in the early stages of infection. This again implies that the immune response in the lungs is more robust than necessary for bacterial control. The delayed IFN-γ levels may be responsible for the reduced NOS2 gene expression, or this may also result from the deficiency of macrophages, the cells that produce NOS2, in the lungs. In any event, the control of bacterial growth in the lungs of CCR2-/- mice following low dose infection suggests that the level of NOS2 production is sufficient; however, at higher doses, this level of macrophage activation was apparently not adequate to control bacterial growth.

One striking difference between the low dose and high dose infection in CCR2-/- mice was the neutrophilic infiltration to the lungs. The increased neutrophilic infiltration as a result of CCR2 deficiency was previously observed [62]; the results in the low dose infected mice suggest that the continued infiltration of neutrophils may be due to uncontrolled bacterial replication in the high dose model rather than a direct result of CCR2 deficiency. It is possible that the presence of large numbers of neutrophils in the lungs is damaging to the tissue, and affects the ability of the macrophages to control infection. In the low dose mice, the neutrophil infiltration is not significantly different at any time point, although there is a trend toward higher numbers of neutrophils in the CCR2-/- lungs. Coincident with the induction of cell-mediated immunity and

control of bacterial growth in the lungs (at 3-4 weeks post-infection), the numbers of neutrophils decreased.

More recently, a more detailed study demonstrated that CCL2-/- mice have very similar infection profile to CCR2-/- mice following low dose aerosol infection [73]. In these studies the authors report fewer macrophages migrating to the lung and a very small transient increase in bacterial burden in the CCL2-/- mice compared to wild type mice. In addition the CCL2-/- mice had a transient reduction in IFNγ production. These data indicate that CCL2 ligation of CCR2 is required for macrophage migration and early lymphocyte focusing in the lung.

In summary, these studies confirm that CCR2 is an important chemokine receptor in the trafficking of macrophages to the lungs during *M. tuberculosis* infection. However, for low dose infection, the prolonged paucity of macrophages and transient delay in T cell recruitment and IFN-γ expression did not noticeably impair control of the infection in the lungs. These results imply that the wild type immune response to *M. tuberculosis* in the lungs is more vigorous than necessary. Clearly, CCR2 is important for macrophage infiltration into the lungs following *M. tuberculosis* infection, and there is not a molecule that can replace CCR2 in this function. This striking phenotype was observed regardless of infection dose, route or strain of *M. tuberculosis*. The importance of macrophages to control of *M. tuberculosis* is well established. The ability of mice to control a low dose, but not a relatively high dose *M. tuberculosis* infection with a substantial deficiency in macrophage numbers in the lungs does not imply that CCR2 is not playing a role in the immune response to this pathogen. Instead, the ability of mice to control a low dose infection with a minimal inflammatory response in the lungs, with respect to macrophages and T cells early in infection, can be observed in these studies. A higher dose infection clearly overwhelms this reduced response, and the reduced subsequent IFN-γ and

macrophage infiltration is not sufficient to gain control of the infection. The induction of T cell response in the lungs in the high dose mice at ~2-3 weeks post-infection coincides with very high bacterial numbers, and thus cannot contribute to the reduction of the bacterial load. This has been observed in other systems as well, including mice deficient in CD4 T cells [7]. However, as with many immunologically deficient mice and tuberculosis, CD4 T cell deficient mice cannot control even low dose aerosol infections [194]. In contrast, in the low dose infection, the minimal innate and inflammatory response that occurs in the absence of CCR2 is sufficient to control the infection until cell mediated immunity is fully induced.

These studies have provided insight into the use of immunologic knockout mice to study *M. tuberculosis*. The use of CFU as the primary measure of the contribution of a specific immune component in the response to this infection can be misleading. In studies designed to unravel a complex system, such as cell migration and granuloma formation, the choice of model can be crucial to the outcome and interpretation of the results. The use of models, in vitro or in vivo, that are deficient in one component enables the assessment of a possible role for that component in cell migration or control of infection. However, the presence of a multitude of components can complicate the interpretation of the data, particularly in *in vivo* studies. An increase in bacterial numbers in a knockout mouse, compared to wild type, has been a standard for determining whether a particular component is essential in the immune response to *M. tuberculosis*. The infiltration of cells to the lungs and subsequent granuloma formation is clearly a complex process requiring a network of molecules and receptors. Nonetheless, although our data confirmed that CCR2 is clearly important in migration of macrophages to the lungs following infection, under certain infection conditions this deficiency does not impair control of bacterial growth in the lungs. Our interpretation of these data is that comparison of bacterial

numbers is only one measure of the function of certain molecules. The data provided here demonstrate that CCR2 is an important molecule in monocyte/macrophage migration, and also affects, perhaps indirectly, T cell migration and IFN-γ expression. In the low dose infection model, other immune components are sufficient to control the infection, whereas when a higher dose is administered to the mice, the absence of CCR2 results in lethal infection. Thus, there is a critical dose that can overwhelm the ability of macrophage-deficient lungs to control infection.

11.0 Summary

My evaluation of cell migration and chemokine expression during *M. tuberculosis* infection has provided novel information that will aid in understanding the cascade of events in response to infection. I have also made important contributions to our general understanding of the immune responses to *M. tuberculosis* and the utility of the mouse model. This study began with a broad focus, which we narrowed to evaluate a specific subset of inducible chemokines. Early analysis of anti-TNF Ab treated mice revealed granuloma deficiency after *M. tuberculosis* infection [106], and one set of logical candidates for control of granuloma formation was chemokines. Therefore, after defining a subset of chemokines that were affected by anti-TNF Ab treatment in vitro, we designed experiments focusing on the expression of those chemokines in vivo and in vitro during *M. tuberculosis* infection. The chemokine functions analyzed fell mainly into three groups based on their receptors: ligands for CXCR3 (CXCL9, 10 and 11), ligands for CCR5 (CCL3, CCL4, CCL5), and ligands for CCR2 (CCL2 and CCL12).

Many cell types are required for an effective, controlled immune response to be initiated and maintained in the lungs during *M. tuberculosis* infection. These cells include CD4 lymphocytes, CD8 lymphocytes, and macrophages. In addition, B lymphocytes and neutrophils are involved in the immune response, but their roles are less defined. In a healthy lung very few immune cells are present, rather the tissue is comprised of airways with walls of ciliated epithelium with some alveolar macrophages and immature dendritic cells present. After infection, cell migration to the lungs begins and the immune system sets up its defense. The organization of the immune system requires many different cells communicating through many different signals. The granuloma structure in the lungs serves as a site for this cascade of communication. Although the granuloma is also a sign of chronic antigenic stimulation and leads to some pathology, it is clearly required for control of infection. The bacterial burdens in

mice plateau at the time when granulomas form and the cell mediated immune response has been initiated. It is at this critical juncture that TNF- deficient mice are unable to form granulomas and control infection. Therefore these studies, focusing on the signals required for granuloma formation and cell migration into the lungs, are very important for understanding the initiation and maintenance of a successful cell mediated immune response to *M. tuberculosis* in the lungs.

Chemokines, or chemotactic cytokines, are responsible for cell migration into and out of lymphatics, the blood and tissue. We demonstrated that many inducible chemokines, both of the C-C and C-X-C classes, are upregulated with *M. tuberculosis* infection.

Differences in the organization of cellular infiltrates found in many chemokine deficient mice, such as CCR2-/- mice, CXCR3-/- mice, CCL2-/- mice or CCR5-/- mice (**Table 1**) did not result in differences in overall control of tuberculosis infection. This is very different from a situation in TNF-deficient mice. In the TNF-deficient mice, even though there are as many cells migrating into the lungs, the infiltrates are not organized. As a general point it appears that early cell migration can be delayed (such as in CCR2-/- mice), but the bacterial burdens must be controlled by 3 or 4 weeks post infection, or an effective cell mediated immune response may not be initiated.

Another important point that can be taken from these studies is that although there may not be differences in the bacterial burden or survival, lessons can be learned about the intricacies of immune system. The table below briefly describes the differences found in the cellular infiltrates during infection of chemokine knockout mice. Not all of these mice illustrate differences in bacterial burden or in survival, but they do show distinct significant differences in the cellular infiltrate to the lungs or the lymph nodes. Therefore CCR2 is required for macrophage migration to the lungs and lymph nodes. CCR5 is required for normal dendritic cell

migration/ retention in the lymph nodes and lung early, influencing T lymphocyte migration late. CXCL10 appears play a role in early lymphocyte migration to the lymph nodes.

Table 11. Cellular infiltrate differences in chemokine or chemokine receptor deficient mice.

Mouse Strain	Cell infiltrate differences observed	When differences observed	Reference
CCR2-/-	Macrophages (Lung, Lymph nodes)	Throughout infection	[63]
CCR5-/-	Dendritic cells (Lymph nodes), T lymphocytes (Lung)	Early, late	Section 9.0
CXCL10-/-	T lymphocytes (Lymph nodes)	Early	Section 8.0
CXCR3-/-	Neutrophils, T lymphocytes (Lung)	Early	[72]

We detected increased expression of CCL2, CCL7 and CCL12, ligands for CCR2, in the mouse after *M. tuberculosis* infection in the lung and in vitro in macrophages. We hypothesized that CCR2 would be required for macrophage migration to the lung. We expected the mice to be susceptible to tuberculosis with a macrophage deficiency. During acute inflammatory responses in CCR2-/- mice there were obvious deficiencies in macrophage and dendritic cell migration. Our studies have demonstrated dose dependent control of *M. tuberculosis* infection in CCR2-/- mice.

Based on our findings that CCR5 ligands were affected by TNF and that CCR5 is on macrophages, dendritic cells and T lymphocytes we hypothesized that the immune response to in CCR5 deficient mice would be impaired due to reduced migration of these cells to the lungs. Our hypothesis was not supported. Our studies suggest that CCR5 has either a direct or indirect

role in dendritic cell migration from the lung to the lymph node. There does not appear to be a direct effect on macrophages or lymphocytes. This may be the consequence of several reasons. CCR5 may not be involved in lymphocyte migration, or the ligands for CCR5, CCL4 and CCL5, could be signaling through CCR1 to induce migration of lymphocytes and macrophages. In addition, other chemokines may be compensating for the loss of CCR5 signaling.

In an effort to recapitulate the pathology observed in the anti-TNF Ab treated mice, these neutralization and receptor knockout models were utilized. We were unable to recreate the pathology observed in the absence of TNF. This is likely due to the number of chemokines influenced, at least in part, by TNF, and it is impossible to recreate a knockout or an effective neutralization model, that could modulate all these chemokines. The effects of TNF may also be temporal, and several chemokines could be modulated at different time points in the infection. The effect TNF has on the immune response is not limited to chemokine expression, and includes such important roles as macrophage activation and modulation of cytokine expression. In addition, chemokines are not solely responsible for cell migration, adhesion molecules play a role in these processes and other factors such as matrix metalloproteinases can be involved in tissue pathology and granuloma formation.

Matrix metalloproteinases (MMPs) are implicated in tissue remodeling processes and chronic inflammatory conditions. In addition, recent evidence indicates that transendothelial migration of lymphocytes is affected by MMPs [195]. MMP-1 (52kDa collagenase) and MMP-9 (92kDa collagenase) are induced in vitro following *M. tuberculosis* infection in THP-1 cells [196], and neutralization of TNF reduced MMP production in response to mycobacteria [197]. These data indicate that chemokine gradient changes may not be solely responsible in the lung pathology observed with anti-TNF Ab treatment in vivo. We performed some gene expression

(array) studies of MMP expression in the lungs of anti-TNF treated mice, and observed no obvious differences between these mice and control mice, but this avenue is complicated by the fact that there is extensive post transcriptional processing of MMPs making interpretation of the data difficult (APPENDIX C).

Through this research we have contributed to generalized concepts of the immune response to *M. tuberculosis*. Through studies on TNF we have learned that the localized gene and protein expression with in the site of a granuloma is very different from expression and activity in the whole lung. Through studies on CCR5-/- mice, we learned that the immune response can be more robust than necessary, but a stronger Th1 response does not lead to increased clearance of the mycobacteria. Through studies in CCR2-/- mice we learned that dose can have a strong influence on survival in immunocompromised mice, and that the immune response can be delayed or reduced without long term detrimental effects to the host, as long as the inoculum is reasonable. Both these studies support the contention that the immune response to *M. tuberculosis* in the lungs of mice is much stronger than necessary, and suggest that there must be some regulation of this response to avoid excessive immunopathology. Overall these studies will have a major impact on the future design of experiments. In many experiments performed for this thesis, there were no differences in mycobacterial burden or survival in gene-deficient mice, yet there were still definable roles and mechanisms of action for a particular factor. In other words, the immune response is a very intricate system and knocking out or blocking essential elements may lead to very obvious or very subtle changes in the response without increased bacterial loads or decreased survival. Therefore, the experiments need to be designed in a way to address mechanisms of action, in addition to outcome of infection in order

to understand the immune response. We have approached this by not simply following bacterial numbers, but also surveying the immune response at many points throughout the infection.

Our studies on cell migration and chemokine expression have deepened the tuberculosis field's understanding of the immune response in the lungs. These studies have shown the importance of very localized controlled chemokine expression. The macrophage appears to orchestrate granuloma formation and maintenance in the lungs, at least in part through the cascade of expression of TNF and chemokines (Figure 44).

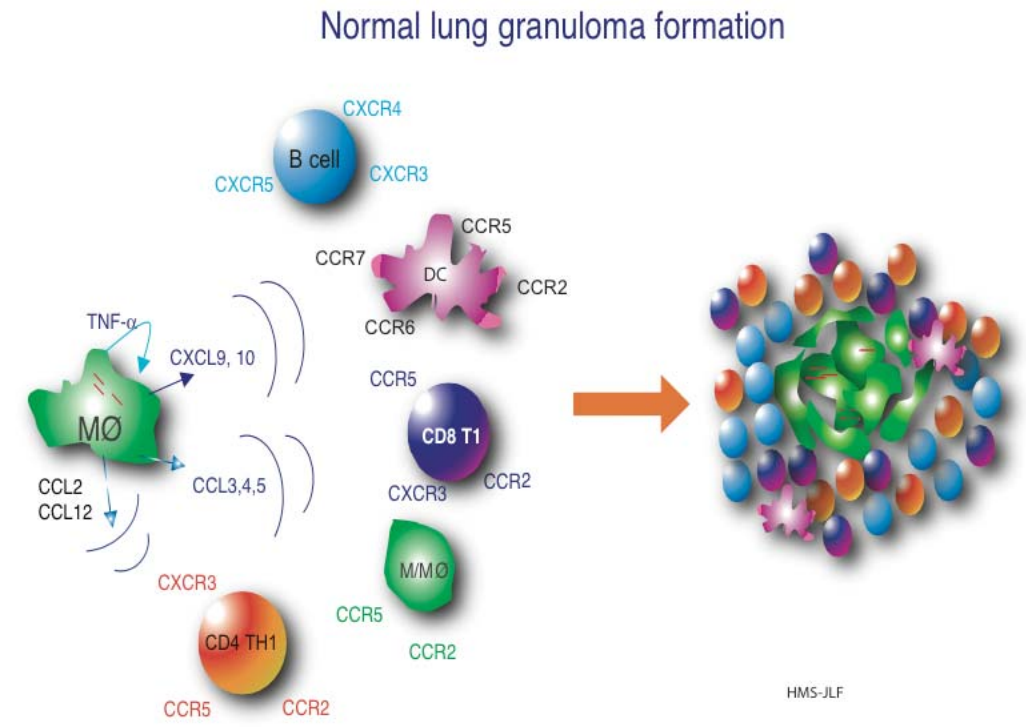

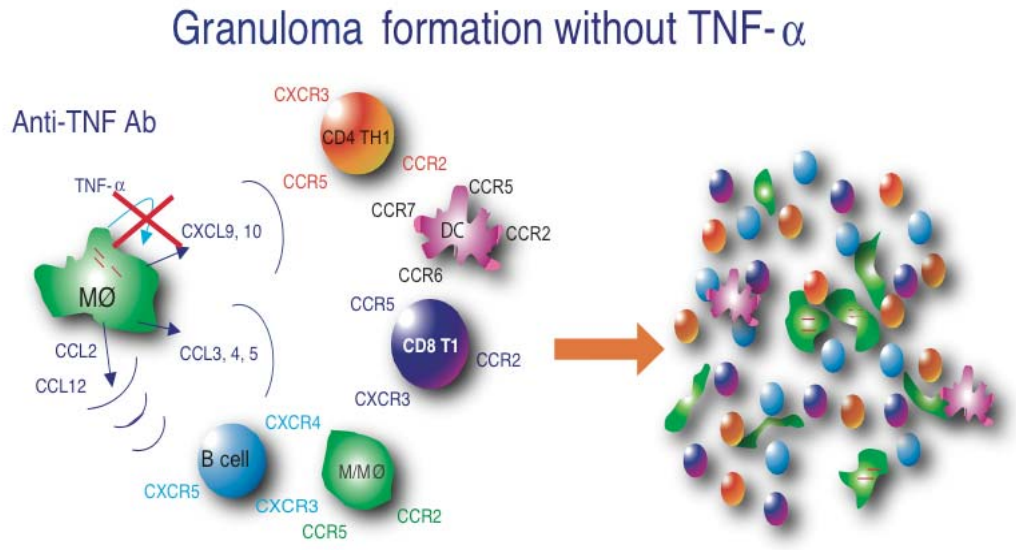

Figure 44. Chemokine expression and cell migration in the absence of TNF.

Chemokines are both down regulated (CCL2, CCL3, CCL4, CCL5, CXCL9, CXCL10) and upregulated (CCL12) in the absence of TNF. In addition granuloma formation is absent and although the cells migrate to the lungs, they do not form organized granulomas.

APPENDIX A

A.0 IL-10 expression during aerosol *M. tuberculosis* infection is a result of increased bacterial burden and does not lead to immunosuppression

Abstract

This study addresses possible interactions between IL-10 and TNF in maintaining a *M. tuberculosis* granulomatous response. The results indicate that IL-10 production seen in TNF neutralized mice was a reaction to the inflammation, rather than contributing to the inflammation through immunosuppressive activity. This response was also observed in other mice that had substantial inflammation or high bacterial numbers in the lungs.

A.1 Introduction

Recent studies indicate that overproduction of IL-10 results in poor immune responses to mycobacterial infections [107, 108]. In vivo production of IL-10 under the control of the IL-2 promoter lead to reactivation of pulmonary tuberculosis in mice [107]. IL-10 and other Th2 cytokines are correlated with impaired control of some intracellular pathogens, such as *Mycobacterium leprae*, *M. bovis* and Leishmania major [108, 198-200].

Additional studies have examined the response of IL-10-/- mice to mycobacterial infections. These studies do not collectively define a role for IL-10 in control of mycobacterial infections. When IL-10-/- mice were infected intravenously with BCG, an avirulent *M. bovis* strain, they maintained lower bacterial burdens than C57BL/6 mice, had larger granulomas and higher expression of ICAM, MHC II, TNF and NOS2 [201, 202]. On the other hand, when IL-10-/- mice were infected via aerosol with BCG, there was no significant difference in disease

progression [203]. *M. avium* infected mice, when treated with neutralizing antibody to IL-10, had increased resistance to disease [204, 205]. There was no difference in bacterial numbers in the organs of IL-10-/- mice within the first 3 months of infection with *M. tuberculosis* [65]. In another study, infection of IL-10-/- mice with *M. tuberculosis* led to transient increases in IFNγ production and initially better control of *M. tuberculosis* than wild type mice, but by 8 weeks post infection, these differences no longer were apparent [109].

IL-10 is an anti-inflammatory cytokine primarily associated with Th2 responses [reviewed in [206, 207]]. IL-10 enhances activation, proliferation and chemotaxis of CD8+ lymphocytes [208], antibody dependent cytotoxicity, B lymphocyte proliferation, differentiation and antibody production. Furthermore, IL-10 can inhibit LPS inducible genes, IFNγ inducible genes, reactive oxygen and nitrogen intermediates [reviewed in [209]].

In this study we sought to determine whether IL-10 and TNF interact in maintaining granuloma structure. When TNF was neutralized in the murine model of chronic persistent tuberculosis, IL-10 mRNA levels increased in the lungs of anti-TNF treated mice, but not in control mice [106]. These mice had substantial lung pathology, as described in the Introduction and Chapter 1 of this thesis. IL-10 transgenic mice were more susceptible to reactivation of chronic *M. tuberculosis* infection and acute BCG infection[67, 108]. These studies suggested that inappropriate regulation of IL-10 may lead to exacerbation of disease.

A.2 Materials and Methods

Animals.

C57BL/6 female mice (Charles River, Rockland, Mass.) and IL10-/- (8-14 weeks old) were used in all experiments. Mice were transferred to the Biomedical Science Tower Biosafety Level 3 animal facility at 7-8 weeks of age. All infected mice were maintained in the BSL3 animal

laboratories and routinely monitored for murine pathogens by means of serological and histological examinations. The University Institutional Animal Care and Use Committee approved all animal protocols employed in this study.

Chemical and reagents.

All chemicals were purchased from Sigma Chemical Co. (St. Louis, MO.) unless otherwise noted. Middlebrook 7H9 liquid medium and 7H10 agar were obtained from Difco Laboratories (Detroit, MI). Antibodies used in flow cytometric analyses were obtained from Pharmingen (San Diego, CA). Pyrazinamide was purchased from Acros. The cell lines, MP6XT-22 (anti-TNF) and JES5-2A5 (anti-IL10), were obtained from DNAX and used to generate ascites (Harlan Bioproducts, Indianapolis,IN). Antibodies were purified endotoxin free from ascites fluid as previously described [106] and mice were treated with antibody intravenously every three days (0.5mg/dose) starting 4 months post infection. Control mice received normal rat IgG (Jackson Immunoresearch Laboratories Inc.,West Grove, PA) with the same dosing regiment.

Mycobacteria and infection of mice.

To prepare bacterial stock, *M. tuberculosis* strain Erdman (Trudeau Institute, Saranac Lake, N.Y.) was used to infect mice, and then bacteria were harvested from their lungs, expanded in 7H9 liquid medium and stored in aliquots at -80◦C. Mice were infected via the aerosol route using a nose-only exposure unit (In Tox Products, Albuquerque, N.M.), and exposed to *M. tuberculosis* (1×10^7 CFU/ml in the nebulizer chamber) for 20 minutes, followed by 5 minutes of air. This resulted in reproducible delivery of 50-100 viable CFU of *M. tuberculosis* as described previously [94], which was confirmed by CFU determination on the lungs of 2-3 infected mice 1 day post-infection. The tissue bacillary load was quantified by plating serial dilutions of the lung, liver, and spleen homogenates onto 7H10 agar as described previously [30].

Flow cytometric analysis of lung cells.

To determine cellular infiltrate in the lung, at 10-day intervals lungs were removed for flow cytometric analysis. Lungs were subjected to a short period (20 minutes) of digestion with 1mg/ml collagenase A and 25 Units/ml DNAse (both from Boehringer Mannheim, Mannheim, Germany) at 37°C. The suspension was pushed through a cell strainer as previously described [63]. Red blood cells were lysed with red blood cell lysis buffer (NH_4Cl/Tris Solution) and the single cell suspension was counted. The samples were stained with 0.2 μg anti-CD4, anti-CD8, anti-CD69, anti-CD25 or 0.2 μg anti-B7.1, anti-B7.2, and 0.15 μg anti-Gr1 and 0.2 μg anti-CD11b in FACS buffer (0.1% NaAzide, 0.1% BSA, 20% mouse serum). Following washes, the cells were fixed in 4% PFA for 1 hour and collected on a FACS Caliber (Beckon Dickinson). Analysis was performed on Cell Quest software (BD-Pharmingen, San Diego, CA).

Histopathology.

Tissue samples for histological studies were fixed in 10% normal buffered formalin followed by paraffin embedment. For histopathological studies 5- to 6- μm sections were stained with Harris' hematoxylin and eosin.

RNase Protection Assay (RPA).

A multiprobe RNase protection assay system (Pharmingen, San Diego, Ca) was used to determine the levels of mRNA for genes of interest at 10 day intervals post-aerosol infection in murine lung or infected macrophages in vitro. At the time of harvest, the lungs were snap frozen in liquid nitrogen and stored at -80°C. Total RNA was extracted using Trizol reagent (Life Technology, Grand Island, N. Y.) followed by treatment with RNase free-DNase (Roche, Indianapolis, IN) and RNase Inhibitor (Roche). The RNA was subjected to RPA according to Pharmingen's protocol. In short, mRNA from macrophages or the lungs was hybridized

overnight to [^{32}P]-UTP-labeled probes. The protected [^{32}P]-UTP-labeled RNA probes were resolved on a 6% polyacrylamide gel and analyzed by autoradiography. Cytokine analysis was performed using a custom-made template set specific for NOS2, IL-4, IL-12p40, TNF, IL-1β, IL-1α, and IFN-γ. The expression of specific genes was quantified on a densitometer (ImageQuant Software, Molecular Dynamics, Sunnyvale, CA), relative to the abundance of housekeeping gene, L32. We also performed phosphorimaging quantification on some samples but found results identical to densitometry; therefore, only densitometry quantifications are shown.

A.3 Results

We followed up our previous work to address the expression and role of IL-10 in *M. tuberculosis* infection. Aerosol infection was performed using a nose only exposure unit to deliver 50-100 CFU to the lungs of IL-10-/- or wild type (C57BL/6) mice. IL-10 was neutralized by administering JES antibody (i.p. 500μg/ mouse every three days) and TNF was neutralized with MP6-XT22 antibody (i.p. 500μg/ mouse every three days).

We have previously reported that IL-10 was expressed at low or undetectable levels in lungs of *M. tuberculosis* aerosol-infected C57Bl/6 mice, as determined by RNase protection assay [106]. On the other hand, when bacterial burdens were high in immunocompromised mice, such as CCR2-/- (high dose i.v.infection), TNFRp55-/-, anti-TNF treated, CD40-/-, or CD4-/- mice, IL-10 expression in the lungs was increased (Table 12) especially when bacterial burdens increased to levels above $1x10^7$ CFU. A good example of the IL-10 expression in mice with high bacterial burdens is in CD40-/- mice where at 3 weeks post infection only some of the mice have high bacterial burdens. The subset of CD40-/- mice with pulmonary bacterial

numbers similar to wild type mice also had wild type (low) IL-10 mRNA expression levels. However, IL-10 expression was 4-5x higher in the lungs of sick CD40-/- mice (Table 12),

Table 12. IL-10 gene expression in the lungs of *M. tuberculosis* infected mice.

Expression of IL-10 was increased in aerosol infected gene-deficient mice that were impaired in the ability to control *M. tuberculosis* infection, compared to wild type C57BL/6 mice. [1]Ratio is the ratio of the intensity of the IL-10 gene over the L32 housekeeping gene. The results are the average of two mice at each time point. This experiment was performed a minimum of twice for each group of mice with similar results.

Strain	"N"	Days Post Infection	Average CFU	Ratio (IL10/L32)
TNFR	3	25	$4x10^7$	0.036
TNFR	3	14	$1x10^5$	0.002
CD4 -/-	3	44	$2x10^7$	0.027
CD4-/-	3	21	$2x10^6$	0.007
CD40-/-	3	21	$4x10^6$	0.005
CD40-/-	2	21	$9x10^7$	0.023
CD40-/-	3	14	$2x10^6$	0.001
CCR2-/-	4	18	$1x10^8$	0.011
CCR2-/-	3	12	$8x10^5$	0.001
GKO	3	28	$9x10^7$	0.014
GKO	3	21	$7x10^6$	0.005
WT	4	21	$1x10^5$	0.002
MP6 txt	3	18	$1x10^7$	0.029
IgG txt	3	18	$1x10^6$	0.001

Acute M. tuberculosis infection in IL-10-/- mice

As previously reported [65], IL-10-/- mice controlled aerosol infection with *M. tuberculosis* similar to wild type mice (Figure 45A). Histologically the granuloma structures were well organized. The macrophages appeared larger and more activated in the IL-10 -/- mice, but RNase Protection Assays on lung RNA revealed no significant differences in the expression of IL-1, IL-15 or IL-12 compared to C57BL/6 mice (data not shown). Based on our previous experience detecting cytokines from the macrophage population, it is possible that our technique was not sensitive enough to detect differences. IFNγ expression was measured at 4, 8, 14, 18, and 22 weeks post infection. While there was a tread towards higher IFNγ expression in the IL-10-/- mice, the differences were only significant at 4 and 14 weeks postinfection.

Therefore, during acute infection, the course of infection in C57BL/6 mice and IL-10-/- was relatively similar.

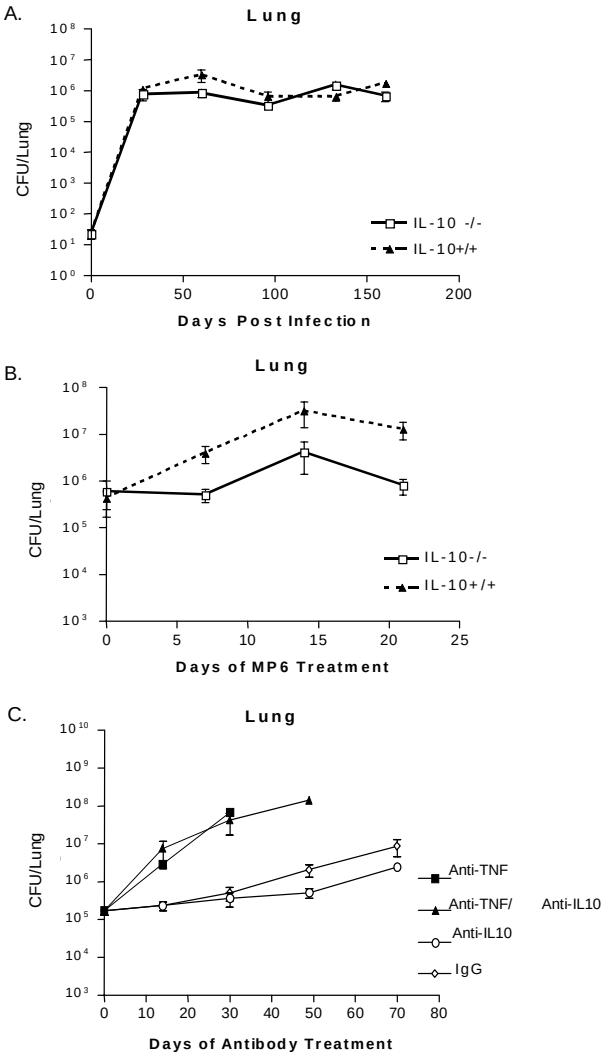

Figure 45. Colony forming units in the lungs of *M. tuberculosis* infected mice.

A. IL-10-/- mice controlled *M. tuberculosis* infection in the lung, spleen, and liver (data not shown). The course of infection in IL-10-/- mice was similar to wild type mice. B. When TNF was neutralized in chronically infected IL-10-/- mice, through MP6 treatment, the IL-10-/- mice maintained better control of the pulmonary bacterial burden. C. IL-10 neutralization alone in chronically infected wild type mice did not alter the course of infection. On the other hand when TNF was neutralized, alone or in conjunction with IL-10, the bacterial burdens in the lungs rose. TNF neutralization alone led to uncontrolled infection and death by 20 days post infection. Dual neutralization of TNF and IL-10 delayed mortality, but only temporarily.

The role of IL-10 during anti-TNF induced reactivation

To address the contribution of IL-10 to the pathology observed during anti-TNF Ab induced reactivation of tuberculosis [106], we treated chronically infected (4-5 months post-infection) IL-10-/- and C57BL/6 mice with anti-TNF antibody. The IL-10-/- mice exhibited reduced bacterial burdens in their lungs, livers and spleens compared to C57BL/6 mice treated with anti-TNF, but that did not influence the survival of the mice (Figure 45B). Both IL-10-/- and wild type mice succumbed to infection by 25 days post anti-TNF antibody treatment. In addition both IL-10-/- and wild type mice developed severe disorganization of the cellular infiltrate in the lungs by 14 days after anti-TNF treatment began (Figure 46).

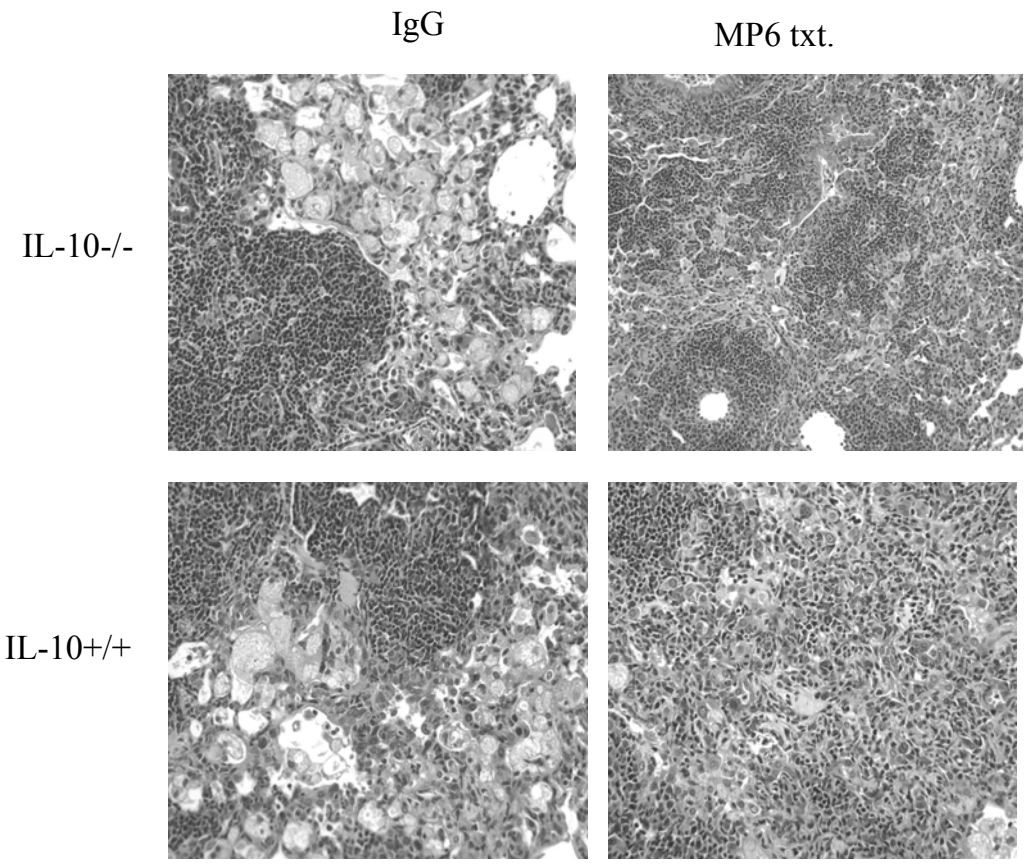

Figure 46. TNF neutralization leads to increased disorganized pulmonary infiltrate in IL-10-/- and wild type mice.

Granuloma formation in IL-10-/- and wild type mice was similar throughout infection (here shown at 4 months post infection). By 14 days post MP6 treatment, cellular infiltrate increased in both groups of mice and granuloma becomes disorganized

When IL-10 was neutralized in conjunction with TNF neutralization in a chronic mouse model, the mean survival time was 8 days longer (m.s.t 24 days (anti-TNF) v. m.s.t. = 32 days (anti-TNF/anti-IL10), but there was no overall difference seen in the histology. These data indicate that IL-10 was probably making a very subtle difference in the immune response. At 10 days post antibody treatment there was a reduction in the mean fluorescence intensity of costimulatory molecules B7.1 (MFI = 240 v. 310: Anti-IL10, anti TNF Abs vs anti-TNF Ab alone) and B7.2 (MFI = 389 v. 592) in the dual neutralized mice compared to the anti-TNF treated mice, but no difference in the percentage of cells expressing these molecules. In addition, the percentage of CD25+ lymphocytes was increased in the dual neutralized mice (31% v. 15% CD25+ in CD8+gate and 39% v. 20% in the CD4+ gate). This suggests that IL-10 may down regulate CD25 expression on lymphocytes, or that a population of proliferating (CD25+) T cells is down-regulated by IL-10. IL-10 neutralization alone resulted in no differences in the course of infection (data not shown).

A.4 Discussion

Recent data suggest that IL-10 overproduction in vivo can reactivate chronic pulmonary tuberculosis in C57BL/6 mice [107]. Although this is evident in the transgenic system, C57BL/6 mice do appear to produce amounts of IL-10 capable of producing detrimental immunosuppressive effects during *M. tuberculosis* infection. IL-10 -/- mice controlled infection slightly longer in the face of TNF neutralization, compared to wild type mice. Clearly, the quantity and timing of IL-10 production influences the effects the cytokine can have on the immune response and control of the infection. In the case of TNF neutralization in wild type

mice, the expression of IL-10 may be slightly detrimental to the induced reactivation. Therefore, the results of our study indicate that IL-10 production in TNF neutralized mice was a reaction to the inflammation in TNF neutralized mice, and although it may contribute to the pathology, it was not responsible for the induction of inflammation observed after TNF neutralization. The data in table 11 also supports this. IL-10 is not expressed in mice where bacterial burdens are below $1x10^7$ CFU. Most of these mice succumb to infection and have severe inflammation due to impaired cell mediated immune responses not due to IL-10 production.

APPENDIX B

B.0 Anti-TNF treatment in the presence of antibiotics.

Anti-TNF treatment quickly results in loss of control of *M. tuberculosis* granulomas and the bacterial burdens increase. The anti-TNF treated mice succumb to infection despite the fact that the number of colony forming units in the lung is not $>10^8$ (a level where wild type C57Bl/6 usually become moribund). The log increase in CFU observed in the anti-TNF treated mice is enough to increase chemokine levels complicating our experimental models by created two variables, no TNF and higher CFU, rather than just no TNF.

To attempt to eliminate the second variable in our experimental model, we treated both the anti-TNF treated and the IgG treated mice with antibiotics 4 months post infection. The treatment led to a reduction in the colony forming units, although the mice treated with MP6XT-22 had a slower reduction, as seen at day 14 (Figure 47). By day 42, *M. tuberculosis* was no longer detected in the lung (limit of detection <40 CFU). As a result no experimental or control mice succumbed due to anti-TNF treatment. The experiment was sustained for 70 days to observe the cellular infiltrate, pathology and colony forming units.

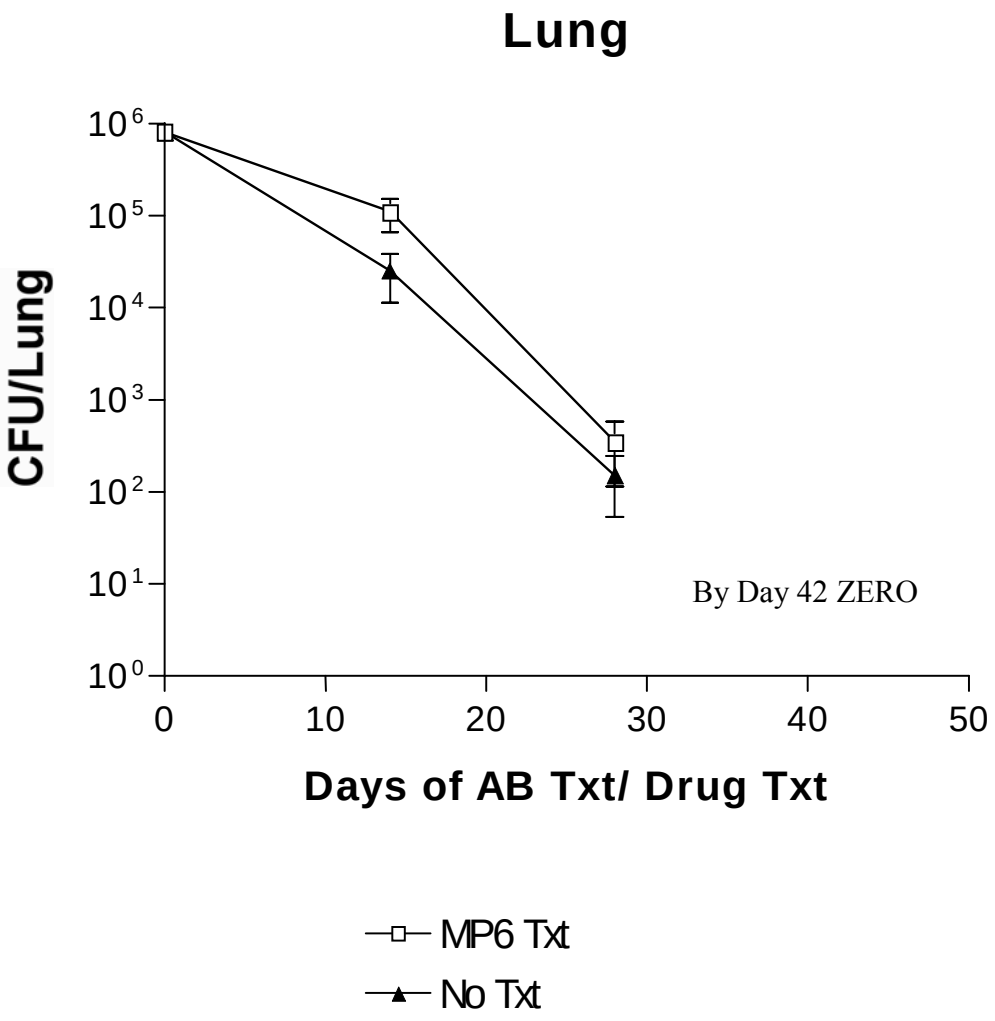

Figure 47. Colony Forming Units in the Lung following antibiotic treatment and antibody treatment in chronically infected mice.

With the antibiotic treatment, we never observed reactivation of disease in either group of mice. Histological samples of the lungs were stained at each time point (Figure 48). Fourteen

days after antibody and antibiotic treatment began, disorganization was observed in the lungs of anti-TNF treated mice. But even when bacterial levels were below detection, the granulomas were still present in the lungs at later time point. The granulomas were still organized even in the anti-TNF treated mice, and the size and number of granulomas was decreased by 42 days post antibody treatment. These data suggest that the bacteria are required to drive the chemokine gradients for granuloma formation. In addition, as described earlier, anti-TNF treatment of macrophages did not abolish, but rather altered chemokine expression in macrophages (Figure 18). The antibiotic treated/ anti-TNF Ab treated mice have very low bacterial burdens compared to anti-TNF Ab treated (without antimycobacterials) mice. If these mice have reduced levels of chemokine similar to observations made in anti-TNF Ab treated mice (See section 7.0), the existing chemokine expression may be enough to control the infection at the later time points.

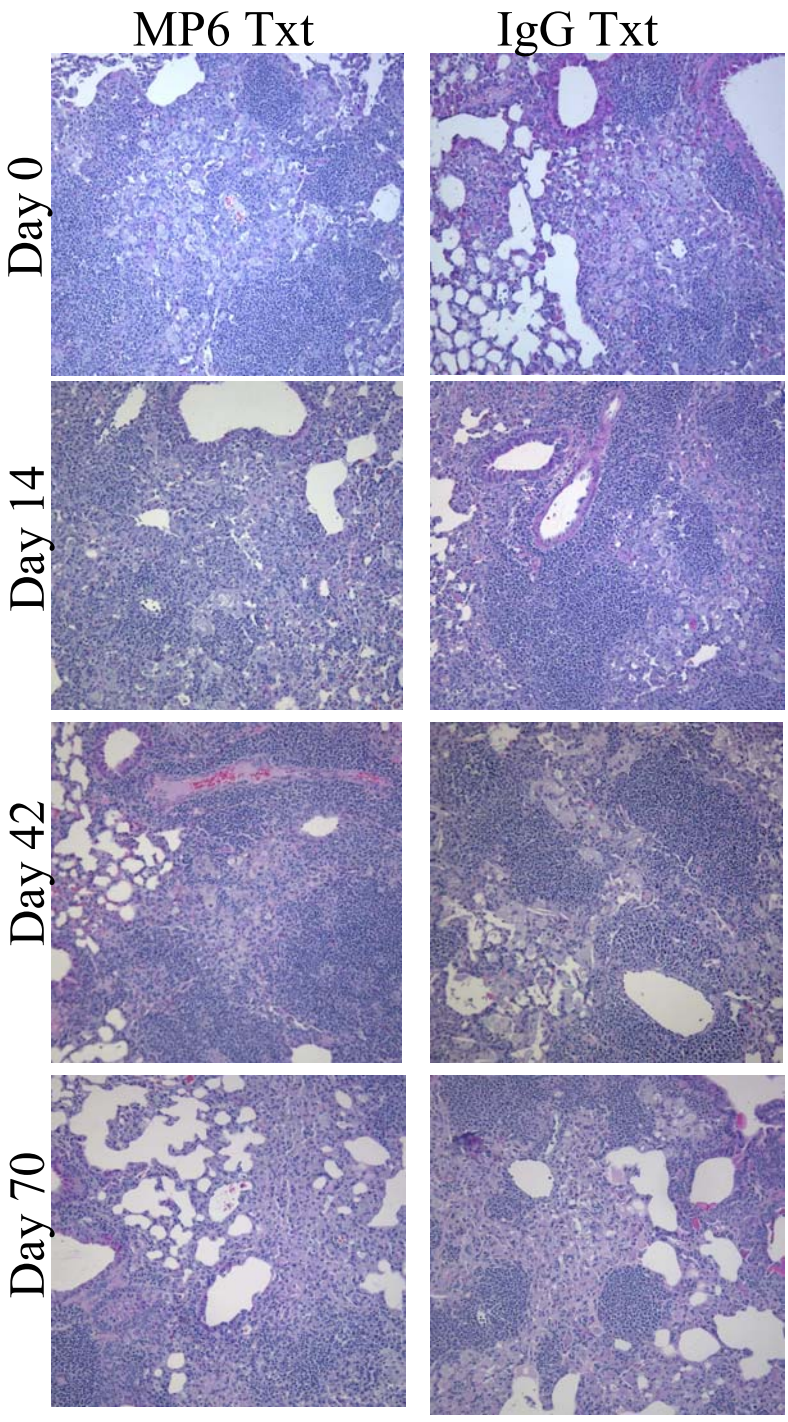

Figure 48. Histological Images of chronically infected mice treated with antibiotics and anti-TNF Ab.

The flow cytometric analysis performed on the lungs of the mice confirmed the observations in the histology. The numbers of cells in the lungs of the mice gradually decreased

as the bacterial burdens reduced (Figure 49). Thirty days post antibody/ antibiotic treatment, the total number of cells in the lungs of anti-TNF treated mice was significantly lower than the IgG treated mice. Two weeks later the number of cells in the IgG treated mice was also much lower and by 70 days after treatment began, the total number of cells in the lungs of both groups was significantly reduced compared to the first day of treatment.

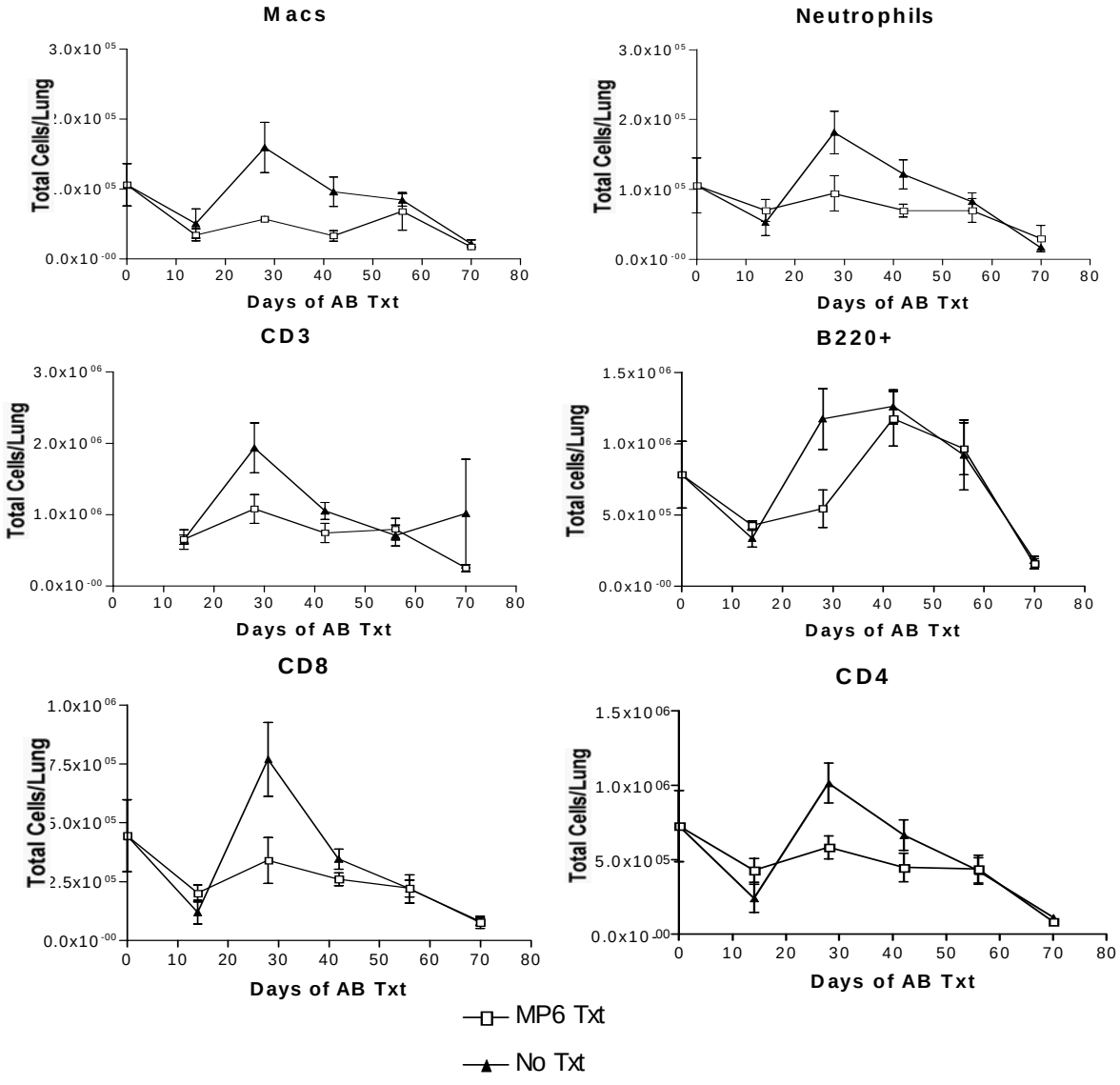

Figure 49. Cellular infiltrate in the lungs of chronically infected mice treated with antibiotics.

Antibiotic treatment reduced the bacterial burdens in the anti-TNF Ab treatment group and the IgG treatment group, eliminating the morbidity of the anti-TNF Ab treated mice. Unfortunately due to the reduced bacterial burden and the decreasing cellular infiltrate in the lungs, the pathological changes usually observed with antibiotic/anti-TNF Ab treatment were transient and not as profound. The antibiotic/anti-TNF treated mice cleared the bacteria more slowly than the antibiotic/IgG treated mice therefore there were still differences in bacterial burden at 14 days post infection. Therefore using this method did not eliminate the variable of bacterial burden differences.

APPENDIX C

C.0 mRNA expression of extracellular matrix proteins and adhesion molecules during *M. tuberculosis* infection.

C.1 Introduction.

TNF is clearly required for granuloma formation and control of tuberculosis infection. This study was performed to address other molecules and processes in granuloma formation and cell migration that might be influenced by TNF during infection. The two major groups of molecules that were addressed include adhesion molecules and matrix metalloproteinases.

The process of cell migration and cellular infiltration is mediated in part through the interaction of cells with cellular adhesion molecules. As leukocytes migrate through blood vessels they are only slightly tethered to the vessel walls. This interaction is through a group of molecules called selectins, which bind to carbohydrate moieties on the leukocytes. Subsequently firm adhesion and transmigration is mediated through another group of molecules, cellular adhesion molecules (such as VCAM, ICAM, or PECAM). Another critical component to cell transmigration is chemokine expression and gradient formation. The gradient can directly influence cell migration by inducing cytoskeletal changes and upregulate the adhesion expression, avidity and affinity inducing firm adhesion.

Cell infiltration and tissue reconstruction can be influenced my matrix metalloproteinases. There is some evidence that TNF may affect the expression of MMP-2 and MMP-9.

C.2 Materials and Methods.

Animals. C57BL/6 female mice (Charles River, Rockland, Mass.) 8-14 weeks old were used in all experiments. All infected mice were maintained in the BSL3 animal laboratories and routinely monitored for murine pathogens by means of serological and histological examinations. The University Institutional Animal Care and Use Committee approved all animal protocols employed in this study.

Chemicals, antibodies and reagents. All chemicals were purchased from Sigma Chemical Co. (St. Louis, MO.) unless otherwise noted. Middlebrook 7H9 liquid medium and 7H10 agar were obtained from Difco Laboratories (Detroit, MI). The cell lines, MP6XT-22 (anti-TNF) and was obtained from DNAX and used to generate ascites (Harlan Bioproducts, Indianapolis,IN). Antibodies were purified endotoxin free from ascites fluid as previously described [106] and mice were treated with antibody intravenously every three days (0.5mg/dose) starting 4 months post infection. Control mice received normal rat IgG (Jackson Immunoresearch Laboratories Inc.,West Grove, PA) with the same dosing regiment.

Mycobacteria and infection of mice. To prepare bacterial stock, *M. tuberculosis* strain Erdman (Trudeau Institute, Saranac Lake, N.Y.) was used to infect mice, and then bacteria were harvested from their lungs, expanded in 7H9 liquid medium and stored in aliquots at -80°C. Mice were infected via the aerosol route using a nose-only exposure unit (InTox Products, Albuquerque, N.M.), and exposed to *M. tuberculosis* (1×10^7 CFU/ml in the nebulizer chamber) for 20 minutes, followed by 5 minutes of air. This resulted in reproducible delivery of 50-100 viable CFU of *M. tuberculosis* as described previously [94], which was confirmed by CFU determination on the lungs of 2-3 mice 1 day post-infection. In acute experiments where a higher inoculum was used, the concentration of *M. tuberculosis* in the nebulizer was increased, and day 1 CFU were determined in the lungs. The tissue bacillary load was quantified by plating

serial dilutions of the lung, liver, and spleen homogenates onto 7H10 agar as described previously [30].

RNA Isolation. RNA was isolated from the lung or cells using the TRIZOL isolation protocol with slight modifications. The lung was homogenized in 3ml (cells were lysed in 1ml TRIZOL/ $2x10^6$ cells) of TRIZOL reagent and then two chloroform extractions were performed. Following an isopropanol precipitation, the RNA was washed with 70% ethanol and treated with RNase Inhibitor (Applied Biosystems, Foster City, CA) for 45 minutes. Following complete resuspension of the RNA at 65° C for 15 minutes the RNA was cleaned and DNase digested using the Qiagen RNA isolation kit, as directed by the manufacturer (Qiagen Inc., Valencia, CA).

GEArray Q series KIT. Total RNA was used as the template for ^{32}-P labeled cDNA probe synthesis using the following procedure. 5μg of RNA was combined with the GEAprimer Mix (Buffer A, SuperArray, Bethesda, MD) and heated to 70C for 3 minutes and then transferred to 42C for 2 minutes. The labeling mix(GEA labeling buffer, 3μCi ^{32}P dCTP, RNase Inhibitor, Reverse Transcriptase, RNase-free H_20) was prepared as described by the manufacturer. The mRNA was reverse transcribed and labeled for 25 minutes at 42C. The reaction was stopped through addition of Buffer C and then the probe was denatured. The labeled cDNA was added to hybridization mix and exposed to a prehybridized filter array O/N with continuous agitation at 60C, as described by the manufacturer. The filters were then washed in multiple changes of wash solution (2X SCC, 1% SDS). The filters were then exposed to X-ray film for 24 hours and 48 hours. Analysis was performed using the manufacturer's instructions. In short, the X-ray film was scanned and then a raw data file extracted using the suggested software (Scanalyze by Michael Eisen).

C.3 Results and Discussion.

Chronically infected mice were treated with either anti-TNF Ab or IgG at 4 months post infection. At 3, 6, 9, and 12 days after antibody treatments began, RNA was isolated from the lungs and used in the GEArray, filter array technology by SuperArray Inc. This array allowed us to address the mRNA expression through use of a cDNA radiolabelled probe. The results of the array are presented in Figure 50,Figure 51, and Figure 52. Figure 50 shows the graphs on the immunoglobulin superfamily, cadherin and catenin adhesion molecules. Figure 51 shows the graphs of the integrin adhesion molecules. Figure 52 shows the data generated on the matrix metalloproteinase expression.

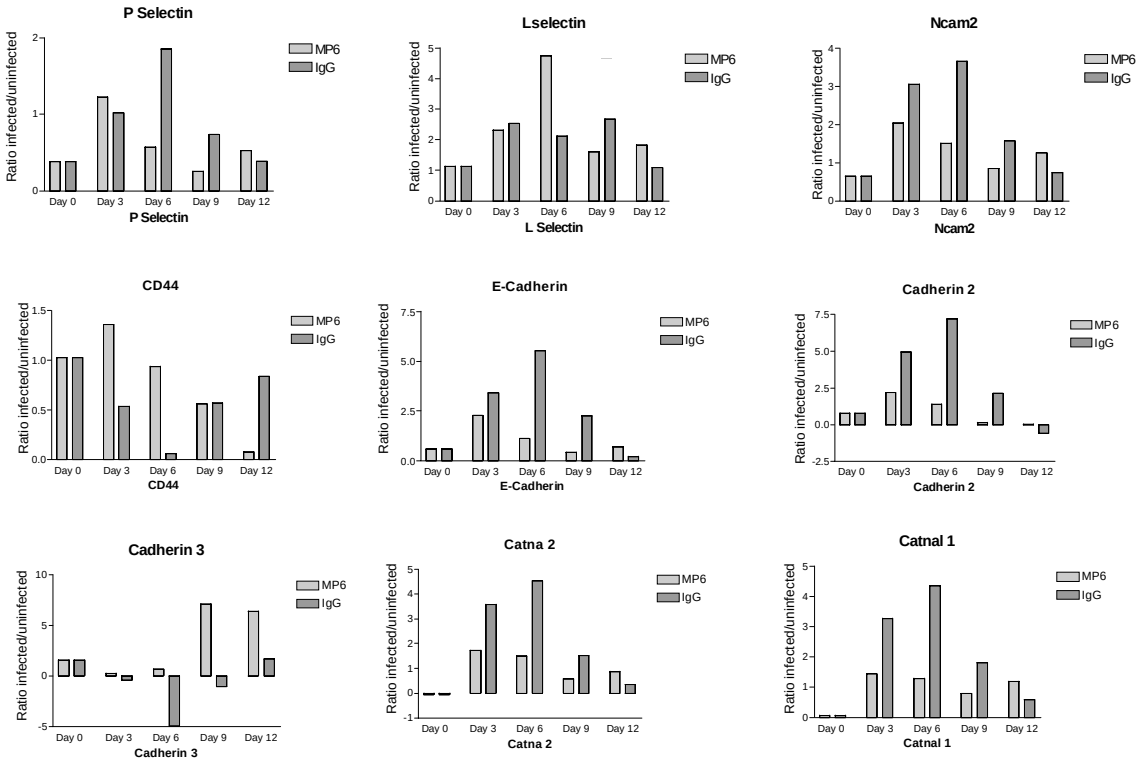

Figure 50. Cell Adhesion Molecules (Ig Superfamily, Cadherins and Catenins, Selectins).

Expression of cell adhesion molecule mRNAs was determined using the GEArray Mouse Extracellular Matrix and Adhesion Molecule Gene Array. The graph represents the ratio of the expression of the sample of interest over uninfected.

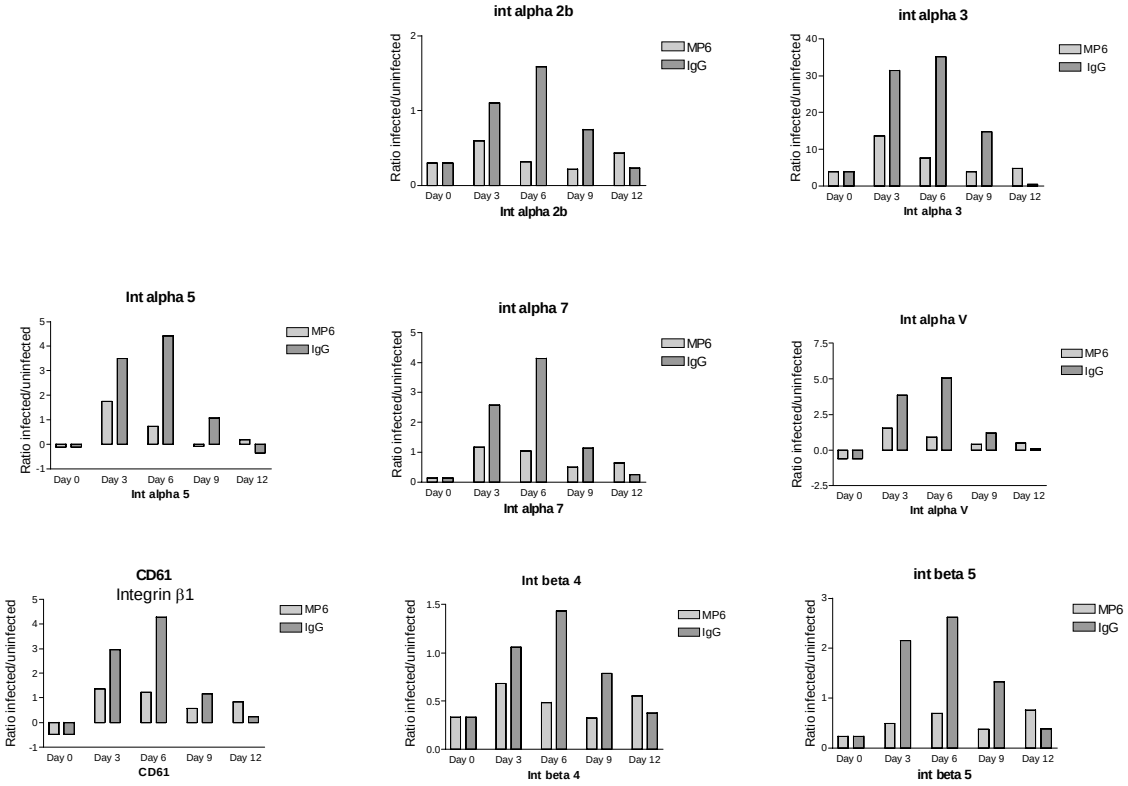

Figure 51. Cell adhesion Molecules (Integrins).

Expression of cell adhesion molecule mRNAs was determined using the GEArray Mouse Extracellular Matrix and Adhesion Molecule Gene Array. The graph represents the ratio of the expression of the sample of interest over uninfected.

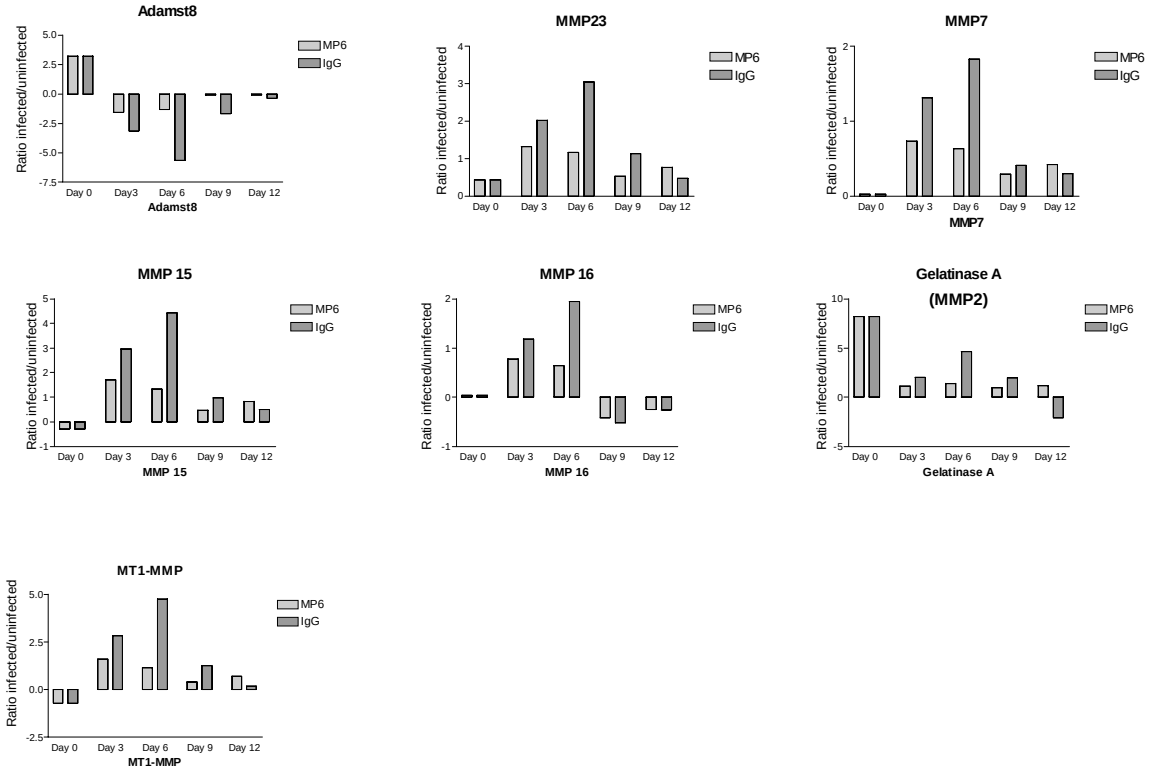

Figure 52. Matrix Metalloproteinases.

Expression of cell adhesion molecule mRNAs was determined using the GEArray Mouse Extracellular Matrix and Adhesion Molecule Gene Array. The graph represents the ratio of the expression of the sample of interest over uninfected.

Expression of many adhesion molecules was different between the MP6 treated and IgG treated mice. Unfortunately within a chronic infection, especially within the IgG treated mice, we did not expect to see such variation. This variability indicates that the assay may be fairly sensitive, but the data analysis procedure must be considered carefully because if both a gene has expression less than background in both the uninfected sample and in the true sample, a false positive value will be generated. In addition, the mRNA analysis performed here can only be a first step when addressing whether these changes in mRNA expression translate to changes in

protein production, and consequently have functional consequences. In addition matrix metalloproteinases are highly post transcriptionally regulated.

In conclusion, our analysis of extracellular matrix and adhesion molecules did not revealed any stricking differences between MP6 treated and IgG treated mice. Even when differences were detected between the groups of mice, there was often increased or decreased expression in the IgG treated mice compared to other time points. Further analysis to address the protein expression of the proteins is necessary to draw any conclusion as to how TNF affects the expression of these molecules.

BIBLIOGRAPHY

1. Agger, E.M. and P. Andersen, *A novel TB vaccine; towards a strategy based on our understanding of BCG failure.* Vaccine., 2002. **21**(1-2): p. 7-14.
2. World Health Organization, *Global Tuberculosis Control: Surveillance, Planning, Financing. WHO Report 2003.* 2003, World Health Organization: Geneva, Switzerland.
3. Corbett, E.L., et al., *The growing burden of tuberculosis: global trends and interactions with the HIV epidemic.* Archives of Internal Medicine., 2003. **163**(9): p. 1009-21.
4. Center for Disease Control, *Trends in Tuberculosis Morbidity ---United States, 1992--2002. Morbidity and Mortality Weekly Report*. 2003, Center for Disease Control: Atlanta. p. 217-222.
5. Styblo, K., *Recent advances in epidemiological research in tuberculosis.* Advances in Tuberculosis Research., 1980. **20**: p. 1-63.
6. Tufariello, J.M., J. Chan, and J.L. Flynn, *Latent tuberculosis: mechanisms of host and bacillus that contribute to persistent infection.* The Lancet Infectious Diseases., 2003. **3**(9): p. 578-90.
7. Caruso, A.M., et al., *Mice deficient in CD4 T cells have only transiently diminished levels of IFN-gamma, yet succumb to tuberculosis.* Journal of Immunology., 1999. **162**(9): p. 5407-16.
8. Scanga, C.A., et al., *Depletion of CD4(+) T cells causes reactivation of murine persistent tuberculosis despite continued expression of interferon gamma and nitric oxide synthase 2.* Journal of Experimental Medicine., 2000. **192**(3): p. 347-58.
9. Saunders, B.M., et al., *CD4 is required for the development of a protective granulomatous response to pulmonary tuberculosis.* Cellular Immunology., 2002. **216**(1-2): p. 65-72.
10. Serbina, N.V., V. Lazarevic, and J.L. Flynn, *CD4(+) T cells are required for the development of cytotoxic CD8(+) T cells during Mycobacterium tuberculosis infection.* Journal of Immunology, 2001. **167**(12): p. 6991-7000.
11. Barnes, P.F., D.L. Lakey, and W.J. Burman, *Tuberculosis in Patients with HIV Infection.* Infectious Disease Clinics of North America, 2002. **16**(1): p. 353-362.
12. Wagner, K.R. and W.R. Bishai, *Issues in the treatment of M. tuberculosis in patients with human immunodeficiency virus infection.* AIDS, 2001. **15**(suppl 5): p. S203-S212.
13. Janicki, B.W., et al., *Immune responses in rhesus monkeys after bacillus Calmette-Guerin vaccination and aerosol challenge with Mycobacterium tuberculosis.* American Review of Respiratory Disease., 1973. **107**(3): p. 359-66.
14. Chaparas, S.D., R.C. Good, and B.W. Janicki, *Tuberculin-induced lymphocyte transformation and skin reactivity in monkeys vaccinated or not vaccinated with Bacille Calmette-Guerin, then challenged with virulent Mycobacterium tuberculosis.* American Review of Respiratory Disease., 1975. **112**(1): p. 43-7.
15. Barclay, W.R., et al., *Protection of monkeys against airborne tuberculosis by aerosol vaccination with bacillus Calmette-Guerin.* American Review of Respiratory Disease., 1973. **107**(3): p. 351-8.

16. Good, R.C., *Diseases in Nonhuman Primates*, in *The Mycobacteria: a Sourcebook*. 1984, Wayne Kubica. p. 903-921.
17. Capuano III, S.V., et al., *Experimental Mycobacterium tuberculosis infection of cynomolgus macaques closely resembles the various manifestations of human M. tuberculosis infection.* Infect. Immun., 2003. **in press**.
18. McMurray, D.N., *Disease model: pulmonary tuberculosis.* Trends in Molecular Medicine., 2001. **7**(3): p. 135-7.
19. Allen, S.S. and D.N. McMurray, *Coordinate cytokine gene expression in vivo following induction of tuberculous pleurisy in guinea pigs.* Infection & Immunity., 2003. **71**(8): p. 4271-7.
20. Jeevan, A., et al., *Effect of Mycobacterium bovis BCG vaccination on interleukin-1 beta and RANTES mRNA expression in guinea pig cells exposed to attenuated and virulent mycobacteria.* Infection & Immunity., 2002. **70**(3): p. 1245-53.
21. Jeevan, A., et al., *Differential expression of gamma interferon mRNA induced by attenuated and virulent Mycobacterium tuberculosis in guinea pig cells after Mycobacterium bovis BCG vaccination.* Infection & Immunity., 2003. **71**(1): p. 354-64.
22. Lyons, M.J., T. Yoshimura, and D.N. McMurray, *Mycobacterium bovis BCG vaccination augments interleukin-8 mRNA expression and protein production in guinea pig alveolar macrophages infected with Mycobacterium tuberculosis.* Infection & Immunity., 2002. **70**(10): p. 5471-8.
23. Flynn, J.L. and J. Chan, *Immunology of tuberculosis.* Annual Review of Immunology., 2001. **19**: p. 93-129.
24. Collins, F.M., *Immunolgy of Tuberculosis.* American Review of Respiratory Disease., 1982. **125**: p. S42-S49.
25. Medina, E. and R. North, *Genetic susceptible mice remain proportionally more susceptible to tuberculosis after vaccination.* Immunology, 1999. **96**: p. 16-21.
26. Gonzalez-Juarrero, M., et al., *Temporal and spatial arrangement of lymphocytes within lung granulomas induced by aerosol infection with Mycobacterium tuberculosis.* Infection & Immunity., 2001. **69**(3): p. 1722-8.
27. Flynn, J.L. and J. Chan, *Tuberculosis: latency and reactivation.* Infection & Immunity., 2001. **69**(7): p. 4195-201.
28. McCune, R.M., F.M. Feldmann, and W. McDermott, *Microbial persistence. II. Characteristics of the sterile state of tubercle bacilli.* Journal of Experimental Medicine., 1966. **123**(3): p. 469-86.
29. McCune, R.M., et al., *Microbial persistence. I. The capacity of tubercle bacilli to survive sterilization in mouse tissues.* Journal of Experimental Medicine., 1966. **123**(3): p. 445-68.
30. Scanga, C.A., et al., *Reactivation of latent tuberculosis: variations on the Cornell murine model.* Infection & Immunity., 1999. **67**(9): p. 4531-8.
31. Ernst, J.D., *Macrophage receptors for Mycobacterium tuberculosis.* Infection & Immunity., 1998. **66**(4): p. 1277-81.
32. Aderem, A. and D.M. Underhill, *Mechanisms of phagocytosis in macrophages.* Annual Review of Immunology., 1999. **17**: p. 593-623.
33. Kang, B.K. and L.S. Schlesinger, *Characterization of mannose receptor-dependent phagocytosis mediated by Mycobacterium tuberculosis lipoarabinomannan.* Infection & Immunity., 1998. **66**(6): p. 2769-77.

34. Leemans, J.C., et al., *CD44 is a macrophage binding site for Mycobacterium tuberculosis that mediates macrophage recruitment and protective immunity against tuberculosis.* Journal of Clinical Investigation., 2003. **111**(5): p. 681-9.
35. Melo, M.D., et al., *Utilization of CD11b knockout mice to characterize the role of complement receptor 3 (CR3, CD11b/CD18) in the growth of Mycobacterium tuberculosis in macrophages.* Cellular Immunology., 2000. **205**(1): p. 13-23.
36. Hu, C., et al., *Mycobacterium tuberculosis infection in complement receptor 3-deficient mice.* Journal of Immunology., 2000. **165**(5): p. 2596-602.
37. Zimmerli, S., S. Edwards, and J.D. Ernst, *Selective receptor blockade during phagocytosis does not alter the survival and growth of Mycobacterium tuberculosis in human macrophages.* American Journal of Respiratory Cell & Molecular Biology., 1996. **15**(6): p. 760-70.
38. Velasco-Velazquez, M.A., et al., *Macrophage--Mycobacterium tuberculosis interactions: role of complement receptor 3.* Microbial Pathogenesis., 2003. **35**(3): p. 125-31.
39. Stokes, R.W., et al., *Mycobacteria-macrophage interactions. Macrophage phenotype determines the nonopsonic binding of Mycobacterium tuberculosis to murine macrophages.* Journal of Immunology., 1993. **151**(12): p. 7067-76.
40. Schlesinger, L.S., et al., *Differences in mannose receptor-mediated uptake of lipoarabinomannan from virulent and attenuated strains of Mycobacterium tuberculosis by human macrophages.* Journal of Immunology., 1996. **157**(10): p. 4568-75.
41. Tailleux, L., et al., *DC-SIGN is the major Mycobacterium tuberculosis receptor on human dendritic cells.[comment].* Journal of Experimental Medicine., 2003. **197**(1): p. 121-7.
42. Reddy, V.M. and D.A. Hayworth, *Interaction of Mycobacterium tuberculosis with human respiratory epithelial cells (HEp-2).* Tuberculosis., 2002. **82**(1): p. 31-6.
43. Leemans, J.C., et al., *Depletion of alveolar macrophages exerts protective effects in pulmonary tuberculosis in mice.* Journal of Immunology., 2001. **166**(7): p. 4604-11.
44. Ferrari, G., et al., *A coat protein on phagosomes involved in the intracellular survival of mycobacteria.* Cell., 1999. **97**(4): p. 435-47.
45. Deretic, V. and R.A. Fratti, *Mycobacterium tuberculosis phagosome.* Molecular Microbiology., 1999. **31**(6): p. 1603-9.
46. Stenger, S., et al., *Differential effects of cytolytic T cell subsets on intracellular infection.* Science., 1997. **276**(5319): p. 1684-7.
47. Heldwein, K.A. and M.J. Fenton, *The role of Toll-like receptors in immunity against mycobacterial infection.* Microbes & Infection., 2002. **4**(9): p. 937-44.
48. Medvedev, A.E., et al., *Induction of tolerance to lipopolysaccharide and mycobacterial components in Chinese hamster ovary/CD14 cells is not affected by overexpression of Toll-like receptors 2 or 4.* Journal of Immunology., 2001. **167**(4): p. 2257-67.
49. Gehring, A.J., et al., *The Mycobacterium tuberculosis 19-kilodalton lipoprotein inhibits gamma interferon-regulated HLA-DR and Fc gamma R1 on human macrophages through Toll-like receptor 2.* Infection & Immunity., 2003. **71**(8): p. 4487-97.
50. Noss, E.H., et al., *Toll-like receptor 2-dependent inhibition of macrophage class II MHC expression and antigen processing by 19-kDa lipoprotein of Mycobacterium tuberculosis.* Journal of Immunology., 2001. **167**(2): p. 910-8.

51. Pai, R.K., et al., *Inhibition of IFN-gamma-induced class II transactivator expression by a 19-kDa lipoprotein from Mycobacterium tuberculosis: a potential mechanism for immune evasion.* Journal of Immunology., 2003. **171**(1): p. 175-84.
52. Lopez, M., et al., *The 19-kDa Mycobacterium tuberculosis protein induces macrophage apoptosis through Toll-like receptor-2.* Journal of Immunology., 2003. **170**(5): p. 2409-16.
53. Means, T.K., et al., *Differential effects of a Toll-like receptor antagonist on Mycobacterium tuberculosis-induced macrophage responses.* Journal of Immunology., 2001. **166**(6): p. 4074-82.
54. Underhill, D.M., et al., *Toll-like receptor-2 mediates mycobacteria-induced proinflammatory signaling in macrophages.* Proceedings of the National Academy of Sciences of the United States of America., 1999. **96**(25): p. 14459-63.
55. Brightbill, H.D., et al., *Host defense mechanisms triggered by microbial lipoproteins through toll-like receptors.* Science., 1999. **285**(5428): p. 732-6.
56. Reiling, N., et al., *Cutting edge: Toll-like receptor (TLR)2- and TLR4-mediated pathogen recognition in resistance to airborne infection with Mycobacterium tuberculosis.* Journal of Immunology., 2002. **169**(7): p. 3480-4.
57. Abel, B., et al., *Toll-like receptor 4 expression is required to control chronic Mycobacterium tuberculosis infection in mice.* Journal of Immunology., 2002. **169**(6): p. 3155-62.
58. Pedrosa, J., et al., *Neutrophils play a protective nonphagocytic role in systemic Mycobacterium tuberculosis infection of mice.* Infection & Immunity, 2000. **68**(2): p. 577-83.
59. Chackerian, A.A., et al., *Dissemination of Mycobacterium tuberculosis is influenced by host factors and precedes the initiation of T-cell immunity.* Infection & Immunity., 2002. **70**(8): p. 4501-9.
60. Gonzalez-Juarrero, M. and I.M. Orme, *Characterization of murine lung dendritic cells infected with Mycobacterium tuberculosis.* Infection & Immunity., 2001. **69**(2): p. 1127-33.
61. Ehlers, S., et al., *Lethal granuloma disintegration in mycobacteria-infected TNFRp55-/- mice is dependent on T cells and IL-12.* Journal of Immunology, 2000. **165**(1): p. 483-92.
62. Peters, W., et al., *Chemokine receptor 2 serves an early and essential role in resistance to Mycobacterium tuberculosis.* Proceedings of the National Academy of Sciences of the United States of America., 2001. **98**(14): p. 7958-63.
63. Scott, H.M. and J.L. Flynn, *Mycobacterium tuberculosis in chemokine receptor 2-deficient mice: influence of dose on disease progression.* Infection & Immunity., 2002. **70**(11): p. 5946-54.
64. Flynn, J.L., et al., *An essential role for interferon gamma in resistance to Mycobacterium tuberculosis infection.* Journal of Experimental Medicine, 1993. **178**(6): p. 2249-54.
65. North, R.J., *Mice incapable of making IL-4 or IL-10 display normal resistance to infection with Mycobacterium tuberculosis.* Clinical & Experimental Immunology., 1998. **113**(1): p. 55-8.
66. Cooper, A.M., et al., *Interleukin 12 (IL-12) is crucial to the development of protective immunity in mice intravenously infected with mycobacterium tuberculosis.* Journal of Experimental Medicine., 1997. **186**(1): p. 39-45.

67. Cooper, A.M., et al., *Mice lacking bioactive IL-12 can generate protective, antigen-specific cellular responses to mycobacterial infection only if the IL-12 p40 subunit is present.* Journal of Immunology., 2002. **168**(3): p. 1322-7.
68. Ladel, C.H., et al., *Lethal tuberculosis in interleukin-6-deficient mutant mice.* Infection & Immunity., 1997. **65**(11): p. 4843-9.
69. Flynn, J.L., et al., *Major histocompatibility complex class I-restricted T cells are required for resistance to Mycobacterium tuberculosis infection.* Proceedings of the National Academy of Sciences of the United States of America., 1992. **89**(24): p. 12013-7.
70. Bosio, C.M., D. Gardner, and K.L. Elkins, *Infection of B cell-deficient mice with CDC 1551, a clinical isolate of Mycobacterium tuberculosis: delay in dissemination and development of lung pathology.* Journal of Immunology., 2000. **164**(12): p. 6417-25.
71. Cooper, A.M., et al., *Expression of the nitric oxide synthase 2 gene is not essential for early control of Mycobacterium tuberculosis in the murine lung.* Infection & Immunity, 2000. **68**(12): p. 6879-82.
72. Seiler, P., et al., *Early granuloma formation after aerosol Mycobacterium tuberculosis infection is regulated by neutrophils via CXCR3-signaling chemokines.* European Journal of Immunology, 2003. **33**(10): p. 2676-86.
73. Kipnis, A., et al., *Role of chemokine ligand 2 in the protective response to early murine pulmonary tuberculosis.* Immunology., 2003. **109**(4): p. 547-51.
74. Boros, D.L., *T helper cell populations, cytokine dynamics, and pathology of the schistosome egg granuloma.* Microbes & Infection., 1999. **1**(7): p. 511-6.
75. Palma, G.I. and N.G. Saravia, *In situ characterization of the human host response to Leishmania panamensis.* American Journal of Dermatopathology., 1997. **19**(6): p. 585-90.
76. Reyes-Flores, O., *Granulomas induced by living agents.* International Journal of Dermatology., 1986. **25**(3): p. 158-65.
77. Rumbley, C.A. and S.M. Phillips, *The schistosome granuloma: an immunoregulatory organelle.* Microbes & Infection., 1999. **1**(7): p. 499-504.
78. Modlin, R.L., et al., *Learning from lesions: patterns of tissue inflammation in leprosy.* Proceedings of the National Academy of Sciences of the United States of America., 1988. **85**(4): p. 1213-7.
79. Pulendran, B., K. Palucka, and J. Banchereau, *Sensing pathogens and tuning immune responses.* Science., 2001. **293**(5528): p. 253-6.
80. Hickman, S.P., J. Chan, and P. Salgame, *Mycobacterium tuberculosis induces differential cytokine production from dendritic cells and macrophages with divergent effects on naive T cell polarization.* Journal of Immunology., 2002. **168**(9): p. 4636-42.
81. Tascon, R.E., et al., *Protection against Mycobacterium tuberculosis infection by CD8+ T cells requires the production of gamma interferon.* Infection & Immunity., 1998. **66**(2): p. 830-4.
82. Bodnar, K.A., N.V. Serbina, and J.L. Flynn, *Fate of Mycobacterium tuberculosis within murine dendritic cells.* Infection & Immunity., 2001. **69**(2): p. 800-9.
83. Lande, R., et al., *IFN-alpha beta released by Mycobacterium tuberculosis-infected human dendritic cells induces the expression of CXCL10: selective recruitment of NK and activated T cells.* Journal of Immunology., 2003. **170**(3): p. 1174-82.

84. Yu, K., et al., *Toxicity of nitrogen oxides and related oxidants on mycobacteria: M. tuberculosis is resistant to peroxynitrite anion.* Tubercle & Lung Disease, 1999. **79**(4): p. 191-8.
85. Tailleux, L., et al., *Constrained intracellular survival of Mycobacterium tuberculosis in human dendritic cells.* Journal of Immunology., 2003. **170**(4): p. 1939-48.
86. Uehira, K., et al., *Dendritic cells are decreased in blood and accumulated in granuloma in tuberculosis.* Clinical Immunology., 2002. **105**(3): p. 296-303.
87. Scanga, C.A., et al., *The inducible nitric oxide synthase locus confers protection against aerogenic challenge of both clinical and laboratory strains of Mycobacterium tuberculosis in mice.* Infection & Immunity, 2001. **69**(12): p. 7711-7.
88. Nagabhushanam, V., et al., *Innate Inhibition of Adaptive Immunity: Mycobacterium tuberculosis- Induced IL-6 Inhibits Macrophage Responses to IFN-gamma.* Journal of Immunology, 2003. **171**: p. 4750-4757.
89. Ulrichs, T., et al., *T-cell responses to CD1-presented lipid antigens in humans with Mycobacterium tuberculosis infection.* Infection & Immunity., 2003. **71**(6): p. 3076-87.
90. Canaday, D.H., et al., *CD4(+) and CD8(+) T cells kill intracellular Mycobacterium tuberculosis by a perforin and Fas/Fas ligand-independent mechanism.* Journal of Immunology., 2001. **167**(5): p. 2734-42.
91. Turner, J., et al., *CD8- and CD95/95L-dependent mechanisms of resistance in mice with chronic pulmonary tuberculosis.* American Journal of Respiratory Cell & Molecular Biology., 2001. **24**(2): p. 203-9.
92. Behar, S.M., et al., *Susceptibility of mice deficient in CD1D or TAP1 to infection with Mycobacterium tuberculosis.* Journal of Experimental Medicine., 1999. **189**(12): p. 1973-80.
93. Dieli, F., et al., *Granulysin-dependent killing of intracellular and extracellular Mycobacterium tuberculosis by Vgamma9/Vdelta2 T lymphocytes.* Journal of Infectious Diseases., 2001. **184**(8): p. 1082-5.
94. Serbina, N.V., et al., *CD8+ CTL from lungs of Mycobacterium tuberculosis-infected mice express perforin in vivo and lyse infected macrophages.* Journal of Immunology., 2000. **165**(1): p. 353-63.
95. Serbina, N.V. and J.L. Flynn, *Early emergence of CD8(+) T cells primed for production of type 1 cytokines in the lungs of Mycobacterium tuberculosis-infected mice.* Infection & Immunity., 1999. **67**(8): p. 3980-8.
96. Turner, J., et al., *The progression of chronic tuberculosis in the mouse does not require the participation of B lymphocytes or interleukin-4.* Experimental Gerontology., 2001. **36**(3): p. 537-45.
97. Vordermeier, H.M., et al., *Increase of tuberculous infection in the organs of B cell-deficient mice.* Clinical & Experimental Immunology., 1996. **106**(2): p. 312-6.
98. Cooper, A.M., et al., *Disseminated tuberculosis in interferon gamma gene-disrupted mice.* Journal of Experimental Medicine, 1993. **178**(6): p. 2243-7.
99. Ottenhof, T.H., D. Kumararatne, J. L. Casanova, *Novel human immunodeficiencies reveal the essential role of type-1 cytokines in immunity to intracellular bacteria.* Immunol. Today, 1998. **19**: p. 491-4.
100. Pearl, J.E., et al., *Inflammation and lymphocyte activation during mycobacterial infection in the interferon-gamma-deficient mouse.* Cellular Immunology, 2001. **211**(1): p. 43-50.

101. Flynn, J.L., et al., *Tumor necrosis factor-alpha is required in the protective immune response against Mycobacterium tuberculosis in mice.* Immunity, 1995. **2**(6): p. 561-72.
102. Ehlers, S., et al., *Fatal granuloma necrosis without exacerbated mycobacterial growth in tumor necrosis factor receptor p55 gene-deficient mice intravenously infected with Mycobacterium avium.* Infection & Immunity, 1999. **67**(7): p. 3571-9.
103. Bean, A.G., et al., *Structural deficiencies in granuloma formation in TNF gene-targeted mice underlie the heightened susceptibility to aerosol Mycobacterium tuberculosis infection, which is not compensated for by lymphotoxin.* Journal of Immunology, 1999. **162**(6): p. 3504-11.
104. Keane, J., et al., *Tuberculosis associated with infliximab, a tumor necrosis factor alpha-neutralizing agent.* New England Journal of Medicine, 2001. **345**(15): p. 1098-104.
105. Gardam, M.A., et al., *Anti-tumour necrosis factor agents and tuberculosis risk: mechanisms of action and clinical management.[comment].* The Lancet Infectious Diseases., 2003. **3**(3): p. 148-55.
106. Mohan, V.P., et al., *Effects of tumor necrosis factor alpha on host immune response in chronic persistent tuberculosis: possible role for limiting pathology.* Infection & Immunity, 2001. **69**(3): p. 1847-55.
107. Turner, J., et al., *In vivo IL-10 production reactivates chronic pulmonary tuberculosis in C57BL/6 mice.* Journal of Immunology., 2002. **169**(11): p. 6343-51.
108. Murray, P.J., et al., *T cell-derived IL-10 antagonizes macrophage function in mycobacterial infection.* Journal of Immunology., 1997. **158**(1): p. 315-21.
109. Roach, D.R., et al., *Endogenous inhibition of antimycobacterial immunity by IL-10 varies between mycobacterial species.* Scandinavian Journal of Immunology., 2001. **54**(1-2): p. 163-70.
110. Jacobs, M., et al., *Enhanced immune response in Mycobacterium bovis bacille calmette guerin (BCG)-infected IL-10-deficient mice.* Clinical Chemistry & Laboratory Medicine., 2002. **40**(9): p. 893-902.
111. Rolph, M.S., et al., *MHC class Ia-restricted T cells partially account for beta2-microglobulin-dependent resistance to Mycobacterium tuberculosis.* European Journal of Immunology., 2001. **31**(6): p. 1944-9.
112. D'Souza, C.D., et al., *An anti-inflammatory role for gamma delta T lymphocytes in acquired immunity to Mycobacterium tuberculosis.* Journal of Immunology., 1997. **158**(3): p. 1217-21.
113. North, R.J. and A.A. Izzo, *Granuloma formation in severe combined immunodeficient (SCID) mice in response to progressive BCG infection. Tendency not to form granulomas in the lung is associated with faster bacterial growth in this organ.* American Journal of Pathology., 1993. **142**(6): p. 1959-66.
114. Gutierrex-Ramos, J.C., et al., *Non-redundant functional groups of chemokines operate in a coordinate manner during the inflammatory response in the lung.* Immunological Reviews., 2000. **177**: p. 31-42.
115. Allavena, P., et al., *The chemokine receptor switch paradigm and dendritic cell migration: its significance in tumor tissues.* Immunological Reviews., 2000. **177**: p. 141-9.
116. Sallusto, F., C.R. Mackay, and A. Lanzavecchia, *The role of chemokine receptors in primary, effector, and memory immune responses.* Annual Review of Immunology., 2000. **18**: p. 593-620.

117. Sallusto, F., et al., *Functional subsets of memory T cells identified by CCR7 expression.* Current Topics in Microbiology & Immunology., 2000. **251**: p. 167-71.
118. Kurihara, T. and R. Bravo, *Cloning and functional expression of mCCR2, a murine receptor for the C-C chemokines JE and FIC.* Journal of Biological Chemistry, 1996. **271**(20): p. 11603-7.
119. Farber, J.M., *Mig and IP-10: CXC chemokines that target lymphocytes.* Journal of Leukocyte Biology., 1997. **61**(3): p. 246-57.
120. Park, M.K., et al., *The CXC chemokine murine monokine induced by IFN-gamma (CXC chemokine ligand 9) is made by APCs, targets lymphocytes including activated B cells, and supports antibody responses to a bacterial pathogen in vivo.* Journal of Immunology., 2002. **169**(3): p. 1433-43.
121. Rossi, D. and A. Zlotnik, *The biology of chemokines and their receptors.* Annual Review of Immunology, 2000. **18**(217-242).
122. Josse, C., et al., *Importance of post-transcriptional regulation of chemokine genes by oxidative stress.* Biochemistry Journal, 2001. **360**: p. 321-333.
123. Jaramillo, M. and M. Olivier, *Hydrogen Peroxide Induces Murine Macrophage Chemokine Gene Transcription Via Extracellular Signal -Regulated Kinase and Cyclic Adenosine 5'- Monophosphate (cAMP)-Dependent Pathways: Involvement of NFkB, Activator Protein 1 and cAMP Response Element Binding Protein.* Journal of Immunology, 2002. **169**: p. 7026-7038.
124. Swanson, B.J., et al., *RANTES production by Memory Phenotype T Cells Is Controlled by a Posttranscriptional, TCR-Dependent Process.* Immunity, 2002. **17**: p. 605-615.
125. Rhoades, E.R., A.M. Cooper, and I.M. Orme, *Chemokine response in mice infected with Mycobacterium tuberculosis.* Infection & Immunity., 1995. **63**(10): p. 3871-7.
126. Sadek, M.I., et al., *Chemokines induced by infection of mononuclear phagocytes with mycobacteria and present in lung alveoli during active pulmonary tuberculosis.* American Journal of Respiratory Cell & Molecular Biology., 1998. **19**(3): p. 513-21.
127. Saukkonen, J.J., et al., *Beta-chemokines are induced by Mycobacterium tuberculosis and inhibit its growth.* Infection & Immunity., 2002. **70**(4): p. 1684-93.
128. Lin, Y., M. Zhang, and P.F. Barnes, *Chemokine production by a human alveolar epithelial cell line in response to Mycobacterium tuberculosis.* Infection & Immunity., 1998. **66**(3): p. 1121-6.
129. Indrigo, J., R.L. Hunter, Jr., and J.K. Actor, *Influence of trehalose 6,6'-dimycolate (TDM) during mycobacterial infection of bone marrow macrophages.* Microbiology., 2002. **148**(Pt 7): p. 1991-8.
130. Mohammed, K.A., et al., *Mycobacterium-mediated chemokine expression in pleural mesothelial cells: role of C-C chemokines in tuberculous pleurisy.* Journal of Infectious Diseases., 1998. **178**(5): p. 1450-6.
131. Riedel, D.D. and S.H. Kaufmann, *Chemokine secretion by human polymorphonuclear granulocytes after stimulation with Mycobacterium tuberculosis and lipoarabinomannan.* Infection & Immunity., 1997. **65**(11): p. 4620-3.
132. Sauty, A., et al., *The T cell-specific CXC chemokines IP-10, Mig, and I-TAC are expressed by activated human bronchial epithelial cells.* Journal of Immunology., 1999. **162**(6): p. 3549-58.

133. Miotto, D., et al., *Expression of IFN-gamma-inducible protein; monocyte chemotactic proteins 1, 3, and 4; and eotaxin in TH1- and TH2-mediated lung diseases.* Journal of Allergy & Clinical Immunology., 2001. **107**(4): p. 664-70.
134. Kurashima, K., et al., *Elevated chemokine levels in bronchoalveolar lavage fluid of tuberculosis patients.* American Journal of Respiratory & Critical Care Medicine., 1997. **155**(4): p. 1474-7.
135. Mayanja-Kizza, H., et al., *Activation of beta-chemokines and CCR5 in persons infected with human immunodeficiency virus type 1 and tuberculosis.* Journal of Infectious Diseases., 2001. **183**(12): p. 1801-4.
136. Juffermans, N.P., et al., *Up-regulation of HIV coreceptors CXCR4 and CCR5 on CD4(+) T cells during human endotoxemia and after stimulation with (myco)bacterial antigens: the role of cytokines.* Blood., 2000. **96**(8): p. 2649-54.
137. Zhu, G., et al., *Gene expression in the tuberculous granuloma: analysis by laser capture microdissection and real-time PCR.* Cellular Microbiology., 2003. **5**(7): p. 445-53.
138. Rojas, M., et al., *TNF-alpha and IL-10 modulate the induction of apoptosis by virulent Mycobacterium tuberculosis in murine macrophages.* Journal of Immunology., 1999. **162**(10): p. 6122-31.
139. Balcewicz-Sablinska, M.K., et al., *Pathogenic Mycobacterium tuberculosis evades apoptosis of host macrophages by release of TNF-R2, resulting in inactivation of TNF-alpha.* Journal of Immunology., 1998. **161**(5): p. 2636-41.
140. Gordon, S., *Alternative activation of macrophages.* Nature Reviews. Immunology., 2003. **3**(1): p. 23-35.
141. Hodge-Dufour, J., et al., *Inhibition of interferon gamma induced interleukin 12 production: a potential mechanism for the anti-inflammatory activities of tumor necrosis factor.* Proceedings of the National Academy of Sciences of the United States of America., 1998. **95**(23): p. 13806-11.
142. Botha, T. and B. Ryffel, *Reactivation of latent tuberculosis infection in TNF-deficient mice.* Journal of Immunology, 2003. **171**(6): p. 3110-8.
143. Roach, D.R., et al., *TNF regulates chemokine induction essential for cell recruitment, granuloma formation, and clearance of mycobacterial infection.* Journal of Immunology., 2002. **168**(9): p. 4620-7.
144. Pfeffer, K., et al., *Mice deficient for the 55 kd tumor necrosis factor receptor are resistant to endotoxic shock, yet succumb to L. monocytogenes infection.* Cell., 1993. **73**(3): p. 457-67.
145. Curran, S., et al., *Laser capture microscopy.* Molecular Pathology., 2000. **53**(2): p. 64-8.
146. Bermudez, L.E., et al., *The efficiency of the translocation of Mycobacterium tuberculosis across a bilayer of epithelial and endothelial cells as a model of the alveolar wall is a consequence of transport within mononuclear phagocytes and invasion of alveolar epithelial cells.* Infection & Immunity., 2002. **70**(1): p. 140-6.
147. Fuller, C.L., J. Flynn, and T.A. Reinhart, *Abundant expression of pro-inflammatory chemokines and cytokines in pulmonary granulomas developing in cynomolgus macaques experimentally infected with Mycobacterium tuberculosis: an in situ study.* Infect. Immun., 2003. **in press**.
148. Proost, P., et al., *Amino-terminal truncation of CXCR3 agonists impairs receptor signaling and lymphocyte chemotaxis, while preserving antiangiogenic properties.* Blood., 2001. **98**(13): p. 3554-61.

149. Lambeir, A.M., et al., *Kinetic investigation of chemokine truncation by CD26/dipeptidyl peptidase IV reveals a striking selectivity within the chemokine family.* Journal of Biological Chemistry., 2001. **276**(32): p. 29839-45.
150. Roach, T.I., et al., *Macrophage activation: lipoarabinomannan from avirulent and virulent strains of Mycobacterium tuberculosis differentially induces the early genes c-fos, KC, JE, and tumor necrosis factor-alpha.* Journal of Immunology, 1993. **150**(5): p. 1886-96.
151. Lu, B., et al., *Structure and function of the murine chemokine receptor CXCR3.* European Journal of Immunology., 1999. **29**(11): p. 3804-12.
152. Soejima, K. and B.J. Rollins, *A functional IFN-gamma-inducible protein-10/CXCL10-specific receptor expressed by epithelial and endothelial cells that is neither CXCR3 nor glycosaminoglycan.* Journal of Immunology., 2001. **167**(11): p. 6576-82.
153. Balashov, K.E., et al., *CCR5(+) and CXCR3(+) T cells are increased in multiple sclerosis and their ligands MIP-1alpha and IP-10 are expressed in demyelinating brain lesions.* Proceedings of the National Academy of Sciences of the United States of America., 1999. **96**(12): p. 6873-8.
154. Dufour, J.H., et al., *IFN-gamma-inducible protein 10 (IP-10; CXCL10)-deficient mice reveal a role for IP-10 in effector T cell generation and trafficking.* Journal of Immunology., 2002. **168**(7): p. 3195-204.
155. Khan, I.A., et al., *IP-10 is critical for effector T cell trafficking and host survival in Toxoplasma gondii infection.* Immunity., 2000. **12**(5): p. 483-94.
156. Wu, L., et al., *Interaction of chemokine receptor CCR5 with its ligands: multiple domains for HIV-1 gp120 binding and a single domain for chemokine binding.* Journal of Experimental Medicine, 1997. **186**(8): p. 1373-81.
157. Mack, M., et al., *Expression and characterization of the chemokine receptors CCR2 and CCR5 in mice.* Journal of Immunology, 2001. **166**(7): p. 4697-704.
158. Fraziano, M., et al., *Expression of CCR5 is increased in human monocyte-derived macrophages and alveolar macrophages in the course of in vivo and in vitro Mycobacterium tuberculosis infection.* AIDS Research & Human Retroviruses., 1999. **15**(10): p. 869-74.
159. Sato, N., et al., *Defects in the generation of IFN-gamma are overcome to control infection with Leishmania donovani in CC chemokine receptor (CCR) 5-, macrophage inflammatory protein-1 alpha-, or CCR2-deficient mice.* Journal of Immunology., 1999. **163**(10): p. 5519-25.
160. Huffnagle, G.B., et al., *Cutting Edge: Role of C-C Chemokine Receptor 5 in Organ-Specific and Innate Immunity to Cryptococcus neoformans.* J Immunology, 1999. **163**: p. 4642-4646.
161. Aliberti, J., et al., *CCR5 provides a signal for microbial induced production of IL-12 by CD8 alpha+ dendritic cells.* Nature Immunology, 2000. **1**(1): p. 83-7.
162. Zhou, Y., et al., *Imparied macrophage function an enhanced T cell-dependent immune response in mice lacking CCR5, the mouse homologue of the major HIV-1 coreceptor.* J Immunology, 1998. **160**(8): p. 4018-4025.
163. Dawson, T.C., et al., *Contrasting effects of CCR5 and CCR2 deficiency in the pulmonary inflammatory response to influenza A virus.* American Journal of Pathology., 2000. **156**(6): p. 1951-9.

164. Olszewski, M.A., et al., *Regulatory effects of macrophage inflammatory protein 1alpha/CCL3 on the development of immunity to Cryptococcus neoformans depend on expression of early inflammatory cytokines.* Infection & Immunity, 2001. **69**(10): p. 6256-63.
165. Liu, W. and D.A. Saint, *A new quantitative method of real time reverse transcription polymerase chain reaction assay based on simulation of polymerase chain reaction kinetics.* Analytical Biochemistry., 2002. **302**(1): p. 52-9.
166. Luther, S.A. and J.G. Cyster, *Chemokines as regulators of T cell differentiation.* Nature Immunology, 2001. **2**(2): p. 102-7.
167. Shevach, E.M., *CD4+ CD25+ suppressor T cells: more questions than answers.* Nature Reviews. Immunology., 2002. **2**(6): p. 389-400.
168. Andres, P.G., et al., *Mice with a selective deletion of the CC chemokine receptors 5 or 2 are protected from dextran sodium sulfate-mediated colitis: lack of CC chemokine receptor 5 expression results in a NK1.1+ lymphocyte-associated Th2-type immune response in the intestine.* Journal of Immunology., 2000. **164**(12): p. 6303-12.
169. Algeciras-Schimnich, A., et al., *CCR5 mediates Fas- and caspase-8 dependent apoptosis of both uninfected and HIV infected primary human CD4 T cells.* Aids., 2002. **16**(11): p. 1467-78.
170. Henderson, R.A., S.C. Watkins, and J.L. Flynn, *Activation of human dendritic cells following infection with Mycobacterium tuberculosis.* Journal of Immunology., 1997. **159**(2): p. 635-43.
171. Tascon, R.E., et al., *Mycobacterium tuberculosis-activated dendritic cells induce protective immunity in mice.* Immunology., 2000. **99**(3): p. 473-80.
172. Legge, K.L. and T.J. Braciale, *Accelerated migration of respiratory dendritic cells to the regional lymph nodes is limited to the early phase of pulmonary infection.* Immunity., 2003. **18**(2): p. 265-77.
173. Bozza, S., et al., *Dendritic cells transport conidia and hyphae of Aspergillus fumigatus from the airways to the draining lymph nodes and initiate disparate Th responses to the fungus.* Journal of Immunology., 2002. **168**(3): p. 1362-71.
174. Vermaelen, K.Y., et al., *Specific migratory dendritic cells rapidly transport antigen from the airways to the thoracic lymph nodes.* Journal of Experimental Medicine., 2001. **193**(1): p. 51-60.
175. Caux, C., et al., *Regulation of dendritic cell recruitment by chemokines.* Transplantation., 2002. **73**(1 Suppl): p. S7-11.
176. Scott, H.M., J. Chan, and J.F. Flynn, *Chemokines and tuberculosis.* Cytokines and Growth Factors Reviews, 2003. **14**(6): p. 467-477.
177. Chan, J., et al., *Effects of nitric oxide synthase inhibitors on murine infection with Mycobacterium tuberculosis.* Infection & Immunity, 1995. **63**(2): p. 736-40.
178. Chan, J., et al., *Killing of virulent Mycobacterium tuberculosis by reactive nitrogen intermediates produced by activated murine macrophages.* Journal of Experimental Medicine, 1992. **175**(4): p. 1111-22.
179. Shang, X., et al., *Chemokine receptor 1 knockout abrogates natural killer cell recruitment and impairs type-1 cytokines in lymphoid tissue during pulmonary granuloma formation.* American Journal of Pathology, 2000. **157**(6): p. 2055-63.

180. Qiu, B., et al., *Chemokine expression dynamics in mycobacterial (type-1) and schistosomal (type-2) antigen-elicited pulmonary granuloma formation.* American Journal of Pathology, 2001. **158**(4): p. 1503-15.
181. Chensue, S.W., et al., *Role of monocyte chemoattractant protein-1 (MCP-1) in Th1 (mycobacterial) and Th2 (schistosomal) antigen-induced granuloma formation: relationship to local inflammation, Th cell expression, and IL-12 production.* Journal of Immunology, 1996. **157**(10): p. 4602-8.
182. Chensue, S.W., et al., *Mycobacterial and schistosomal antigen-elicited granuloma formation in IFN-gamma and IL-4 knockout mice: analysis of local and regional cytokine and chemokine networks.* Journal of Immunology, 1997. **159**(7): p. 3565-73.
183. Huffnagle, G.B., et al., *Leukocyte recruitment during pulmonary Cryptococcus neoformans infection.* Immunopharmacology, 2000. **48**(3): p. 231-6.
184. Boring, L., et al., *Impaired monocyte migration and reduced type 1 (Th1) cytokine responses in C-C chemokine receptor 2 knockout mice.* Journal of Clinical Investigation, 1997. **100**(10): p. 2552-61.
185. Kurihara, T., et al., *Defects in macrophage recruitment and host defense in mice lacking the CCR2 chemokine receptor.* Journal of Experimental Medicine, 1997. **186**(10): p. 1757-62.
186. Orme, I.M. and F.M. Collins, *Mouse Model of Tuberculosis*, in *Tuberculosis: Pathogenesis, Protection, and Control*, B.R. Bloom, Editor. 1994, ASM Press: Washington DC. p. 113-134.
187. Kuziel, W.A., et al., *Severe reduction in leukocyte adhesion and monocyte extravasation in mice deficient in CC chemokine receptor 2.* Proceedings of the National Academy of Sciences of the United States of America, 1997. **94**(22): p. 12053-8.
188. Peters, W., M. Dupuis, and I.F. Charo, *A mechanism for the impaired IFN-gamma production in C-C chemokine receptor 2 (CCR2) knockout mice: role of CCR2 in linking the innate and adaptive immune responses.* Journal of Immunology, 2000. **165**(12): p. 7072-7.
189. Fife, B.T., et al., *CC chemokine receptor 2 is critical for induction of experimental autoimmune encephalomyelitis.* Journal of Experimental Medicine, 2000. **192**(6): p. 899-905.
190. Peters, W. and I.F. Charo, *Involvement of chemokine receptor 2 and its ligand, monocyte chemoattractant protein-1, in the development of atherosclerosis: lessons from knockout mice.* Current Opinion in Lipidology, 2001. **12**(2): p. 175-80.
191. Traynor, T.R., et al., *CCR2 expression determines T1 versus T2 polarization during pulmonary Cryptococcus neoformans infection.* Journal of Immunology, 2000. **164**(4): p. 2021-7.
192. Jouanguy, E., et al., *A human IFNGR1 small deletion hotspot associated with dominant susceptibility to mycobacterial infection.* Nature Genetics, 1999. **21**(4): p. 370-8.
193. Warmington, K.S., et al., *Effect of C-C chemokine receptor 2 (CCR2) knockout on type-2 (schistosomal antigen-elicited) pulmonary granuloma formation: analysis of cellular recruitment and cytokine responses.* American Journal of Pathology, 1999. **154**(5): p. 1407-16.
194. Serbina, N.V. and J.L. Flynn, *CD8(+) T cells participate in the memory immune response to Mycobacterium tuberculosis.* Infection & Immunity, 2001. **69**(7): p. 4320-8.

195. Faveeuw, C., G. Preece, and A. Ager, *Transendothelial migration of lymphocytes across high endothelial venules into lymph nodes is affected by metalloproteinases.* Blood., 2001. **98**(3): p. 688-95.
196. Friedland, J.S., et al., *Differential regulation of MMP-1/9 and TIMP-1 secretion in human monocytic cells in response to Mycobacterium tuberculosis.* Matrix Biology., 2002. **21**(1): p. 103-10.
197. Quiding-Jarbrink, M., D.A. Smith, and G.J. Bancroft, *Production of matrix metalloproteinases in response to mycobacterial infection.* Infection & Immunity., 2001. **69**(9): p. 5661-70.
198. Lima, M.C., et al., *Immunological cytokine correlates of protective immunity and pathogenesis in leprosy.* Scandinavian Journal of Immunology., 2000. **51**(4): p. 419-28.
199. Wangoo, A., et al., *Contribution of Th1 and Th2 cells to protection and pathology in experimental models of granulomatous lung disease.* Journal of Immunology., 2001. **166**(5): p. 3432-9.
200. Belkaid, Y., et al., *The role of interleukin (IL)-10 in the persistence of Leishmania major in the skin after healing and the therapeutic potential of anti-IL-10 receptor antibody for sterile cure.* Journal of Experimental Medicine., 2001. **194**(10): p. 1497-506.
201. Jacobs, M., et al., *Increased resistance to mycobacterial infection in the absence of interleukin-10.* Immunology., 2000. **100**(4): p. 494-501.
202. Murray, P.J. and R.A. Young, *Increased antimycobacterial immunity in interleukin-10-deficient mice.* Infection & Immunity., 1999. **67**(6): p. 3087-95.
203. Erb, K.J., et al., *IL-4, IL-5 and IL-10 are not required for the control of M. bovis-BCG infection in mice.* Immunology & Cell Biology., 1998. **76**(1): p. 41-6.
204. Denis, M. and E. Ghadirian, *IL-10 neutralization augments mouse resistance to systemic Mycobacterium avium infections.* Journal of Immunology., 1993. **151**(10): p. 5425-30.
205. Bermudez, L.E. and J. Champsi, *Infection with Mycobacterium avium induces production of interleukin-10 (IL-10), and administration of anti-IL-10 antibody is associated with enhanced resistance to infection in mice.* Infection & Immunity., 1993. **61**(7): p. 3093-7.
206. Opal, S.M., J.C. Wherry, and P. Grint, *Interleukin-10: potential benefits and possible risks in clinical infectious diseases.* Clinical Infectious Diseases., 1998. **27**(6): p. 1497-507.
207. Lalani, I., K. Bhol, and A.R. Ahmed, *Interleukin-10: biology, role in inflammation and autoimmunity.[erratum appears in Ann Allergy Asthma Immunol 1998 Mar;80(3):A-6].* Annals of Allergy, Asthma, & Immunology., 1997. **79**(6): p. 469-83.
208. Groux, H., et al., *Inhibitory and stimulatory effects of IL-10 on human CD8+ T cells.* Journal of Immunology., 1998. **160**(7): p. 3188-93.
209. Bogdan, C. and C. Nathan, *Modulation of macrophage function by transforming growth factor beta, interleukin-4, and interleukin-10.* Annals of the New York Academy of Sciences., 1993. **685**: p. 713-39.